Immuno-phenotyping and Inflammatory Mediators in SARS-CoV-2 Infection and Degenerative Aortic Valve Disease

Dissertation

der Mathematisch-Naturwissenschaftlichen Fakultät

der Eberhard Karls Universität Tübingen

zur Erlangung des Grades eines

Doktors der Naturwissenschaften

(Dr. rer. nat.)

vorgelegt von

Carolin Prang

aus Hamburg

Tübingen

2023

Gedruckt mit Genehmigung der Mathematisch-Naturwissenschaftlichen Fakultät der Eberhard Karls Universität Tübingen.

Tag der mündlichen Qualifikation:	22.06.2023
Dekan:	Prof. Dr. Thilo Stehle
1. Berichterstatter/-in:	PD Dr. Karin Müller
2. Berichterstatter/-in:	Prof. Dr. Alex Weber

Erklärung:

Ich erkläre, dass ich die zur Promotion eingereichte Arbeit mit dem Titel:

„Immuno-phenotyping and inflammatory mediators in SARS-CoV-2 infection and degenerative aortic valve disease “

selbständig verfasst, nur die angegebenen Quellen und Hilfsmittel benutzt und wörtlich oder inhaltlich übernommene Stellen als solche gekennzeichnet habe. Ich erkläre, dass die Richtlinien zur Sicherung guter wissenschaftlicher Praxis der Universität Tübingen beachtet wurden. Ich versichere an Eides statt, dass diese Angaben wahr sind und dass ich nichts verschwiegen habe. Mir ist bekannt, dass die falsche Abgabe einer Versicherung an Eides statt mit Freiheitsstrafe bis zu drei Jahren oder mit Geldstrafe bestraft wird.

Tübingen, den ....

Datum Unterschrift

Table of Content

ABBREVIATIONS ..... **II**

SUMMARY ..... **IV**

ZUSAMMENFASSUNG ..... **VI**

PUBLICATION LIST ..... **VIII**

PERSONAL CONTRIBUTIONS ..... **IX**

1 INTRODUCTION **1**

1.1 SARS-CoV-2 INFECTION 1

1.1.1 Cardiovascular complications *4*

1.1.2 Important immune cells in SARS-CoV-2 infection *5*

1.1.2.1 Monocytes 5

1.1.2.2 Thrombocytes 7

1.1.3 Furin *8*

1.1.4 Long-term consequences of COVID-19 ..... *8*

1.2 CALCIFIC AORTIC VALVE STENOSIS 10

1.2.1 Thrombocytes and monocytes in aortic stenosis *12*

1.2.2 Cytokines and chemokines in aortic stenosis *14*

2 AIM OF THIS WORK **16**

3 GENERAL RESULTS AND DISCUSSION **18**

3.1 HIGH PLASMA LEVELS OF FURIN PREDICT SEVERE CLINICAL OUTCOME IN CAD INFECTED SARS-COV-2 PATIENTS 18

3.2 REDUCTION OF NON-CLASSICAL MONOCYTES IS CHARACTERISTIC FOR CAD INFECTED SARS-COV-2 PATIENTS 22

3.3 MIF IS HIGHLY INCREASED IN PATIENTS AFTER RECOVERY OF SARS-COV-2 INFECTION 26

3.4 IMMUNO-PHENOTYPING IN AORTIC STENOSIS 30

3.5 CONCLUSION 36

4 LITERATURE **38**

5 ACKNOWLEDGMENT **53**

6 APPENDIX **54**

Abbreviations

ACE	Angiotensin Converting Enzyme
Afib	Atrial fibrillation
ALT	Alanine amino-transferase
ARDS	Acute respiratory distress syndrome
ARB	Angiotensin II Receptor Blockers
AS	Aortic stenosis
ASA	Acetylsalicylic acid
AST	Aspartate-aminotransferase
BMI	Body mass index
BMP	Bone morphogenetic proteins
CAD	Coronary artery disease
CAS	Calcific aortic stenosis
CK	Creatinine kinase
COVID-19	Coronavirus disease-19
CPDA	Citrate-phosphat-dextrose-adenin
CRP	Collagen related peptide
CVD	Cardio vascular disease
DCs	Dendritic cells
DM	Diabetes milletus
EP	Clinical endpoint
FC	Flow cytometry
FMO	Fluorescence minus one
g	Gramm
GFR-MDRD	Glomerular filtration rate
h	Hour
Hb	Hemoglobin
HI	Horovitz index
Hs TNI	High sensitive Troponin I
ICU	Intensive care unit
IFN	Interferon
INR	International normalized ratio
IL	Interleukin
IQR	Interquartile range
L	Liter
LDH	Lactate dehydrogenase
LDL	Low density lipoprotein
MIF	Macrophage migration inhibitory factor
NT-pro-BNP	N-terminal pro- brain natriuretic peptide,
Pap Sys	Pulmonary arterial pressure systolic
PBMC	Peripheral blood mononuclear cell
PBS	Phosphate buffered saline
PCR	Real-time reverse transcriptase polymerase chain reaction
PCT	Procalcitonin

PFA	Paraformaldehyde
PRP	Platelet-rich plasma
PTT	Partial thromboplastin time
RAAS	Renin-angiotensin-aldosterone system
RT	Room temperature
SARS-CoV-2	Severe acute respiratory syndrome coronavirus-2
SD	Standard deviation
SDF-1	Stromal cell-derived factor 1
TNF	Tumor necrosis factor
VECs	Valvular endothelial cells
VICs	Valvular interstitial cells

Summary

The new emerging SARS-CoV-2 is responsible for more than 640,395,651 cases and over 6,618,579 deaths worldwide. The SARS-CoV-2 infection is responsible for several concomitants, including severe thrombotic events, systemic inflammation, changes in hemostasis, and coagulation. Primary, the lung is affected regarding thrombi formation, but the heart, brain, liver, and kidney are also highly perceptible. Clinical cardiovascular complications frequently occur in hospitalized COVID-19 patients like acute heart failure and stroke, arrhythmias, venous thromboembolism, cardiogenic shock, arterial thrombosis, and myocarditis. Patients with cardiovascular diseases like coronary artery disease (CAD) are prone to develop severe clinical courses with worsening prognoses and life-threatening heart and lung injuries. Our study characterized important peripheral monocytes and thrombocytes in patients with a cardiovascular disease associated with an acute SARS-CoV-2 infection. Patients with a predisposition like CAD and an acute SARS-CoV-2 infection demonstrated a reduced number of peripheral non-classical monocytes with a changed phenotype indicating a defective migration and T cell activation behavior compared to CAD patients without infection. Further, a reduced number of non-classical monocytes below the calculated median represents a prognostic marker for rapidly progressive respiratory failure indicated by a HI < 200mmHg with subsequent mechanical ventilation. Characterizing peripheral thrombocytes in CAD patients following SARS-CoV-2 infection showed increased systemic platelet activation and hyper-inflammation. In addition, plasma levels of the convertase furin were significantly reduced in ICU-treated patients compared to patients with a mild disease progression. Further, furin functions as a prognostic plasma marker for a poor clinical outcome in SARS-CoV-2 positive CAD patients. SARS-CoV-2 infected patients with cardiovascular diseases demonstrated a significantly increased concentration of intracellular MIF in monocyte subsets after a recovery phase of three months. Further, phenotype of monocytes differed comparing acutely infected patients with a follow-up of three months. These results imply a prolonged immune response upon severe acute SARS-CoV-2 infection related to increased intracellular MIF expression and changes in monocyte phenotypes.

In summary, we demonstrated that the number of circulating non-classical monocytes can be used as a prognostic marker for rapidly progressive respiratory failure, and an association of the convertase furin with a poor clinical outcome upon SARS-CoV-2 infection.

The other part of the thesis gives insight into the role of thrombocytes and monocytes in patients with calcific aortic valve stenosis. Calcific aortic valve stenosis represents the most prevalent valve disease in western countries, particularly in the aging population. The aortic valve is affected by accelerating inflammation, fibrotic and calcific remodeling of the valve leaflets, thickening, and osteogenic formation leading to valve obstruction. Until now, no

pharmaceutical strategies are available to prevent inflammation, calcification, and osteogenic formation at an early stage of aortic stenosis. Thus, it is urgent to find new diagnostic and therapeutic targets to prevent severe disease progression. A huge cohort of patients with severe aortic stenosis demonstrated different phenotypes of slow and fast disease progression. Patients with a slow disease progression showed a calcific, pro-osteogenic and TGF-ß1 dependent phenotype. However, fast progressive aortic stenosis was characterized by an inflammatory and MIF-dependent phenotype. Further, the chemokine-like MIF may predict a fast disease progression in patients and is related to a local aortic valve tissue inflammation.

Zusammenfassung

Das neu auftretende Virus SARS-CoV-2, ist weltweit für mehr als 640,395,651 Fälle und über 6,618,579 Todesfälle verantwortlich. Eine SARS-CoV-2 Infektion verursacht verschiedene Begleiterscheinungen, darunter schwere thrombotische Ereignisse, systemische Entzündungen, Veränderungen der Hämostase und der Gerinnung. Nicht nur die Lunge ist von der Thrombenbildung betroffen, sondern auch Herz, Gehirn, Leber und Niere können häufig betroffen sein. Bei hospitalisierten COVID-19 Patienten, treten häufig klinische kardiovaskuläre Komplikationen auf, wie zum Beispiel akutes Herzversagen, Herzrhythmusstörungen, venöse Thromboembolien, kardiogener Schock, arterielle Thrombosen, akuter Schlaganfall und Myokarditis. Herz-Kreislauf-Erkrankungen wie die koronare Herzkrankheit erhöhen das Risiko, bei einer SARS-CoV-2 Infektion schwere Verläufe zu entwickeln, die unter anderem lebensbedrohliche Herz- und Lungenverletzungen umfassen. Ziel unserer Studie war es, die zirkulierenden peripheren Monozyten und Thrombozyten bei Patienten mit kardiovaskulären Vorerkrankungen im Zusammenhang mit einer akuten SARS-CoV-2 Infektion zu charakterisieren. Patienten mit einer Prädisposition wie KHK und einer akuten SARS-CoV-2 Infektion weisen, im Vergleich zu KHK-Patienten ohne Infektion, eine reduzierte Anzahl peripherer nicht-klassischer Monozyten mit einem veränderten Phänotyp auf, der auf ein verändertes Migrations- und T-Zell-Aktivierungsverhalten hinweist. Darüber hinaus, kann eine verringerte Anzahl nicht-klassischer Monozyten unterhalb des berechneten Medians als prognostischer Marker für ein rasch fortschreitendes Atemversagen dienen, dass durch einen HI < 200 mmHg mit anschließender mechanischer Beatmung beschrieben wird. Eine Charakterisierung der peripheren Thrombozyten bei KHK Patienten mit einer SARS-CoV-2 Infektion, zeigte eine erhöhte systemische Thrombozyten Aktivierung und eine Hyperinflammation. Darüber hinaus ist der Plasmaspiegel der Konvertase Furin bei Patienten, die auf der Intensivstation behandelt wurden, im Vergleich zu einem leichten Krankheitsverlauf, deutlich reduziert. Außerdem kann Furin, als prognostischer Plasmamarker für ein schlechten klinischen Verlauf, bei SARS-CoV-2-positiven KHK Patienten verwendet werden. SARS-CoV-2 infizierte Patienten mit kardiovaskulären Erkrankungen, zeigten nach einer Erholungsphase von drei Monaten eine signifikant erhöhte intrazelluläre MIF Konzentration in Monozyten auf. Darüber hinaus, zeigen die Monozyten unterschiedliche Phänotypen, im Vergleich zu akut infizierten Patienten und einem Follow-up von drei Monaten. Die Ergebnisse deuten auf eine langanhaltende Immunantwort nach einer schweren akuten SARS-CoV-2 Infektion hin, die mit einer erhöhten intrazellulären MIF Expression und Veränderungen des Monozyten Phänotyps einhergeht.

Zusammenfassend konnten wir zeigen, dass die Anzahl der zirkulierenden nicht-klassischen Monozyten, als prognostischer Marker für ein rasch fortschreitendes Lungenversagen

verwendet werden kann und dass die Konvertase Furin mit einem schlechten klinischen Ergebnis nach einer SARS-CoV-2 Infektion assoziiert ist.

Der weitere Teil der Arbeit trägt dazu bei, Erkenntnisse über die Rolle von Thrombozyten und Monozyten bei Patienten mit schwerer kalzifizierter Aortenklappenstenose zu gewinnen. Die Aortenklappenstenose ist die häufigste Klappenerkrankung in den westlichen Ländern, vor allem in der alternden Bevölkerung. Die Aortenklappe ist von einer beschleunigten Entzündung, fibrotischem und kalzifiziertem Umbau der Klappensegel, Verdickung und osteogener Knochenbildung betroffen, was zu einer Klappenobstruktion führt. Bisher gibt es keine pharmazeutischen Strategien zur Verhinderung von Entzündungen, Verkalkung und osteogener Bildung, in einem frühen Stadium der Aortenstenose. Daher müssen dringend neue diagnostische und therapeutische Ziele gefunden werden, um ein schweres Voranschreiten der Erkrankung zu verhindern. Die Analyse einer Kohorte von Patienten mit schwerer Aortenstenose, zeigt unterschiedliche Phänotypen von langsam und schnell progredienten Patienten. Patienten mit einer langsam fortschreitenden Erkrankung zeigen einen kalzifizierten, pro-osteogenen und TGF-ß1-abhängigen Phänotyp. Im Gegensatz dazu, zeigen Patienten mit einer schnell fortschreitenden Erkrankung, einen entzündlichen und MIF-abhängigen Phänotyp. Darüber hinaus kann das Chemokin-ähnliche MIF, zur Vorhersage eines schnellen Fortschreitens der Erkrankung bei Patienten mit einer Aortenklappenstenose verwendet werden und steht in Zusammenhang mit einer lokalen Entzündung des Aortenklappen Gewebes.

Publication list

Parts of this thesis have previously been published:

1. Mueller KAL, Langnau C, Günter M, Pöschel S, Gekeler S, Petersen-Uribe Á, Kreisselmeier KP, Klingel K, Bösmüller H, Li B, Jaeger P, Castor T, Rath D, Gawaz MP, Autenrieth SE. Numbers and phenotype of non-classical CD14dimCD16+ monocytes are predictors of adverse clinical outcome in patients with coronary artery disease and severe SARS-CoV-2 infection. Cardiovasc Res. 2021 Jan 1;117(1):224-239. doi: 10.1093/cvr/cvaa328. PMID: 33188677; PMCID: PMC7665325.

2. Langnau C, Rohlfing AK, Gekeler S, Günter M, Pöschel S, Petersen-Uribe Á, Jaeger P, Avdiu A, Harm T, Kreisselmeier KP, Castor T, Bakchoul T, Rath D, Gawaz MP, Autenrieth SE, Mueller KAL. Platelet Activation and Plasma Levels of Furin Are Associated With Prognosis of Patients With Coronary Artery Disease and COVID-19. Arterioscler Thromb Vasc Biol. 2021 Jun;41(6):2080-2096. doi: 10.1161/ATVBAHA.120.315698. Epub 2021 Apr 29. PMID: 33910372; PMCID: PMC8147700.

3. Langnau C, Janing H, Kocaman H, Gekeler S, Günter M, Petersen Á, Jaeger P, Koch B, Kreisselmeier KP, Castor T, Rath D, Gawaz M, Autenrieth SE, Mueller K. Recovery of systemic hyperinflammation in patients with severe SARS-CoV-2 infection. Biomarkers. 2022 Nov 15:1-19. doi: 10.1080/1354750X.2022.2148745. Epub ahead of print. PMID: 36377411.

Parts of this thesis have previously been submitted or are in revision:

4. Karin Anne Lydia Mueller, Carolin Langnau, Tobias Harm, Manuel Sigle, Madeleine Ilg, Anne-Katrin Rohlfing, Sarah Gekeler, Bo Li, Manina Günter, Nora Goebel, Ulrich F.W. Franke, Nura Rashed, Zeanub Khan, Klaus-Peter Kreisselmeier, Tatsiana Castor, Iris Irmgard Mueller, Stella E. Autenrieth, Meinrad Paul Gawaz (2022). Expression of migration inhibitory factor (MIF) in valve tissue, circulating platelets and monocytes is associated with fast progression of aortic stenosis. *In revision*

Personal contributions

1. Publication

Mueller KAL, Langnau C, Günter M, Pöschel S, Gekeler S, Petersen-Uribe Á, Kreisselmeier KP, Klingel K, Bösmüller H, Li B, Jaeger P, Castor T, Rath D, Gawaz MP, Autenrieth SE. Numbers and phenotype of non-classical CD14dimCD16+ monocytes are predictors of adverse clinical outcome in patients with coronary artery disease and severe SARS-CoV-2 infection. Cardiovasc Res. 2021 Jan 1;117(1):224-239. doi: 10.1093/cvr/cvaa328. PMID: 33188677; PMCID: PMC7665325.

I planned and executed the following experiments under the guidance of PD Dr. Karin Müller and PD Dr. Stella Autenrieth. I prepared all patients' samples and performed all of the flow cytometry staining and measurements with assistance from the technician Sarah Gekeler. I performed all supplemental experiments and data analysis and prepared parts of the revision. Furthermore, I analyzed all data, prepared all figures and tables. I included corrections and editing's of the manuscript and wrote the method part and figure legends under the supervision of Dr. Karin Müller and PD Dr. Stella Autenrieth. Karin Klingel prepared the histological staining of the lung and heart tissue.

2. Publication

Langnau C, Rohlfing AK, Gekeler S, Günter M, Pöschel S, Petersen-Uribe Á, Jaeger P, Avdiu A, Harm T, Kreisselmeier KP, Castor T, Bakchoul T, Rath D, Gawaz MP, Autenrieth SE, Mueller KAL. Platelet Activation and Plasma Levels of Furin Are Associated With Prognosis of Patients With Coronary Artery Disease and COVID-19. Arterioscler Thromb Vasc Biol. 2021 Jun;41(6):2080-2096. doi: 10.1161/ATVBAHA.120.315698. Epub 2021 Apr 29. PMID: 33910372; PMCID: PMC8147700.

I planned and executed the following experiments under the guidance of PD Dr. Karin Müller and PD Dr. Stella Autenrieth. I prepared all patients' samples and performed all of the flow cytometry staining and measurements with assistance from the technician Sarah Gekeler. Further, I conducted the Image Steam analysis with the assistance from Simone Pöschel. I performed the LegendPlex staining and measurements as well as analysis of the data with assistance from Sarah Gekeler. I executed the ELISA with assistance of Dr. Anne-Katrin Rohlfing. PD Dr. Karin Müller and I performed the statistical analysis and Kaplan-Mayer curve. Tobias Harm ran the Vulcano plot analysis. Dr. Anne-Katrin Rohlfing performed the microscopy staining.

I analyzed all the data, prepared all figures and tables. I performed the supplemental experiments and data analysis with assistance from Dr. Anne-Katrin Rohlfing. I included

corrections and editing's, and wrote parts of the manuscript and the figure legends under the supervision of PD Dr. Karin Müller and Prof. Dr. Meinrad Gawaz.

3. Publication

Langnau C, Janing H, Kocaman H, Gekeler S, Günter M, Petersen Á, Jaeger P, Koch B, Kreisselmeier KP, Castor T, Rath D, Gawaz M, Autenrieth SE, Mueller K. Recovery of systemic hyperinflammation in patients with severe SARS-CoV-2 infection. Biomarkers. 2022 Nov 15:1-19. doi: 10.1080/1354750X.2022.2148745. Epub ahead of print. PMID: 36377411.

I planned and executed the following experiments under the guidance of PD Dr. Karin Müller and PD Dr. Stella Autenrieth. I prepared all patients' samples and performed all of the flow cytometry staining and measurements with assistance from the technician Sarah Gekeler. I performed the OMIQ analysis and evaluation of flow cytometry data. Further, I performed the LegendPlex staining and measurements as well as analysis of the data with assistance from Sarah Gekeler. I analyzed all data, prepared the figures and tables. I included corrections and editing's and wrote parts of the manuscript and the figure legends under the supervision of Dr. Karin Müller and Prof. Dr. Meinrad Gawaz.

4. Publication

Karin Anne Lydia Mueller, Carolin Langnau, Tobias Harm, Manuel Sigle, Madeleine Ilg, Anne-Katrin Rohlfing, Sarah Gekeler, Bo Li, Manina Günter, Nora Goebel, Ulrich F.W. Franke, Nura Rashed, Zeanub Khan, Klaus-Peter Kreisselmeier, Tatsiana Castor, Iris Irmgard Mueller, Stella E. Autenrieth, Meinrad Paul Gawaz (2022). Expression of migration inhibitory factor (MIF) in valve tissue, circulating platelets and monocytes is associated with fast progression of aortic stenosis. *In revision*

I planned and executed the following experiments under the guidance of PD Dr. Karin Müller and PD Dr. Stella Autenrieth. I prepared all patients' samples and performed all of the flow cytometry staining and measurements with assistance from the technician Sarah Gekeler. I performed the OMIQ analysis of flow cytometry data and prepared the figures under the supervision of PD Dr. Stella Autenrieth. Further, I performed the LegendPlex staining and measurements as well as analysis of the data with assistance from Sarah Gekeler. Madeleine Ilg, Sarah Gekeler, Bo Li, Nura Rashed, and Zeanub Khan performed the (immune-) histological staining. Tobias Harm and Manuel Sigle ran the Vulcano plot and pathway analysis. Furthermore, I analyzed the data, prepared the figures and tables. I included corrections and editing's and wrote the method part and figure legends of the manuscript under the supervision of Dr. Karin Müller and PD Dr. Stella Autenrieth.

1 Introduction

1.1 SARS-CoV-2 infection

The new emerging severe acute respiratory syndrome coronavirus 2 (SARS-CoV-2) primary causes asymptomatic infections or a common cold affecting the upper airways in healthy individuals. However, several predispositions lead to severe and lethal complications, for example, acute respiratory distress syndrome (ARDS) (Lamers and Haagmans, 2022, Zheng et al., 2020b). Worldwide, more than 640,395,651 cases of the coronavirus disease 2019 (COVID-19) (WHO, 2022) and over 6,618,579 deaths (WHO, 2022) have been reported since it emerged in 2020. SARS-CoV-2 belongs to the genus *Betacoronavirus* in the family *Coronaviridae.* It is closely associated to SARS-CoV and Middle East respiratory syndrome CoV (Fehr and Perlman, 2015, Kim et al., 2020).

Chronic cardiovascular disorders like ischemic heart disease and heart failure, as well as hypertension and diabetes mellitus (DM), outline specific predispositions of hospitalized patients with cardiovascular risk factors. SARS-CoV-2 infection is linked to a broad range of disease severity, from asymptomatic or mild infection to critical illness with multi-organ failure. Hospitalized patients infected with SARS-CoV-2 are characterized by common complications like sepsis, respiratory failure, pneumonia, and ARDS (Guzik et al., 2020, Huang et al., 2020a, Giacca, 2022, Lamers and Haagmans, 2022, Zheng et al., 2020b). Further, SARS-CoV-2 infection symptoms include severe thrombotic events, systemic inflammation, changes in hemostasis, and coagulation. Primary, the lung is affected regarding thrombi formation, but the liver, brain, heart, and kidney are also highly susceptible. In addition, cardiac arrhythmias, myocardial infarction, heart failure, and myocarditis have been monitored in infected patients. Elevated plasma D-dimer levels and massive thrombotic events were predictive for coagulation-associated complications (Nishiga et al., 2020, Oren Ohad, 2020, Al-Samkari et al., 2020, Gorog et al., 2022, Zhou et al., 2020, Giacca, 2022). An overproduction of early pro-inflammatory cytokines and chemokines, is an additional characteristic of a SARS-CoV-2 infection. This phenomenon is called cytokine storm and increases the risk for vascular hyperpermeability and if permanent, multi-organ injury and death in COVID-19 patients (Jose and Manuel, 2020, Tang et al., 2020a).

The mechanism of cell entry of the SARS-CoV-2 virus is well described in the literature (Figure 1). Initiation of the entry process of the virus starts with attachment on the host cell's membrane, resulting in membrane fusion facilitated by the virus S glycoprotein. Beforehand, the S glycoprotein is cleaved into S1 and S2 subunits by the subtilisin-like proprotein convertase furin within the virus producing-cell during biosynthesis and maturation. After cleavage of the S glycoprotein and release of the virus, the subunit S1 binds to its receptor

angiotensin-converting enzyme 2 (ACE2) on the host cell's surface. The subunit S2 is responsible for anchoring the S protein into the host membrane (Huang et al., 2020b, Jackson et al., 2022, Shang et al., 2020). The primary cell entry receptor for SARS-CoV-2, like in airway epithelial cells, has been identified as ACE2. ACE2 is expressed on several immune cells like monocytes, macrophages, and respiratory and vascular endothelial cells (Clarke and Turner, 2012, Datta et al., 2020, Abassi et al., 2020).

Cleavage of the S2 site by target-cell proteases is followed by ACE2-mediated membrane fusion. Depending on the entry route, the S2 site is either cleaved by transmembrane protease serine 2 (TMPRSS2) on the target cell or by cathepsin L upon internalization via clathrin-mediated endocytosis. Conformational changes of both subunits allow fusion of the viral and target host cell membrane, inducing the formation of a fusion pore and causing insertion of the viral genome to reach the target cell cytoplasm (Figure 1A+B) (Bayati et al., 2021, Huang et al., 2020b, Shang et al., 2020, Jackson et al., 2022, Huang et al., 2006, Glowacka et al., 2011).

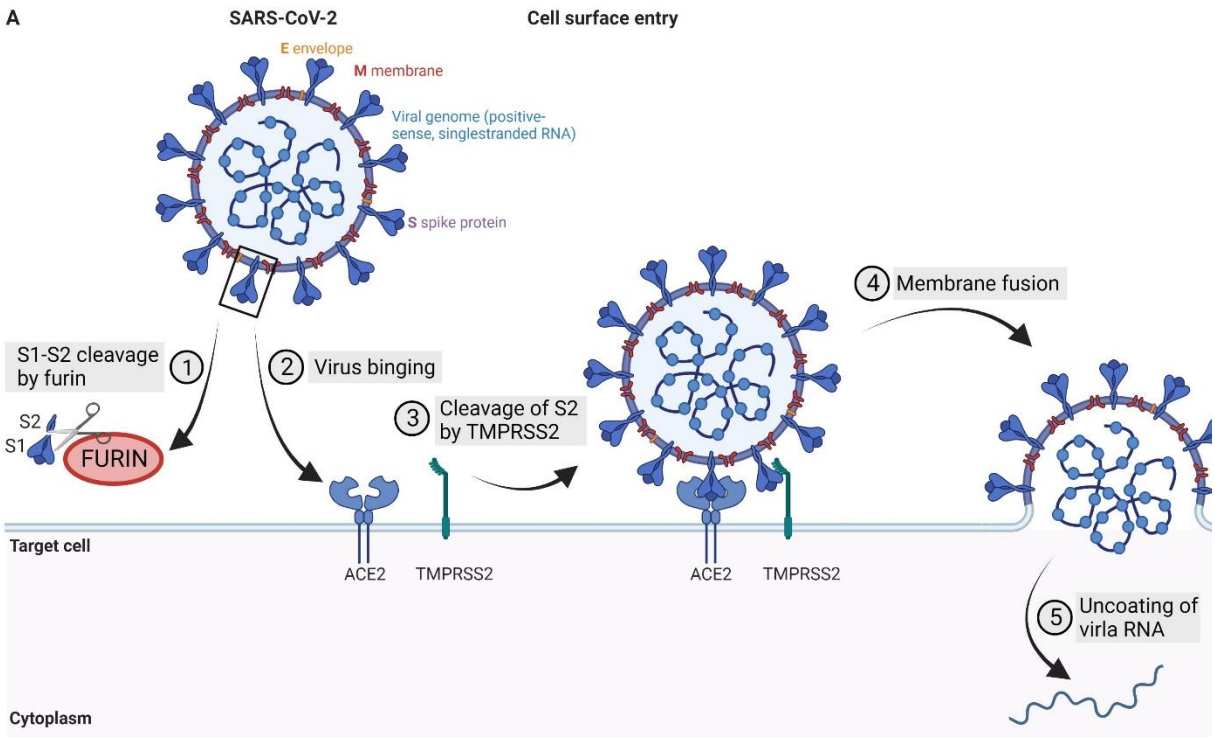

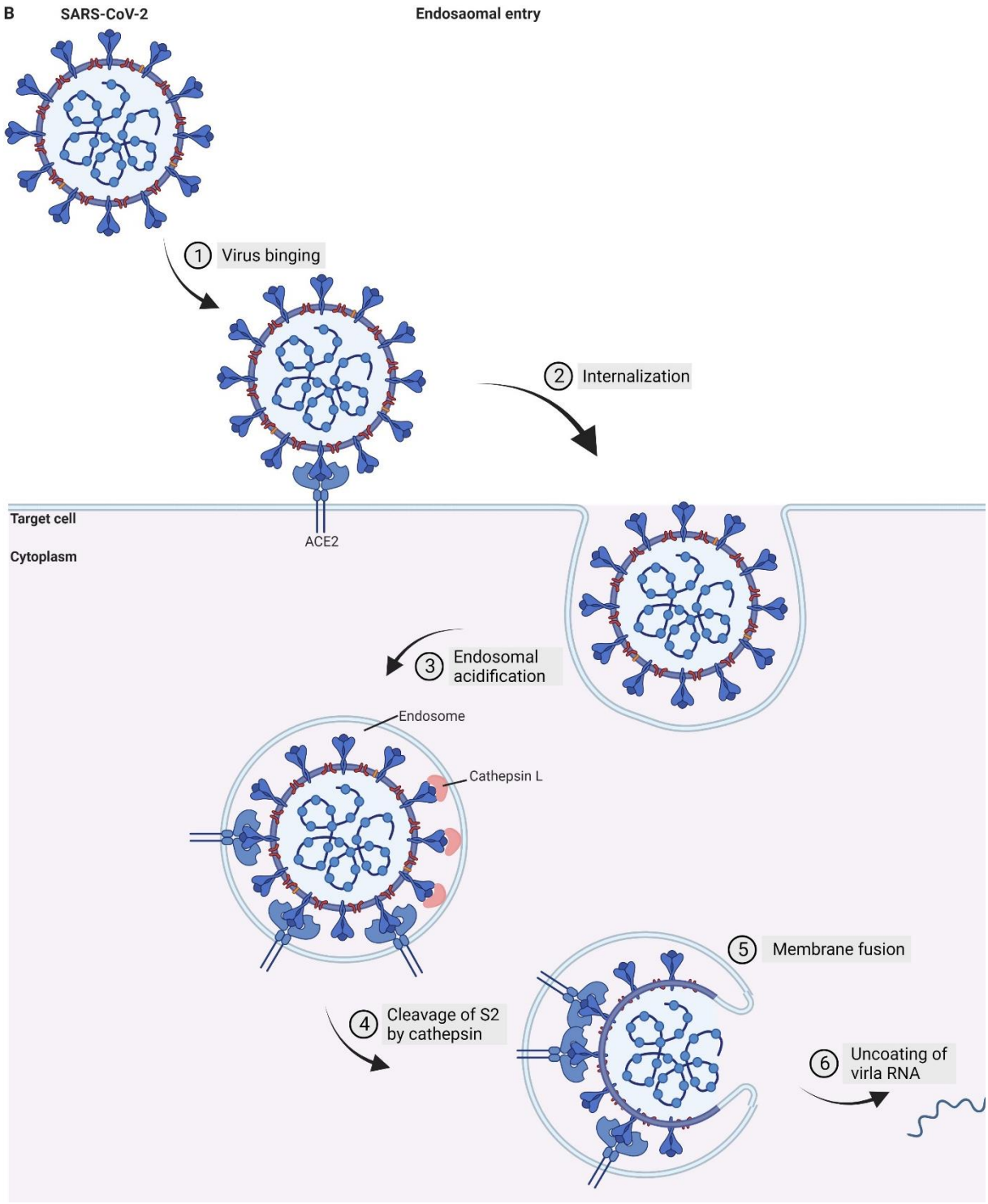

Figure 1: Cell entry of SARS-CoV-2. The SARS-CoV-2 virus is able to enter the target host cell either by cell surface entry (A) or endosomal entry (B). Cell entry of the virus requires two cleavages of the spike S glycoprotein. First, the S1-S2 junction has to be cleaved by the enzyme furin, which is necessary during the maturation process of the virus within the infected cell. The S2 site is either cleaved by TMPRSS2 or cathepsin L, dependent on the cell entry mechanism. **(A)** The cell surface entry starts with the S1-S2 cleavage within the infected cell by furin, followed by binding to ACE2, resulting in conformation changes within the S1 subunit. Cleavage of the S2 site by the enzyme TMPRSS2 on the cell surface results in conformational changes of the S2 site. Viral and target membranes can fuse and form a fusion pore while releasing the viral RNA into the host cell cytoplasm. **(B)** The endosomal entry starts similar to the cell surface entry with the S1-S2 cleavage within the infected cell by furin, followed by binding to ACE2, resulting in conformation changes within the S1 subunit. Without the enzyme

TMPRSS2 on the surface, the complex of the virus and ACE2 is internalized via clathrin-mediated endocytosis. The S2 site is cleaved by the enzyme cathepsin L within the endosome resulting in conformational changes of the S2 site. Viral and endosome membranes can fuse and form a fusion pore while releasing the viral RNA into the host cell cytoplasm. Adapted from (Jackson et al., 2022, Rangu et al., 2022) and created with BioRender.com

1.1.1 Cardiovascular complications

Clinical cardiovascular complications mainly occur in hospitalized COVID-19 patients and comprise arterial thrombosis, arrhythmias, acute heart failure, cardiogenic shock, venous thromboembolism, acute stroke, myocardial ischemia or infarction, and myocarditis (Giacca, 2022, Nishiga et al., 2020). In particular, patients with cardiovascular comorbidities like coronary artery disease (CAD) are prone to develop severe clinical courses with worsening prognosis, including life-threatening heart and lung injury and high mortality following SARS-CoV-2 infection (Nishiga et al., 2020, Task Force for the management of, 2022, Oren Ohad, 2020). Further, a cytokine storm may promote cardiovascular dysfunctions in COVID-19 patients, caused by a dysfunction of T-cell activation and cytokine release (Task Force for the management of, 2022).

In general, atherogenesis and disease progression in CAD are characterized by chronic alterations of inflammatory molecules such as pro-inflammatory cytokines, adhesion molecules, or C-reactive protein (CRP) (Wolf and Ley, 2019). Immune cells like monocytes are recruited to the vessel wall upon increased regulation of cytokines and chemokines, causing atherosclerotic lesion formation (Wolf and Ley, 2019). Inflammatory immune cells like monocytes and macrophages are associated with several heart diseases, for example, CAD, myocardial infarction, myocarditis, and heart failure (Wolf and Ley, 2019, Swirski and Nahrendorf, 2018, Woollard and Geissmann, 2010). Further, thrombocytes play an essential role during disease progression and contribute to inflammatory processes in atherosclerosis and CAD. Activated, hyper-aggregable thrombocytes can affect endothelial and immune cell function and atherosclerotic plaque formation by thrombo-inflammatory immune responses. Thrombocytes connect the local inflammatory responses at the vascular wall with the development of an atherogenic milieu (Nording et al., 2020, Reinthaler et al., 2016, Huilcaman et al., 2022).

In CAD patients, a SARS-CoV-2 infection causes a pro-inflammatory and pro-thrombotic immune response resulting in cardiovascular disorders like heart failure, acute coronary syndrome or myocardial injury (Xiong et al., 2020, Nishiga et al., 2020). Furthermore, the development of acute right heart failure is a massive problem in CAD patients resulting from predispositions like right heart and diastolic dysfunction and increased pulmonary artery pressure. Further, these patients develop pulmonary embolisms because of infect-related

coagulopathy causing acute right heart failure and distributed intravascular coagulation (Task Force for the management of, 2022, Oren Ohad, 2020, Tang et al., 2020b). Other high-risk conditions like DM and CAD in COVID-19 patients may also increase the risk for severe respiratory failure, increased mortality, and organ injury (Zheng et al., 2020b, Task Force for the management of, 2022, Rath et al., 2020, Nishiga et al., 2020).

1.1.2 Important immune cells in SARS-CoV-2 infection

Fighting against virus infections require a first line defense achieved by the innate immune system. Important immune cells sense the body via pattern recognition receptors resulting in inflammatory pathways and viral clearance. In particular, the innate immune system executes important functions like prevention of viral entry and replication of the virus, removal of infected cell debris and contribution to boost adaptive immune responses. Immune responses are carried out by important cells like monocytes, macrophages, neutrophils, and natural killer cells, promoting inflammatory signaling pathways and immune responses (Rouse and Sehrawat, 2010, Diamond and Kanneganti, 2022). In particular, monocytes are recruited to the side of infection and are critical for controlling and clearing microbial infections. However, monocytes are also related to the pathogeneses of inflammatory and degenerative diseases (Shi and Pamer, 2011).

Besides the critical role of monocytes in fighting against virus infections, thrombocytes also regulate meaningful immune cell responses. Thrombocytes express surface receptors enabling them to sense invading pathogens and secrete antimicrobial agents controlling the innate and adaptive immune responses. Activation of thrombocytes and their cell count are related to an elevated risk for thrombotic complications (Assinger, 2014, Portier and Campbell, 2021).

Therefore, the role of monocytes and thrombocytes are of high interest and should be further investigated regarding virus infections associated with cardiovascular diseases.

1.1.2.1 Monocytes

The maturation of monocytes occurs within the bone marrow, followed by their release into the bloodstream. Monocytes are able to function as precursor cells, enabling the differentiation into macrophages or dendritic cells. Dependent on the surface expression of CD14 and CD16, monocytes have been characterized into three subsets: classical ($CD14^{++}CD16^{-}$ ~85 %), intermediate ($CD14^{+}CD16^{+}$ ~5 %), and non-classical ($CD14^{dim}CD16^{++}$ ~10 %) monocytes which perform different functions at different stages of their maturation (Ziegler-Heitbrock et al., 2010, Shantsila et al., 2011, Kapellos et al., 2019). CD14 is an endotoxin receptor binding to lipopolysaccharides. Especially monocytes and tissue-resident macrophages are CD14 positive, whereas neutrophils and B-lymphocytes only weakly express CD14 (Naeim F, 2018).

However, CD16 functions as the antibody-dependent cellular-cytotoxicity as a low-affinity Fcγ transmembrane receptor showing expression on tissue-resident macrophages, dendritic cells, monocytes, natural killer cells, and granulocytes (Naeim F, 2018, Stern-Ginossar and Mandelboim, 2009). Circulating peripheral monocytes play an essential role during innate and adaptive immune responses such as inflammation and recognition of dead cells or pathogens with subsequent removal. Additionally, monocytes are involved in tissue repair, emphasizing their importance and multi-functionality (Kratofil et al., 2017, Boyette et al., 2017). In general, monocytes get activated and migrate to the site of infection, and boosting antimicrobial activity against a broad range of pathogenic microorganisms. Further, monocytes are able to enter draining lymph nodes and facilitate adaptive immunity following infection. Various adhesion and migration molecules are essential for the recruitment of monocytes, described as rolling, adhesion, and transmigration. Important adhesion molecules are lymphocyte function-associated antigen 1 (αLβ2 integrin), L-selectin (CD62L), macrophage receptor 1, very late antigen 4, and platelet endothelial cell adhesion molecule (Ziegler-Heitbrock, 2007, Shi and Pamer, 2011).

Classical monocytes show a pro-inflammatory phenotype based on their function and secretion of inflammatory molecules. They can differentiate into monocyte-derived DCs, under the right conditions. Classical monocytes show a high surface expression of CD36, CCR2, and CD64, making them distinguishable from the other subsets. Classical monocytes adhere to the endothelium, migrate, and phagocytose pathogens. Thus, they directly promote antimicrobial immune responses by sensing their environment. They rapidly migrate into inflamed tissue and contribute to control of inflammation and tissue repair (Kapellos et al., 2019, Merad and Martin, 2020, Lassalle et al., 2022). In contrast, intermediate monocytes are focused on antigen processing and presentation, cytokine secretion (TNFα, IL-1β, IL-6), apoptosis, and transendothelial migration. Intermediate monocytes express high surface levels of CCR5 and HLA-DR (Kapellos et al., 2019). A recent study shows that intermediate monocytes are significantly increased in peripheral blood in SARS-CoV-2 patients who required intensive care unit (ICU) treatment compared to patients without ICU treatment (Merad and Martin, 2020). However, non-classical monocytes play an essential role during anti-viral immune responses and maintain vascular homeostasis (Kapellos et al., 2019, Narasimhan et al., 2019, Buscher et al., 2017). In addition, non-classical monocytes express high levels of CX3CR1 and patrol within the vascular system alongside the endothelium of blood vessels, indicating a role in the innate local surveillance of tissue (Cros et al., 2010, Auffray et al., 2009). Further studies showed that non-classical monocytes execute functions in the complement system and FcR-mediated phagocytosis (Kapellos et al., 2019). Additionally, patrolling non-classical monocytes have been related to athero-protective, anti-inflammatory, and pro-homeostatic functions (Thomas et al., 2015, Cros et al., 2010, Buscher et al., 2017).

1.1.2.2 Thrombocytes

Thrombocytes are small anucleated cells formed by the strangulation of megakaryocytes in the bone marrow. They are mainly responsible for thrombus formation, vascular integrity, leakage avoidance, inflammation, and leukocyte interaction (Deppermann and Kubes, 2018, Gros et al., 2014, Lievens and von Hundelshausen, 2011). The promotion of inflammatory responses is either achieved by direct interaction with pathogens or indirectly by recruiting and stimulating other immune cells (Deppermann and Kubes, 2018). Thrombocytes and their activation represent a crucial connection between inflammation, atherosclerosis, and infectious diseases (Gawaz et al., 2005, Koupenova et al., 2018). Thrombocytes can affect several cell types within the blood and are able to associate the immune system with thrombo-inflammation due to the release of several cytokines and chemokines. Thus, they are critical mediators of inflammation (Ribeiro et al., 2019).

Thrombocyte activation and coagulopathy are also associated with infectious diseases like SARS-CoV-2, causing thrombotic complications like pulmonary embolism and deep vein thrombosis (Guzik et al., 2020, Connors and Levy, 2020, Zaid et al., 2020). COVID-19 patients show alterations in their thrombocyte count. In particular, severely ill patients exhibit thrombocytopenia, thrombocyte activation, and characteristic coagulopathy early during infection (Connors and Levy, 2020, Barrett et al., 2021, Zaid et al., 2020). It is well described that thrombocytes are hyper-activated, indicated by an increased surface expression of P-Selectin or other factors in COVID-19 patients at hospital admission (Grobler et al., 2020, Langnau et al., 2021, Bongiovanni et al., 2021, Colling and Kanthi, 2020). This hyperactive state is mainly described during ARDS in SARS-CoV-2 infection, while it is distinct in other acute respiratory distress syndromes like influenza (Zaid et al., 2021). Uncontrolled hyper-inflammation is characterized by high activation of thrombocytes and is attended to hypofibrinolysis. COVID-19 patients have an increased risk to develop progressive respiratory failure, multiple organ failure, and death. Especially COVID-19 patients with a severe outcome often have pre-existing cardiovascular conditions and suffer from obesity, DM, hypertension or are at an advanced age. All of these cardiovascular risk factors are well described to have an impact on thrombocyte activation. Further, patients with SARS-CoV-2 infection showed increased formation of circulating thrombocyte/leukocyte co-aggregation (Guzik et al., 2020, Gu et al., 2021, Zheng et al., 2020b, Manne et al., 2020). The formation of thrombocyte aggregates is associated with a worse clinical outcome in COVID-19 patients (Hottz et al., 2020). Several studies demonstrate the critical role of thrombocytes with thrombosis in SARS-CoV-2 infected patients (Connors and Levy, 2020, Giacca, 2022, Gu et al., 2021). Patients suffering from COVID-19 are predisposed to thrombocytopenia, and the lung shows infiltration of pulmonary megakaryocytes. Mild thrombocytopenia is also associated with severe end-stage disease (Barrett et al., 2021, Giacca, 2022, Gu et al., 2021). In summary, SARS-CoV-2

infection is characterized by thrombocyte hyper-reactivity, increased expression of surface CD62P, and scattering of fibrinogen and collagen. Further, increased levels of circulating aggregates of thrombocytes with monocytes or T cells and increased thrombocyte degranulation were highly consistent in COVID-19 patients (Giacca, 2022).

1.1.3 Furin

Furin is a subtilisin-like proprotein convertase, and its expression is ubiquitous. Furin controls various physiological functions, such as the complement system, blood clotting, and the cleavage of viral-envelope glycoproteins, membrane receptors, and bacterial exotoxins (Braun and Sauter, 2019, Nakayama, 1997). Most importantly, furin enables viral attachment of SARS-CoV-2 on the host cell membrane (Coutard et al., 2020, Hoffmann et al., 2020b, Walls et al., 2020, Shang et al., 2020). In detail, furin is able to cleave the S glycoprotein into the subunits S1 and S2 within the Golgi apparatus during biosynthesis and maturation in the infected host cell (Hoffmann et al., 2020a, Shang et al., 2020, Jackson et al., 2022). Further, furin may have critical functions in cardiovascular disease, for example, CAD and the cardiovascular risk factor DM. In patients with acute myocardial infarction, furin plasma levels have been further related to all-cause mortality and cardiovascular events (Yakala et al., 2019, Wang et al., 2020, Fernandez et al., 2018). In atherosclerotic plaques, furin expression was observed mainly in macrophages. Variants of furin were identified which are associated with CAD, and their differential expression levels affected the migration behavior of monocytes and macrophages (Stawowy et al., 2005, Yang et al., 2020b, Zhao et al., 2018, Yakala et al., 2019).

1.1.4 Long-term consequences of COVID-19

SARS-CoV-2 infection is characterized by serious clinical symptoms like severe systemic inflammatory responses and cytokine storm, resulting in thrombotic complications, microcirculatory disturbances, and organ failure. Therefore, SARS-CoV-2 may have long-term consequences on the cardiovascular and immune system (Xiong et al., 2020, Lamers and Haagmans, 2022, Zheng et al., 2020b). Until now, these long-term consequences are not fully understood. Thus, it is critical to study the impact of the SARS-CoV-2 virus on immune cells and immune response pathologies along with clinically relevant complications like fatigue, muscle weakness, dyspnea, arrhythmias, anxiety, and depression (Huang et al., 2021).

Long-COVID is a new term describing symptoms of COVID-19 patients that persist after an acute infection of 4-12 weeks up to several months (Giacca, 2022). Another study described that ‘long COVID’ should be considered in two phases. The continuous phase with symptoms lasts between 4-12 weeks. The second phase is named “post-COVID-19 syndrome” and lasts over 12 weeks, depending on the duration of symptoms (Raman et al., 2022). The long-COVID

symptoms are highly heterogenous and refer to various organ systems, including fatigue, myalgia, impaired concentration, breathlessness, sleep quality, short-term memory loss, joint swelling or pain, chest pain, overall mood dysfunctions, dermatological complications, and lung fibrosis. Several physiological mechanisms of the virus are responsible for these long-term complications. Less common are cardiovascular problems, including late pericarditis, acute coronary syndromes, stroke, venous and arterial thromboembolism (Desai et al., 2022, Higgins et al., 2021, Giacca, 2022). A possible explanation for the pathophysiological mechanism is the direct tissue damage by the entry receptor for ACE2, expressed in several locations within the body. Therefore, the virus has various possibilities to enter the body, causing direct tissue damage. Further, long-term pulmonary complications were reported upon COVID-19 infection (Desai et al., 2022). Other studies observed long-term complications following SARS-CoV-2 infection affecting mental health, like anxiety, depression, PTSD, and sleep disturbances (Bourmistrova et al., 2022). Similar long-term complications were observed in studies about the SARS-CoV-1 virus, which emerged in 2003 (Desai et al., 2022).

1.2 Calcific aortic valve stenosis

Calcific aortic valve stenosis (CAS) represents the most prevalent heart valve disease in western countries, particularly in the aging population (Osnabrugge et al., 2013, Nkomo et al., 2006). The aortic valve is affected by accelerating inflammation, fibrotic and calcific remodeling of the valve leaflets, thickening, and osteogenic formation, finally leading to valve obstruction. Until now, no pharmaceutical strategies are available to prevent inflammation, calcification, fibrotic and osteogenic formation at an early stage of aortic stenosis. Only surgical and transcatheter aortic valve replacement is available, whereas the time point for surgical intervention is critical. Current clinical guidelines recommend intervention with evidence of left ventricular decompensation (Pawade et al., 2015, Goody et al., 2020, Everett et al., 2018). Important CAS risk factors such as male sex, hypertension, smoking, and increased low-density lipoprotein (LDL) are associated with a similar disease called atherosclerosis (Akat et al., 2009, Rajamannan et al., 2007). Calcification of the aortic valve is not only a passive, age-related process. It is currently described as an active process similar to atherosclerosis, sharing common characteristics. Active regulatory mechanisms, and inflammatory reactions, play a significant role during disease progression (Lerman et al., 2015, Rajamannan et al., 2011). Calcification of the aortic valve is a mostly slow-progressing disease with several clinical symptoms like abnormal heart sound or chest pain, starting with a slight asymptomatic thickening of the pocket valves, through pronounced calcifying changes to a symptomatic high-grade aortic valve stenosis (Freeman and Otto, 2005).

In detail, calcific aortic stenosis is triggered by progressive inflammatory and fibro-calcific processes regulated by circulating inflammatory and valve resident endothelial and interstitial cells. Disease progression can be subdivided into two phases (Figure 2). The initial phase comprises lipid deposition and oxidation, encouraged by injury and inflammatory immune responses. The second phase is characterized by disease progression due to osteogenic differentiation and calcification with the formation of bone-like structures (Goody et al., 2020). The cellular and molecular mechanisms of pathology are complex and still need to be fully understood. The pathophysiology of aortic stenosis comprises mechanical stress, endothelial damage, and dysfunction of valvular endothelial cells (VECs). In turn, this causes lipid accumulation and differentiation of myofibroblasts and valvular interstitial cells (VICs) into calcifying phenotypes, finally causing calcification of the aortic valve. The thickening of the valve leaflets continues and reduces the valve opening with increased blood flow velocity (Pawade et al., 2015, Goody et al., 2020, Dweck et al., 2013). In addition, infiltration of activated circulating immune cells like monocytes, $CD4^+$ as well as $CD8^+$ T-lymphocytes occur within the valve tissue and accelerate myofibroblastic and osteoblastic differentiation of valve

resident cells, inducing tissue calcification (Goody et al., 2020, Raddatz et al., 2019, Bouchareb et al., 2019).

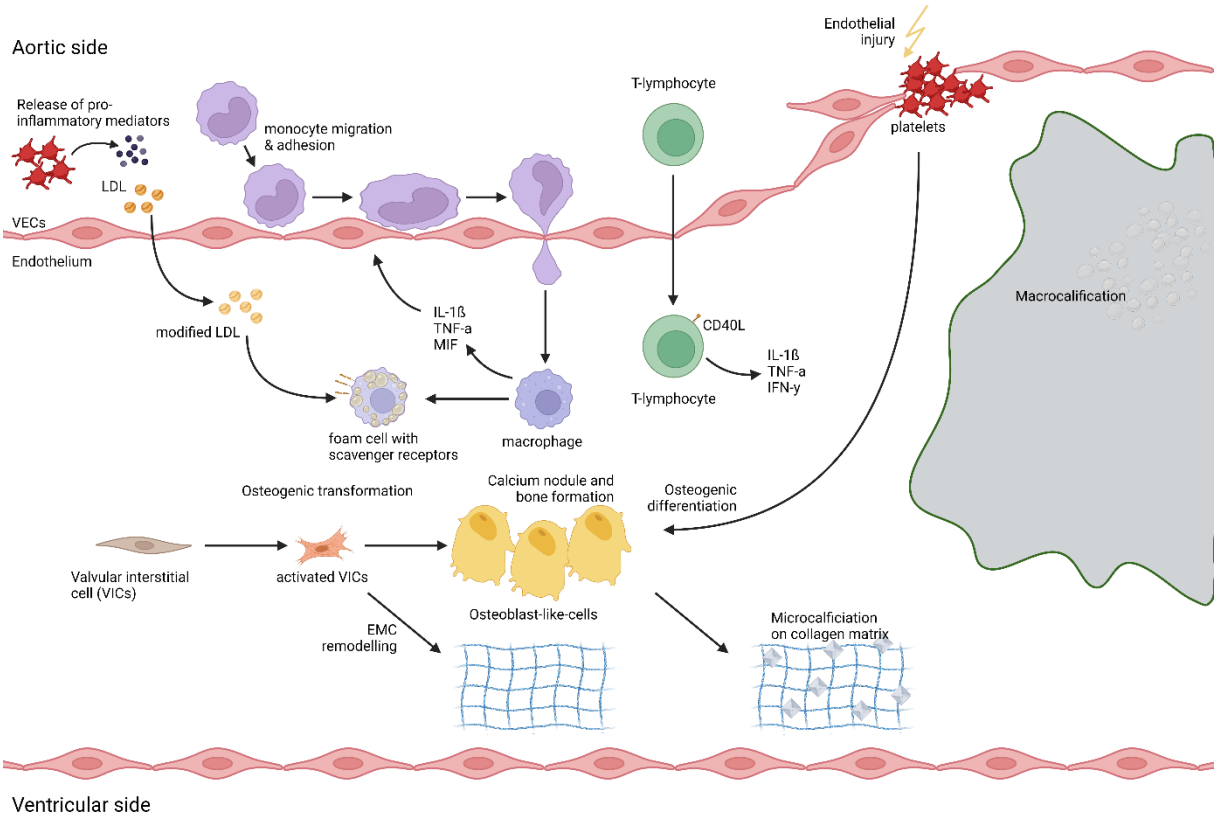

Figure 2: Inflammation and calcification processes in the aortic valve. Aortic stenosis is triggered by progressive inflammatory and fibro-calcific processes regulated by circulating inflammatory, valve resident endothelial, and interstitial cells. Disease progression can be subdivided into two phases. The initial phase comprises lipid deposition and oxidation encouraged by injury and inflammatory responses. The second phase is characterized by disease progression due to osteogenic differentiation and calcification. The pathophysiology of aortic stenosis comprises mechanical stress, endothelial damage, and dysfunction of valvular endothelial cells (VECs). In turn, this causes lipid accumulation and differentiation of myofibroblasts and valvular interstitial cells (VICs) into calcifying phenotypes, finally causing calcification of the aortic valve. In addition, infiltration occurs of activated circulating immune cells like monocytes, $CD4^+$ and $CD8^+$ T-lymphocytes into the valve tissue. Infiltration accelerates myofibroblastic and osteoblastic differentiation of valve resident cells inducing tissue calcification. In particular, monocytes differentiate into macrophages, whereas macrophages can take up modified LDL and differentiate into foam cells. Macrophages and T-lymphocytes produce pro-inflammatory cytokines and chemokines like IL-1β, TNF-α, and IFN-γ. Adapted from (Salas et al., 2012, Zheng et al., 2020a) and created with BioRender.com

The aortic valve is covered by an endothelial layer consisting of VECs on the aortic and the ventricular side (Figure 3). The aortic valve is structured into three layers: laminae fibrosa, spongiosa, and ventricularis and is composed of VICs and a complex extracellular matrix. The lamina fibrosa on the aortic side forms the most significant part of the valve with abundant type I collagen fibrils and comprises dense tissue and a few nuclear cells. The fibrosa increases stability through collagen. The lamina ventricularis can distribute radial forces during valve opening on the ventricular side due to collagen, elastin, and smooth muscle cells. The middle

of the valve forms the spongiosa, consisting mainly of connective tissue, and VICs provide the necessary flexibility for the cardiac cycle through glycosaminoglycans (Goody et al., 2020).

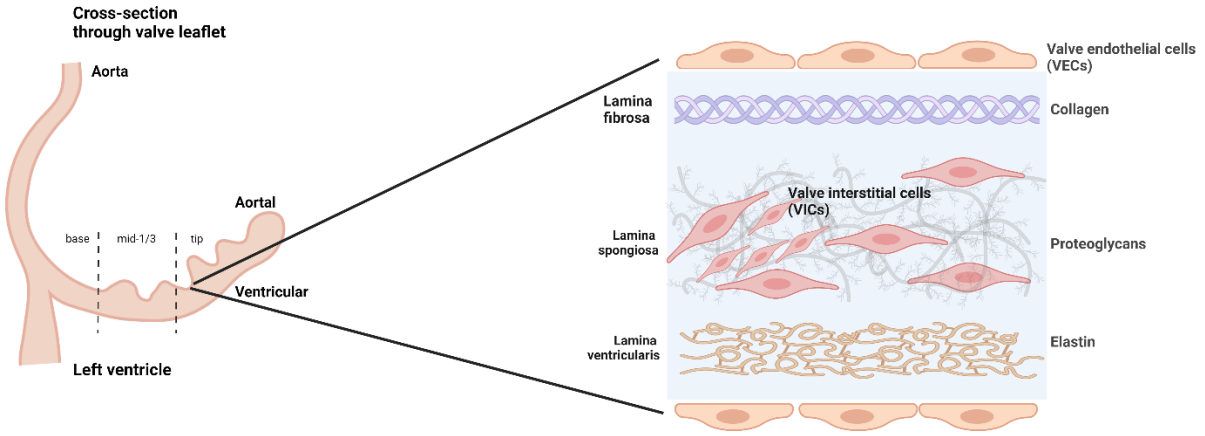

Figure 3: Structure of the aortic valve. The human aortic valve is structured into three layers, while valvular endothelial cells (VECs) cover the ventricular and aortal side. The lamina fibrosa forms the most extensive layer on the aortal side and is composed of dense tissue, a few nuclear cells, and type I collagen fibrils, increasing stability. The lamina spongiosa consists mainly of connective tissue and valvular interstitial cells (VICs) providing the necessary flexibility for the cardiac cycle through glycosaminoglycans. The lamina ventricularis is built with elastin, collagen, and smooth muscle cells. Adapted from (Rutkovskiy et al., 2017) and created with BioRender.com

1.2.1 Thrombocytes and monocytes in aortic stenosis

Studies have shown that thrombocytes, in particular thrombocyte adhesion and activation, play a critical role in local and systemic inflammation, as well as atherogenesis (Bouchareb et al., 2019, Huo et al., 2003, Massberg et al., 2002). Further, thrombocytes mediate osteogenic differentiation in aortic stenosis (Bouchareb et al., 2019). At the beginning of aortic stenosis, it has been demonstrated that the increased shear stress, developed due to turbulent flow pattern within the stenotic aortic valve, causes an elevated release of thrombin and activation of thrombocytes (Natorska et al., 2011, Bouchareb et al., 2019). The primary functions of thrombocytes are hemostasis and thrombosis, as well as vascular inflammation, particularly thrombo-inflammation. Thrombocytes can adhere to activated endothelium and contribute to the development of vascular inflammation and atheroprogression (Massberg et al., 2002). Under normal physiological conditions, thrombocytes cannot adhere to the vascular endothelium. Due to endothelium dysfunction, the endothelium gets activated and contributes to pro-thrombotic events due to transformation into a pro-inflammatory phenotype or injury of the endothelium. Endothelium dysfunction is associated with cardiovascular diseases like hypertension, CAD, chronic heart failure, DM, and severe viral infections. Endothelium activation causes thrombocytes activation, adhesion, and secretion of several inflammatory mediators like chemokines and cytokines that boost vascular inflammation and lead to the recruitment of inflammatory cells (Rajendran et al., 2013, Bakogiannis et al., 2019, Strussmann et al., 2013, Wirtz et al., 2015). Further, increased thrombocyte and decreased lymphocyte

count in blood circulation has been associated with increased cardiovascular morbidity and mortality (Iijima et al., 2007, Nikolsky et al., 2007). At the site of lesions formation and tissue injury, thrombocytes get activated and aggregate to the surface of the valve, implying that thrombocytes significantly contribute to the inflammatory processes which promote calcification and predispose the sclerotic valve to form septic thrombi (Kerrigan et al., 2002, Massberg et al., 2002). Furthermore, thrombocyte activation and subsequent modulation of innate immune cells is a critical step in host defense to facilitate bacterial clearance and prevent pathogen dissemination. However, thrombocytes also mediate the formation of septic thrombi on the surface of injured valves, most commonly caused by *Streptococci viridans* (Ribeiro et al., 2019, Kerrigan et al., 2002).

Besides the role of thrombocytes, monocytes and macrophages also execute essential functions during thrombo-inflammation. It is already known that monocyte subsets have different roles in heart failure, stroke, pathogenesis, and the outcome of acute coronary syndromes (Shantsila et al., 2011, Woollard and Geissmann, 2010). Like thrombocytes, monocytes rapidly infiltrate inflamed tissue and differentiate into macrophages, monocyte-derived dendritic cells, or remain monocytes. Monocyte subsets perform different functions. For example, non-classical monocytes patrol the endothelial surface in the presence of oxidized LDL and contribute to endothelial integrity (Marcovecchio et al., 2017, Yang et al., 2014, Zernecke et al., 2020). Further, monocytes secrete cytokines and chemokines, resulting in the migration of other immune cells, differentiation into foam cells, formation of local inflammation, and fibrotic and calcifying nodules (Wirtz et al., 2015, Zernecke et al., 2020, Pawade et al., 2015, Badimon and Vilahur, 2014, Zernecke and Weber, 2005). The interaction of thrombocytes and monocytes may lead to pro-inflammatory events, causing calcification in response to endothelial signals (Kral et al., 2016, Nording et al., 2015, Pawade et al., 2015).

Thrombocytes and monocytes express inflammatory and antimicrobial active chemokines and cytokines within the affected aortic valves, influencing the valve's local inflammation and defense reaction. The secreted chemokines and cytokines have an impact on the recruitment of monocytes, the osteoblastic transformation, and the synthesis of connective tissue in inflamed aortic valves (Bartoli-Leonard et al., 2021, Zernecke and Weber, 2005, Kang et al., 2021, Yeaman, 2014, von Hundelshausen and Schmitt, 2014). Many studies show that the development of aortic stenosis is driven by the local inflammatory responses followed by calcification and osteogenic differentiation of the valvular cells (Lindman et al., 2016). In summary, activated thrombocytes mediate a pro-inflammatory, pro-atherosclerotic, and pro-osteogenic response in the inflamed valve, thus, triggering disease progression (Bouchareb et al., 2019). However, the exact pathomechanism and significance of the pro-inflammatory and pro-atherosclerotic factors in developing aortic valve disease have not yet been investigated.

1.2.2 Cytokines and chemokines in aortic stenosis

Cytokines play a critical role during immune responses as a second messenger. They are small secreted proteins produced by different immune cells affecting specific interactions and communications between cells, cell growth and differentiation. Typically, cytokines are produced in a cascade, meaning one cytokine stimulates the target cell resulting in additional cytokine production (Zhang and An, 2007). According to their function during inflammation, cytokines can be divided into pro- and anti-inflammatory cytokines like the interleukins IL-1β and IL-10, respectively (Kany et al., 2019). A subgroup of cytokines represents the chemokines that induce chemotaxis of leukocytic cell types in their soluble phase. Besides this, it is known that chemokines can be transported and presented by endothelial surfaces, triggering integrin-mediated arrest of rolling leukocytes (Laudanna and Alon, 2006).

Potent inflammatory mediators of interest are the chemokines CXCL12 and CXCL14 and the chemokine-like macrophage migration inhibitory factor (MIF), which regulate the function and activation of circulatory inflammatory cells, including monocytes, macrophages, and bone marrow-derived progenitor cells and modulate thrombocytes survival and thrombotic potential (Witte et al., 2021, Chatterjee et al., 2014, Chatterjee and Geisler, 2016, Chatterjee et al., 2015). Several studies have demonstrated that thrombocytes intracellularly store CXCL12, CXCL14, and MIF and secrete large amounts of these chemokines after activation (Chatterjee et al., 2014, Chatterjee et al., 2015, Witte et al., 2017). Thrombocyte activation and accumulation are essential triggers for chemotaxis, migration, and differentiation of monocytes, which play a critical role in thrombus inflammation (Kral et al., 2016, Koupenova et al., 2018, Colling et al., 2021).

The chemokine CXCL14 may play a role in the context of atherosclerosis since its mRNA showed increased values in the left descending coronary artery. Atherosclerosis and CAS share several similarities regarding symptoms and pathomechanism. Thus, CXCL14 might also influence the progression of CAS. Furthermore, leukocytes, in particular monocytes and B-lymphocytes, showed CXCL14 expression. In addition, CXCL14 might have a regulatory function on CXCL12-mediated CXCR4 signaling during the absence of CXCL12. However, this topic is in discussion and requires further investigation (Lu et al., 2016).

Another thrombocyte-derived chemokine is the stromal cell-derived factor1a (CXCL12/SDF-1a), promoting leukocyte and progenitor cell recruitment and adhesion to injured and inflamed tissues, implying an essential role in the initiation of vascular remodeling. CXCL12 is highly expressed in atherosclerotic lesions and associated with acute coronary syndrome (Gao et al., 2019, Massberg et al., 2006, Wurster et al., 2013). Furthermore, it was shown that thrombocyte expression of CXCL12 correlates with the severity of aortic valve stenosis in affected patients

(Wurster et al., 2014). CXCR7 regulates CXCL12/CXCR4 pathway due to heterodimerization with CXCL12 or scavenging (Hughes and Nibbs, 2018). This observation is confirmed when considering the binding affinity for CXCL12 to CXCR7, which is higher than CXCR4. CXCR7 is expressed and exposed on the surface of monocytes. Upon binding of CXCL12, the receptor may be internalized. Among other things, CXCL12 appears to be upregulated during inflammation, recruits immune cells, and monitors and regulate immune development by promoting the differentiation of T-lymphocytes towards a regulatory phenotype (Sanchez-Martin et al., 2013). Other studies verified abnormal high amounts of CXCL12 in atherosclerosis lesions in comparison to healthy vessels ascribing a lesion-protective role for CXCL12 (van der Vorst et al., 2015). Furthermore, it has been shown that the phagocytosis of apoptotic thrombocytes by monocytes and macrophages was facilitated by CXCL12, promoting foam cell formation due to the monocytic expression of CXCR4 and CXCR7 (Chatterjee et al., 2015). CXCR7 is required for heart valve development, qualifying this receptor for further investigation in the context of CAS. The chemokine receptor CXCR4 shows expression among all leukocytes (Rich, 2019). Upon exposure to MIF, CXCR4 expressing cells showed enhanced migration (Hughes and Nibbs, 2018).

MIF is a pleiotropic pro-inflammatory cytokine with chemokine-like functions and is implicated in several acute and chronic inflammatory diseases, autoimmune diseases, cardiovascular diseases, and atherogenesis (Zernecke et al., 2008, Muller et al., 2014b, Morand et al., 2006). Further studies showed that thrombocytes pre-store MIF, secreted upon thrombocyte activation, and play a functional role in leukocyte activation (Strussmann et al., 2013, Bernhagen et al., 2007, Wirtz et al., 2015). MIF functions as a pro-atherogenic factor and interacts with the chemokine receptors CXCR2 and CXCR4, promoting atherogenic monocyte adhesion, migration, differentiation, and survival, as well as leukocyte arrest on aortic endothelium (Bernhagen et al., 2007, Cheng et al., 2010, Muller et al., 2014a). Further, it was shown that in LDLR-deficient mice, deficiency of MIF reduces atherogenesis (Pan et al., 2004). A recent study could observe that MIF plasma levels are related to all-cause mortality and cardiovascular events in patients with acute myocardial infarction (Zhao et al., 2019). Further, MIF was associated with a pro-inflammatory and pro-atherosclerotic role in patients with CAD and myocardial infarction. Thus, MIF might play a critical role in thrombo-inflammation during valve calcification (van der Vorst et al., 2015).

2 Aim of this work

The discovery and development of new diagnostic and therapeutic approaches are critical steps in the fight against diseases, especially when their current treatments are inadequate. Thus, my thesis aims the analyzation of important immune cells and inflammatory mediators during SARS-CoV-2 infection and cardiovascular diseases to increase the knowledge about disease pathology and progression and finally to find new targets for diagnostic and therapeutic approaches.

The first part of the thesis addresses the ongoing pandemic of the SARS-CoV-2 virus. SARS-CoV-2 is responsible for more than 640,395,651 cases and over 6,618,579 deaths worldwide (WHO, 2022). The SARS-CoV-2 infection is responsible for several concomitants, including severe thrombotic events, systemic inflammation, changes in hemostasis, and coagulation. Primary, the lung is affected regarding thrombi formation, but the brain, heart, kidney, and liver are also highly perceptible. Clinical cardiovascular complications are highly occurring in hospitalized COVID-19 patients like venous thromboembolism, acute heart failure, cardiogenic shock, arrhythmias, acute stroke, arterial thrombosis, and myocarditis. Patients with cardiovascular diseases have an increased risk of developing a SARS-CoV-2 infection with a severe prognosis comprising life-threatening lung and heart injury (Huang et al., 2020a, Lamers and Haagmans, 2022, Giacca, 2022). Thus, it is significant to study immune responses during SARS-CoV-2 infection and to increase the knowledge about the pathology of COVID-19. This work aimed to address the following questions:

1. How are the phenotype and activation of thrombocytes altered in patients with pre-existing CAD and acute SARS-CoV-2 infection? What is the role of furin and its association with the severity of disease progression?
2. Is the function and phenotype of circulating monocytes altered during acute SARS-CoV-2 infection? Have circulating monocytes a prognostic role in patients with CAD and an increased risk for severe complications comprising life-threatening heart and lung injury upon SARS-CoV-2 infection?
3. How is the monocyte phenotype and function altered in SARS-CoV-2 infected patients after a three months follow-up?

The second part of the thesis aims to gain insight into the critical role of thrombocytes and monocytes in calcific aortic stenosis. Aortic valve stenosis represents the most prevalent valve disease in western countries, particularly in the aging population (Osnabrugge et al., 2013, Nkomo et al., 2006). The aortic valve is affected by accelerating inflammation, fibrotic and calcific remodeling of the valve leaflets, thickening, and osteogenic formation, leading to valve obstruction. Until now, no pharmaceutical strategies are available to prevent inflammation, calcification, and fibrotic and osteogenic formation at an early stage of aortic stenosis (Goody et al., 2020, Everett et al., 2018). The aim of this work was to address the following question:

1. Do thrombocytes, thrombocyte-derived mediators, and thrombocyte-monocyte interactions impact the acceleration of local valvular inflammation and mineralization?

3 General Results and Discussion

The overall aim of my thesis was to characterize phenotypes of immune cells, such as peripheral circulating monocytes and thrombocytes, in patients with cardiovascular diseases and acute SARS-CoV-2 infection. The focus of our studies was to contribute and increase the knowledge about the pathology, immune responses, and disease progression of infection with the SARS-CoV-2 virus affecting the whole world population. In particular, we analyzed several plasma inflammatory mediators and the function and activation of circulating monocytes and thrombocytes during acute infection and after three months of recovery in patients with pre-existing cardiovascular diseases.

Furthermore, we analyzed the phenotypes of monocytes and thrombocytes and inflammatory mediators in patients with severe calcific aortic valve stenosis. Calcific aortic valve stenosis remains the most frequent heart valve disease in western countries, particularly in the aging population (Osnabrugge et al., 2013, Nkomo et al., 2006). The mechanisms of disease pathology of aortic stenosis are not fully understood. Currently, the only treatment option of patients is to replace the aortic valve upon the onset of severe symptoms (Goody et al., 2020, Everett et al., 2018). Therefore, the aim was to investigate molecular mechanisms, disease pathology, and the role of monocytes and thrombocytes in patients with severe aortic stenosis. Getting more insights and knowledge about the involved immune cells and inflammatory mediators, which may play a critical role during disease progression, will give us new perspectives for further therapeutically and diagnostical targets.

3.1 High plasma levels of furin predict severe clinical outcome in CAD infected SARS-CoV-2 patients

We characterized immune cells and critical inflammatory mediators during the first wave of the SARS-CoV-2 pandemic in 2020. We focused on the role of thrombocytes and plasma furin levels in acute SARS-CoV-2 infected patients with pre-existing CAD. We included CAD patients with and without SARS-CoV-2 infection and healthy controls in our cohort. The aim was to investigate how thrombocytes' function and activation status differ between uninfected CAD patients and CAD patients upon SARS-CoV-2 infection (Langnau et al., 2021). We concentrated, particularly on CAD patients, because they have an increased risk for respiratory failure and cardiac death. SARS-CoV-2 infection is characterized by pro-inflammatory and pro-thrombotic events causing in CAD patients acute coronary syndrome with subsequent impairment of left or right ventricular function (Task Force for the management of, 2022, Xiong et al., 2020).

Our flow cytometry data represented that CAD patients infected with SARS-CoV-2 are characterized by a significantly high number of peripheral thrombocytes and increased activation of thrombocytes, indicated by an increased CD62P surface expression, compared to uninfected CAD patients. We defined thrombocyte/leukocyte aggregates as $CD42b^+CD61^+$ aggregates and demonstrated an increased frequency and activation status in infected CAD patients. Flow cytometry imaging analysis revealed that $CD14^+$ monocytes adhere to thrombocytes and form aggregates (Langnau et al., 2021). We focused on circulating thrombocytes because thrombocytes have been studied not only regarding thrombosis. They are also key mediators of inflammation and thrombo-immunity. The role of thrombocytes in vascular biology has been studied because of their association with myocardial infarction, stroke, and venous thromboembolism. Thrombocytes can interact with the vessel wall but can also induce changes in the vessel wall environment affecting other immune cells (Morrell et al., 2014, Koupenova et al., 2018).

Further, thrombocytes release various potent cytokines or chemokines upon microbial infection (Yeaman, 2010, Maouia et al., 2020) and associate with leukocytes and endothelial cells, promoting vascular and tissue inflammation (Dib et al., 2020, Li et al., 2020). The literature already characterized virus infections by thrombocytopenia, thrombocyte hyperactive-reactivity, and aggregation of thrombocytes with leukocytes (Raadsen et al., 2021, Hottz et al., 2018, Rapkiewicz et al., 2020). Critically ill patients showed decreased thrombocyte count and leukocytosis with an increased risk of high mortality following SARS-CoV-2 infection (Bao et al., 2020, Yang et al., 2020a). Further, enhanced thrombocyte apoptosis has been observed in COVID-19 patients who required ICU treatment (Althaus K, 2020), as well as extensive thrombocyte and neutrophil activation (Nicolai et al., 2020). Our data support and amplify the current knowledge that thrombocyte activation occurs directly at the beginning of SARS-CoV-2 infection as soon as the infection is confirmed by PCR and not only in progressive SARS-CoV-2 infection (Langnau et al., 2021).

Our data indicate that circulating thrombocytes have a pro-thrombotic role during the systemic thrombo-inflammation named hyper-inflammation, directly at the beginning of infection (Langnau et al., 2021). Studies confirm the importance of controlling the disease progression of SARS-CoV-2 infection at an early stage of infection for preventing a systemic thrombi-inflammation and cytokine storm (Xie et al., 2020, Xiong et al., 2020, Nishiga et al., 2020, Leblond et al., 2006). Other studies already demonstrated a relationship between an acute SARS-CoV-2 infection with altered thrombocytes activation, increased number of circulating aggregates of thrombocytes with leukocytes, and characteristic coagulopathy. In turn, this causes thrombotic complications such as pulmonary embolism, deep vein thrombosis, and arrhythmia (Guzik et al., 2020, Connors and Levy, 2020, Zaid et al., 2020, Manne et al., 2020). Another study showed that elevated thrombocyte activation and thrombocyte/leukocyte co-

aggregates were related to a severe clinical prognosis of patients with COVID-19 (Hottz et al., 2020). Interestingly, high thrombocyte activity and aggregation of thrombocytes with leukocytes or monocytes can be found in CAD patients affecting the stability of CAD and can be used as a biomarker throughout atheroprogression as well as for monocyte inflammation in cardiovascular diseases (Allen et al., 2019, Linden et al., 2007, Furman et al., 1998, Brambilla et al., 2008). Additionally, another cardiovascular disease such as acute coronary syndrome, is promoted by hyper-reactivity of thrombocytes (Martin et al., 2012), and COVID-19 may be associated with myocardial injury and a worsened outcome in COVID-19 patients (Bonow et al., 2020, Guo et al., 2020). As already mentioned, patients with cardiac predispositions have an increased risk for severe clinical outcomes and increased mortality due to COVID-19 (Rath et al., 2020, Clerkin et al., 2020, Inciardi et al., 2020). Another critical factor during COVID-19 disease are pro-thrombotic complications (Connors and Levy, 2020). A microcirculatory arrest may increase the risk in SARS-CoV-2 infected patients for thromboses such as pulmonary embolism and deep vein thrombosis, emphasizing the critical role of thrombocytes during SARS-CoV-2 infection (Poissy et al., 2020, Lax et al., 2020).

Various studies demonstrated that uncontrolled hyper-inflammation upon SARS-CoV-2 infection increased the risk of developing severe complications like multiple organ failure, progressive respiratory failure, and death (Jose and Manuel, 2020, Guzik et al., 2020). To analyze the hyper-inflammation in our cohort, we performed different LegendPlex analyses to measure cytokine and chemokine concentrations in patient plasma. CAD-SARS-CoV-2^{positive} patients demonstrated significantly increased concentrations of plasma IFN-γ, IL-1β, CCL2, and CXCL8-10 (Langnau et al., 2021). Our results are in line with the current literature showing that a highly increased expression of cytokines may result in severe cytokine release syndrome, which increases the severity of the disease even more (Hsu et al., 2022). In particular, IL-1β is a pro-inflammatory cytokine associated with infection and inflammation. During SARS-CoV-2, IL-1β gets activated, causing the activation of other pro-inflammatory cytokines, including IL-6 and TNF-α. IL-1β is further associated with hypercoagulation, disseminated intravascular coagulation, and regarding COVID-19 patients, with a severe clinical outcome (Hsu et al., 2022). Additionally, current studies demonstrated that the chemokines CXCL8, CCL2, and CCL8 function as infiltration signals of the lung and mediate the recruitment of mononuclear phagocytes to SARS-CoV-2 infected lung tissue (Hsu et al., 2022).

Interestingly, the plasma concentration of the subtilisin-like proprotein convertase furin was significantly increased in CAD-SARS-CoV-2^{positive} patients compared to CAD-SARS-CoV-2^{negative} patients and healthy controls (Langnau et al., 2021). Furin is associated with essential functions during complement system and in the blood-clotting, as well as in the cleavage of bacterial exotoxins, viral-envelope glycoproteins, and membrane receptors due to the

regulation of a variety of physiological functions (Nakayama, 1997). Most importantly, furin enables viral attachment of SARS-CoV-2 (Coutard et al., 2020, Hoffmann et al., 2020b, Walls et al., 2020, Shang et al., 2020). In detail, furin is able to cleave the S glycoprotein into its subunits S1 and S2 within the Golgi apparatus during biosynthesis and maturation in the infected cell (Hoffmann et al., 2020a, Shang et al., 2020, Jackson et al., 2022). Further, furin plays a critical role in cardiovascular disease, for example, in CAD and DM, a cardiovascular risk factor. Furin plasma levels have been further investigated in patients with acute myocardial infarction showing a relation to all-cause mortality and cardiovascular events (Yakala et al., 2019, Wang et al., 2020, Fernandez et al., 2018). In atherosclerotic plaques, furin expression was observed mainly in macrophages. Variants of furin were identified and are associated with CAD, and their differential expression levels affect the behavior of monocytes and macrophages (Stawowy et al., 2005, Yang et al., 2020b, Zhao et al., 2018, Yakala et al., 2019). These data demonstrate that furin is crucial for SARS-CoV-2 attachment on the host cell membrane and indicates an association with CAD. Thus, we further focused on furin in more detail and studied whether furin levels are associated with a severe course during infection characterized by required ICU treatment. CAD-SARS-CoV-2^{positive} patients who required ICU treatment showed increased levels of plasma furin compared to patients without ICU treatment. Therefore, elevated furin plasma concentrations can be used as an initial biomarker for progressive respiratory failure and required ICU treatment at hospital admission. Our volcano plot analysis confirmed an increased plasma concentration of furin in CAD-SARS-CoV-2^{positive} patients (Langnau et al., 2021).

Furthermore, correlation analysis displays that thrombocyte activation correlated with plasma levels of CCL5, an outstanding thrombocyte chemokine released upon activation. The number of circulating CD42b^{+}CD61^{+} thrombocyte/leukocyte aggregates correlated with enhanced IL-6 and the chemokines CCL2 and CXCL10, implying thrombocyte activation and interaction with leukocytes contribute to hyper-inflammation (Langnau et al., 2021).

We found that plasma furin levels are significantly increased in CAD-SARS-CoV-2^{positive} patients, in particular CAD-SARS-CoV-2^{positive} patients who required ICU treatment, indicating an association of increased plasma furin with a severe clinical course during SARS-CoV-2 infection. Therefore, Kaplan-Meier analyses were performed to determine whether plasma furin levels predict a severe clinical prognosis in SARS-CoV-2 infected CAD patients. As the clinical endpoint, we defined the appearance of a HI <200mmHg, and mechanical ventilation after 60 days. After the calculation of the median of furin (0.064 ng/ml), we observed that furin levels above the calculated median were associated with an adverse clinical outcome. Calculations show that significantly more CAD-SARS-CoV-2^{positive} patients with a furin level above the median had a worse clinical prognosis due to a HI <200mmHg, and mechanical ventilation after 60 days (Langnau et al., 2021).

Due to the association of thrombocytes-derived inflammatory mediators and their impact on atheroprogression and thrombo-inflammation, we next analyzed whether furin can be stored in thrombocytes. Our immunofluorescence staining showed that furin is highly stored in thrombocytes and expressed on the thrombocyte surface upon activation with several mediators (Langnau et al., 2021). Studies implicate that furin might cleave the SARS-CoV-2 spike protein implying an essential role during the virus entry process. Thus, furin may be a therapeutic target (Coutard et al., 2020, Hoffmann et al., 2020b, Cheng et al., 2020). Another study confirmed our data showing that thrombocytes can contain significant amounts of furin (Leblond et al., 2006).

Limitations of our study are that our study is rather an observational or hypothesis-generating study. For example, no causalities or conclusions about therapeutic options are possible. Additionally, further experiments are required to analyze the association of platelet activation and furin expression and its impact on severe clinical outcomes in more detail. Further studies and increased patient cohort are needed to show whether patients with increased furin plasma levels show differences in their disease outcome, clinical symptoms, comorbidities, and courses of the disease. In addition, it would be interesting to know, since platelets store and release amounts of furin upon activation, whether platelets play a critical role during virus entry and cleavage similar to furin. An advantage of an observational study is that correlations can be analyzed between important factors. In our case, we analyzed correlations between furin plasma levels and clinical parameters related to a severe clinical outcome. Further, we observed correlations between plasma levels of pro-inflammatory cytokines and activation of platelets or platelet/leukocyte aggregates. Other strengths of our study are the straightforward approach of measuring furin plasma levels in patients directly after hospital admission. Elevated furin plasma levels may predict a severe clinical outcome or course of patients infected with SARS-CoV-2. Measuring the plasma levels by ELISA would be easily implementable tool in standard diagnostic tests (Langnau et al., 2021).

Though we could not confirm that thrombocyte-derived furin is associated with SARS-CoV-2 activation, we can presume that activated thrombocytes facilitate tissue and vascular inflammation and may contribute to replication and cell fusion. Antithrombotic therapeutics which reduce thrombocyte release might be manageable and efficient prevention for severe clinical outcomes and thromboembolic events.

3.2 Reduction of non-classical monocytes is characteristic for CAD infected SARS-CoV-2 patients

We analyzed circulating peripheral monocytes in patients with a cardiac predisposition for SARS-CoV-2 infection directly at the beginning of the pandemic. In our study, we included

patients with and without acute SARS-CoV-2 infection and the underlying health condition CAD and healthy controls (Mueller et al., 2021). Our study focused on patients with CAD because they have an increased risk for progressive lung and heart failure following SARS-CoV-2 infection. Patients with chronic cardiovascular disease may become unstable due to an imbalance between the metabolic demand of infectious disease and reduced heart function. In particular, CAD patients have an increased risk for coronary plaque rupture caused by virus-induced systemic inflammation (Task Force for the management of, 2022, Xiong et al., 2020). Thus, the aim was to analyze the prognostic impact of monocyte subsets in a risk evaluation of patients with CAD and SARS-CoV-2 infection.

Interestingly, we found a significantly reduced number of non-classical monocytes in CAD+SARS-CoV-2 patients in comparison to healthy controls and CAD patients without infection. Similar to this, we observed a significant reduction of classical monocytes in CAD+SARS-CoV-2 patients compared to healthy controls. However, the number of intermediate monocytes was not altered between the groups (Mueller et al., 2021). Our results are in line with other publications, showing a reduced number of total monocytes in hospitalized patients because of SARS-CoV-2 infection in comparison to healthy controls (Qin et al., 2020). Another study demonstrates a reduction of intermediate and non-classical monocytes in patients with severe progression of SARS-CoV-2 infection (Knoll et al., 2021, Gatti et al., 2020). Further, a study showed an association between a reduced number of CD16 negative monocytes and patients who required ICU treatment (Vasse et al., 2021).

In order to analyze whether the reduction of non-classical monocytes is related to a severe course during infection, we stratified CAD+SARS-CoV-2 patients dependent on ICU treatment into ICU and non-ICU. CAD+SARS-CoV-2 patients who required ICU treatment showed a significant reduction of non-classical monocytes compared to non-ICU patients. No differences in monocyte number were observed for intermediate and classical monocytes. Furthermore, CAD+SARS-CoV-2 patients admitted to ICU were stratified depending on their Horovitz Index (HI). Progressive respiratory failure and required mechanical ventilation were specified by ICU+HI≤200mmHg. Non-classical monocytes were significantly decreased in ICU+HI≤200mmHg patient group compared to ICU+HI>200mmHg patients. A similar reduction was observed in ICU+HI≤200mmHg patients for intermediate monocytes. These results demonstrate that especially patients with progressive respiratory failure and who require mechanical ventilation have a significant reduction of non-classical monocytes, indicating an association between the number of non-classical monocytes and a reduced clinical outcome upon SARS-CoV-2 infection (Mueller et al., 2021).

In order to analyze whether the function of monocytes is impaired or altered, several activation, migration, and T cell activation markers on the monocyte surface were analyzed. CD54,

CD62L, and CD80 were significantly increased in non-classical monocytes in CAD patients compared to CAD+SARS-CoV-2 patients and healthy controls. Further, expression of CD62L was less in patients with ICU treatment and HI<200mmHg, while CD54 and CD80 surface expression levels show no differences. CX3CR1 expression was significantly reduced in non-classical monocytes in CAD+SARS-CoV-2 patients. Further, we observed a CX3CR1 reduction in patients with HI<200mmHg. In contrast, no differential expression between CAD and CAD+SARS-CoV-2 patients could be observed for HLA-DR, while HLA-DR expression was significantly increased in healthy controls. Our data indicate an altered migration behavior and T cell activation function of the residual non-classical monocytes in the bloodstream. This observation is surprising because we would expect an increased expression of migration and activation markers on the surface of non-classical monocytes upon virus infection (Mueller et al., 2021). Various studies showed that SARS-CoV-2 infection results in a cytokine storm due to the increased release of pro-inflammatory cytokines. This cytokine storm should increase the expression of activation and migration markers on the surface of monocytes. Thereby monocytes were able to migrate to infected or inflamed tissue and fight against invading pathogens (Shi and Pamer, 2011). An explanation for our observation of a decreased cell number could be an increased infiltration of non-classical monocytes via CD62L and CX3CR1 (Fang et al., 2018) into the inflamed heart and lung tissue.

In order to confirm our hypothesis of an infiltration of monocytes into the lung and heart, we analyzed immunohistochemistry staining of lung and heart tissue of CAD patients with and without SARS-CoV-2 infection. We observed different expressions of $CD14^+$ and $CD16^+$ monocytes and $CD68^+$ macrophages, which infiltrated the myocardium in CAD+SARS-CoV-2 patients in comparison to control and CAD patients. In detail, we observed a significantly higher number of $CD14^+$, $CD16^+$, and $CD68^+$ inflammatory immune cells in CAD+SARS-CoV-2 in comparison to control and CAD patients without infection. Similar results were observed in the lung tissue of CAD+SARS-CoV-2 patients. In summary, we observed an infiltration of high numbers of inflammatory cells like $CD68^+$ macrophages, $CD14^+$, and $CD16^+$ monocytes into the lung and heart tissue in CAD patients with SARS-CoV-2 (Mueller et al., 2021). These findings assume that classical and non-classical monocytes, as well as macrophages, migrate to inflamed myocardial tissue and promote local inflammation in SARS-CoV-2 associated myocarditis, which would explain our observation of the reduced number of non-classical monocytes in peripheral blood (Knoll et al., 2021, Sanchez-Cerrillo et al., 2020, Mueller et al., 2021). Another study showed that CAD patients have elevated cell numbers and activation status of non-classical monocytes (Thomas et al., 2015, Huang et al., 2012). Therefore, it is more surprising that CAD+SARS-CoV-2 patients show significantly reduced cell numbers and activation markers. We assume that non-classical monocytes migrate into the inflamed lung and heart tissue in order to boost and sustain local inflammation and tissue damage. Our

results are in line with other studies showing that monocytes migrate into inflamed tissue caused by viral infections to boost antimicrobial immune responses against invading pathogens (Shi and Pamer, 2011). In addition, inflammatory monocytes migrate into the inflamed lung during SARS-CoV-2 infection and differentiate into pulmonary macrophages, contributing to tissue damage (Knoll et al., 2021).

Next, Kaplan-Meier curves were performed to identify diagnostic markers for CAD patients infected with SARS-CoV-2. The clinical endpoint was specified as the appearance of a Horovitz index ≤200 mmHg specifying progressive respiratory failure and mechanical ventilation after a follow-up of 30 days. Based on the calculated median (median 1443 cells/ml) of non-classical monocytes, CAD+SARS-CoV-2 patients were stratified into two groups. Results show that patients with a cell count below the calculated median attained the clinical EP significantly more often. 41.7% of ICU+HI>200mmHg patients had a cell count below the median, in contrast to 81.8% of ICU+HI<200mmHg patients indicating rapid failure. Cox regression analysis predicts non-classical monocyte cell count as the only predictor for the primary endpoint pointed as the appearance of progressive respiratory failure. Cox regression includes the pre-defined confounding factors: oral anticoagulation, gender, and age. Thus, determination of the non-classical monocyte number would be an easy, additional, and new tool that would improve an early diagnosis of SARS-CoV-2 infection and may predict a worse outcome of infection (Mueller et al., 2021).

Limitations of our study are that our study is rather an observational or hypothesis-generating study. No causalities or conclusions about therapeutic options are possible. Additionally, further experiments are required to analyze the mechanism of decreased number of non-classical monocytes. It is important to investigate the exact pathological mechanisms in order to achieve diagnostic and therapeutic goals as quickly as possible. Furthermore, the patient's number should be increased in order to include more patients with adverse clinical events like myocardial infarction, stroke or death. It would be interesting to analyze whether the number of non-classical monocytes is associated to severe clinical events. An advantage of an observational study is that correlations can be analyzed between important factors. We observed a decreased number of non-classical monocytes in CAD infected patients compared to patients without SARS-CoV-2 infection. Our study demonstrated that a decreased number of non-classical monocytes is related to rapidly progressive respiratory failure and changed phenotype of monocyte subsets in CAD infected patients. Our results imply a critical role of non-classical monocytes in patients with a severe clinical outcome. Measuring of monocyte number directly at the beginning of hospital admission would be an easy tool to detect patients at risk for a worsen clinical course (Mueller et al., 2021).

3.3 MIF is highly increased in patients after recovery of SARS-CoV-2 infection

The worldwide pandemic of SARS-CoV-2 has affected the population in many ways. The current research mainly focused on acute infection and its pathology, but more and more studies demonstrate the long-term consequences after SARS-CoV-2 infection. In order to analyze these long-term COVID-19 consequences in more detail, we included patients at cardiovascular risk or who were diagnosed with cardiovascular diseases and acute SARS-CoV-2 infection in our cohort. These patients were further analyzed during a follow-up of three months post-infection, and healthy participants were included as a control group. We compared the patient groups regarding subgroups of peripheral circulating monocytes and plasma chemokine profiling to analyze whether the acute inflammation and phenotyping of monocytes are altered after a recovery phase of three months (Langnau et al., 2022). In a previous study with the same patient cohort, we already showed that non-classical monocytes are significantly reduced in SARS-CoV-2 infected patients in comparison to healthy controls and CVD patients without infection. Further, rapidly progressive respiratory failure was associated with the reduction of non-classical monocytes because of inflamed lung and heart tissue (Mueller et al., 2021).

Characterizing COVID-19 patients after a follow-up of three months, we observed an increased white blood cell count by trend as well as an increased thrombocyte count compared to patients during the acute infection (Langnau et al., 2022). Interestingly, in line with our previous study, non-classical monocytes were significantly decreased in acutely infected patients. In contrast, after a recovery phase of three months, the cell count of non-classical monocytes almost matches that of healthy controls. After a three month recovery, we could observe a similar increase for circulating classical monocytes, while intermediate monocytes showed no differences (Langnau et al., 2022). The infectious disease COVID-19 has affected the population worldwide during the last 2 ½ years. Scientific research has taken much effort to analyze the underlying pathology and disease progression in SARS-CoV-2 infected patients. One important problem during COVID-19 is the uncontrolled systemic hyper-inflammation which is also related to organ failure, microcirculatory dysfunction, and respiratory stress syndrome (Jose and Manuel, 2020, Giacca, 2022). Previously, we showed that non-classical monocytes are significantly reduced and functionally altered in CVD-infected patients compared to controls. Further, the reduced number of non-classical monocytes is associated with a severe clinical outcome with respiratory failure upon infection (Mueller et al., 2021, Chilunda et al., 2021, Degauque et al., 2021). Our data indicate that monocytes are essential during organ dysfunction and respiratory distress in COVID-19 patients (Langnau et al., 2022).

Going into more detail, we analyzed the function of monocytes by surface marker expression, which are important for T-cell activation, migration, and adhesion (Langnau et al., 2022). Previously, we observed an impaired function and activation potential of peripheral monocytes in patients with severe acute SARS-CoV-2 infection and pre-existing CVD compared to uninfected CVD patients (Mueller et al., 2021). We demonstrated a significant increase in activation marker CD11b expression on all three monocyte subsets in patients during the acute infection, in the current study. The adhesion marker CD11a was enhanced on classical and intermediate monocytes during acute infection compared to patients in the recovery phase. Non-classical monocytes only showed a reduction by trend in the follow-up phase compared to healthy controls and acutely infected patients. Our results imply monocytes' altered adhesion, activation, and migration function during a severe acute SARS-CoV-2 infection (Langnau et al., 2022). Further, the surface expression of CCR2 was analyzed, important for mediating monocyte migration and ACKR2/CXCL12, inducing chemokine-dependent cell survival. CCR2 is significantly increased in classical and non-classical monocytes in healthy controls and acutely infected patients compared to patients during the recovery phase, indicating an impaired migration property. In contrast, intermediate monocytes showed a significantly increased CCR2 expression in patients during the acute infection. The CXCL12 receptor ACKR3 shows a similar surface expression on all three monocyte subsets in acute and recovered patients in contrast to healthy controls showing a significantly decreased expression. Our data imply an altered adhesion, migration, chemotaxis, and B/T cell activation of monocyte subsets during acute SARS-CoV-2 infection, at least in parts, after a recovery phase of three months. In contrast, not all surface marker adapts to a level of healthy controls after a three-month recovery (Langnau et al., 2022).

For a deeper characterization of monocyte subsets, we performed unsupervised data analysis using "uniform manifold approximation and projection (UMAP) (Leland McInnes, 2020) dimension reduction of gated monocytes to group phenotypically similar events". PhenoGraph (Levine et al., 2015) clustering analysis was performed to study monocyte marker profiles and clustering changes. Equivalent to our manual gating strategy, we observed an increased surface expression of activation and migration marker CCR2 and CD11a in the clusters MT23, MT17, and MT14 during the acute infection. Unsupervised clustering with PhenoGraph of the monocyte chemokine receptor flow cytometry panel results in 28 clusters (MT01-MT28). All clusters showed significant differences in frequency between acutely infected and recovered patients. Cluster MT03 and MT24 demonstrate an elevated intracellular expression of CXCL12, while CXCL14 is reduced in patients during the acute infection compared to a recovery phase of three months. In contrast, MT27 showed an elevated expression of the chemokines CXCL12 and CXCL14 during the acute phase of infection. The activation marker CD11b is decreased in monocytes in the clusters MT27, MT14, MT03, and MT24 after three

months of recovery compared to the acute infection. These results are alike to our manual gating strategy. The unsupervised analysis of multicolor flow cytometry data confirmed the data received by the manual gating strategy (Langnau et al., 2022).

We measured the intracellular expression of CXCL12 and MIF in all three monocyte subsets for a more specific and deeper pro-inflammatory cytokine characterization (Langnau et al., 2022). We focused on CXCL12 and MIF in patients with CVD and subsequent SARS-CoV-2 infection to analyze whether their expression is different after a follow-up of three months. Intracellular CXCL12 is significantly increased in all three monocyte subsets during acutely infected patients, while the expression is similar between the healthy controls and patients during the recovery phase. In contrast, the cytokine MIF is highly increased in classical and intermediate monocytes in patients three months following SARS-CoV-2 infection in comparison to healthy controls and acutely infected patients (Langnau et al., 2022). The cytokines CXCL12 and MIF are critical during atherosclerotic and inflammatory immune responses due to the chemotactic control of lymphocytes and monocytes (Calandra and Roger, 2003, Gao et al., 2019, van der Vorst et al., 2015). In particular, CXCL12 promotes leukocyte and progenitor cell recruitment and adhesion to injured and inflamed tissues, indicating an essential role in initiating vascular remodeling. CXCL12 is highly expressed in atherosclerosis lesions and associated with acute coronary syndrome (Gao et al., 2019, Massberg et al., 2006, Wurster et al., 2013). Other studies verified abnormally high amounts of CXCL12 in atherosclerosis lesions in comparison to healthy vessels ascribing a lesion-protective role for CXCL12 (van der Vorst et al., 2015). Furthermore, it has been shown that the phagocytosis of apoptotic thrombocytes by monocytes and macrophages was facilitated by CXCL12 promoting foam cell formation due to the monocytic expression of CXCR4 and CXCR7 (Chatterjee et al., 2015). Further, MIF is a pleiotropic pro-inflammatory cytokine with chemokine-like functions and is implicated in various chronic and acute inflammatory diseases, autoimmune diseases, cardiovascular diseases, and atherogenesis (Zernecke et al., 2008, Muller et al., 2014b, Morand et al., 2006). Further studies showed that thrombocytes pre-store MIF which is secreted upon thrombocyte activation and plays a functional role in leukocyte activation (Strussmann et al., 2013, Bernhagen et al., 2007, Wirtz et al., 2015). MIF functions as a pro-atherogenic factor and interacts with the chemokine receptors CXCR2 and CXCR4, promoting atherogenic monocyte adhesion, migration, differentiation, and survival, as well as leukocyte arrest on aortic endothelium (Bernhagen et al., 2007, Cheng et al., 2010, Muller et al., 2014a).

In order to analyze the systemic inflammation during acute and recovered SARS-CoV-2 infection, we performed chemokine profiling with LegendPlex analysis to measure plasma levels of several chemokines and cytokines. We observed increased plasma concentrations of pro-inflammatory cytokines and chemokines like IFN-y, CCL2, IL-18, IL-8, CXCL10,

CXCL11, IL-6, and MIF in CVD-infected SARS-CoV-2 patients. In contrast, we also could measure several inflammatory mediators like CCL20, IL-33, CCL11, CXCL1, CXCL5, CCL4, and IL-17A in CVD patients during the three months of the recovery phase (Langnau et al., 2022).

Our current study aimed to characterize monocyte immuno-phenotypes and plasma chemokine profiling during the acute phase of infection in comparison to a recovery of three months in patients with pre-existing cardiovascular disease. Our clinical assessment showed that almost all patients recovered from severe COVID-19 disease after three month follow-up. None of the patients suffered from post-COVID-19 symptoms and had cardiovascular or neurological consequences. In contrast, by analyzing the phenotype of systemic peripheral monocytes, we observed changes in their subpopulations, comparing acute infection with a follow-up. One significant outcome was the patients' high intracellular expression of MIF in monocytes after three months post-infection. In contrast, MIF was not altered during acute infection compared to healthy controls (Langnau et al., 2022). As already described, MIF is expressed ubiquitously and executes chemokine-like functions essential during innate immunity (Calandra and Roger, 2003, Sun et al., 1996). In particular, the binding of MIF results in the activation of downstream signaling pathways like NF-kB and inflammation, as well as immune cell survival or migration (Calandra and Roger, 2003, Kim et al., 2017). Our findings imply an important role of MIF and peripheral monocytes during the immune-defense mechanisms against viral infections like SARS-CoV-2. A continued expression of intracellular MIF in peripheral monocytes seems to promote the defense response mechanisms in COVID-19 (Langnau et al., 2022). Monocytes belong to the innate blood cells and execute their function directly at the beginning of acute infections (Jakubzick et al., 2017). Monocyte subpopulations differ regarding their function during immune responses (Ziegler-Heitbrock et al., 2010, Shantsila et al., 2011, Kapellos et al., 2019). Classical monocytes ($CD14^{++}CD16^{-}$) are circulating cells essential during initial inflammatory responses (Kapellos et al., 2019). In contrast, non-classical monocytes ($CD14^{dim}CD16^{++}$) are called "patrolling" monocytes with anti-inflammatory responses in the innate immune system (Buscher et al., 2017). Thus, it may be feasible to speculate that intracellular MIF in monocytes is characteristic of a severe course of SARS-CoV-2 infection contributing to immunity and re-infection. This implication is supported due to the fact that several cytokines and chemokines (e.g., CXCL1, IL17A, CCL17, IL-33) are highly increased after a three month recovery from SARS-CoV-2 infection. The cytokine IL-33 is vital for inducing priming of T-helper 2 cells (Komai-Koma et al., 2007), whereas CCL17 induces chemotactic regulation for regulatory T-cells. Neutrophil migration can be induced by CXCL1 (Metzemaekers et al., 2020, Sawant et al., 2016), and IL-17A was linked to immune responses during infectious diseases (Ge et al., 2020).

Limitations of our study are that our study is rather described as a hypothesis-generating or observational study. No causalities or conclusions about therapeutic options are possible. Additionally, further experiments for MIF are required to analyze how MIF may play a role in an extended immune response upon SARS-CoV-2 infection. For example, exploring the direct impact of MIF on the function and activation of monocytes or thrombocytes can be performed *in vitro* experiments. Another limitation of our study is the small patient number. Further, large randomized studies are essential to verify our results and the predictive value of MIF and other pro-inflammatory cytokines regarding the recovery of the immune response after acute COVID-19 infection. In order to analyze whether the increased MIF expression in monocytes correlates with or is related to clinical parameters or adverse clinical events, an increased cohort of SARS-CoV-2 patients with clinical follow-up is required. To be able to make a statement about long-COVID in our Cohort, a follow-up of 6 up to 12 months would be necessary (Langnau et al., 2022). An advantage of an observational study is that correlations can be analyzed between important factors. Including a healthy control group allows us to show whether the activation and migration surface marker of monocytes reach a level of healthy controls after recovery of three months. Increased MIF expression levels and pro-inflammatory monocyte function show a prolonged and persistent immune response following a three month recovery. Analyzing immune pathology and reactions after SARS-CoV-2 is critical to prevent and treat long-term complications (Langnau et al., 2022).

3.4 Immuno-phenotyping in aortic stenosis

Calcific aortic stenosis remains the most frequent heart valve disease in developed countries, particularly in the aging population (Osnabrugge et al., 2013, Nkomo et al., 2006). The disease progression of patients with aortic stenosis is highly variable, and the underlying mechanisms are not fully understood (Writing Committee et al., 2021, Surendran et al., 2020). Currently, a “watch and wait” strategy is used for CAS patients because no pharmacological strategies are available (Writing Committee et al., 2021, Vahanian et al., 2021, Everett et al., 2018). Patients undergo surgery or interventional therapy after onset of symptoms associated with poor prognosis (Pawade et al., 2015, Goody et al., 2020). Thus, it is critical to investigate pathological mechanisms in order to prevent disease onset and progression.

We hypothesized that alterations of thrombocyte activity, thrombocyte-derived mediators, and thrombocyte-monocyte interaction have a predictive function during the accelerated course of systemic thrombo-inflammation in AS patients. We stratified our patient cohort into two groups depending on the change of the maximum transvalvular flow velocity (ΔVmax) over time, indicating the rate of disease progression. 238 patients were included in slow progressive AS (SP-AS), and 237 patients were included in fast progressive AS (FP-AS) (Mueller et al., *in revision*).

Analyzing the local inflammation within the valve, histological analysis of pentachrome staining demonstrated that collagen is significantly increased in the tissue of FP-AS patients compared to SP-AS patients. However, mineralization in the AV was highly increased in SP-AS, visualized by von Kossa staining. Furthermore, the immunohistochemical staining of AV tissue showed a significantly increased cellularity in FP-AS, suggesting extravasation and infiltration of immune cells into the AV tissue. Further, the number of $CD16^+$ monocytes and $CD68^+$ macrophages was significantly increased in FP-AS patients. Interestingly, also $CD42b^+$ thrombocytes are significantly elevated in FP-AS patients compared to SP-AS patients. Results indicate that thrombocyte accumulation is associated with elevated tissue inflammation, immune cell infiltration, and thrombocyte activation. Further, immunostaining revealed that $CD42b^+$ thrombocytes mainly infiltrate and accumulate within the aortal side in contrast to the ventricular side. Similarly, we observed a higher total cell count, mainly on the aortal side than on the ventricular side. In summary, analysis demonstrates that FP-AS are characterized by infiltrating inflammatory cells and thrombocytes and high collagen content but less calcification compared to SP-AS patients (Mueller et al., *in revision*).

Studies already show that the beginning of disease progression is characterized by infiltration of immune cells and the differentiation of VICs into myofibroblastic and osteoblastic phenotypes. This process is regulated by cytokines and extracellular vesicles secreted by thrombocytes and immune cells (Jansen et al., 2017, Goody et al., 2020). Our data confirm the current knowledge about thrombocyte accumulation and its relation to an inflammatory valvular phenotype indicated by infiltrating macrophages and monocytes into the aortic valve. Our data imply that thrombocytes and immune cells may affect the differentiation of VICs and VECs, leading finally to fibrosis and calcification (Mueller et al., *in revision*). Another study already demonstrates a critical function of thrombocyte-mediated osteogenic differentiation of AS (Bouchareb et al., 2019). The primary function of thrombocytes is to maintain hemostasis and regulation of thrombosis, but besides this, they are important during vascular inflammation, particularly thrombo-inflammation. Due to adhesion on the activated endothelium, thrombocytes promote vascular inflammation and atheroprogression (Massberg et al., 2002). Studies in mouse models demonstrate that inhibition of thrombocyte adhesion leads to less inflammation of the aortic root and less atheroprogression (Massberg et al., 2002, Huo et al., 2003) as well as reduced vascular inflammation and plaque formation (Massberg et al., 2002).

In order to analyze the AV of SP- and FP-AS patients in more detail, gene expression analyses were performed by NanoString technology. Total RNA was extracted from aortic valves from formalin-fixed paraffin-embedded valve tissues, followed by ribonucleic acid profiling. Hierarchical cluster analysis of the top 50 differentially expressed genes revealed a different RNA expression in the aortic valve tissue of SP- and FP-AS patients. 23 genes of the tested 594 were significantly upregulated. In comparison, two genes were downregulated in FP-AS

compared to SP-AS patients. The differently regulated genes were mainly inflammatory. Two important downregulated gene expression signals are critical regulators of the toll-like receptor/inflammasome pathway (transforming growth factor-ß1 (TGF-β1) and MAP kinase-activated protein kinase 2). In contrast, the pro-inflammatory and apoptotic signaling, mediated e.g., by NF-κB or MIF, is upregulated in FP-AS (Mueller et al., *in revision*). Furthermore, analysis with row-wise comparisons of Nanostring® data (GeneCardSuite, 2021) depicts differences in the TGF-β1- and MIF-dependent pathways between the two patient groups. In detail, the MIF-associated gene expression was highly increased in FP-AS patients, while TGF-β1-associated gene expression was characteristic for SP-AS patients. In order to address the role of MIF in more detail, we performed MIF immunohistochemistry of AV. Analysis shows a significantly increased MIF expression within the aortic valve tissue in FP-AS patients. Interestingly, MIF expression was mainly observed in the aortal side in the AV compared to the ventricular side. However, TGF-β1 expression was highly increased in SP-AS patients confirming an essential role of MIF in FP-AS and a TGF-β1 important role in SP-AS (Mueller et al., *in revision*).

Due to increased infiltration of $CD16^+$ monocytes and $CD68^+$ macrophages and thrombocyte accumulation within the aortic valve, we performed a correlation coefficient Spearman's p analysis to analyze important clinical factors and thrombo-inflammation-related parameters in patients with FP- and SP-AS. Correlation analysis resulted in a significant correlation of plasma levels of MIF with AV tissue cell infiltration and collagen content. In addition, intracellular MIF in thrombocytes correlates inversely with an accumulation of $CD42b^+$ thrombocytes and $CD16^+$ monocytes, as well as positively with calcification area. To sum up, correlation analysis demonstrates different systemic MIF expressions in plasma, thrombocytes, and monocytes, indicating an important role of MIF during the disease progression of AS (Mueller et al., *in revision*).

The next step aims the investigation of systemic inflammation during AS progression. Thrombocytes get activated upon adhesion to the endothelium and secrete several inflammatory mediators, including cytokines and chemokines like MIF, causing an increase in vascular inflammation (Bakogiannis et al., 2019, Strussmann et al., 2013, Wirtz et al., 2015). Chemokine profiling showed that plasma levels of TGF-β1 and MIF were significantly increased in FP-AS patients (Mueller et al., *in revision*).

Further, we analyzed the role of thrombocytes by multicolor flow cytometry because studies already showed that thrombocytes and thrombocyte-derived mediators play an essential role during inflammation (Gawaz et al., 2005). The role of thrombocytes during atherosclerosis is highly investigated, while their role during aortic stenosis is poorly understood. Thrombocytes get activated due to shear stress from turbulent flow patterns within the calcific aortic valve

(Bouchareb et al., 2019). Analyzing the thrombocyte count, we could not detect any differences between SP- and FP-AS patients, while thrombocyte activation, indicated by surface CD62P expression, was significantly increased in FP-AS patients. In addition, the expression of thrombocyte markers CD31 and CD41 were highly elevated on thrombocytes in FP-AS patients compared to SP-AS patients (Mueller et al., *in revision*). Intracellular MIF expression was decreased in FP-AS patients, which can be explained by an increased activation status of thrombocytes in FP-AS patients (Mueller et al., *in revision*) because thrombocytes release inflammatory mediators by granules into the plasma (Koupenova et al., 2018). In order to analyze the flow cytometry data in more detail, unsupervised data analysis was performed by OMIQ. First, uniform manifold approximation and projection (UMAP) dimension reduction (Leland McInnes, 2020) was applied, showing similar events between SP- and FP-AS patients. Afterwards, an unsupervised clustering analysis PhenoGraph (Levine et al., 2015) showed a significant clustering of thrombocytes between SP- and FP-AS patients. PhenoGraph clustering results in 42 clusters, while seven differ in frequency between the two groups (Mueller et al., *in revision*). Heatmap analysis showed the median marker expression of the significantly different clusters and revealed that clusters P35, P03, P06, and P38 expressed an increased amount of intracellular MIF in SP-AS patients. These data are conformed with the results of our manual gating strategy. Our data demonstrate that thrombocyte activation is not only a characteristic of local valve inflammation but also occurs during systemic inflammation. Thrombocytes accumulate within the aortic valve, which correlates with elevated tissue inflammation and increased activation of thrombocytes. Our data implicate that thrombocyte accumulation and activation play an essential role in the genesis and progression of AS, but further studies are needed (Mueller et al., *in revision*). Our data are supported by several studies demonstrating that thrombocytes play a critical role in inflammation and atherogenesis (Bouchareb et al., 2019, Huo et al., 2003, Massberg et al., 2002).

Furthermore, we analyzed peripheral circulating monocytes by flow cytometry because we observed a high infiltration of monocytes and macrophages in the aortic valve by immunohistochemistry staining indicating an important role during local inflammation (Mueller et al., *in revision*). Monocytes and macrophages also secrete cytokines and chemokines, which in turn induce infiltration of other inflammatory cells and can differentiate into foam cells resulting in local inflammation (Wirtz et al., 2015, Zernecke et al., 2020, Pawade et al., 2015, Badimon and Vilahur, 2014, Zernecke and Weber, 2005). For the number of classical, intermediate, and non-classical monocytes, we could not see any differences between SP- and FP-AS patients. Interestingly, intracellular MIF expression was differently expressed in intermediate and non-classical monocytes. In detail, FP-AS patients showed a significantly increased expression. MIF expression in intermediate and non-classical monocytes correlated with the activation of thrombocytes and intracellular MIF expression in thrombocytes (Mueller

et al., *in revision*). To gain more insights into the activation of monocytes, we used a high-dimensional flow cytometric activation marker panel and pre-gated on monocytes. Further, we performed unsupervised data analysis UMAP and PhenoGraph as described above. Monocytes were clustered into 35 clusters, where five showed a different frequency between SP- and FP-AS patients. These five clusters showed different expression levels of CD11b, CD62L, HLA-DR, and intracellular MIF, CXCL12, and CXCL14. In summary, we could demonstrate differences in the expression of systemic inflammation markers on monocytes between slow and fast progressive AS patients, while MIF stands out the most (Mueller et al., *in revision*).

The interaction of thrombocytes and monocytes can trigger pro-inflammatory events, resulting in calcification processes in response to endothelial signals (Kral et al., 2016, Nording et al., 2015, Pawade et al., 2015). By flow cytometry analysis, we observed thrombocyte and monocyte phenotypes that were associated with clinical disease progression, specifically in FP-AS. These phenotypes are characterized by altered activation and adhesion markers in thrombocytes and monocytes, as well as cytokines and chemokines. Our results indicate a crucial role of thrombocyte and monocyte interactions during disease progression in AS patients, which are in line with other studies (Mueller et al., *in revision*). These studies show close interactions of neutrophils, lymphocytes, and thrombocytes which are associated with disease severity in AS patients (Song et al., 2015, Erdogan et al., 2021, Edem et al., 2016). To analyze the interaction of thrombocytes with leukocytes and the formation of aggregates in more detail, further investigations are needed, like a more precise multicolor flow cytometry panel focusing on aggregates of thrombocytes with monocytes (Mueller et al., *in revision*).

Further, our study implies a pivotal role of the cytokine MIF in the regulatory processes in local and systemic thrombo-inflammation in AS patients (Mueller et al., *in revision*). Our flow cytometry data indicate that fast progressive aortic stenosis patients are characterized by circulating thrombocytes with increased activation marker CD62P, secretion of MIF, and interaction with leukocytes (Mueller et al., *in revision*). Other studies already demonstrated an important function of MIF in monocyte function and regulation, while thrombocytes are able to store large amounts of MIF (Zernecke et al., 2008, Bernhagen et al., 2007, Schober et al., 2004). MIF is a cytokine with different effects on inflammatory responses and induction of signaling via CXCR2/4 and CD74 causing inflammatory cell recruitment and pro-inflammatory gene expression (Bernhagen, Krohn et al. 2007). Analysis of the atherosclerosis mouse model $LDLR^{-/-}$ showed that MIF executes a crucial role in atherogenesis and atheroprogression indicated by reduced atherogenesis due to MIF deficiency (Pan et al., 2004). The cytokine MIF was already investigated in a murine model showing that MIF promotes the migration of classical $Ly6^{high}$ monocytes, which execute a similar function as the human classical $CD14^{+}$

monocytes (Ruiz-Rosado Jde et al., 2016). Further, MIF was associated with cardiovascular diseases and atheroprogression (Muller et al., 2014a, Muller et al., 2014b). Plasma MIF levels were related to all-cause mortality and cardiovascular events in patients with acute myocardial infarction (Zhao et al., 2019). A possible pharmacological strategy regarding the critical prognostic factor MIF would be direct inhibition of thrombocyte degranulation or inhibition of MIF by antagonists. Inhibition of thrombocyte degranulation with MIF may reduce the acceleration of inflammation within the aortic valve and, thus, the disease progression. In pre-clinical trials, MIF antagonists have been developed and investigated to improve atherosclerosis (Kontos et al., 2020). Other studies demonstrated that the bone morphogenic protein antagonist Gremlin-1 could inhibit MIF-related monocyte function and reduce atherosclerotic plaque growth in an $ApoE^{-/-}$ mouse model (Muller et al., 2013, Muller et al., 2014a). These preliminary works support that MIF is a promising prognostic marker for severe aortic stenosis, emphasizing the benefit of early recognition of an accelerated disease progression to prevent irreversible inflammatory and calcific damages within the aortic valve.

A chord diagram was performed to summarize all data on significant MIF-related gene expression and local and systemic inflammation markers in SP- and FP-AS patients. In detail, the chord diagram represents *ex vivo* data, differentially expressed gene pathways, and changes in clinical parameters between SP- and FP-AS patients. Most interestingly, patients with a fast progressive disease progression showed increased MIF levels and altered MIF-regulated pathways. In contrast, slow progressive patients were associated with TGF-β1 pathways confirming our immunohistochemistry and flow cytometry analysis data (Mueller et al., *in revision*). TGF-β1 signaling is already well known during the calcification and fibrotic processes in aortic stenosis inducing osteoblastic differentiation of VICs, and VECs (Song et al., 2015, Pawade et al., 2015). Our results demonstrate a significantly increased gene expression of TGF-β1 within the AV of SP-AS patients, while plasma levels of TGF-β1 are significantly increased in FP-AS patients (Mueller et al., *in revision*).
In order to verify our hypothesis of MIF plasma levels and thrombocyte MIF as a prognostic factor for accelerated disease progression in AS patients, we performed a step-wise linear regression analysis to show that these factors are independent of demographic, clinical, and functional cofounders. Our results represent that plasma MIF and cell-based MIF markers (called “liquid biopsy”) are highly connected to patients with fast progressive disease, independent from cardiovascular comorbidities and valvular function parameters. Only the “liquid biopsy” is still significantly correlated with FP-AS (Mueller et al., *in revision*).

Limitations of our study are that our study is rather an observational or hypothesis-generating study. No causalities or conclusions about therapeutic options are possible. Furthermore, additional analysis about the mechanism of MIF and its role during disease progression in CAS

has to be done. For example, *in vitro* assays can be performed to analyze the impact of MIF on the function, phenotype and activation status of isolated VICs and VECs as well as function and activation of monocytes and thrombocytes. This would increase the knowledge about MIF and its direct influence on immune responses and tissue pathology within the aortic valve. Another limitation of our study is the definition of rapid and slow progression of AS which is not easy and rather challenging as it is not well defined, neither in the guidelines nor in the literature (Mueller et al., *in revision*).

An advantage of an observational study is that correlations can be analyzed between important factors. In our case, we analyzed correlations between MIF levels and immune cells infiltrated the aortic valve, calcification and collagen content. Further, we observed correlations between activation of platelets, MIF+ platelets and MIF expression in monocyte subsets. A further strength of our study is the huge number of included patients with AS. A huge patient number allows important statements about the applicability of our results (Mueller et al., *in revision*).

In conclusion, our results imply a critical role of thrombocyte-derived MIF and its interaction with circulating and valve resident monocytes during local and systemic inflammation in fast-progressive AS patients. Liquid biopsy may help to identify patients at risk for fast progressive disease pathology (Mueller et al., *in revision*).

3.5 Conclusion

My thesis characterized circulating peripheral monocytes and thrombocytes in patients with cardiovascular diseases in association with an acute SARS-CoV-2 infection or patients with severe calcific aortic stenosis. The new emerging SARS-CoV-2 virus is affecting the whole world population and causes severe and life-threatening complications like ARDS, pneumonia, sepsis, as well as respiratory failure (Giacca, 2022, Lamers and Haagmans, 2022, Zhou et al., 2020, Zheng et al., 2020b, Huang et al., 2020a). Thus, it is of fundamental need to characterize disease pathology and to find new diagnostic and therapeutic targets. Besides this, severe aortic stenosis is the most common valve disease affecting mainly elderly adults (Osnabrugge et al., 2013, Nkomo et al., 2006). The only therapeutic option for patients with aortic stenosis is surgical replacement of the aortic valve upon onset of severe symptoms (Goody et al., 2020, Everett et al., 2018). Thus, it is urgent to find new diagnostic and therapeutic targets, to prevent severe disease progression.

Patients with a predisposition like CAD and an acute SARS-CoV-2 infection demonstrated a reduced number of peripheral non-classical monocytes with a changed phenotype indicating an altered migration and T cell activation behavior compared to CAD patients without infection. Further, a reduced number of non-classical monocytes below the calculated median function

as a prognostic marker for rapidly progressive respiratory failure indicated by an HI<200 mmHg with subsequent mechanical ventilation (Mueller et al., 2021). Characterizing peripheral thrombocytes in CAD patients upon SARS-CoV-2 infection showed increased systemic thrombocyte activation and hyper-inflammation. In addition, plasma levels of subtilisin-like proprotein convertase furin were significantly reduced in ICU-treated patients compared to patients with mild disease progression. Further, furin can be used as a prognostic plasma marker for a poor clinical outcome in SARS-CoV-2 positive CAD patients (Langnau et al., 2021). SARS-CoV-2 infected patients with cardiovascular diseases showed a significantly increased concentration of intracellular MIF in monocyte subsets after a recovery phase of three months (Langnau et al., 2022). Further, monocytes showed different phenotypes comparing acutely infected patients with a follow-up of three months. Results imply a long-lasting immune response upon severe acute SARS-CoV-2 infection related to increased intracellular MIF expression and changes in monocyte phenotypes (Langnau et al., 2022).

Analysis of a cohort of patients with severe aortic stenosis demonstrated different phenotypes of slow and fast progressive AS patients. Patients with a slow progressive disease showed a calcific, pro-osteogenic, and TGF-β1 dependent phenotype. In contrast, fast progressive AS patients showed an inflammatory and MIF-dependent phenotype. Further, the chemokine-like MIF can predict fast progression in AS patients and is related to local aortic valve tissue inflammation. Our results are of major importance to increase the knowledge about disease pathology and progression in order that AS patients finally receive the best possible treatment (Mueller et al., *in revision*).

4 Literature

ABASSI, Z., KNANEY, Y., KARRAM, T. & HEYMAN, S. N. 2020. The Lung Macrophage in SARS-CoV-2 Infection: A Friend or a Foe? *Front Immunol,* 11**,** 1312.

AKAT, K., BORGGREFE, M. & KADEN, J. J. 2009. Aortic valve calcification: basic science to clinical practice. *Heart,* 95**,** 616-23.

AL-SAMKARI, H., KARP LEAF, R. S., DZIK, W. H., CARLSON, J. C. T., FOGERTY, A. E., WAHEED, A., GOODARZI, K., BENDAPUDI, P. K., BORNIKOVA, L., GUPTA, S., LEAF, D. E., KUTER, D. J. & ROSOVSKY, R. P. 2020. COVID-19 and coagulation: bleeding and thrombotic manifestations of SARS-CoV-2 infection. *Blood,* 136**,** 489-500.

ALLEN, N., BARRETT, T. J., GUO, Y., NARDI, M., RAMKHELAWON, B., ROCKMAN, C. B., HOCHMAN, J. S. & BERGER, J. S. 2019. Circulating monocyte-platelet aggregates are a robust marker of platelet activity in cardiovascular disease. *Atherosclerosis,* 282**,** 11-18.

ALTHAUS K, M. I., JAN ZLAMAL, LISANN PELZL, HELENE HÄBERLE, MARTIN MEHRLÄNDER, STEFANIE HAMMER, HARALD SCHULZE, MICHAEL BITZER, NISAR MALEK, DOMINIK RATH, HANS BÖSMÜLLER, BERNARD NIESWANDT, MEINRAD GAWAZ, TAMAM BAKCHOUL, PETER ROSENBERGER 2020. Severe COVID-19 infection is associated with increased antibody-mediated platelet apoptosis. *medRxiv*.

ASSINGER, A. 2014. Platelets and infection - an emerging role of platelets in viral infection. *Front Immunol,* 5**,** 649.

AUFFRAY, C., FOGG, D. K., NARNI-MANCINELLI, E., SENECHAL, B., TROUILLET, C., SAEDERUP, N., LEEMPUT, J., BIGOT, K., CAMPISI, L., ABITBOL, M., MOLINA, T., CHARO, I., HUME, D. A., CUMANO, A., LAUVAU, G. & GEISSMANN, F. 2009. CX3CR1+ CD115+ CD135+ common macrophage/DC precursors and the role of CX3CR1 in their response to inflammation. *J Exp Med,* 206**,** 595-606.

BADIMON, L. & VILAHUR, G. 2014. Thrombosis formation on atherosclerotic lesions and plaque rupture. *J Intern Med,* 276**,** 618-32.

BAKOGIANNIS, C., SACHSE, M., STAMATELOPOULOS, K. & STELLOS, K. 2019. Platelet-derived chemokines in inflammation and atherosclerosis. *Cytokine,* 122**,** 154157.

BAO, C., TAO, X., CUI, W., YI, B., PAN, T., YOUNG, K. H. & QIAN, W. 2020. SARS-CoV-2 induced thrombocytopenia as an important biomarker significantly correlated with abnormal coagulation function, increased intravascular blood clot risk and mortality in COVID-19 patients. *Exp Hematol Oncol,* 9**,** 16.

BARRETT, T. J., BILALOGLU, S., CORNWELL, M., BURGESS, H. M., VIRGINIO, V. W., DRENKOVA, K., IBRAHIM, H., YURIDITSKY, E., APHINYANAPHONGS, Y., LIFSHITZ, M., XIA LIANG, F., ALEJO, J., SMITH, G., PITTALUGA, S., RAPKIEWICZ, A. V., WANG, J., IANCU-RUBIN, C., MOHR, I., RUGGLES, K., STAPLEFORD, K. A., HOCHMAN, J. & BERGER, J. S. 2021. Platelets contribute to disease severity in COVID-19. *J Thromb Haemost,* 19**,** 3139-3153.

BARTOLI-LEONARD, F., ZIMMER, J. & AIKAWA, E. 2021. Innate and adaptive immunity: the understudied driving force of heart valve disease. *Cardiovasc Res,* 117**,** 2506-2524.

BAYATI, A., KUMAR, R., FRANCIS, V. & MCPHERSON, P. S. 2021. SARS-CoV-2 infects cells after viral entry via clathrin-mediated endocytosis. *J Biol Chem,* 296**,** 100306.

BERNHAGEN, J., KROHN, R., LUE, H., GREGORY, J. L., ZERNECKE, A., KOENEN, R. R., DEWOR, M., GEORGIEV, I., SCHOBER, A., LENG, L., KOOISTRA, T., FINGERLE-ROWSON, G., GHEZZI, P.,

KLEEMANN, R., MCCOLL, S. R., BUCALA, R., HICKEY, M. J. & WEBER, C. 2007. MIF is a noncognate ligand of CXC chemokine receptors in inflammatory and atherogenic cell recruitment. *Nat Med,* 13**,** 587-96.

BONGIOVANNI, D., KLUG, M., LAZAREVA, O., WEIDLICH, S., BIASI, M., URSU, S., WARTH, S., BUSKE, C., LUKAS, M., SPINNER, C. D., SCHEIDT, M. V., CONDORELLI, G., BAUMBACH, J., LAUGWITZ, K. L., LIST, M. & BERNLOCHNER, I. 2021. SARS-CoV-2 infection is associated with a pro-thrombotic platelet phenotype. *Cell Death Dis,* 12**,** 50.

BONOW, R. O., O'GARA, P. T. & YANCY, C. W. 2020. Cardiology and COVID-19. *JAMA,* 324**,** 1131-1132.

BOUCHAREB, R., BOULANGER, M. C., TASTET, L., MKANNEZ, G., NSAIBIA, M. J., HADJI, F., DAHOU, A., MESSADEQ, Y., ARSENAULT, B. J., PIBAROT, P., BOSSE, Y., MARETTE, A. & MATHIEU, P. 2019. Activated platelets promote an osteogenic programme and the progression of calcific aortic valve stenosis. *Eur Heart J,* 40**,** 1362-1373.

BOURMISTROVA, N. W., SOLOMON, T., BRAUDE, P., STRAWBRIDGE, R. & CARTER, B. 2022. Long-term effects of COVID-19 on mental health: A systematic review. *J Affect Disord,* 299**,** 118-125.

BOYETTE, L. B., MACEDO, C., HADI, K., ELINOFF, B. D., WALTERS, J. T., RAMASWAMI, B., CHALASANI, G., TABOAS, J. M., LAKKIS, F. G. & METES, D. M. 2017. Phenotype, function, and differentiation potential of human monocyte subsets. *PLoS One,* 12**,** e0176460.

BRAMBILLA, M., CAMERA, M., COLNAGO, D., MARENZI, G., DE METRIO, M., GIESEN, P. L., BALDUINI, A., VEGLIA, F., GERTOW, K., BIGLIOLI, P. & TREMOLI, E. 2008. Tissue factor in patients with acute coronary syndromes: expression in platelets, leukocytes, and platelet-leukocyte aggregates. *Arterioscler Thromb Vasc Biol,* 28**,** 947-53.

BRAUN, E. & SAUTER, D. 2019. Furin-mediated protein processing in infectious diseases and cancer. *Clin Transl Immunology,* 8**,** e1073.

BUSCHER, K., MARCOVECCHIO, P., HEDRICK, C. C. & LEY, K. 2017. Patrolling Mechanics of Non-Classical Monocytes in Vascular Inflammation. *Front Cardiovasc Med,* 4**,** 80.

CALANDRA, T. & ROGER, T. 2003. Macrophage migration inhibitory factor: a regulator of innate immunity. *Nat Rev Immunol,* 3**,** 791-800.

CHATTERJEE, M., BORST, O., WALKER, B., FOTINOS, A., VOGEL, S., SEIZER, P., MACK, A., ALAMPOUR-RAJABI, S., RATH, D., GEISLER, T., LANG, F., LANGER, H. F., BERNHAGEN, J. & GAWAZ, M. 2014. Macrophage migration inhibitory factor limits activation-induced apoptosis of platelets via CXCR7-dependent Akt signaling. *Circ Res,* 115**,** 939-49.

CHATTERJEE, M. & GEISLER, T. 2016. Inflammatory Contribution of Platelets Revisited: New Players in the Arena of Inflammation. *Semin Thromb Hemost,* 42**,** 205-14.

CHATTERJEE, M., VON UNGERN-STERNBERG, S. N., SEIZER, P., SCHLEGEL, F., BUTTCHER, M., SINDHU, N. A., MULLER, S., MACK, A. & GAWAZ, M. 2015. Platelet-derived CXCL12 regulates monocyte function, survival, differentiation into macrophages and foam cells through differential involvement of CXCR4-CXCR7. *Cell Death Dis,* 6**,** e1989.

CHENG, Q., MCKEOWN, S. J., SANTOS, L., SANTIAGO, F. S., KHACHIGIAN, L. M., MORAND, E. F. & HICKEY, M. J. 2010. Macrophage migration inhibitory factor increases leukocyte-endothelial interactions in human endothelial cells via promotion of expression of adhesion molecules. *J Immunol,* 185**,** 1238-47.

CHENG, Y. W., CHAO, T. L., LI, C. L., CHIU, M. F., KAO, H. C., WANG, S. H., PANG, Y. H., LIN, C. H., TSAI, Y. M., LEE, W. H., TAO, M. H., HO, T. C., WU, P. Y., JANG, L. T., CHEN, P. J., CHANG, S. Y. & YEH, S. H. 2020. Furin Inhibitors Block SARS-CoV-2 Spike Protein Cleavage to Suppress Virus Production and Cytopathic Effects. *Cell Rep,* 33**,** 108254.

CHILUNDA, V., MARTINEZ-AGUADO, P., XIA, L. C., CHENEY, L., MURPHY, A., VEKSLER, V., RUIZ, V., CALDERON, T. M. & BERMAN, J. W. 2021. Transcriptional Changes in CD16+ Monocytes May Contribute to the Pathogenesis of COVID-19. *Front Immunol,* 12**,** 665773.

CLARKE, N. E. & TURNER, A. J. 2012. Angiotensin-converting enzyme 2: the first decade. *Int J Hypertens,* 2012**,** 307315.

CLERKIN, K. J., FRIED, J. A., RAIKHELKAR, J., SAYER, G., GRIFFIN, J. M., MASOUMI, A., JAIN, S. S., BURKHOFF, D., KUMARAIAH, D., RABBANI, L., SCHWARTZ, A. & URIEL, N. 2020. COVID-19 and Cardiovascular Disease. *Circulation,* 141**,** 1648-1655.

COLLING, M. E. & KANTHI, Y. 2020. COVID-19-associated coagulopathy: An exploration of mechanisms. *Vasc Med,* 25**,** 471-478.

COLLING, M. E., TOURDOT, B. E. & KANTHI, Y. 2021. Inflammation, Infection and Venous Thromboembolism. *Circ Res,* 128**,** 2017-2036.

CONNORS, J. M. & LEVY, J. H. 2020. COVID-19 and its implications for thrombosis and anticoagulation. *Blood,* 135**,** 2033-2040.

COUTARD, B., VALLE, C., DE LAMBALLERIE, X., CANARD, B., SEIDAH, N. G. & DECROLY, E. 2020. The spike glycoprotein of the new coronavirus 2019-nCoV contains a furin-like cleavage site absent in CoV of the same clade. *Antiviral Res,* 176**,** 104742.

CROS, J., CAGNARD, N., WOOLLARD, K., PATEY, N., ZHANG, S. Y., SENECHAL, B., PUEL, A., BISWAS, S. K., MOSHOUS, D., PICARD, C., JAIS, J. P., D'CRUZ, D., CASANOVA, J. L., TROUILLET, C. & GEISSMANN, F. 2010. Human CD14dim monocytes patrol and sense nucleic acids and viruses via TLR7 and TLR8 receptors. *Immunity,* 33**,** 375-86.

DATTA, P. K., LIU, F., FISCHER, T., RAPPAPORT, J. & QIN, X. 2020. SARS-CoV-2 pandemic and research gaps: Understanding SARS-CoV-2 interaction with the ACE2 receptor and implications for therapy. *Theranostics,* 10**,** 7448-7464.

DEGAUQUE, N., HAZIOT, A., BROUARD, S. & MOONEY, N. 2021. Endothelial cell, myeloid, and adaptive immune responses in SARS-CoV-2 infection. *FASEB J,* 35**,** e21577.

DEPPERMANN, C. & KUBES, P. 2018. Start a fire, kill the bug: The role of platelets in inflammation and infection. *Innate Immun,* 24**,** 335-348.

DESAI, A. D., LAVELLE, M., BOURSIQUOT, B. C. & WAN, E. Y. 2022. Long-term complications of COVID-19. *Am J Physiol Cell Physiol,* 322**,** C1-C11.

DIAMOND, M. S. & KANNEGANTI, T. D. 2022. Innate immunity: the first line of defense against SARS-CoV-2. *Nat Immunol,* 23**,** 165-176.

DIB, P. R. B., QUIRINO-TEIXEIRA, A. C., MERIJ, L. B., PINHEIRO, M. B. M., ROZINI, S. V., ANDRADE, F. B. & HOTTZ, E. D. 2020. Innate immune receptors in platelets and platelet-leukocyte interactions. *J Leukoc Biol,* 108**,** 1157-1182.

DWECK, M. R., KHAW, H. J., SNG, G. K., LUO, E. L., BAIRD, A., WILLIAMS, M. C., MAKIELLO, P., MIRSADRAEE, S., JOSHI, N. V., VAN BEEK, E. J., BOON, N. A., RUDD, J. H. & NEWBY, D. E. 2013.

Aortic stenosis, atherosclerosis, and skeletal bone: is there a common link with calcification and inflammation? *Eur Heart J,* 34**,** 1567-74.

EDEM, E., REYHANOGLU, H., KUCUKUKUR, M., KIRDOK, A. H., KINAY, A. O., TEKIN, U. I., OZCAN, K., ERTURK, M., SENTURK, C., KIRILMAZ, B., GUNGOR, H. & DURMAZ, I. 2016. Predictive value of platelet-to-lymphocyte ratio in severe degenerative aortic valve stenosis. *J Res Med Sci,* 21**,** 93.

ERDOGAN, M., OZTURK, S., KARDESLER, B., YIGITBASI, M., KASAPKARA, H. A., BASTUG, S., ERDOL, M. A., AKAR BAYRAM, N., AKCAY, M. & DURMAZ, T. 2021. The relationship between calcific severe aortic stenosis and systemic immune-inflammation index. *Echocardiography,* 38**,** 737-744.

EVERETT, R. J., CLAVEL, M. A., PIBAROT, P. & DWECK, M. R. 2018. Timing of intervention in aortic stenosis: a review of current and future strategies. *Heart,* 104**,** 2067-2076.

FANG, P., LI, X., DAI, J., COLE, L., CAMACHO, J. A., ZHANG, Y., JI, Y., WANG, J., YANG, X. F. & WANG, H. 2018. Immune cell subset differentiation and tissue inflammation. *J Hematol Oncol,* 11**,** 97.

FEHR, A. R. & PERLMAN, S. 2015. Coronaviruses: an overview of their replication and pathogenesis. *Methods Mol Biol,* 1282**,** 1-23.

FERNANDEZ, C., RYSA, J., ALMGREN, P., NILSSON, J., ENGSTROM, G., ORHO-MELANDER, M., RUSKOAHO, H. & MELANDER, O. 2018. Plasma levels of the proprotein convertase furin and incidence of diabetes and mortality. *J Intern Med,* 284**,** 377-387.

FREEMAN, R. V. & OTTO, C. M. 2005. Spectrum of calcific aortic valve disease: pathogenesis, disease progression, and treatment strategies. *Circulation,* 111**,** 3316-26.

FURMAN, M. I., BENOIT, S. E., BARNARD, M. R., VALERI, C. R., BORBONE, M. L., BECKER, R. C., HECHTMAN, H. B. & MICHELSON, A. D. 1998. Increased platelet reactivity and circulating monocyte-platelet aggregates in patients with stable coronary artery disease. *J Am Coll Cardiol,* 31**,** 352-8.

GAO, J. H., YU, X. H. & TANG, C. K. 2019. CXC chemokine ligand 12 (CXCL12) in atherosclerosis: An underlying therapeutic target. *Clin Chim Acta,* 495**,** 538-544.

GATTI, A., RADRIZZANI, D., VIGANO, P., MAZZONE, A. & BRANDO, B. 2020. Decrease of Non-Classical and Intermediate Monocyte Subsets in Severe Acute SARS-CoV-2 Infection. *Cytometry A,* 97**,** 887-890.

GAWAZ, M., LANGER, H. & MAY, A. E. 2005. Platelets in inflammation and atherogenesis. *J Clin Invest,* 115**,** 3378-84.

GE, Y., HUANG, M. & YAO, Y. M. 2020. Biology of Interleukin-17 and Its Pathophysiological Significance in Sepsis. *Front Immunol,* 11**,** 1558.

GENECARDSUITE. 2021. [Accessed].

GIACCA, M., SHAH, A.M. 2022. The pathological maelstrom of COVID-19 and cardiovascular disease. *Nat Cardiovasc Res,* 1, 200–210

GLOWACKA, I., BERTRAM, S., MULLER, M. A., ALLEN, P., SOILLEUX, E., PFEFFERLE, S., STEFFEN, I., TSEGAYE, T. S., HE, Y., GNIRSS, K., NIEMEYER, D., SCHNEIDER, H., DROSTEN, C. & POHLMANN, S. 2011. Evidence that TMPRSS2 activates the severe acute respiratory syndrome coronavirus spike protein for membrane fusion and reduces viral control by the humoral immune response. *J Virol,* 85**,** 4122-34.

GOODY, P. R., HOSEN, M. R., CHRISTMANN, D., NIEPMANN, S. T., ZIETZER, A., ADAM, M., BONNER, F., ZIMMER, S., NICKENIG, G. & JANSEN, F. 2020. Aortic Valve Stenosis: From Basic Mechanisms to Novel Therapeutic Targets. *Arterioscler Thromb Vasc Biol,* 40**,** 885-900.

GOROG, D. A., STOREY, R. F., GURBEL, P. A., TANTRY, U. S., BERGER, J. S., CHAN, M. Y., DUERSCHMIED, D., SMYTH, S. S., PARKER, W. A. E., AJJAN, R. A., VILAHUR, G., BADIMON, L., BERG, J. M. T., CATE, H. T., PEYVANDI, F., WANG, T. T. & BECKER, R. C. 2022. Current and novel biomarkers of thrombotic risk in COVID-19: a Consensus Statement from the International COVID-19 Thrombosis Biomarkers Colloquium. *Nat Rev Cardiol,* 19**,** 475-495.

GROBLER, C., MAPHUMULO, S. C., GROBBELAAR, L. M., BREDENKAMP, J. C., LAUBSCHER, G. J., LOURENS, P. J., STEENKAMP, J., KELL, D. B. & PRETORIUS, E. 2020. Covid-19: The Rollercoaster of Fibrin(Ogen), D-Dimer, Von Willebrand Factor, P-Selectin and Their Interactions with Endothelial Cells, Platelets and Erythrocytes. *Int J Mol Sci,* 21.

GROS, A., OLLIVIER, V. & HO-TIN-NOE, B. 2014. Platelets in inflammation: regulation of leukocyte activities and vascular repair. *Front Immunol,* 5**,** 678.

GU, S. X., TYAGI, T., JAIN, K., GU, V. W., LEE, S. H., HWA, J. M., KWAN, J. M., KRAUSE, D. S., LEE, A. I., HALENE, S., MARTIN, K. A., CHUN, H. J. & HWA, J. 2021. Thrombocytopathy and endotheliopathy: crucial contributors to COVID-19 thromboinflammation. *Nat Rev Cardiol,* 18**,** 194-209.

GUO, T., FAN, Y., CHEN, M., WU, X., ZHANG, L., HE, T., WANG, H., WAN, J., WANG, X. & LU, Z. 2020. Cardiovascular Implications of Fatal Outcomes of Patients With Coronavirus Disease 2019 (COVID-19). *JAMA Cardiol,* 5**,** 811-818.

GUZIK, T. J., MOHIDDIN, S. A., DIMARCO, A., PATEL, V., SAVVATIS, K., MARELLI-BERG, F. M., MADHUR, M. S., TOMASZEWSKI, M., MAFFIA, P., D'ACQUISTO, F., NICKLIN, S. A., MARIAN, A. J., NOSALSKI, R., MURRAY, E. C., GUZIK, B., BERRY, C., TOUYZ, R. M., KREUTZ, R., WANG, D. W., BHELLA, D., SAGLIOCCO, O., CREA, F., THOMSON, E. C. & MCINNES, I. B. 2020. COVID-19 and the cardiovascular system: implications for risk assessment, diagnosis, and treatment options. *Cardiovasc Res,* 116**,** 1666-1687.

HIGGINS, V., SOHAEI, D., DIAMANDIS, E. P. & PRASSAS, I. 2021. COVID-19: from an acute to chronic disease? Potential long-term health consequences. *Crit Rev Clin Lab Sci,* 58**,** 297-310.

HOFFMANN, M., KLEINE-WEBER, H. & POHLMANN, S. 2020a. A Multibasic Cleavage Site in the Spike Protein of SARS-CoV-2 Is Essential for Infection of Human Lung Cells. *Mol Cell,* 78**,** 779-784 e5.

HOFFMANN, M., KLEINE-WEBER, H., SCHROEDER, S., KRUGER, N., HERRLER, T., ERICHSEN, S., SCHIERGENS, T. S., HERRLER, G., WU, N. H., NITSCHE, A., MULLER, M. A., DROSTEN, C. & POHLMANN, S. 2020b. SARS-CoV-2 Cell Entry Depends on ACE2 and TMPRSS2 and Is Blocked by a Clinically Proven Protease Inhibitor. *Cell,* 181**,** 271-280 e8.

HOTTZ, E. D., AZEVEDO-QUINTANILHA, I. G., PALHINHA, L., TEIXEIRA, L., BARRETO, E. A., PAO, C. R. R., RIGHY, C., FRANCO, S., SOUZA, T. M. L., KURTZ, P., BOZZA, F. A. & BOZZA, P. T. 2020. Platelet activation and platelet-monocyte aggregate formation trigger tissue factor expression in patients with severe COVID-19. *Blood,* 136**,** 1330-1341.

HOTTZ, E. D., BOZZA, F. A. & BOZZA, P. T. 2018. Platelets in Immune Response to Virus and Immunopathology of Viral Infections. *Front Med (Lausanne),* 5**,** 121.

HSU, R. J., YU, W. C., PENG, G. R., YE, C. H., HU, S., CHONG, P. C. T., YAP, K. Y., LEE, J. Y. C., LIN, W. C. & YU, S. H. 2022. The Role of Cytokines and Chemokines in Severe Acute Respiratory Syndrome Coronavirus 2 Infections. *Front Immunol,* 13**,** 832394.

HUANG, C., HUANG, L., WANG, Y., LI, X., REN, L., GU, X., KANG, L., GUO, L., LIU, M., ZHOU, X., LUO, J., HUANG, Z., TU, S., ZHAO, Y., CHEN, L., XU, D., LI, Y., LI, C., PENG, L., LI, Y., XIE, W., CUI, D., SHANG, L., FAN, G., XU, J., WANG, G., WANG, Y., ZHONG, J., WANG, C., WANG, J., ZHANG, D. & CAO, B. 2021. 6-month consequences of COVID-19 in patients discharged from hospital: a cohort study. *Lancet,* 397**,** 220-232.

HUANG, C., WANG, Y., LI, X., REN, L., ZHAO, J., HU, Y., ZHANG, L., FAN, G., XU, J., GU, X., CHENG, Z., YU, T., XIA, J., WEI, Y., WU, W., XIE, X., YIN, W., LI, H., LIU, M., XIAO, Y., GAO, H., GUO, L., XIE, J., WANG, G., JIANG, R., GAO, Z., JIN, Q., WANG, J. & CAO, B. 2020a. Clinical features of patients infected with 2019 novel coronavirus in Wuhan, China. *Lancet,* 395**,** 497-506.

HUANG, I. C., BOSCH, B. J., LI, F., LI, W., LEE, K. H., GHIRAN, S., VASILIEVA, N., DERMODY, T. S., HARRISON, S. C., DORMITZER, P. R., FARZAN, M., ROTTIER, P. J. & CHOE, H. 2006. SARS coronavirus, but not human coronavirus NL63, utilizes cathepsin L to infect ACE2-expressing cells. *J Biol Chem,* 281**,** 3198-203.

HUANG, Y., YANG, C., XU, X. F., XU, W. & LIU, S. W. 2020b. Structural and functional properties of SARS-CoV-2 spike protein: potential antivirus drug development for COVID-19. *Acta Pharmacol Sin,* 41**,** 1141-1149.

HUANG, Y., YIN, H., WANG, J., MA, X., ZHANG, Y. & CHEN, K. 2012. The significant increase of FcgammaRIIIA (CD16), a sensitive marker, in patients with coronary heart disease. *Gene,* 504**,** 284-7.

HUGHES, C. E. & NIBBS, R. J. B. 2018. A guide to chemokines and their receptors. *FEBS J,* 285**,** 2944-2971.

HUILCAMAN, R., VENTURINI, W., FUENZALIDA, L., CAYO, A., SEGOVIA, R., VALENZUELA, C., BROWN, N. & MOORE-CARRASCO, R. 2022. Platelets, a Key Cell in Inflammation and Atherosclerosis Progression. *Cells,* 11.

HUO, Y., SCHOBER, A., FORLOW, S. B., SMITH, D. F., HYMAN, M. C., JUNG, S., LITTMAN, D. R., WEBER, C. & LEY, K. 2003. Circulating activated platelets exacerbate atherosclerosis in mice deficient in apolipoprotein E. *Nat Med,* 9**,** 61-7.

IIJIMA, R., NDREPEPA, G., MEHILLI, J., BRUSKINA, O., SCHULZ, S., SCHOMIG, A. & KASTRATI, A. 2007. Relationship between platelet count and 30-day clinical outcomes after percutaneous coronary interventions. Pooled analysis of four ISAR trials. *Thromb Haemost,* 98**,** 852-7.

INCIARDI, R. M., ADAMO, M., LUPI, L. & METRA, M. 2020. Atrial fibrillation in the COVID-19 era: simple bystander or marker of increased risk? *Eur Heart J,* 41**,** 3094.

JACKSON, C. B., FARZAN, M., CHEN, B. & CHOE, H. 2022. Mechanisms of SARS-CoV-2 entry into cells. *Nat Rev Mol Cell Biol,* 23**,** 3-20.

JAKUBZICK, C. V., RANDOLPH, G. J. & HENSON, P. M. 2017. Monocyte differentiation and antigen-presenting functions. *Nat Rev Immunol,* 17**,** 349-362.

JANSEN, F., XIANG, X. & WERNER, N. 2017. Role and function of extracellular vesicles in calcific aortic valve disease. *Eur Heart J,* 38**,** 2714-2716.

JOSE, R. J. & MANUEL, A. 2020. COVID-19 cytokine storm: the interplay between inflammation and coagulation. *Lancet Respir Med,* 8**,** e46-e47.

KANG, H., LI, X., XIONG, K., SONG, Z., TIAN, J., WEN, Y., SUN, A. & DENG, X. 2021. The Entry and Egress of Monocytes in Atherosclerosis: A Biochemical and Biomechanical Driven Process. *Cardiovasc Ther,* 2021**,** 6642927.

KANY, S., VOLLRATH, J. T. & RELJA, B. 2019. Cytokines in Inflammatory Disease. *Int J Mol Sci,* 20.

KAPELLOS, T. S., BONAGURO, L., GEMUND, I., REUSCH, N., SAGLAM, A., HINKLEY, E. R. & SCHULTZE, J. L. 2019. Human Monocyte Subsets and Phenotypes in Major Chronic Inflammatory Diseases. *Front Immunol,* 10**,** 2035.

KERRIGAN, S. W., DOUGLAS, I., WRAY, A., HEATH, J., BYRNE, M. F., FITZGERALD, D. & COX, D. 2002. A role for glycoprotein Ib in Streptococcus sanguis-induced platelet aggregation. *Blood,* 100**,** 509-16.

KIM, D., LEE, J. Y., YANG, J. S., KIM, J. W., KIM, V. N. & CHANG, H. 2020. The Architecture of SARS-CoV-2 Transcriptome. *Cell,* 181**,** 914-921 e10.

KIM, M. J., KIM, W. S., KIM, D. O., BYUN, J. E., HUY, H., LEE, S. Y., SONG, H. Y., PARK, Y. J., KIM, T. D., YOON, S. R., CHOI, E. J., HA, H., JUNG, H. & CHOI, I. 2017. Macrophage migration inhibitory factor interacts with thioredoxin-interacting protein and induces NF-kappaB activity. *Cell Signal,* 34**,** 110-120.

KNOLL, R., SCHULTZE, J. L. & SCHULTE-SCHREPPING, J. 2021. Monocytes and Macrophages in COVID-19. *Front Immunol,* 12**,** 720109.

KOMAI-KOMA, M., XU, D., LI, Y., MCKENZIE, A. N., MCINNES, I. B. & LIEW, F. Y. 2007. IL-33 is a chemoattractant for human Th2 cells. *Eur J Immunol,* 37**,** 2779-86.

KONTOS, C., EL BOUNKARI, O., KRAMMER, C., SINITSKI, D., HILLE, K., ZAN, C., YAN, G., WANG, S., GAO, Y., BRANDHOFER, M., MEGENS, R. T. A., HOFFMANN, A., PAULI, J., ASARE, Y., GERRA, S., BOURILHON, P., LENG, L., ECKSTEIN, H. H., KEMPF, W. E., PELISEK, J., GOKCE, O., MAEGDEFESSEL, L., BUCALA, R., DICHGANS, M., WEBER, C., KAPURNIOTU, A. & BERNHAGEN, J. 2020. Designed CXCR4 mimic acts as a soluble chemokine receptor that blocks atherogenic inflammation by agonist-specific targeting. *Nat Commun,* 11**,** 5981.

KOUPENOVA, M., CLANCY, L., CORKREY, H. A. & FREEDMAN, J. E. 2018. Circulating Platelets as Mediators of Immunity, Inflammation, and Thrombosis. *Circ Res,* 122**,** 337-351.

KRAL, J. B., SCHROTTMAIER, W. C., SALZMANN, M. & ASSINGER, A. 2016. Platelet Interaction with Innate Immune Cells. *Transfus Med Hemother,* 43**,** 78-88.

KRATOFIL, R. M., KUBES, P. & DENISET, J. F. 2017. Monocyte Conversion During Inflammation and Injury. *Arterioscler Thromb Vasc Biol,* 37**,** 35-42.

LAMERS, M. M. & HAAGMANS, B. L. 2022. SARS-CoV-2 pathogenesis. *Nat Rev Microbiol,* 20**,** 270-284.

LANGNAU, C., JANING, H., KOCAMAN, H., GEKELER, S., GUNTER, M., PETERSEN, A., JAEGER, P., KOCH, B., KREISSELMEIER, K. P., CASTOR, T., RATH, D., GAWAZ, M., AUTENRIETH, S. E. & MUELLER, K. 2022. Recovery of systemic hyperinflammation in patients with severe SARS-CoV-2 infection. *Biomarkers***,** 1-19.

LANGNAU, C., ROHLFING, A. K., GEKELER, S., GUNTER, M., POSCHEL, S., PETERSEN-URIBE, A., JAEGER, P., AVDIU, A., HARM, T., KREISSELMEIER, K. P., CASTOR, T., BAKCHOUL, T., RATH, D., GAWAZ, M. P., AUTENRIETH, S. E. & MUELLER, K. A. L. 2021. Platelet Activation and Plasma Levels of Furin Are Associated With Prognosis of Patients With Coronary Artery Disease and COVID-19. *Arterioscler Thromb Vasc Biol,* 41**,** 2080-2096.

LASSALLE, F., ROSA, M., STAELS, B., VAN BELLE, E., SUSEN, S. & DUPONT, A. 2022. Circulating Monocyte Subsets and Transcatheter Aortic Valve Replacement. *Int J Mol Sci,* 23.

LAUDANNA, C. & ALON, R. 2006. Right on the spot. Chemokine triggering of integrin-mediated arrest of rolling leukocytes. *Thromb Haemost,* 95**,** 5-11.

LAX, S. F., SKOK, K., ZECHNER, P., KESSLER, H. H., KAUFMANN, N., KOELBLINGER, C., VANDER, K., BARGFRIEDER, U. & TRAUNER, M. 2020. Pulmonary Arterial Thrombosis in COVID-19 With Fatal Outcome : Results From a Prospective, Single-Center, Clinicopathologic Case Series. *Ann Intern Med,* 173**,** 350-361.

LEBLOND, J., LAPRISE, M. H., GAUDREAU, S., GRONDIN, F., KISIEL, W. & DUBOIS, C. M. 2006. The serpin proteinase inhibitor 8: an endogenous furin inhibitor released from human platelets. *Thromb Haemost,* 95**,** 243-52.

LELAND MCINNES, J. H., JAMES MELVILLE 2020. UMAP: Uniform Manifold Approximation and Projection for Dimension Reduction. *Cornell University*.

LERMAN, D. A., PRASAD, S. & ALOTTI, N. 2015. Calcific Aortic Valve Disease: Molecular Mechanisms and Therapeutic Approaches. *Eur Cardiol,* 10**,** 108-112.

LEVINE, J. H., SIMONDS, E. F., BENDALL, S. C., DAVIS, K. L., AMIR EL, A. D., TADMOR, M. D., LITVIN, O., FIENBERG, H. G., JAGER, A., ZUNDER, E. R., FINCK, R., GEDMAN, A. L., RADTKE, I., DOWNING, J. R., PE'ER, D. & NOLAN, G. P. 2015. Data-Driven Phenotypic Dissection of AML Reveals Progenitor-like Cells that Correlate with Prognosis. *Cell,* 162**,** 184-97.

LI, C., LI, J. & NI, H. 2020. Crosstalk Between Platelets and Microbial Pathogens. *Front Immunol,* 11**,** 1962.

LIEVENS, D. & VON HUNDELSHAUSEN, P. 2011. Platelets in atherosclerosis. *Thromb Haemost,* 106**,** 827-38.

LINDEN, M. D., FURMAN, M. I., FRELINGER, A. L., 3RD, FOX, M. L., BARNARD, M. R., LI, Y., PRZYKLENK, K. & MICHELSON, A. D. 2007. Indices of platelet activation and the stability of coronary artery disease. *J Thromb Haemost,* 5**,** 761-5.

LINDMAN, B. R., CLAVEL, M. A., MATHIEU, P., IUNG, B., LANCELLOTTI, P., OTTO, C. M. & PIBAROT, P. 2016. Calcific aortic stenosis. *Nat Rev Dis Primers,* 2**,** 16006.

LU, J., CHATTERJEE, M., SCHMID, H., BECK, S. & GAWAZ, M. 2016. CXCL14 as an emerging immune and inflammatory modulator. *J Inflamm (Lond),* 13**,** 1.

MANNE, B. K., DENORME, F., MIDDLETON, E. A., PORTIER, I., ROWLEY, J. W., STUBBEN, C., PETREY, A. C., TOLLEY, N. D., GUO, L., CODY, M., WEYRICH, A. S., YOST, C. C., RONDINA, M. T. & CAMPBELL, R. A. 2020. Platelet gene expression and function in patients with COVID-19. *Blood,* 136**,** 1317-1329.

MAOUIA, A., REBETZ, J., KAPUR, R. & SEMPLE, J. W. 2020. The Immune Nature of Platelets Revisited. *Transfus Med Rev,* 34**,** 209-220.

MARCOVECCHIO, P. M., THOMAS, G. D., MIKULSKI, Z., EHINGER, E., MUELLER, K. A. L., BLATCHLEY, A., WU, R., MILLER, Y. I., NGUYEN, A. T., TAYLOR, A. M., MCNAMARA, C. A., LEY, K. & HEDRICK, C. C. 2017. Scavenger Receptor CD36 Directs Nonclassical Monocyte Patrolling Along the Endothelium During Early Atherogenesis. *Arterioscler Thromb Vasc Biol,* 37**,** 2043-2052.

MARTIN, J. F., KRISTENSEN, S. D., MATHUR, A., GROVE, E. L. & CHOUDRY, F. A. 2012. The causal role of megakaryocyte-platelet hyperactivity in acute coronary syndromes. *Nat Rev Cardiol,* 9**,** 658-70.

MASSBERG, S., BRAND, K., GRUNER, S., PAGE, S., MULLER, E., MULLER, I., BERGMEIER, W., RICHTER, T., LORENZ, M., KONRAD, I., NIESWANDT, B. & GAWAZ, M. 2002. A critical role of platelet adhesion in the initiation of atherosclerotic lesion formation. *J Exp Med,* 196**,** 887-96.

MASSBERG, S., KONRAD, I., SCHURZINGER, K., LORENZ, M., SCHNEIDER, S., ZOHLNHOEFER, D., HOPPE, K., SCHIEMANN, M., KENNERKNECHT, E., SAUER, S., SCHULZ, C., KERSTAN, S., RUDELIUS, M., SEIDL, S., SORGE, F., LANGER, H., PELUSO, M., GOYAL, P., VESTWEBER, D., EMAMBOKUS, N. R., BUSCH, D. H., FRAMPTON, J. & GAWAZ, M. 2006. Platelets secrete stromal cell-derived factor 1alpha and recruit bone marrow-derived progenitor cells to arterial thrombi in vivo. *J Exp Med,* 203**,** 1221-33.

MERAD, M. & MARTIN, J. C. 2020. Pathological inflammation in patients with COVID-19: a key role for monocytes and macrophages. *Nat Rev Immunol,* 20**,** 355-362.

METZEMAEKERS, M., GOUWY, M. & PROOST, P. 2020. Neutrophil chemoattractant receptors in health and disease: double-edged swords. *Cell Mol Immunol,* 17**,** 433-450.

MORAND, E. F., LEECH, M. & BERNHAGEN, J. 2006. MIF: a new cytokine link between rheumatoid arthritis and atherosclerosis. *Nat Rev Drug Discov,* 5**,** 399-410.

MORRELL, C. N., AGGREY, A. A., CHAPMAN, L. M. & MODJESKI, K. L. 2014. Emerging roles for platelets as immune and inflammatory cells. *Blood,* 123**,** 2759-67.

MUELLER, K. A. L., LANGNAU, C., GUNTER, M., POSCHEL, S., GEKELER, S., PETERSEN-URIBE, A., KREISSELMEIER, K. P., KLINGEL, K., BOSMULLER, H., LI, B., JAEGER, P., CASTOR, T., RATH, D., GAWAZ, M. P. & AUTENRIETH, S. E. 2021. Numbers and phenotype of non-classical CD14dimCD16+ monocytes are predictors of adverse clinical outcome in patients with coronary artery disease and severe SARS-CoV-2 infection. *Cardiovasc Res,* 117**,** 224-239.

MUELLER, K. A. L., LANGNAU, C., HARM, T., SIGLE, M., DROPPA, M., ILG, M., ROHLFING, A. K., GEKELER, S., LI, B., GÜNTER, M., GÖBEL, N., FRANKE, U., RADWAN, M., SCHLENSAK, C., RASHED, N., JANNING, H., KHAN, Z., RATH, D., KREISSELMEIER, K. P., CASTOR, T., MUELLER, I., AUTENRIETH, S. E. & GAWAZ, M. *in revision*. Macrophage migration inhibitory factor promotes thrombo-inflammation in fast progressive aortic stenosis and predicts unfavorable outcome.

MULLER, II, CHATTERJEE, M., SCHNEIDER, M., BORST, O., SEIZER, P., SCHONBERGER, T., VOGEL, S., MULLER, K. A., GEISLER, T., LANG, F., LANGER, H. & GAWAZ, M. 2014a. Gremlin-1 inhibits macrophage migration inhibitory factor-dependent monocyte function and survival. *Int J Cardiol,* 176**,** 923-9.

MULLER, II, MULLER, K. A., KARATHANOS, A., SCHONLEBER, H., RATH, D., VOGEL, S., CHATTERJEE, M., SCHMID, M., HAAS, M., SEIZER, P., LANGER, H., SCHAEFFELER, E., SCHWAB, M., GAWAZ, M. & GEISLER, T. 2014b. Impact of counterbalance between macrophage migration inhibitory factor and its inhibitor Gremlin-1 in patients with coronary artery disease. *Atherosclerosis,* 237**,** 426-32.

MULLER, I., SCHONBERGER, T., SCHNEIDER, M., BORST, O., ZIEGLER, M., SEIZER, P., LEDER, C., MULLER, K., LANG, M., APPENZELLER, F., LUNOV, O., BUCHELE, B., FAHRLEITNER, M., OLBRICH, M., LANGER, H., GEISLER, T., LANG, F., CHATTERJEE, M., DE BOER, J. F., TIETGE, U. J., BERNHAGEN, J., SIMMET, T. & GAWAZ, M. 2013. Gremlin-1 is an inhibitor of macrophage migration inhibitory factor and attenuates atherosclerotic plaque growth in ApoE-/- Mice. *J Biol Chem,* 288**,** 31635-45.

NAEIM F, R. P., SONG S, PHAN R 2018. *Atlas of Hematopathology*

Morphology, Immunophenotype, Cytogenetics, and Molecular Approaches, Elsevier.

NAKAYAMA, K. 1997. Furin: a mammalian subtilisin/Kex2p-like endoprotease involved in processing of a wide variety of precursor proteins. *Biochem J,* 327 (Pt 3)**,** 625-35.

NARASIMHAN, P. B., MARCOVECCHIO, P., HAMERS, A. A. J. & HEDRICK, C. C. 2019. Nonclassical Monocytes in Health and Disease. *Annu Rev Immunol,* 37**,** 439-456.

NATORSKA, J., BYKOWSKA, K., HLAWATY, M., MAREK, G., SADOWSKI, J. & UNDAS, A. 2011. Increased thrombin generation and platelet activation are associated with deficiency in high molecular weight multimers of von Willebrand factor in patients with moderate-to-severe aortic stenosis. *Heart,* 97**,** 2023-8.

NICOLAI, L., LEUNIG, A., BRAMBS, S., KAISER, R., WEINBERGER, T., WEIGAND, M., MUENCHHOFF, M., HELLMUTH, J. C., LEDDEROSE, S., SCHULZ, H., SCHERER, C., RUDELIUS, M., ZOLLER, M., HOCHTER, D., KEPPLER, O., TEUPSER, D., ZWISSLER, B., VON BERGWELT-BAILDON, M., KAAB, S., MASSBERG, S., PEKAYVAZ, K. & STARK, K. 2020. Immunothrombotic Dysregulation in COVID-19 Pneumonia Is Associated With Respiratory Failure and Coagulopathy. *Circulation,* 142**,** 1176-1189.

NIKOLSKY, E., GRINES, C. L., COX, D. A., GARCIA, E., TCHENG, J. E., SADEGHI, M., MEHRAN, R., LANSKY, A. J., NA, Y. & STONE, G. W. 2007. Impact of baseline platelet count in patients undergoing primary percutaneous coronary intervention in acute myocardial infarction (from the CADILLAC trial). *Am J Cardiol,* 99**,** 1055-61.

NISHIGA, M., WANG, D. W., HAN, Y., LEWIS, D. B. & WU, J. C. 2020. COVID-19 and cardiovascular disease: from basic mechanisms to clinical perspectives. *Nat Rev Cardiol,* 17**,** 543-558.

NKOMO, V. T., GARDIN, J. M., SKELTON, T. N., GOTTDIENER, J. S., SCOTT, C. G. & ENRIQUEZ-SARANO, M. 2006. Burden of valvular heart diseases: a population-based study. *Lancet,* 368**,** 1005-11.

NORDING, H., BARON, L. & LANGER, H. F. 2020. Platelets as therapeutic targets to prevent atherosclerosis. *Atherosclerosis,* 307**,** 97-108.

NORDING, H. M., SEIZER, P. & LANGER, H. F. 2015. Platelets in inflammation and atherogenesis. *Front Immunol,* 6**,** 98.

OREN OHAD, K. S. L., GLUCKMAN TYLER J., GERSH BERNARD J., BLUMENTHAL ROGER S. . 2020. *Coronavirus Disease 2019 (COVID-19): Epidemiology, Clinical Spectrum and Implications for the Cardiovascular Clinician* [Online]. Available: https://www.acc.org/latest-in-cardiology/articles/2020/04/06/11/08/covid-19-epidemiology-clinical-spectrum-and-implications-for-the-cv-clinician [Accessed May 11, 2020].

OSNABRUGGE, R. L., MYLOTTE, D., HEAD, S. J., VAN MIEGHEM, N. M., NKOMO, V. T., LEREUN, C. M., BOGERS, A. J., PIAZZA, N. & KAPPETEIN, A. P. 2013. Aortic stenosis in the elderly: disease prevalence and number of candidates for transcatheter aortic valve replacement: a meta-analysis and modeling study. *J Am Coll Cardiol,* 62**,** 1002-12.

PAN, J. H., SUKHOVA, G. K., YANG, J. T., WANG, B., XIE, T., FU, H., ZHANG, Y., SATOSKAR, A. R., DAVID, J. R., METZ, C. N., BUCALA, R., FANG, K., SIMON, D. I., CHAPMAN, H. A., LIBBY, P. & SHI, G. P. 2004. Macrophage migration inhibitory factor deficiency impairs atherosclerosis in low-density lipoprotein receptor-deficient mice. *Circulation,* 109**,** 3149-53.

PAWADE, T. A., NEWBY, D. E. & DWECK, M. R. 2015. Calcification in Aortic Stenosis: The Skeleton Key. *J Am Coll Cardiol,* 66**,** 561-77.

POISSY, J., GOUTAY, J., CAPLAN, M., PARMENTIER, E., DUBURCQ, T., LASSALLE, F., JEANPIERRE, E., RAUCH, A., LABREUCHE, J., SUSEN, S. & LILLE, I. C. U. H. C.-G. 2020. Pulmonary

Embolism in Patients With COVID-19: Awareness of an Increased Prevalence. *Circulation,* 142**,** 184-186.

PORTIER, I. & CAMPBELL, R. A. 2021. Role of Platelets in Detection and Regulation of Infection. *Arterioscler Thromb Vasc Biol,* 41**,** 70-78.

QIN, C., ZHOU, L., HU, Z., ZHANG, S., YANG, S., TAO, Y., XIE, C., MA, K., SHANG, K., WANG, W. & TIAN, D. S. 2020. Dysregulation of Immune Response in Patients With Coronavirus 2019 (COVID-19) in Wuhan, China. *Clin Infect Dis,* 71**,** 762-768.

RAADSEN, M., DU TOIT, J., LANGERAK, T., VAN BUSSEL, B., VAN GORP, E. & GOEIJENBIER, M. 2021. Thrombocytopenia in Virus Infections. *J Clin Med,* 10.

RADDATZ, M. A., MADHUR, M. S. & MERRYMAN, W. D. 2019. Adaptive immune cells in calcific aortic valve disease. *Am J Physiol Heart Circ Physiol,* 317**,** H141-H155.

RAJAMANNAN, N. M., BONOW, R. O. & RAHIMTOOLA, S. H. 2007. Calcific aortic stenosis: an update. *Nat Clin Pract Cardiovasc Med,* 4**,** 254-62.

RAJAMANNAN, N. M., EVANS, F. J., AIKAWA, E., GRANDE-ALLEN, K. J., DEMER, L. L., HEISTAD, D. D., SIMMONS, C. A., MASTERS, K. S., MATHIEU, P., O'BRIEN, K. D., SCHOEN, F. J., TOWLER, D. A., YOGANATHAN, A. P. & OTTO, C. M. 2011. Calcific aortic valve disease: not simply a degenerative process: A review and agenda for research from the National Heart and Lung and Blood Institute Aortic Stenosis Working Group. Executive summary: Calcific aortic valve disease-2011 update. *Circulation,* 124**,** 1783-91.

RAJENDRAN, P., RENGARAJAN, T., THANGAVEL, J., NISHIGAKI, Y., SAKTHISEKARAN, D., SETHI, G. & NISHIGAKI, I. 2013. The vascular endothelium and human diseases. *Int J Biol Sci,* 9**,** 1057-69.

RAMAN, B., BLUEMKE, D. A., LUSCHER, T. F. & NEUBAUER, S. 2022. Long COVID: post-acute sequelae of COVID-19 with a cardiovascular focus. *Eur Heart J,* 43**,** 1157-1172.

RANGU, R., WANDER, P. L., BARROW, B. M. & ZRAIKA, S. 2022. Going viral in the islet: mediators of SARS-CoV-2 entry beyond ACE2. *J Mol Endocrinol,* 69**,** R63-R79.

RAPKIEWICZ, A. V., MAI, X., CARSONS, S. E., PITTALUGA, S., KLEINER, D. E., BERGER, J. S., THOMAS, S., ADLER, N. M., CHARYTAN, D. M., GASMI, B., HOCHMAN, J. S. & REYNOLDS, H. R. 2020. Megakaryocytes and platelet-fibrin thrombi characterize multi-organ thrombosis at autopsy in COVID-19: A case series. *EClinicalMedicine,* 24**,** 100434.

RATH, D., PETERSEN-URIBE, A., AVDIU, A., WITZEL, K., JAEGER, P., ZDANYTE, M., HEINZMANN, D., TAVLAKI, E., MULLER, K. & GAWAZ, M. P. 2020. Impaired cardiac function is associated with mortality in patients with acute COVID-19 infection. *Clin Res Cardiol,* 109**,** 1491-1499.

REINTHALER, M., BRAUNE, S., LENDLEIN, A., LANDMESSER, U. & JUNG, F. 2016. Platelets and coronary artery disease: Interactions with the blood vessel wall and cardiovascular devices. *Biointerphases,* 11**,** 029702.

RIBEIRO, L. S., MIGLIARI BRANCO, L. & FRANKLIN, B. S. 2019. Regulation of Innate Immune Responses by Platelets. *Front Immunol,* 10**,** 1320.

ROUSE, B. T. & SEHRAWAT, S. 2010. Immunity and immunopathology to viruses: what decides the outcome? *Nat Rev Immunol,* 10**,** 514-26.

RUIZ-ROSADO JDE, D., OLGUIN, J. E., JUAREZ-AVELAR, I., SAAVEDRA, R., TERRAZAS, L. I., ROBLEDO-AVILA, F. H., VAZQUEZ-MENDOZA, A., FERNANDEZ, J., SATOSKAR, A. R., PARTIDA-SANCHEZ, S. & RODRIGUEZ-SOSA, M. 2016. MIF Promotes Classical Activation and Conversion of

Inflammatory Ly6C(high) Monocytes into TipDCs during Murine Toxoplasmosis. *Mediators Inflamm,* 2016**,** 9101762.

RUTKOVSKIY, A., MALASHICHEVA, A., SULLIVAN, G., BOGDANOVA, M., KOSTAREVA, A., STENSLOKKEN, K. O., FIANE, A. & VAAGE, J. 2017. Valve Interstitial Cells: The Key to Understanding the Pathophysiology of Heart Valve Calcification. *J Am Heart Assoc,* 6.

SALAS, M. J., SANTANA, O., ESCOLAR, E. & LAMAS, G. A. 2012. Medical therapy for calcific aortic stenosis. *J Cardiovasc Pharmacol Ther,* 17**,** 133-8.

SANCHEZ-CERRILLO, I., LANDETE, P., ALDAVE, B., SANCHEZ-ALONSO, S., SANCHEZ-AZOFRA, A., MARCOS-JIMENEZ, A., AVALOS, E., ALCARAZ-SERNA, A., DE LOS SANTOS, I., MATEU-ALBERO, T., ESPARCIA, L., LOPEZ-SANZ, C., MARTINEZ-FLETA, P., GABRIE, L., DEL CAMPO GUEROLA, L., DE LA FUENTE, H., CALZADA, M. J., GONZALEZ-ALVARO, I., ALFRANCA, A., SANCHEZ-MADRID, F., MUNOZ-CALLEJA, C., SORIANO, J. B., ANCOCHEA, J., MARTIN-GAYO, E., REINMUN, C. & GROUPS, E. 2020. COVID-19 severity associates with pulmonary redistribution of CD1c+ DCs and inflammatory transitional and nonclassical monocytes. *J Clin Invest,* 130**,** 6290-6300.

SANCHEZ-MARTIN, L., SANCHEZ-MATEOS, P. & CABANAS, C. 2013. CXCR7 impact on CXCL12 biology and disease. *Trends Mol Med,* 19**,** 12-22.

SAWANT, K. V., POLURI, K. M., DUTTA, A. K., SEPURU, K. M., TROSHKINA, A., GAROFALO, R. P. & RAJARATHNAM, K. 2016. Chemokine CXCL1 mediated neutrophil recruitment: Role of glycosaminoglycan interactions. *Sci Rep,* 6**,** 33123.

SCHOBER, A., BERNHAGEN, J., THIELE, M., ZEIFFER, U., KNARREN, S., ROLLER, M., BUCALA, R. & WEBER, C. 2004. Stabilization of atherosclerotic plaques by blockade of macrophage migration inhibitory factor after vascular injury in apolipoprotein E-deficient mice. *Circulation,* 109**,** 380-5.

SHANG, J., WAN, Y., LUO, C., YE, G., GENG, Q., AUERBACH, A. & LI, F. 2020. Cell entry mechanisms of SARS-CoV-2. *Proc Natl Acad Sci U S A,* 117**,** 11727-11734.

SHANTSILA, E., WRIGLEY, B., TAPP, L., APOSTOLAKIS, S., MONTORO-GARCIA, S., DRAYSON, M. T. & LIP, G. Y. 2011. Immunophenotypic characterization of human monocyte subsets: possible implications for cardiovascular disease pathophysiology. *J Thromb Haemost,* 9**,** 1056-66.

SHI, C. & PAMER, E. G. 2011. Monocyte recruitment during infection and inflammation. *Nat Rev Immunol,* 11**,** 762-74.

SONG, R., FULLERTON, D. A., AO, L., ZHENG, D., ZHAO, K. S. & MENG, X. 2015. BMP-2 and TGF-beta1 mediate biglycan-induced pro-osteogenic reprogramming in aortic valve interstitial cells. *J Mol Med (Berl),* 93**,** 403-12.

STAWOWY, P., KALLISCH, H., BORGES PEREIRA STAWOWY, N., STIBENZ, D., VEINOT, J. P., GRAFE, M., SEIDAH, N. G., CHRETIEN, M., FLECK, E. & GRAF, K. 2005. Immunohistochemical localization of subtilisin/kexin-like proprotein convertases in human atherosclerosis. *Virchows Arch,* 446**,** 351-9.

STERN-GINOSSAR, N. & MANDELBOIM, O. 2009. An integrated view of the regulation of NKG2D ligands. *Immunology,* 128**,** 1-6.

STRUSSMANN, T., TILLMANN, S., WIRTZ, T., BUCALA, R., VON HUNDELSHAUSEN, P. & BERNHAGEN, J. 2013. Platelets are a previously unrecognised source of MIF. *Thromb Haemost,* 110**,** 1004-13.

SUN, H. W., BERNHAGEN, J., BUCALA, R. & LOLIS, E. 1996. Crystal structure at 2.6-A resolution of human macrophage migration inhibitory factor. *Proc Natl Acad Sci U S A,* 93**,** 5191-6.

SURENDRAN, A., EDEL, A., CHANDRAN, M., BOGAERT, P., HASSAN-TASH, P., KUMAR ASOKAN, A., HIEBERT, B., SOLATI, Z., SANDHAWALIA, S., RAABE, M., KASS, M., SHAH, A., JASSAL, D. S., JALEEL, A. & RAVANDI, A. 2020. Metabolomic Signature of Human Aortic Valve Stenosis. *JACC Basic Transl Sci,* 5**,** 1163-1177.

SWIRSKI, F. K. & NAHRENDORF, M. 2018. Cardioimmunology: the immune system in cardiac homeostasis and disease. *Nat Rev Immunol,* 18**,** 733-744.

TANG, L., YIN, Z., HU, Y. & MEI, H. 2020a. Controlling Cytokine Storm Is Vital in COVID-19. *Front Immunol,* 11**,** 570993.

TANG, N., BAI, H., CHEN, X., GONG, J., LI, D. & SUN, Z. 2020b. Anticoagulant treatment is associated with decreased mortality in severe coronavirus disease 2019 patients with coagulopathy. *J Thromb Haemost,* 18**,** 1094-1099.

TASK FORCE FOR THE MANAGEMENT OF, C.-O. T. E. S. O. C. 2022. European Society of Cardiology guidance for the diagnosis and management of cardiovascular disease during the COVID-19 pandemic: part 1-epidemiology, pathophysiology, and diagnosis. *Eur Heart J,* 43**,** 1033-1058.

THOMAS, G., TACKE, R., HEDRICK, C. C. & HANNA, R. N. 2015. Nonclassical patrolling monocyte function in the vasculature. *Arterioscler Thromb Vasc Biol,* 35**,** 1306-16.

VAHANIAN, A., BEYERSDORF, F., PRAZ, F., MILOJEVIC, M., BALDUS, S., BAUERSACHS, J., CAPODANNO, D., CONRADI, L., DE BONIS, M., DE PAULIS, R., DELGADO, V., FREEMANTLE, N., GILARD, M., HAUGAA, K. H., JEPPSSON, A., JUNI, P., PIERARD, L., PRENDERGAST, B. D., SADABA, J. R., TRIBOUILLOY, C., WOJAKOWSKI, W. & GROUP, E. E. S. D. 2021. 2021 ESC/EACTS Guidelines for the management of valvular heart disease. *Eur J Cardiothorac Surg,* 60**,** 727-800.

VAN DER VORST, E. P., DORING, Y. & WEBER, C. 2015. MIF and CXCL12 in Cardiovascular Diseases: Functional Differences and Similarities. *Front Immunol,* 6**,** 373.

VASSE, M., ZUBER, B., GOUBEAU, L., BALLESTER, M. C., ROUMIER, M., DELCOMINETTE, F., HABAROU, F., JOLLY, E., ACKERMANN, F., CERF, C., FARFOUR, E., PASCREAU, T. & GROUP, S. A.-C.-F. H. S. 2021. A low level of CD16(pos) monocytes in SARS-CoV-2 infected patients is a marker of severity. *Clin Chem Lab Med,* 59**,** 1315-1322.

VON HUNDELSHAUSEN, P. & SCHMITT, M. M. 2014. Platelets and their chemokines in atherosclerosis-clinical applications. *Front Physiol,* 5**,** 294.

WALLS, A. C., PARK, Y. J., TORTORICI, M. A., WALL, A., MCGUIRE, A. T. & VEESLER, D. 2020. Structure, Function, and Antigenicity of the SARS-CoV-2 Spike Glycoprotein. *Cell,* 181**,** 281-292 e6.

WANG, Y. K., TANG, J. N., HAN, L., LIU, X. D., SHEN, Y. L., ZHANG, C. Y. & LIU, X. B. 2020. Elevated FURIN levels in predicting mortality and cardiovascular events in patients with acute myocardial infarction. *Metabolism,* 111**,** 154323.

WHO. 2022. *WHO Coronavirus (COVID-19) Dashboard* [Online]. Available: https://covid19.who.int/ [Accessed 05.12.2022].

WIRTZ, T. H., TILLMANN, S., STRUSSMANN, T., KRAEMER, S., HEEMSKERK, J. W., GROTTKE, O., GAWAZ, M., VON HUNDELSHAUSEN, P. & BERNHAGEN, J. 2015. Platelet-derived MIF: a novel platelet chemokine with distinct recruitment properties. *Atherosclerosis,* 239**,** 1-10.

WITTE, A., CHATTERJEE, M., LANG, F. & GAWAZ, M. 2017. Platelets as a Novel Source of Pro-Inflammatory Chemokine CXCL14. *Cell Physiol Biochem,* 41**,** 1684-1696.

WITTE, A., ROHLFING, A. K., DANNENMANN, B., DICENTA, V., NASRI, M., KOLB, K., SUDMANN, J., CASTOR, T., RATH, D., BORST, O., SKOKOWA, J. & GAWAZ, M. 2021. The chemokine CXCL14 mediates platelet function and migration via direct interaction with CXCR4. *Cardiovasc Res,* 117**,** 903-917.

WOLF, D. & LEY, K. 2019. Immunity and Inflammation in Atherosclerosis. *Circ Res,* 124**,** 315-327.

WOOLLARD, K. J. & GEISSMANN, F. 2010. Monocytes in atherosclerosis: subsets and functions. *Nat Rev Cardiol,* 7**,** 77-86.

WRITING COMMITTEE, M., OTTO, C. M., NISHIMURA, R. A., BONOW, R. O., CARABELLO, B. A., ERWIN, J. P., 3RD, GENTILE, F., JNEID, H., KRIEGER, E. V., MACK, M., MCLEOD, C., O'GARA, P. T., RIGOLIN, V. H., SUNDT, T. M., 3RD, THOMPSON, A., TOLY, C., MEMBERS, A. A. J. C., O'GARA, P. T., BECKMAN, J. A., LEVINE, G. N., AL-KHATIB, S. M., ARMBRUSTER, A., BIRTCHER, K. K., CIGGAROA, J., DESWAL, A., DIXON, D. L., FLEISHER, L. A., DE LAS FUENTES, L., GENTILE, F., GOLDBERGER, Z. D., GORENEK, B., HAYNES, N., HERNANDEZ, A. F., HLATKY, M. A., JOGLAR, J. A., JONES, W. S., MARINE, J. E., MARK, D., PALANIAPPAN, L., PIANO, M. R., SPATZ, E. S., TAMIS-HOLLAND, J., WIJEYSUNDERA, D. N. & WOO, Y. J. 2021. 2020 ACC/AHA guideline for the management of patients with valvular heart disease: A report of the American College of Cardiology/American Heart Association Joint Committee on Clinical Practice Guidelines. *J Thorac Cardiovasc Surg,* 162**,** e183-e353.

WURSTER, T., STELLOS, K., HAAP, M., SEIZER, P., GEISLER, T., OTTON, J., INDERMUEHLE, A., ISHIDA, M., SCHUSTER, A., NAGEL, E., GAWAZ, M. & BIGALKE, B. 2013. Platelet expression of stromal-cell-derived factor-1 (SDF-1): an indicator for ACS? *Int J Cardiol,* 164**,** 111-5.

WURSTER, T., TEGTMEYER, R., BORST, O., RATH, D., GEISLER, T., GAWAZ, M. & BIGALKE, B. 2014. Platelet expression of stromal cell-derived factor-1 is associated with the degree of valvular aortic stenosis. *PLoS One,* 9**,** e97405.

XIE, J., TONG, Z., GUAN, X., DU, B. & QIU, H. 2020. Clinical Characteristics of Patients Who Died of Coronavirus Disease 2019 in China. *JAMA Netw Open,* 3**,** e205619.

XIONG, T. Y., REDWOOD, S., PRENDERGAST, B. & CHEN, M. 2020. Coronaviruses and the cardiovascular system: acute and long-term implications. *Eur Heart J,* 41**,** 1798-1800.

YAKALA, G. K., CABRERA-FUENTES, H. A., CRESPO-AVILAN, G. E., RATTANASOPA, C., BURLACU, A., GEORGE, B. L., ANAND, K., MAYAN, D. C., CORLIANO, M., HERNANDEZ-RESENDIZ, S., WU, Z., SCHWERK, A. M. K., TAN, A. L. J., TRIGUEROS-MOTOS, L., CHEVRE, R., CHUA, T., KLEEMANN, R., LIEHN, E. A., HAUSENLOY, D. J., GHOSH, S. & SINGARAJA, R. R. 2019. FURIN Inhibition Reduces Vascular Remodeling and Atherosclerotic Lesion Progression in Mice. *Arterioscler Thromb Vasc Biol,* 39**,** 387-401.

YANG, J., ZHANG, L., YU, C., YANG, X. F. & WANG, H. 2014. Monocyte and macrophage differentiation: circulation inflammatory monocyte as biomarker for inflammatory diseases. *Biomark Res,* 2**,** 1.

YANG, X., YANG, Q., WANG, Y., WU, Y., XU, J., YU, Y. & SHANG, Y. 2020a. Thrombocytopenia and its association with mortality in patients with COVID-19. *J Thromb Haemost,* 18**,** 1469-1472.

YANG, X., YANG, W., MCVEY, D. G., ZHAO, G., HU, J., POSTON, R. N., REN, M., WILLEIT, K., COASSIN, S., WILLEIT, J., WEBB, T. R., SAMANI, N. J., MAYR, M., KIECHL, S. & YE, S. 2020b. FURIN

Expression in Vascular Endothelial Cells Is Modulated by a Coronary Artery Disease-Associated Genetic Variant and Influences Monocyte Transendothelial Migration. *J Am Heart Assoc,* 9**,** e014333.

YEAMAN, M. R. 2010. Platelets in defense against bacterial pathogens. *Cell Mol Life Sci,* 67**,** 525-44.

YEAMAN, M. R. 2014. Platelets: at the nexus of antimicrobial defence. *Nat Rev Microbiol,* 12**,** 426-37.

ZAID, Y., GUESSOUS, F., PUHM, F., ELHAMDANI, W., CHENTOUFI, L., MORRIS, A. C., CHEIKH, A., JALALI, F., BOILARD, E. & FLAMAND, L. 2021. Platelet reactivity to thrombin differs between patients with COVID-19 and those with ARDS unrelated to COVID-19. *Blood Adv,* 5**,** 635-639.

ZAID, Y., PUHM, F., ALLAEYS, I., NAYA, A., OUDGHIRI, M., KHALKI, L., LIMAMI, Y., ZAID, N., SADKI, K., BEN EL HAJ, R., MAHIR, W., BELAYACHI, L., BELEFQUIH, B., BENOUDA, A., CHEIKH, A., LANGLOIS, M. A., CHERRAH, Y., FLAMAND, L., GUESSOUS, F. & BOILARD, E. 2020. Platelets Can Associate with SARS-Cov-2 RNA and Are Hyperactivated in COVID-19. *Circ Res*.

ZERNECKE, A., BERNHAGEN, J. & WEBER, C. 2008. Macrophage migration inhibitory factor in cardiovascular disease. *Circulation,* 117**,** 1594-602.

ZERNECKE, A. & WEBER, C. 2005. Inflammatory mediators in atherosclerotic vascular disease. *Basic Res Cardiol,* 100**,** 93-101.

ZERNECKE, A., WINKELS, H., COCHAIN, C., WILLIAMS, J. W., WOLF, D., SOEHNLEIN, O., ROBBINS, C. S., MONACO, C., PARK, I., MCNAMARA, C. A., BINDER, C. J., CYBULSKY, M. I., SCIPIONE, C. A., HEDRICK, C. C., GALKINA, E. V., KYAW, T., GHOSHEH, Y., DINH, H. Q. & LEY, K. 2020. Meta-Analysis of Leukocyte Diversity in Atherosclerotic Mouse Aortas. *Circ Res,* 127**,** 402-426.

ZHANG, J. M. & AN, J. 2007. Cytokines, inflammation, and pain. *Int Anesthesiol Clin,* 45**,** 27-37.

ZHAO, G., YANG, W., WU, J., CHEN, B., YANG, X., CHEN, J., MCVEY, D. G., ANDREADI, C., GONG, P., WEBB, T. R., SAMANI, N. J. & YE, S. 2018. Influence of a Coronary Artery Disease-Associated Genetic Variant on FURIN Expression and Effect of Furin on Macrophage Behavior. *Arterioscler Thromb Vasc Biol,* 38**,** 1837-1844.

ZHAO, Q., MEN, L., LI, X. M., LIU, F., SHAN, C. F., ZHOU, X. R., SONG, N., ZHU, J. J., GAO, X. L., MA, Y. T., DU, X. J., GAO, X. M. & YANG, Y. N. 2019. Circulating MIF Levels Predict Clinical Outcomes in Patients With ST-Elevation Myocardial Infarction After Percutaneous Coronary Intervention. *Can J Cardiol,* 35**,** 1366-1376.

ZHENG, K. H., TZOLOS, E. & DWECK, M. R. 2020a. Pathophysiology of Aortic Stenosis and Future Perspectives for Medical Therapy. *Cardiol Clin,* 38**,** 1-12.

ZHENG, Y. Y., MA, Y. T., ZHANG, J. Y. & XIE, X. 2020b. COVID-19 and the cardiovascular system. *Nat Rev Cardiol,* 17**,** 259-260.

ZHOU, F., YU, T., DU, R., FAN, G., LIU, Y., LIU, Z., XIANG, J., WANG, Y., SONG, B., GU, X., GUAN, L., WEI, Y., LI, H., WU, X., XU, J., TU, S., ZHANG, Y., CHEN, H. & CAO, B. 2020. Clinical course and risk factors for mortality of adult inpatients with COVID-19 in Wuhan, China: a retrospective cohort study. *Lancet,* 395**,** 1054-1062.

ZIEGLER-HEITBROCK, L. 2007. The CD14+ CD16+ blood monocytes: their role in infection and inflammation. *J Leukoc Biol,* 81**,** 584-92.

ZIEGLER-HEITBROCK, L., ANCUTA, P., CROWE, S., DALOD, M., GRAU, V., HART, D. N., LEENEN, P. J., LIU, Y. J., MACPHERSON, G., RANDOLPH, G. J., SCHERBERICH, J., SCHMITZ, J., SHORTMAN, K., SOZZANI, S., STROBL, H., ZEMBALA, M., AUSTYN, J. M. & LUTZ, M. B. 2010. Nomenclature of monocytes and dendritic cells in blood. *Blood,* 116**,** e74-80.

5 Acknowledgment

At this point, I would like to thank all the people who contributed to the success of my dissertation.

First, I want to thank PD Dr. Karin Müller and Prof. Dr. Stella Autenrieth, my supervisors, who allowed me to work on this exciting project in their excellent working groups. I want to thank both of them for their support at any time, for any kind of question or problem, and for always giving me the help, advice, and helpful discussions I needed. I especially want to thank PD Dr. Karin Müller for her optimistic nature, which has always inspired me, and her confidence allowed me to develop my projects.

I want to thank my second supervisor Prof. Dr. Alex Weber, for his help, constructive discussions, and the evaluation of my PhD thesis.

My special thanks go to Sarah Gekeler, who helped me with everything around the lab, for always being there, answering every question, and helping with lab experiments. It was always fun working with you.

Furthermore, I want to thank the whole working group AG Autenrieth and AG Müller for making the last years inside and outside the lab so pleasant, and I thank AG Gawaz, especially Dr. Anne-Katrin Rohlfing, for the continuing good mood, great support and productive cooperation.

Lastly, I want to thank my family, especially my parents, for everything they have done for me over the past years, their support and their belief in me.

And of course, Sven for always being at my side and encouraging me. Without him, I would not have made it.

6 Appendix

1. Numbers and phenotype of non-classical CD14dimCD16+ monocytes are predictors of adverse clinical outcome in patients with coronary artery disease and severe SARS-CoV-2 infection

2. Recovery of systemic hyperinflammation in patients with severe SARS-CoV-2 infection

3. Platelet Activation and Plasma Levels of Furin Are Associated With Prognosis of Patients With Coronary Artery Disease and COVID-19

4. Macrophage migration inhibitory factor (MIF) promotes local and systemic thrombo-inflammation in fast progressive aortic stenosis and predicts unfavorable outcome

Numbers and phenotype of non-classical CD14dimCD16+ monocytes are predictors of adverse clinical outcome in patients with coronary artery disease and severe SARS-CoV-2 infection

Karin Anne Lydia Mueller[1], Carolin Langnau[1], Manina Günter[2], Simone Pöschel[2], Sarah Gekeler[1], Álvaro Petersen-Uribe[1], Klaus-Peter Kreisselmeier[1], Karin Klingel[3], Hans Bösmüller[3], Bo Li[1], Philippa Jaeger[1], Tatsiana Castor[1], Dominik Rath[1], Meinrad Paul Gawaz[1], Stella E. Autenrieth[2]

[1]University Hospital Tuebingen, Department of Cardiology and Angiology, Eberhard Karls University Tuebingen, Tuebingen, Germany

[2]University Hospital Tuebingen, Department of Hematology, Oncology, clinical Immunology and Rheumatology, Eberhard Karls University Tuebingen, Tuebingen, Germany

[3]University Hospital Tuebingen, Department of Molecular Pathology, Eberhard Karls University Tuebingen, Tuebingen, Germany

Mueller, Karin Anne Lydia et al. “Numbers and phenotype of non-classical CD14dimCD16+ monocytes are predictors of adverse clinical outcome in patients with coronary artery disease and severe SARS-CoV-2 infection.” Cardiovascular research vol. 117,1 (2021): 224-239. doi:10.1093/cvr/cvaa328

Numbers and phenotype of non-classical CD14^{dim}CD16^{+} monocytes are predictors of adverse clinical outcome in patients with coronary artery disease and severe SARS-CoV-2 infection

Karin Anne Lydia Mueller[1], Carolin Langnau[1], Manina Günter[2], Simone Pöschel[2], Sarah Gekeler[1], Álvaro Petersen-Uribe[1], Klaus-Peter Kreisselmeier[1], Karin Klingel[3], Hans Bösmüller[3], Bo Li[1], Philippa Jaeger[1], Tatsiana Castor[1], Dominik Rath[1], Meinrad Paul Gawaz[1], Stella E. Autenrieth[2]

[1]University Hospital Tuebingen, Department of Cardiology and Angiology, Eberhard Karls University Tuebingen, Tuebingen, Germany

[2]University Hospital Tuebingen, Department of Hematology, Oncology, clinical Immunology and Rheumatology, Eberhard Karls University Tuebingen, Tuebingen, Germany

[3]University Hospital Tuebingen, Department of Molecular Pathology, Eberhard Karls University Tuebingen, Tuebingen, Germany

Corresponding author:

Karin Anne Lydia Mueller, MD

Department of Cardiology and Angiology

University Hospital of the Eberhard Karls University Tuebingen

Otfried-Müller Str.10, 72076 Tuebingen, Germany

Tel: +49-7071-29-83688

Fax: +49-7071-29-4473

E-mail: k.mueller@med.uni-tuebingen.de

Short title: Monocytes predict outcome in COVID-19 patients

Keywords: Coronary artery disease; SARS-CoV-2 infection; respiratory failure; immuno-response; non-classical monocytes

Abstract

Aims: To elucidate the prognostic role of monocytes in the immune response of patients with coronary artery disease (CAD) at risk for life-threatening heart and lung injury as major complications of SARS-CoV-2 infection.

Methods and Results: From February to April 2020, we prospectively studied a cohort of 96 participants comprising 47 consecutive patients with CAD and acute SARS-CoV-2 infection (CAD+SARS-CoV-2), 19 CAD patients without infections, and 30 healthy controls. Clinical assessment included blood sampling, echocardiography, and electrocardiography within 12 hours of admission. Respiratory failure was stratified by the Horovitz Index (HI) as moderately/severely impaired when HI $\leq$ 200mmHg. The clinical endpoint (EP) was defined as HI $\leq$ 200mmHg with subsequent mechanical ventilation within a follow-up of 30 days.

The numbers of $CD14^{dim}CD16^{+}$ non-classical monocytes in peripheral blood were remarkably low in CAD+SARS-CoV-2 compared to CAD patients without infection and healthy controls ($p<0.0001$). Moreover, these $CD14^{dim}CD16$ monocytes showed decreased expression of established markers of adhesion, migration, and T cell activation (CD54, CD62L, CX3CR1, CD80, HLA-DR). Decreased numbers of $CD14^{dim}CD16^{+}$ monocytes were associated with the occurrence of EP. Kaplan-Meier curves illustrate that CAD+SARS-CoV-2 patients with numbers below the median of $CD14^{dim}CD16^{+}$ monocytes (median 1443 cells/mL) reached EP significantly more often compared to patients with numbers above the median (log-rank 5.03, $p=0.025$).

Conclusion: Decreased numbers of $CD14^{dim}CD16^{+}$ monocytes are associated with rapidly progressive respiratory failure in CAD+SARS-CoV-2 patients. Intensified risk assessments comprising monocyte sub- and phenotypes may help to identify patients at risk for respiratory failure.

Translational Perspective

Patients with coronary artery disease (CAD) are at risk of life-threatening heart and lung injury accelerated by the pro-inflammatory and pro-thrombotic immune response during SARS-CoV-2 infection. We found substantially low numbers of $CD14^{dim}CD16^{+}$ non-classical monocytes with an

altered phenotype suggesting impaired migration behaviour and T cell activation capacity in peripheral blood of SARS-CoV-2 patients with CAD, compared to CAD patients without infection or healthy controls. Decreased numbers of $CD14^{dim}CD16^{+}$ monocytes predicted rapidly progressive respiratory failure (Horovitz index $\leq$ 200mmHg) with subsequent mechanical ventilation. Therefore, early sub- and phenotyping of $CD14^{dim}CD16^{+}$ monocytes using simple flow cytometry might predict worsening of respiratory failure at an early stage of SARS-CoV-2 infection in high-risk CAD patients, who require an extensive heart failure and anti-thrombotic therapy to improve their clinical outcome.

1. Introduction

Patients with coronary artery disease (CAD) are at risk to develop severe courses of SARS-CoV-2 infection comprising life-threatening heart and lung injury which are some of the most frequent complications according to the current assessment of the European Society of Cardiology.[1, 2] SARS-CoV-2 infection leads to a pro-inflammatory and pro-thrombotic immune response which, in the presence of CAD, can often lead to acute coronary syndrome with subsequent impairment of left or right ventricular function.[3, 4] An accompanying myocarditis caused by SARS-CoV-2 infection has also been described in the literature.[5, 6] Viral myocarditis comprises a broad spectrum of symptoms ranging from asymptomatic to most severe clinical courses resulting in congestive heart failure and inflammatory cardiomyopathy with potentially life-threatening functional impairment of the ventricle and poor prognosis.[3, 5, 7] Patients with CAD are also particularly at risk for acute right heart failure due to pre-existing right heart and diastolic dysfunction as well as elevated pulmonary artery pressure.[1, 2] Right heart dysfunction is triggered by SARS-CoV-2 infection as pneumonic infiltrates and lung involvement, often associated with progressive respiratory failure and acute respiratory distress syndrome (ARDS), lead to an additional increase of pulmonary pressure and tricuspid regurgitation resulting in right heart overload and finally failure.[3] Furthermore, patients are at risk to develop pulmonary embolisms due to infect-associated coagulopathy resulting in acute right heart failure and disseminated intravascular coagulation.[4] These clinical scenarios explain the increased rate of organ failure, admissions to the intensive care unit (ICU) with rapidly progressive respiratory failure, and mortality in cardiovascular patients when SARS-CoV-2 infection occurs.[1-3, 7]

Chronic alterations of inflammatory mediators, like C-reactive protein (CRP), pro-inflammatory cytokines, or adhesion molecules trigger atherogenesis and -progression in CAD.[8] Up-regulation of the involved cytokines and chemokines recruit inflammatory cells like monocytes to the vessel wall causing atherosclerotic lesions.[8] Inflammatory cells like monocytes and macrophages have been implicated in many inflammatory heart diseases, e.g. CAD, myocardial infarction, myocarditis, and heart failure.[8-10] In humans, three distinct monocyte subpopulations have been classified based on their surface receptor expression into classical ($CD14^{+}CD16^{-}$), intermediate ($CD14^{+}CD16^{+}$), and non-classical ($CD14^{dim}CD16^{+}$) monocytes.[11, 12]

Classical monocytes secrete soluble mediators and differentiate into monocyte-derived dendritic cells (DCs) and therefore show a rather pro-inflammatory phenotype. Intermediate monocytes are specialized in antigen presentation, whereas non-classical monocytes are important for the anti-viral immune responses.[11-13] Non-classical monocytes predominantly remain in the vascular system and migrate along the endothelium. This process is termed patrolling and is mediated by their expression of the adhesion-related receptor CX3CR1 among others.[14, 15] An athero-protective role and also anti-inflammatory and pro-homeostatic effects of these patrolling non-classical monocytes have recently been suggested.[14] During infections viral RNA and DNA is recognized by non-classical ($CD14^{dim}CD16^{+}$) monocytes via TLR7 expression leading to the production of TNF-α, IL-1β, and CCL3.[14] In addition, in HIV-infected patients, a central role of TNF overproduction by non-classical monocytes has been proposed, indicating that they could be considered as key players in the immune hyperactivation of the disease.[12] Moreover, in viraemic HIV-infected patients a pivotal role by TNF overproduction was shown for non-classical monocytes, indicating that they might be considered as a major actor in the immune hyperactivation of the disease.[16] Furthermore, patients with HIV and subclinical atherosclerosis show altered expression of activation markers on non-classical monocytes.[17]

Coronavirus disease 2019 (COVID-19) has spread rapidly worldwide and is associated with significant mortality, especially in risk groups with poor prognostic features, such as CAD.[18] In hospitalized patients infected with SARS-CoV-2, the causative agent of COVID-19, pneumonia, sepsis, respiratory failure and ARDS are common complications.[18-20] The pathophysiology of SARS-CoV-2 is characterized by an early production of proinflammatory cytokines (tumour necrosis factor (TNF), IL-6, and IL-1β) described as a cytokine storm, resulting in an increased risk of vascular hyperpermeability and, if long-lasting, multiorgan failure, and eventually death.[20] This is mediated after entry of the coronavirus and the release of RNA as genomic material into the cell by activation of TLRs. The frequency of monocytes is reduced in patients with severe SARS-CoV-2 infection[21], however, the different monocyte subsets were not analysed in detail yet. On the other hand, increased frequencies of non-classical monocytes have been associated with the occurrence of acute coronary syndromes in the general population.[22] Thus, we analysed numbers of monocyte subsets and their

surface marker expression in CAD patients with and without SARS-CoV-2 infection in order to determine prognostic markers for treatment options.

2. Methods

Study design, participants, and assessment of clinical parameters

From February to April 2020 we prospectively studied a consecutive cohort of 96 participants. Out of these, 47 consecutive patients with pre-existing CAD and acute SARS-CoV-2 infection (CAD+SARS-CoV-2) were admitted with progressive respiratory failure. N=19 patients with pre-existing stable CAD without any infections were matched for the group of CAD+SARS-CoV-2 patients. N=30 healthy participants served as controls. All patients underwent clinical and cardiac assessment including echocardiography, electrocardiography, concomitant medication, comorbidities, and blood sampling for routine laboratory parameters and phenotyping of monocytes within 12 hours of admission. SARS-CoV-2 infection was diagnosed by RNA detection from nasopharyngeal secretions with real-time reverse transcriptase polymerase chain reaction. CAD was determined by coronary angiography in all patients before hospital admission. CAD was defined as >25-50% diameter luminal stenosis of two or more coronary vessels or left main or proximal left anterior descending coronary artery stenosis >50%. Respiratory failure was stratified into four groups by the Horovitz Index (HI) as follows: normal HI > 300 mmHg, mildly impaired HI 201 - 300 mmHg, moderately impaired HI 101 - 200 mmHg, severely impaired ≤ 100 mmHg.[23] All patients were admitted and treated at the Department of Cardiology and Angiology of the University Hospital of Tübingen, Germany.

Inclusion criteria of our study were an age older than 18 years and confirmed coronary artery disease with or without SARS-CoV-2 infection. Exclusion criteria were other viral or bacterial co-infections and cancer. The study was approved by the local ethics committee (240/2018BO2) and complies with the declaration of Helsinki and the good clinical practice guidelines on the approximation of the laws, regulations and administrative provisions of the member states relating to the implementation of good clinical practice in the conduct of clinical trials on medicinal products for human use. Written informed consent was obtained from every patient.

N terminal-pro-B-type natriuretic peptide (NT-pro-BNP, >300 ng/L), high sensitive troponine I (hs TNI, >37 ng/L) and C-reactive protein (CRP, >0.5 mg/dL) were classified as elevated laboratory markers of myocardial and inflammatory distress. Echocardiographic parameters included left and

right ventricular function, right ventricular dilatation, presence of tricuspid valve regurgitation, and pericardial effusion according to current guidelines.[24,25]

Clinical Follow-up

The clinical endpoint (EP) was defined as rapidly progressive respiratory failure with indication to mechanical ventilation characterized by a moderately or severely impaired Horovitz Index (moderately impaired HI defined as 101 - 200 mmHg, severely impaired HI defined as ≤ 100 mmHg) within a follow-up of 30 days. All patients were followed for 30 days after study inclusion for the occurrence of the primary EP.

Flow Cytometry staining

Blood samples of patients with coronary artery disease (including SARS-CoV-2 infection) and healthy human were collected in CPDA monovettes for flow cytometry staining in order to stain monocytes. 10 x RBC Lysis buffer (BioLegend) was diluted 1:10 in Millipore water and whole blood was lysed and incubated for 15 min at RT in the dark. After two washing steps with PBS containing 1 % FCS, 2 mM EDTA and 1 % sodium azide, cell count was adjusted to 3 x 10^6 cells per well in a 96 well plate (Falcon). Unspecific antibody binding was blocked by cell incubation with human IgG (Sigma) for 20 min at 4 °C. First, extracellular staining with CX3CR1 PE/Dazzle antibody (clone 2A9-1, BioLegend) was performed for 1 h at 37 °C followed by staining with HLA-DR PerCP-Vio77 (clone REA805Miltenyi), CD54 PE (clone REA266, Miltenyi), CD3 BV510 (clone OKT3), CD15 BV510 (clone W603), CD19 BV510 (clone HLB19), CD20 BV510 (clone 2H7), CD56 BV510 (clone HCD56), CD14 FITC (clone M5E2), CD16 BV711 (clone 3G8), CD62L PE-Cy7 (clone DREG-56), CD80 BV786 (clone 2D10), and Zombie NIR (BioLegend) for 20 min at 4 °C and washed with PBS containing 1 % FCS, 2 mM EDTA and 1 % sodium azide. Next, cells were fixed overnight at 4°C with FoxP3 Staining Buffer Set (eBioscience) according to manufacturer's instructions and acquired using the LSR Fortessa (BD Biosciences). Supplementary Figure 1 shows the gating strategy of human monocyte subsets. Data analysis was done with FlowJo software V.10.6.2 (Tree Star).

Histopathological and immunohistological analysis of heart and lung tissue

Specimens were gained from heart and lung tissue of healthy controls, CAD, and CAD+SARS-CoV-2 patients and fixed in 4 % buffered formaldehyde for immunohistology. Paraffin-embedded EMB were stained with hematoxylin/eosin (H&E) and analyzed by light microscopy.[26, 27] Histological analysis followed the Dallas criteria complemented by immunohistology to assess ongoing inflammation. For immunohistological staining, tissue sections were treated with an avidin–biotin–immunoperoxidase method (Vectastain-Elite ABC Kit, Vector, Burlingame, CA, USA), in combination with the following monoclonal antibodies: anti-CD68 (macrophages; DAKO, Hamburg, Germany), anti-CD14 (Santa Cruz Biotechnology, USA), and anti-CD16 (Santa Cruz Biotechnology, USA).

Statistical analysis

We determined clinical and laboratory baseline characteristics in relation to measured monocyte phenotypes, marker expression, and clinical outcome. Continuous, not normally distributed variables are expressed as median and interquartile range (IQR) and were compared using Mann–Whitney *U* test for two group comparison and Kruskal-Wallis test for three group comparison, where applicable. Continuous parameters were dichotomized at established cut-off values if necessary. Categorical data are presented as total numbers and proportions and were analysed by chi-squared test. Correlation analysis was performed by Spearman rank correlation coefficient r. Survival curves of patients grouped by pre-specified variables were calculated by Kaplan-Meier analyses and compared using the log-rank test. Cox proportional-hazards regression analysis was carried out for multivariable analysis to assess the association of risk factors with the primary endpoint. The risk for endpoint occurrence is presented as a hazard ratio (HR) with 95% confidence interval (CI). Comparisons were considered statistically significant if two-sided p-value was <0·05. Statistical analysis of all participants was performed using SPSS Statistics Version 26 (SPSS, Inc.) and GraphPad Prism Version 8.4.0 (GraphPad Software).

Results

Demographic and clinical characteristics of patients with coronary artery disease and SARS-CoV-2 infection

We prospectively studied a consecutive cohort of 96 participants from February to April 2020. 47 out of 96 patients with pre-existing CAD and acute SARS-CoV-2 infection (CAD + SARS-CoV-2) were admitted with progressive respiratory symptoms. 19 patients with pre-existing stable CAD without any infections were matched to CAD + SARS-CoV-2 patients, while 30 healthy participants served as controls. Baseline characteristics and demographics of the overall cohort are given in Table 1. The median age of the population was 62 (IQR 48–79) years; 44 (45.8%) patients were men. Of the 47 CAD+SARS-CoV-2 patients, 14 (29.8%) were admitted to the intensive care unit (ICU) due to progressive respiratory, circulatory, or multiorgan failure, as they required vasopressor therapy or high-flow oxygen to correct hypoxaemia (Table 2). 11 out of 14 (78.6%) patients showed rapidly progressive respiratory failure defined by a Horovitz Index (HI) of ≤ 200 mmHg and required mechanical ventilation (Table 3). This was the pre-defined clinical endpoint (EP) during a follow-up of 30 days.

Patients with SARS-CoV-2 infection show significantly lower numbers of $CD14^{dim}CD16^{+}$ monocytes in peripheral blood

We analysed subtypes of monocytes in an intensified risk assessment of patients with CAD and SARS-CoV-2 infection to elucidate their prognostic impact during the cause of the disease. Therefore, we stratified monocytes in peripheral blood by their expression of CD14 and CD16 into classical $CD14^{+}$ $CD16^{-}$, intermediate $CD14^{+}CD16^{+}$ and non-classical $CD14^{dim}CD16^{+}$subtypes using flow cytometry. We found no difference in the numbers of classical monocytes in patients with CAD (median 227550, IQR [143400–115800]) compared to CAD + SARS-CoV-2 (median 223380, IQR [115800–329600]) and healthy controls (median 291745, IQR [236228–408465]), whereas significantly less classical monocytes were detected in CAD + SARS-CoV-2 patients compared to healthy controls (p=0.018 for overall comparison in Kruskal-Wallis test, CAD vs CAD + SARS-CoV-2 p=0.99, CAD vs healthy control p=0.18, healthy control vs CAD + SARS-CoV-2 p=0.017) (Fig.

1A). In contrast, slightly increased numbers of intermediate monocytes were observed in CAD (median 31030, IQR [23100–45540]) compared to healthy controls (median 22600, IQR [15645–36735], CAD vs healthy control p=0.22) whereas these numbers were similar to healthy controls in CAD + SARS-CoV-2 patients (median 23230, IQR [7840–34560], p=0.99, CAD vs CAD + SARS-CoV-2 p=0.048) (Fig. 1A). Most interestingly, the numbers of non-classical monocytes were substantially reduced by 82 or 75% in CAD + SARS-CoV-2 patients (median 1443, IQR [649–4266]) compared to CAD patients (median 27820, IQR [18600–50840]) and healthy controls (median 21180, IQR [12788–34185]), respectively ($p<0.0001$ for overall comparison in Kruskal-Wallis test, CAD vs CAD + SARS-CoV-2 $p<0.0001$, CAD vs healthy control p=0.63, healthy control vs CAD + SARS-CoV-2 $p<0.0001$) (Fig. 1A). Spearman rank correlation analysis revealed an inverse, yet significant association of $CD14^{dim}CD16^{+}$ non-classical monocytes with CRP levels in the overall cohort of healthy controls, CAD patients, and CAD + SARS-CoV-2 patients (r=-0.674 and $p< 0.0001$). In subgroup analysis of the CAD + SARS-CoV-2 patients the observed association remained significant with r=-0.373 and p= 0.010 (data not shown).

As current literature suggested gender-specific immune response in patients with SARS-CoV-2 infection, we stratified our data by gender to detect differences between men and women in our cohort.[28-30]

Interestingly, there were no statistically relevant, gender-specific differences regarding monocyte subtypes in the overall cohort and in the comparison of controls vs CAD vs CAD + SARS-CoV-2 patients (supplementary Fig. 2A-C).

CAD patients with SARS-CoV-2 infection admitted to ICU show the lowest numbers of $CD14^{dim}CD16^{+}$ monocytes

Analysis of CAD + SARS-CoV-2 patients admitted to ICU (here referred to as ICU patients) (median 712, IQR [161.3–2769]) showed significantly less $CD14^{dim}CD16^{+}$ monocytes compared to non-ICU patients (median 2150, IQR [879–4878], p=0.03), whereas no differences were found for $CD14^{+}$ $CD16^{-}$ and $CD14^{+}CD16^{+}$ monocytes (p=0.29 and p=0.30, respectively) (Fig. 1B). Gender-specific

subgroup analysis showed similar results for female and male ICU patients compared to non-ICU patients (supplementary Fig. 3A, B).

Moreover, the lowest number of $CD14^{dim}CD16^{+}$ monocytes was detected in ICU patients with progressive respiratory failure, an HI ≤ 200 mmHg, and mechanical ventilation (here referred to as ICU + HI ≤ 200 mmHg; median 388, IQR [129–858]) compared to ICU + HI > 200 mmHg (median 2324, IQR [917.5–4577]), p=0.0017) (Fig. 1C). ICU + HI ≤ 200 mmHg patients (median 6020, IQR [1980–7840]) showed also lower numbers of $CD14^{+}CD16^{+}$ monocytes compared to ICU + HI > 200 mmHg patients (median 25900, IQR [15233–40920]), p=0.001) (Fig. 1C). When further stratified by gender, there were no statistically relevant differences between men and women in the group of patients with HI ≤ 200 mmHg compared to HI > 200 mmHg (supplementary Fig. 3C, D).

Remaining $CD14^{dim}CD16^{+}$ monocytes in peripheral blood of CAD + SARS-CoV-2 patients are functionally impaired

We further assessed the expression of activation markers on $CD14^{dim}CD16^{+}$ monocytes important for adhesion, migration and T cell activation like CD54, CD62L, CX3CR1, CD80 and HLA-DR. CD54 and CD62L mediate adhesion and trans-endothelial migration. The expression of CD54 and the frequency of $CD62L^{+}CD14^{dim}CD16^{+}$ monocytes was significantly increased by two- and eight-fold on CAD patients (CD54: median 16117, IQR [14349–18633], CD62L: median 0.12, IQR [0.073–0.17]) compared to healthy controls (CD54: median 7262, IQR [6298–8775], CD62L: median 0.0046, IQR [0.0033–0.0103]), CD54: p<0.0001, CD62L: p<0.0001), respectively (Fig. 2A-B). Interestingly, this increase was absent in CAD + SARS-CoV-2 patients (CD54: median 8153, IQR [2115–11299], CD62L: median 0.0068, IQR [0.0015–0.014], CAD versus CAD + SARS-CoV-2 CD54: p<0.0001, CD62L: p<0.0001) (Fig. 2A-B), indicating impaired migration of the remaining $CD14^{dim}CD16^{+}$ monocyte to the site of tissue injury. Moreover, CX3CR1, binding fraktaline, which mediates tissue extravasation, was less expressed on $CD14^{dim}CD16^{+}$ monocytes in CAD + SARS-CoV-2 patients (median 20365, IQR [11990–32958]) compared to CAD patients (median 41732, IQR [36812–46084], p<0.0001), and to healthy controls (median 40150 IQR [36089–43352], p<0.0001) (Fig. 2C). In addition, HLA-DR expression was reduced on $CD14^{dim}CD16^{+}$ monocytes in CAD (median 25458,

IQR [21512–26573]) and CAD + SARS-CoV-2 (median 25580, IQR [17327–32643]) patients compared to healthy controls (median 36128, IQR [28089–45615], CAD versus healthy controls: p<0.0001, CAD + SARS-CoV-2 versus healthy controls: p<0.0001) (Fig. 2D), while CD80 expression was four-fold higher in CAD patients (median2240, IQR [1946–2609] compared to healthy controls (median 589, IQR [458–719], p<0.0001) (Fig. 2E). Similarly as for CD54 and CD62L described above, this increase in CD80 expression on $CD14^{dim}CD16^{+}$ monocytes was absent in CAD + SARS-CoV-2 patients (median 503, IQR [391–489], p<0.0001) (Fig. 2E). These data suggest impaired migration behaviour and T cell activation capacity of the remaining $CD14^{dim}CD16^{+}$ monocytes.

Subgroup analysis of ICU patients reveals an impaired activation phenotype of $CD14^{dim}CD16^{+}$ monocytes in peripheral blood

In subgroup analysis of ICU patients, assessing the markers described above, we detected an even lower expression of HLA-DR on and even less numbers of $CD62L^{+}CD14^{dim}CD16^{+}$ monocytes compared to non-ICU patients (HLA-DR: ICU patients median 2456, IQR [1221–11368] versus non-ICU patients median 14349, IQR [5274–27282], p=0.015), $CD62L^{+}CD14^{dim}CD16^{+}$ monocytes: ICU patients median 0.0017, IQR [0.00049–0.00659] versus non-ICU patients median 0.00823, IQR [0.00269–0.014], p=0.019, respectively) (Fig. 2B, D). CD54, CD80 and CX3CR1 were reduced for trend but not statistically significant on $CD14^{dim}CD16^{+}$ monocytes (CD54: p=0.12, CD80: p=0.22, and CX3CR1: p=0.11) (Fig. 2A, C, E). Analysis of ICU + HI ≤ 200 mmHg compared to ICU + HI > 200 mmHg patients revealed no difference in CD54 and CD80 expression on $CD14^{dim}CD16^{+}$ monocytes (CD54: p=0.07, CD80: p=0.84) (Fig. 2A, E). In contrast, the frequency of $CD62L^{+}$ and the expression of HLA-DR and CX3CR1 on $CD14^{dim}CD16^{+}$ monocytes were significantly reduced in ICU + HI ≤ 200 mmHg patients (CD62L: median 0.0014, IQR [0.00045–0.0022], HLA-DR: median 2650, IQR [1000–9707], CX3CR1: median 11455, IQR [8913–15967] vs ICU + HI > 200 mmHg CD62L: 0.0075, IQR [0.0032–0.14], HLA-DR: median 14316, IQR [4400–26766], CX3CR1: median 25008, IQR [14425–33356]; p=0.003, p=0.012, p=0.005, respectively) (Fig. 2B-D).

Immunohistochemistry of heart and lung tissue of CAD patients with SARS-CoV-2 infection detects increased infiltration of $CD68^{+}$, $CD14^{+}$, and $CD16^{+}$ positive inflammatory cells

In a subgroup of patients we performed histological and immunohistochemical analysis of heart and lung tissue (Figure 3). Representative heart tissue sections from healthy controls, CAD, and CAD+SARS-CoV-2 patients (n=4 in each group) were stained with anti-CD68, anti-CD14, and anti-CD16. We identified distinct expression patterns of these $CD68^+$, $CD14^+$, and $CD16^+$ inflammatory cells infiltrating the myocardium to maintain local inflammation in CAD+SARS-CoV-2 compared to healthy controls and CAD patients (Figure 3 A). Interestingly, we could detect a dramatically increased number of $CD68^+$, $CD14^+$, and $CD16^+$ cells in CAD+SARS-CoV-2 patients compared to healthy controls and CAD patients (Figure 3 A). These findings suggest that non-classical monocytes and macrophages migrate to affected myocardial tissue and maintain local inflammation in SARS-Cov-2 related myocarditis (Fig. 3 A).

Analysis of affected lung tissue showed similar results. Here, we found substantially higher numbers of $CD68^+$, $CD14^+$, and $CD16^+$ inflammatory cells in CAD+SARS-CoV-2 patients compared to healthy controls (Fig. 3 B).

Low numbers of $CD14^{dim}CD16^+$ monocytes predict outcome in CAD patients with SARS-CoV-2 infection

In order to identify prognostic markers for CAD patients with SARS-CoV-2 infection indicating progressive respiratory failure we elucidated the role of $CD14^{dim}CD16^+$ monocytes during a follow-up of 30 days. 11/47 CAD + SARS-CoV-2 patients (23.4%) reached the primary endpoint defined as the occurrence of a Horovitz index ≤ 200 mmHg and mechanical ventilation. For Kaplan-Meier analysis the number of patients was divided into two groups based on the median of the non-classical monocyte count. This revealed that significantly more patients with EP were below the cut-off value (median 1443 cells/mL). 41.7% ICU + HI > 200 mmHg patients showed a cell number below the median, while this was the case for 81.8% ICU + HI ≤ 200 mmHg patients ($p=0.02$ (Fig. 4A) indicating rapidly progressive respiratory failure. Kaplan–Meier curves illustrate that CAD + SARS-CoV-2 patients with low numbers of $CD14^{dim}CD16^+$ non-classical monocytes reached the clinical endpoint significantly more often compared to patients with cell counts above the median (log-rank 5.03, $p=0.025$) (Fig. 4B). Remarkably, considering the median number of $CD14^{dim}CD16^+$ monocytes from ICU patients in

relation to all CAD + SARS-CoV-2 patients, Kaplan-Meier analysis revealed that patients with a $CD14^{dim}CD16^{+}$ monocyte cell count below the median of 388 cell/mL develop most frequently respiratory failure (log-rank 14.18, $p<0.0001$) (Fig. 4C). Additionally, we performed gender-specific Kaplan-Meier analysis (Supplementary Fig. 4A, B). Even though low numbers of non-classical monocytes could predict the occurrence of the clinical endpoint in women by trend, this was not statistically significant compared to men (men: log-rank, 1.797, p=0.180, supplementary Fig. 4A; women: log-rank 3.78, p=0.052, supplementary Fig. 4B). We also performed cox regression analysis for the occurrence of progressive respiratory failure defined by a Horovitz index of ≤ 200 mmHg. Cox regression analysis taken into account for the pre-defined confounding factors age, gender, and oral anticoagulation use identified $CD14^{dim}CD16^{+}$ non-classical monocyte count to remain the only independent predictor for the primary endpoint (HR 5.10; CI 1.08 – 24.19, p=0.040, supplementary table 1). We performed another cox regression analysis to correct for several comorbidities and confounders including age, gender, oral anticoagulation use, arterial hypertension, hyperlipidemia, diabetes mellitus, and chronic kidney disease. Cox regression analysis identified $CD14^{dim}CD16^{+}$ non-classical monocyte count and hyperlipidemdia as independent predictors for the occurrence of the primary endpoint ($CD14^{dim}CD16^{+}$ non-classical monocyte count: HR 0.18; CI 0.03 – 0.90, p=0.037; hyperlipidemia: HR 6.29; CI 1.17 – 33.93, p=0.032, supplementary table 2).

Discussion

In contrast to other studies on COVID-19[18, 19] we focussed on patients with pre-existing coronary artery disease, which are prone to progressive heart and lung failure when suffering from SARS-CoV-2 infection.[1-3] To our knowledge, this is the first study to show that the clinical outcome of CAD + SARS-CoV-2 patients is associated with reduced numbers of $CD14^{dim}CD16^{+}$ monocytes in peripheral blood. Our data are in accordance with reduced numbers of monocytes (not dissected into the three subsets) in hospitalized patients with SARS-CoV-2 infection compared to healthy controls[21] and a study from Gatti et al. showing reduced frequencies of non-classical and intermediate monocyte subsets in patients with severe SARS-CoV-2 infection.[31] On the contrary, one study addressing the role of intermediate $CD14^{+}CD16^{+}$ monocytes in peripheral blood of SARS-CoV-2 infected patients,

showed an increased frequency of this subsets in peripheral blood and even higher frequencies in severe pulmonary syndrome patients from ICU.[32] However, we cannot compare our data showing reduced numbers of $CD14^{+}CD16^{+}$ monocytes in CAD + SARS-CoV-2 patients compared to CAD patients with this study of Zhou et al.[32] as CAD patients are characterized by doubling of intermediate monocytes which is even associated with cardiovascular outcomes.[33] Zhou et al. do not give information about comorbidities of the cohort, especially not of presence or absence of CAD.[32]

We showed that in infected CAD patients with progressive respiratory failure not only the numbers of monocytes were substantially reduced, but also their function was impaired. More precise, these patients showed less expression of adhesion and activation markers on non-classical monocytes when compared to CAD patients without infection. This was surprising as SARS-CoV-2 infection results in elevated levels of inflammatory mediators, a so-called cytokine storm, e.g. TNF, MCP-1, MIP-1a, and IL-6 described in the plasma of patients.[5, 18, 20] This should increase monocyte numbers and also their activation markers, which we did not observe in our cohort. Most likely these findings are reflected by monocyte invasion of $CD14^{dim}CD16^{+}$ into injured tissue via the adhesion molecules CD62L and CX3CR1[34] where they differentiate into macrophages. Our analysis of affected heart and lung tissue showed increased numbers of $CD68^{+}$, $CD14^{+}$, and $CD16^{+}$ inflammatory cells in CAD+SARS-Cov-2 patients. These $CD68^{+}$, $CD14^{+}$, and $CD16^{+}$ monocytes and macrophages infiltrate the myocardium in SARS-Cov-2 related myocarditis and the affected lungs during progressive respiratory failure. These findings support our hypothesis that non-classical monocytes may migrate from the blood to the lungs and the myocardium in CAD+SARS-CoV-2 patients during the course of the disease and maintain systemic and local inflammation. Monocyte migration to the site of inflammation in affected heart and lung tissue might lead to reduced numbers of non-classical monocytes in peripheral blood with impaired surface marker expression that we observed in our analysis.[35] Moreover, since CAD patients characteristically show increased numbers and activation of non-classical monocytes[34], it was unexpected that patients with CAD and SARS-CoV-2 infection showed an opposite phenotype with drastically decreased numbers and activation markers. Therefore, we speculate that in the context of SARS-CoV-2 infection, these monocytes migrate from the blood into the affected tissue, where they promote and maintain local inflammation and tissue damage. This could be the causal link for the low

number of remaining peripheral $CD14^{dim}CD16^{+}$ monocytes. This extraordinary finding is reflected in the clinical course and is even of prognostic importance. CAD patients with low $CD14^{dim}CD16^{+}$ monocyte counts show more often rapidly progressive respiratory failure with HI ≤ 200 mmHg and mechanical ventilation at an early stage of the infection as demonstrated by the Kaplan-Meier curves. Thus, we propose the additional determination of the monocyte phenotype as a simple and new tool which could improve routine diagnostics at the beginning of the infection.[3, 36] Thus, we speculate that sequestrated, activated non-classical monocytes promote the localized inflammatory response of affected lung tissue. This is of great clinical importance as the decreased number of $CD14^{dim}CD16^{+}$ non-classical monocytes with their impaired phenotype are specifically found in CAD + SARS-CoV-2 infected patients, but not in CAD patients, which is mirrored in the severity of the respiratory failure. Since there is currently no causal therapy for the infection, it is essential to detect and treat prognostically relevant comorbidities at an early stage according to current guidelines in order to prevent a fatal course triggered by the infection. CAD patients with pre-existing burden of cardiac and vascular dysfunction might benefit from intensified heart failure and anti-thrombotic therapy before progression of respiratory failure occurs.[4]

In conclusion, decreased numbers of $CD14^{dim}CD16^{+}$ non-classical monocytes are associated with adverse clinical outcome of CAD + SARS-CoV-2 patients and might serve as a prognostic marker to predict worsening of respiratory failure. An early phenotyping of monocytes using simple flow cytometry analysis may help to identify patients at risk requiring a more intensified heart failure and anti-thrombotic therapy in the course of the infection, especially in patients with pre-existing coronary artery disease.

Funding

This work was supported by the German Research Foundation (DFG) – Project number 374031971–TRR 240 and by the Ministry of Science, Research and the Arts of the State of Baden-Württemberg (COVID-19 Funding). The funder had no role in study design, data collection, data analysis, data interpretation, or writing of the manuscript. The corresponding author had full access to all data in the study and had final responsibility for the decision to submit for publication. Karin Klingel received funding by Deutsche Herzstiftung.

Author contributions

K.A.L.M., M.P.G. and S.E.A. conception and design of the study, interpretation of data, drafting of the manuscript and revising it critically for important intellectual content; C.L., performed experimental analysis, data acquisition and interpretation; M.G., S.P., S.G., B.L. performed experimental analysis; Á.P.-U., P.J. data acquisition and interpretation; K.P.K.: interpretation of data, revising manuscript critically for important intellectual content; T.C., D.R. interpretation of data, revising manuscript critically for important intellectual content. K.K. and H.B. provided and analyzed heart and lung tissue and performed histological and immunohistochemical stainings and analysis.

Conflict of interest

None of the authors has any conflict of interest to declare. Our study complies with the Declaration of Helsinki, our locally appointed ethics committee has approved the research protocol, and informed consent has been obtained from all participants.

Data Availability Statement

For original data, please contact Karin Anne Lydia Mueller, k.mueller@med.uni-tuebingen.de.

References

1. ESC Guidance for the Diagnosis and Management of CV Disease during the COVID-19 Pandemic. 2020.
2. Oren Ohad KSL, Gluckman Tyler J., Gersh Bernard J., Blumenthal Roger S. . Coronavirus Disease 2019 (COVID-19): Epidemiology, Clinical Spectrum and Implications for the Cardiovascular Clinician. 2020.
3. Xiong TY, Redwood S, Prendergast B, Chen M. Coronaviruses and the cardiovascular system: acute and long-term implications. *Eur Heart J* 2020.
4. Tang N, Bai H, Chen X, Gong J, Li D, Sun Z. Anticoagulant treatment is associated with decreased mortality in severe coronavirus disease 2019 patients with coagulopathy. *J Thromb Haemost* 2020;**18**:1094-1099.
5. Chen C, Zhou Y, Wang DW. SARS-CoV-2: a potential novel etiology of fulminant myocarditis. *Herz* 2020;**45**:230-232.
6. Tay JY, Lim PL, Marimuthu K, Sadarangani SP, Ling LM, Ang BSP, Chan M, Leo YS, Vasoo S. De-isolating COVID-19 Suspect Cases: A Continuing Challenge. *Clin Infect Dis* 2020.
7. Shi S, Qin M, Shen B, Cai Y, Liu T, Yang F, Gong W, Liu X, Liang J, Zhao Q, Huang H, Yang B, Huang C. Association of Cardiac Injury With Mortality in Hospitalized Patients With COVID-19 in Wuhan, China. *JAMA Cardiol* 2020.
8. Wolf D, Ley K. Immunity and Inflammation in Atherosclerosis. *Circ Res* 2019;**124**:315-327.
9. Swirski FK, Nahrendorf M. Cardioimmunology: the immune system in cardiac homeostasis and disease. *Nat Rev Immunol* 2018;**18**:733-744.
10. Woollard KJ, Geissmann F. Monocytes in atherosclerosis: subsets and functions. *Nat Rev Cardiol* 2010;**7**:77-86.
11. Narasimhan PB, Marcovecchio P, Hamers AAJ, Hedrick CC. Nonclassical Monocytes in Health and Disease. *Annu Rev Immunol* 2019;**37**:439-456.
12. Kapellos TS, Bonaguro L, Gemund I, Reusch N, Saglam A, Hinkley ER, Schultze JL. Human Monocyte Subsets and Phenotypes in Major Chronic Inflammatory Diseases. *Front Immunol* 2019;**10**:2035.
13. Buscher K, Marcovecchio P, Hedrick CC, Ley K. Patrolling Mechanics of Non-Classical Monocytes in Vascular Inflammation. *Front Cardiovasc Med* 2017;**4**:80.
14. Cros J, Cagnard N, Woollard K, Patey N, Zhang SY, Senechal B, Puel A, Biswas SK, Moshous D, Picard C, Jais JP, D'Cruz D, Casanova JL, Trouillet C, Geissmann F. Human CD14dim monocytes patrol and sense nucleic acids and viruses via TLR7 and TLR8 receptors. *Immunity* 2010;**33**:375-386.
15. Auffray C, Fogg DK, Narni-Mancinelli E, Senechal B, Trouillet C, Saederup N, Leemput J, Bigot K, Campisi L, Abitbol M, Molina T, Charo I, Hume DA, Cumano A, Lauvau G, Geissmann F. CX3CR1+ CD115+ CD135+ common macrophage/DC precursors and the role of CX3CR1 in their response to inflammation. *J Exp Med* 2009;**206**:595-606.
16. Dutertre CA, Amraoui S, DeRosa A, Jourdain JP, Vimeux L, Goguet M, Degrelle S, Feuillet V, Liovat AS, Muller-Trutwin M, Decroix N, Deveau C, Meyer L, Goujard C, Loulergue P, Launay O, Richard Y, Hosmalin A. Pivotal role of M-DC8(+) monocytes from viremic HIV-infected patients in TNFalpha overproduction in response to microbial products. *Blood* 2012;**120**:2259-2268.
17. Mueller KAL, Hanna DB, Ehinger E, Xue X, Baas L, Gawaz MP, Geisler T, Anastos K, Cohen MH, Gange SJ, Heath SL, Lazar JM, Liu C, Mack WJ, Ofotokun I, Tien PC, Hodis HN, Landay AL, Kaplan RC, Ley K. Loss of CXCR4 on non-classical monocytes in participants of the Women's Interagency HIV Study (WIHS) with subclinical atherosclerosis. *Cardiovasc Res* 2019;**115**:1029-1040.
18. Huang C, Wang Y, Li X, Ren L, Zhao J, Hu Y, Zhang L, Fan G, Xu J, Gu X, Cheng Z, Yu T, Xia J, Wei Y, Wu W, Xie X, Yin W, Li H, Liu M, Xiao Y, Gao H, Guo L, Xie J, Wang G, Jiang R, Gao Z, Jin Q,

Wang J, Cao B. Clinical features of patients infected with 2019 novel coronavirus in Wuhan, China. *Lancet* 2020;**395**:497-506.
19. Zhou F, Yu T, Du R, Fan G, Liu Y, Liu Z, Xiang J, Wang Y, Song B, Gu X, Guan L, Wei Y, Li H, Wu X, Xu J, Tu S, Zhang Y, Chen H, Cao B. Clinical course and risk factors for mortality of adult inpatients with COVID-19 in Wuhan, China: a retrospective cohort study. *Lancet* 2020;**395**:1054-1062.
20. Jose RJ, Manuel A. COVID-19 cytokine storm: the interplay between inflammation and coagulation. *Lancet Respir Med* 2020.
21. Qin C, Zhou L, Hu Z, Zhang S, Yang S, Tao Y, Xie C, Ma K, Shang K, Wang W, Tian DS. Dysregulation of immune response in patients with COVID-19 in Wuhan, China. *Clin Infect Dis* 2020.
22. Kashiwagi M, Imanishi T, Tsujioka H, Ikejima H, Kuroi A, Ozaki Y, Ishibashi K, Komukai K, Tanimoto T, Ino Y, Kitabata H, Hirata K, Akasaka T. Association of monocyte subsets with vulnerability characteristics of coronary plaques as assessed by 64-slice multidetector computed tomography in patients with stable angina pectoris. *Atherosclerosis* 2010;**212**:171-176.
23. DesPrez K, McNeil JB, Wang C, Bastarache JA, Shaver CM, Ware LB. Oxygenation Saturation Index Predicts Clinical Outcomes in ARDS. *Chest* 2017;**152**:1151-1158.
24. Lang RM, Badano LP, Mor-Avi V, Afilalo J, Armstrong A, Ernande L, Flachskampf FA, Foster E, Goldstein SA, Kuznetsova T, Lancellotti P, Muraru D, Picard MH, Rietzschel ER, Rudski L, Spencer KT, Tsang W, Voigt JU. Recommendations for cardiac chamber quantification by echocardiography in adults: an update from the American Society of Echocardiography and the European Association of Cardiovascular Imaging. *J Am Soc Echocardiogr* 2015;**28**:1-39 e14.
25. Parasuraman S, Walker S, Loudon BL, Gollop ND, Wilson AM, Lowery C, Frenneaux MP. Assessment of pulmonary artery pressure by echocardiography-A comprehensive review. *Int J Cardiol Heart Vasc* 2016;**12**:45-51.
26. Klingel K, Sauter M, Bock CT, Szalay G, Schnorr JJ, Kandolf R. Molecular pathology of inflammatory cardiomyopathy. *Med Microbiol Immunol* 2004;**193**:101-107.
27. Aretz HT. Myocarditis: the Dallas criteria. *Hum Pathol* 1987;**18**:619-624.
28. Jin JM, Bai P, He W, Wu F, Liu XF, Han DM, Liu S, Yang JK. Gender Differences in Patients With COVID-19: Focus on Severity and Mortality. *Front Public Health* 2020;**8**:152.
29. Takahashi T, Ellingson MK, Wong P, Israelow B, Lucas C, Klein J, Silva J, Mao T, Oh JE, Tokuyama M, Lu P, Venkataraman A, Park A, Liu F, Meir A, Sun J, Wang EY, Casanovas-Massana A, Wyllie AL, Vogels CBF, Earnest R, Lapidus S, Ott IM, Moore AJ, Yale IRT, Shaw A, Fournier JB, Odio CD, Farhadian S, Dela Cruz C, Grubaugh ND, Schulz WL, Ring AM, Ko AI, Omer SB, Iwasaki A. Sex differences in immune responses that underlie COVID-19 disease outcomes. *Nature* 2020.
30. Conti P, Younes A. Coronavirus COV-19/SARS-CoV-2 affects women less than men: clinical response to viral infection. *J Biol Regul Homeost Agents* 2020;**34**:339-343.
31. Gatti A, Radrizzani D, Vigano P, Mazzone A, Brando B. Decrease of Non-Classical and Intermediate Monocyte Subsets in Severe Acute SARS-CoV-2 Infection. *Cytometry A* 2020.
32. Zhou Y, Fu B, Zheng X, Wang D, Zhao C, qi Y, Sun R, Tian Z, Xu X, Wei H. Pathogenic T cells and inflammatory monocytes incite inflammatory storm in severe COVID-19 patients. *National Science Review* 2020.
33. Cappellari R, D'Anna M, Bonora BM, Rigato M, Cignarella A, Avogaro A, Fadini GP. Shift of monocyte subsets along their continuum predicts cardiovascular outcomes. *Atherosclerosis* 2017;**266**:95-102.
34. Fang P, Li X, Dai J, Cole L, Camacho JA, Zhang Y, Ji Y, Wang J, Yang XF, Wang H. Immune cell subset differentiation and tissue inflammation. *J Hematol Oncol* 2018;**11**:97.
35. Sanchez-Cerrillo I, Landete P, Aldave B, Sanchez-Alonso S, Sanchez-Azofra A, Marcos-Jimenez A, Avalos E, Alcaraz-Serna A, de Los Santos I, Mateu-Albero T, Esparcia L, Lopez-Sanz C, Martinez-Fleta P, Gabrie L, Del Campo Guerola L, de la Fuente H, Calzada MJ, Gonzalez-

Alvaro I, Alfranca A, Sanchez-Madrid F, Munoz-Calleja C, Soriano JB, Ancochea J, Martin-Gayo E. COVID-19 severity associates with pulmonary redistribution of CD1c+ DC and inflammatory transitional and nonclassical monocytes. *J Clin Invest* 2020.

36. Zheng YY, Ma YT, Zhang JY, Xie X. COVID-19 and the cardiovascular system. *Nat Rev Cardiol* 2020;**17**:259-260.

Tables

Table 1. Baseline characteristics of the overall cohort (n = 96)

Table 2. Baseline characteristics of patient population stratified by the admission to intensive care unit (ICU)

Table 3. Baseline characteristics of patient population stratified by the occurrence of the clinical endpoint (progressive respiratory failure defined by Horovitz Index HI < 200mmHg and mechanical ventilation)

Figure Legends

Figure 1: Reduced numbers of $CD14^{dim}CD16^{+}$ monocytes in CAD + SARS-CoV-2 infected patients

Whole blood human $CD14^{+}CD16^{-}$, $CD14^{+}CD16^{+}$ and $CD14^{dim}CD16^{+}$ monocytes were analyzed by flow cytometry from (A) healthy controls (n=30), CAD patients (n=19) and CAD + SARS-CoV-2 infected patients (n=47), (B) CAD + SARS-CoV-2 infected patients stratified by ICU admission (no ICU n=33, ICU n=14) and (C) ICU patients with rapidly progressive respiratory failure (Horovitz index HI ≤ 200 mmHg) requiring mechanical ventilation (HI > 200 mmHg; n=36, HI ≤ 200 mmHg n=11). Graphs show the number of $CD14^{+}CD16^{-}$, $CD14^{+}CD16^{+}$ and $CD14^{dim}CD16^{+}$ monocytes (median with interquartile range [IQR]). Kruskal-Wallis or Mann-Whitney test were performed for three or two group comparison, respectively. For this analysis a p-value ≤ 0.050 was considered significant, indicated by *, p-value ≤ 0.010 indicated by **, p-value ≤ 0.001 indicated by *** and p-value ≤ 0.0001 indicated by ****.

Figure 2: Reduced expression of activation markers on $CD14^{dim}CD16^{+}$ monocytes in CAD + SARS-CoV-2 infected patients

(A) CD54, (B) CD62L, (C) CX3CR1, (D) HLA-DR, and (E) CD80 surface marker expression was evaluated by flow cytometry on $CD14^{dim}CD16^{+}$ monocytes in whole blood from (left panel) healthy controls (n=30), CAD patients (n=19), and CAD + SARS-CoV-2 infected patients (n=47), (middle panel) CAD + SARS-CoV-2 infected patients stratified by ICU admission (no ICU n=33, ICU n=14),

and (right panel) ICU patients with rapidly progressive respiratory failure requiring mechanical ventilation (HI > 200 mmHg; n=36, HI ≤ 200 mmHg n=11). Graphs show the median fluorescence of the indicated marker on $CD14^{dim}CD16^{+}$ monocytes as dot plots (median with interquartile range (IQR)). Kruskal-Wallis or Mann-Whitney test were performed for three or two group comparison, respectively. For this analysis a p-value ≤ 0.050 was considered significant, indicated by *, p-value ≤ 0.010 indicated by **, p-value ≤ 0.001 indicated by *** and p-value ≤ 0.0001 indicated by ****.

Figure 3: Histopathological and immunohistological findings in the heart and lung tissue of patients with coronary artery disease and severe SARS-CoV-2 infection.

(A) Representative myocardial tissue sections from patients with coronary artery disease with and without acute SARS-CoV-2 infection and controls without any heart or lung disease. We analyzed n=4 patients in each group and performed histological and immunohistochemical stainings with hematoxylin/eosin (H&E), anti-CD68, anti-CD14 and anti-CD16 antibodies as described in the method section.

The left panel illustrates the findings in normal myocardial tissue of a patient without any heart disease. There is no detection of inflammatory cells within the myocardium.

The middle panel depicts heart tissue of a patient with coronary artery disease. Immunohistochemical stainings for the detection of CD68, CD14 and CD16 show few positive cells indicated by the arrows but no relevant local inflammation.

The right panel shows heart tissue of a patient with coronary artery disease and acute SARS-CoV-2 infection with progressive respiratory failure. Immunohistochemical staining detects dramatically increased numbers of $CD68^{+}$, $CD14^{+}$ and $CD16^{+}$ cells (indicated by arrows). Presence of higher numbers of infiltrating inflammatory cells is a characteristic finding of acute myocardial inflammation during viral infection like SARS-Cov-2 related myocarditis.

(B) Representative lung tissue sections from patients with coronary artery disease with acute SARS-CoV-2 infection and controls without any heart or lung disease. Histological and

immunohistochemical stainings were performed from n=4 patients in each group with hematoxylin/eosin (H&E), anti-CD68, anti-CD14 and anti-CD16 antibodies as described in the method section.

The left panel shows the findings in normal lung tissue from a patient without any heart and lung disease. There is no detection of inflammatory cells within the lung tissue.

The right panel depicts lung tissue of a patient with coronary artery disease and acute SARS-CoV-2 infection. Immunohistochemical staining detects increased numbers of $CD68^{+}$, $CD14^{+}$ and $CD16^{+}$ cells (indicated by arrows). This finding suggests that inflamed lung tissue is characterized by the presence of $CD68^{+}$ macrophages and $CD14^{+}$ and $CD16^{+}$ monocytes which migrated into the lung tissue to trigger and maintain local tissue inflammation during progressive respiratory failure due to SARS-CoV-2 infection.

Figure 4: Low numbers of $CD14^{dim}CD16^{+}$ monocytes are associated with rapidly progressive respiratory failure in CAD + SARS-CoV-2 patients

(A) The number of patients was divided into 2 groups based on the median of the non-classical monocyte count (median 1443 cells/mL). Graph represents the frequency of patients with a $CD14^{dim}CD16^{+}$ monocyte cell count below the median stratified by HI ≤ 200 mmHg. Chi-square test was performed for categorical variables. For this analysis a p-value ≤ 0.050 was considered significant. (B) Kaplan-Meier curves illustrate the occurrence of the clinical study endpoint stratified by $CD14^{dim}CD16^{+}$ monocyte count of all CAD + SARS-CoV-2 patients (median 1443 cell/mL). During a follow-up of 30 days 11/47 patients (23.4%) reached the primary endpoint. The primary study endpoint was defined as rapidly progressive respiratory failure with a Horovitz index ≤ 200 mmHg and mechanical ventilation. Nine out of 11 patients (81.8%) showed a $CD14^{dim}CD16^{++}$ monocyte count below the median of 1443 cells/mL (log-rank 5.03, p=0.025). (C) Kaplan-Meier curves illustrate the occurrence of the clinical study endpoint stratified by $CD14^{dim}CD16^{+}$ monocyte count of all ICU patients (median 388 cell/mL). Six out of 11 patients (54.5%) showed a $CD14^{dim}CD16^{++}$ monocyte count below the median of 388 cells/mL (log-rank 14.18, p<0.0001).

Table 1. Baseline characteristics of patient population

Parameters	All Patients, N=96	CAD+SARS-CoV-2, N=47	CAD, N=19	Control, N=30	p-value
Clinical characteristics					
Age, y	62 (48-79)	79 (59-82)	70 (62-77)	39 (28-53)	**<0.001**
Male	44 (45.8)	24 (51.1)	8 (42.1)	12 (40)	0.596
BMI (kg/m²)	25.5 (23-28.9)	27.8 (25.1-31.8)	25.9 (23.6-27.9)	23 (22-27.3)	**0.001**
Fever	31 (32.3)	31 (65.9)	0 (0)	0 (0)	**<0.001**
hs TNI > 37 (ng/L)	8 (8.3)	8 (17)	0 (0)	0 (0)	0.171
NT-pro BNP > 300 (ng/L)	27 (28.1)	27 (57.4)	0 (0)	0 (0)	**<0.001**
CRP > 0.5 ml/dL	53 (55.2)	44 (93.6)	6 (31.6)	3 (10.0)	**<0.001**
Cardiovascular risk factors					
Arterial hypertension	53 (55.2)	37 (78.7)	15 (78..9)	1 (3..3)	**<0.001**
Dyslipidemia	36 (37.5)	24 (51.1)	11 (57.9)	1 (3.3)	**<0.001**
Diabetes mellitus	14 (14.6)	12 (25.5)	1 (5.3)	1 (3.3)	**0.012**
Current smokers	8 (8.3)	1 (2.1)	3 (15.8)	4 (13.3)	0.100
Atrial fibrillation	16 (16.8)	10 (21.3)	6 (31.6)	0 (0)	**0.007**
Chronic kidney disease	7 (7.3)	7 (14.9)	0 (0)	0 (0)	**0.02**
Parameters of echocardiography					
Left ventricular ejection fraction, %	60 (60-60)	60 (60-60)	60 (60-60)	60 (60-60)	0.872
Right ventricular dilatation	15 (15.6)	15 (31.9)	0 (0)	0 (0)	**0.036**
Right ventricular function (TAPSE in mm)	21 (15.3-26.7)	20 (14.9-25.1)	26 (20.3-31.7)	-	0.104
Tricuspid regurgitation >1	9 (9.3)	6 (12.8)	3 (15.8)	0 (0)	0.205
Pericardial effusion	19 (19.8)	19 (40.4)	0 (0)	0 (0)	**0.010**
Pleural effusion	12 (12.5)	11 (23.4)	1 (5.3)	0 (0)	0.713
PAPsys (mmHg)	25 (20.3-33)	25 (20-30)	26 (22.5-38)	-	0.327
Concomitant cardiac medication at study entry					
Oral anticoagulation	12 (12.5)	5 (10.6)	7 (36.8)	0 (0)	**0.001**
ACE-I or ARB	41 (42.7)	30 (63.8)	11 (57.9)	0 (0)	**0.036**
Aldosterone inhibitors	7 (7.3)	6 (12.8)	1 (5.3)	0 (0)	0.085

Diuretics	22 (22.9)	19 (40.4)	3 (15.8)	0 (0)	**<0.001**
Calcium channel blockers	18 (18.8)	13 (27.7)	5 (26.3)	0 (0)	**0.005**
Beta blockers	25 (26)	18 (38.3)	7 (36.8)	0 (0)	**<0.001**
Statins	26 (27.1)	20 (42.6)	6 (31.6)	0 (0)	**<0.001**
ASA	18 (5.3)	13 (27.7)	5 (26.3)	0 (0)	**0.005**
P2Y12 inhibitors	2 (2.1)	1 (2.1)	1 (5.3)	0 (0)	0.464
Parameters of electrocardiography					
Heart Rate (bpm)	76 (65-83)	77 (69-88)	69 (64-82)	61 (58-74)	0.057
Heart Rhythm					
- Sinus rhythm	46 (49)	29 (61.7)	17 (89.5)	0 (0)	0.463
- Atrial fibrillation	7 (7.3)	6 (12.8)	1 (5.3)	0 (0)	
- Pacemaker with ventricular pacing	4 (4.2)	3 (6.4)	1 (5.3)	0 (0)	
Laboratory parameters and biomarkers					
Leukocytes (1000/µL)	6805 (5112.5-8152.5)	6080 (4190-7650)	7660 (5940-9000)	6890 (6000-7670)	0.051
Lymphocytes (1000/µL)	920 (660.-1730)	690 (590-970)	1540 (1370-2050)	2110 (1545-2425)	**<0.001**
Hb (g/dL)	13.4 (11.8-14.1)	13 (11.2-13.8)	13.9 (12.9-14.6)	13.9 (13-14.2)	**0.025**
Platelets (1000/µL)	211.5 (152.5-285.5)	169 (142-243)	240.5 (203.8-301.5)	252 (218-305)	**0.002**
INR (%)	1.1 (1-1.1)	1.1 (1-1.1)	1 (1-1)	1 (1-1.1)	0.136
PTT (s)	24 (22.75-28)	24 (22-28)	25 (23-33.5)	24 (23-24.5)	0.335
D-Dimer (µg/dL)	0.9 (0.6-1.7)	0.9 (0.7-1.7)	0.3 (0.3-0.3)	0.2 (0.2-0.2)	0.099
Creatinine (mg/dL)	0.8 (0.7-1)	0.9 (0.7-1.2)	0.8 (0.6-0.8)	0.7 (0.7-0.8)	**0.035**
GFR-MDRD (ml/m^2)	80.1 (69.3.-100.5)	75.5 (58.3-98.9)	84.6 (74.1-99.7)	90.1 (80.9-119.3)	**0.012**
Sodium (mmol/L)	139 (136-140)	136 (134-140)	140 (138.8-142.3)	140 (139-142)	**<0.001**
CRP (mg/dL)	1.5 (0.4-9.6.3)	4 (1.4-12.2)	0.3 (0.1-1.2)	0.1 (0-0.5)	**<0.001**
PCT (ng/mL)	0.1 (0.1-0.2)	0.1 (0.1-0.2)	-	-	-
IL-6	19.9 19.9 (10.2-43.5)	13.5 (5.2-27.3)	26.9 (10.2-59.8)	31.9 (16.3-50.1)	**0.013**
TNF-α	55.5 (28.8-149.6)	143.6 (37.5-362.6)	62.3 (43.1-116.4)	27.9 (21.5-55.5)	**<0.001**
hs TNI (ng/dL)	8 (3-19.5)	10 (3-25)	4.0 (3-6.5)	3 (3-3)	0.068
NT-pro-BNP (ng/L)	364 (98-3068)	411 (132-3422)	330 (280-1035)	84 (44.3-168)	**0.030**

CK (U/L)	113 (63-198)	122 (66-250)	74 (52.5-128)	99 (71-165.5)	**0.**065
AST (U/L)	22 (16-38)	35 (20-43.5)	16 (13-20.5)	19 (15.5-25)	**<0.001**
ALT (U/L)	24 (17.5-36)	27 (19-38)	20 (14.8-28)	22.2 (16.5-30.8)	0.259
LDH (U/L)	218 (188.5-285.8)	263.5 (210.3-332.5)	195.5 (176-210.8)	162.5 (147.3-227.3)	**<0.001**
HbA1c (%)	6 (5.6-6.3)	6.2 (6-6.4)	5.6 (5.4-6)	5.4 (5-6)	**0.001**
Lactate (mmol/L)	1.4 (0.9-1.9)	1.4 (0.9-1.9)	-	1.2 (1.2-1.2)	0.772
pH	7.4 (7.4-7.5)	7.4 (4.4-7.5)	-	-	
Intensive Care					
Bacterial co infection	4 (4.2)	4 (8.5)	0 (0)	0 (0)	**0.022**
Acute kidney injury	2 (2.1)	2 (4.3)	0 (0)	0 (0)	0.238
Acute hepatic injury	3 (3.1)	3 (6.4)	0 (0)	0 (0)	0.475
Vasopressors	6 (6.3)	6 (12.8)	0 (0)	0 (0)	**<0.001**
Horovitz Index (mmHg)					
- > 300 mmHg	79 (82.3)	30 (63.8)	19 (100)	30 (100)	**<0.001**
- 201 - 300 mmHg	6 (6.3)	6 (12.8)	0 (0)	0 (0)	
- 101 - 200 mmHg	6 (6.3)	6 (12.8)	0 (0)	0 (0)	
- ≤ 100 mmHg	5 (5.2)	5 (10.6)	0 (0)	0 (0)	

Values are given as numbers (n) and percentage (%) or are given as median and interquartile range (IQR). ACE - Angiotensin Converting Enzyme, Afib - atrial fibrillation, ALT – alanine amino-tranferase, ARB - Angiotensin II Receptor Blockers**,** ASA – Acetylsalicylic acid , AST – aspartate-aminotransferase, BMI – body mass index, CAD – coronary artery disease, CK – creatinine kinase, CRP – C-reactive protein, GFR-MDRD – glomerular filtration rate, Hb – hemoglobin, hs TNI - High sensitive Troponin I, INR – international normalized ratio, LDH – lactate dehydrogenase, NT-pro-BNP – N-terminal pro- brain natriuretic peptide, Pap Sys – pulmonary arterial pressure systolic, PCT – procalcitonin, PTT – partial thromboplastin time, SARS-CoV-2 – severe acute respiratory syndrome coronavirus-2

Table 2. Baseline characteristics of patient population stratified by the admission to intensive care unit (ICU)

Parameters	All Patients, N=47	No ICU, N=33	ICU, N=14	p-value
Clinical characteristics				
Age, y	79 (59-82)	75 (56-81)	79 (67-84.5)	0.264
Male	24 (51..1)	16 (48.5)	8 (57.1)	0.587
BMI (kg/m²)	27.8 (25.1-31.8)	27.5 (25.2-31.9)	28.7 (25-33)	0.644
Fever	31 (65.9)	22 (66.7)	9 (64.3)	0.867
hs TNI > 37 (ng/L)	8 (17)	3 (9.1)	5 (37.7)	**0.034**
NT-pro BNP > 300 (ng/L)	27 (57.4)	15 (45.5)	12 (85.7)	**0.011**
CRP > 0.5 ml/dL	44 (93.6)	30 (90.9)	14 (100)	0.244
Cardiovascular risk factors				
Arterial hypertension	37 (78.7)	24 (72.7)	13 (92.9)	0.123
Dyslipidemia	24 (51.1)	18 (54.5)	6 (42.9)	0.608
Diabetes mellitus	12 (25.5)	8 (24.2)	4 (28.6)	0.756
Current smokers	1 (2.1)	1 (3)	0 (0)	0.526
Atrial fibrillation	10 (21.3)	6 (18.8)	4 (28.6)	0.457
Chronic kidney disease	7 (14.9)	3 (9.1)	4 (28.6)	0.086
Parameters of echocardiography				
Left ventricular ejection fraction, %	60 (60-60)	60 (60-60)	60 (60-60)	0.575
Right ventricular dilatation	15 (31.9)	10 (30.3)	5 (35.7)	0.714
Right ventricular function (TAPSE in mm)	20 (14.9-25.1)	20 (14.7-25.3)	25 (21.3-28.7)	0.304
Tricuspid regurgitation >1	6 (12.8)	4 (12.1)	2 (14.3)	0.152
Pericardial effusion	19 (40.4)	14 (42.4)	5 (35.7)	0.370
Pleural effusion	11 (23.4)	8 (24.2)	3 (21.4)	0.933
PAPsys (mmHg)	25 (20-30)	24 (20-30)	30 (23.8-37.8)	0.081
Concomitant cardiac medication at study entry				
Oral anticoagulation	5 (10.6)	3 (9.1)	2 (14.3)	0.407
ACE-I or ARB	9 (19.1)	7 (21.2)	2 (14.3)	0.541
Aldosterone inhibitors	22 (46.8)	14 (42.4)	8 (57.1)	0.176

Diuretics	6 (12.8)	4 (12.1)	2 (14.3)	0.720
Calcium channel blockers	19 (40.4)	14 (42.4)	5 (35.7)	0.901
Beta blockers	13 (27.7)	10 (30.3)	3 (21.4)	0.686
Statins	18 (38.3)	13 (39.4)	5 (35.7)	0.950
ASA	20 (42.6)	15 (45.5)	5 (35.7)	0.757
P2Y12 inhibitors	13 (27.7)	11 (33.3)	2 (14.3)	0.252
Parameters of electrocardiography				
Heart Rate (bpm)	77 (69.5-87.8)	76 (69-86.5)	77 (68-98)	0.817
Heart Rhythm				
- Sinus rhythm	29 (61.7)	20 (60.6)	9 (64.3)	0.672
- Atrial fibrillation	6 (12.8)	3 (9.1)	3 (21.4)	
- Pacemaker with ventricular pacing	3 (6.4)	2 (6.1)	1 (7.1)	
Laboratory parameters and biomarkers				
Leukocytes (1000/µL)	6080 (4190-7650)	5670 (4150-7375)	6905 (4260-9265)	0.285
Lymphocytes (1000/µL)	690 (590-970)	810 (635-1200)	585 (500-775.5)	**0.008**
Hb (g/dL)	13 (11.2-13.8)	13 (11.7-13.8)	12.5 (9.4-14.4)	0.609
Platelets (1000/µL)	169 (142-243)	173 (142.5-244)	163 (120.8-253.8)	0.545
INR (%)	1.1 (1-1.1)	1.1 (1-1.1)	1.1 (1-1.1)	0.647
PTT (s)	24 (22-28)	24 (22-26.5)	26.5 (23-31)	0.092
D-Dimer (µg/dL)	0.9 (0.7-1.7)	0.8 (0.5-1.1)	1.7 (1-2.7)	**0.003**
Creatinine (mg/dL)	0.9 (0.7-1.2)	0.8 (0.7-1)	1 (0.6-1.5)	0.520
GFR-MDRD (ml/m^2)	75.5 (58.3-98.9)	79 (59.9-99.7)	73 (40.7-96.8)	0.471
Sodium (mmol/L)	136 (134-140)	136 (132.5-139.5)	137 (134.8-140)	0.726
CRP (mg/dL)	4 (1.4-12.2)	2.3 (1.2-6)	12.3 (9.5-21.3)	**<0.001**
PCT (ng/mL)	0.1 (0.1-0.2)	0.1 (0-0.2)	0.1 (0.1-0.7)	**0.004**
IL-6	13.5 (5.2-27.3)	15.2 (5.5-29.4)	11.7 (4.2-19.5)	0.366
TNF-α	143.6 (37.5-362.6)	59.7 (32.3-211.5)	259.9 (146.8-911.5)	**0.019**
hs TNI (ng/dL)	10 (3-25)	7 (2-17)	20 (12-105.8)	**0.010**
NT-pro-BNP (ng/L)	411 (132-3422)	309 (92-826.5)	2328 (639.5-12168.5)	**0.005**
CK (U/L)	122 (66-250)	121 (64-251)	181.5 (115.8-244.3)	0.329

AST (U/L)	35 (20-43.5)	32 (20-42)	40 (24-62.3)	0.073
ALT (U/L)	27 (19-38)	28 (19.5-39.5)	21.5 (17.8-34)	0.306
LDH (U/L)	263.5 (210.3-332.5)	235.5 (193.3-304.3)	327.5 (269.3-405.3)	**0.003**
HbA1c (%)	6.2 (6-6.4)	6.1 (6-6.4)	6.3 (6.05-6.5)	0.325
Lactate (mmol/L)	1.4 (0.9-1.9)	1.3 (0.9-1.8)	1.6 (0.9-2.3)	0.590
pH	7.4 (7.4-7.5)	7.4 (7.4-7.5)	7.4 (7.4-7.5)	0.803
Intensive Care				
Bacterial co infection	4 (8.5)	0 (0)	4 (28.6)	**0.004**
Acute kidney injury	2 (4.3)	0 (0)	2 (14.3)	**0.024**
Acute hepatic injury	3 (6.4)	2 (6.1)	1 (7.1)	0.882
Vasopressors	6 (12.8)	1 (3)	5 (35.7)	**0.001**
Horovitz Index (mmHg)				
- > 300 mmHg	30 (63.8)	26 (78.8)	4 (28.6)	**<0.001**
- 201 - 300 mmHg	6 (12.8)	6 (18.2)	0 (0)	
- 101 - 200 mmHg	6 (12.8)	1 (3)	5 (35.7)	
- ≤ 100 mmHg	5 (10.6)	0 (0)	5 (35.7)	

Values are given as numbers (n) and percentage (%) or are given as median and interquartile range (IQR). Continuous, not normally distributed variables are expressed as median and IQR and were compared using Mann–Whitney U test for two group comparison and Kruskal-Wallis test for three group comparison, where applicable. Continuous parameters were dichotomized at established cut-off values if necessary. Categorical data are presented as total numbers and proportions and were analysed by chi-squared test. Comparisons were considered statistically significant if two-sided p-value was <0.05. ACE - Angiotensin Converting Enzyme, Afib - atrial fibrillation, ALT – alanine amino-tranferase, ARB - Angiotensin II Receptor Blockers, ASA – Acetylsalicylic acid, AST – aspartate-aminotransferase, BMI – body mass index, CAD – coronary artery disease, CK – creatinine kinase, CRP – C-reactive protein, GFR-MDRD – glomerular filtration rate, Hb – hemoglobin, hs TNI - High sensitive Troponin I, INR – international normalized ratio, LDH – lactate dehydrogenase, NT-pro-BNP – N-terminal pro- brain natriuretic peptide, Pap Sys – pulmonary arterial pressure systolic, PCT – procalcitonin, PTT – partial thromboplastin time, SARS-CoV-2 – severe acute respiratory syndrome coronavirus-2

Table 3. Baseline characteristics of patient population stratified by the occurrence of the clinical endpoint (progressive respiratory failure defined by Horovitz Index HI < 200mmHg and mechanical ventilation)

Parameters	All Patients, N=47	HI > 200mmHg, N=36	HI ≤ 200mmHg, N=11	p-Value
Clinical characteristics				
Age, y	79 (59-82)	77 (55.5-81)	79 (68-86)	0.170
Male	24 (51..1)	18 (50)	6 (54.5)	0.792
BMI (kg/m²)	27.8 (25.1-31.8)	27.8 (25.2-31.9)	27.7 (24.8-33.8)	0.959
Fever	31 (67.4)	25 (69.4)	6 (54.5)	0.573
hs TNI > 37 (ng/L)	8 (17)	4 (11.1)	4 (36.4)	0.064
NT-pro BNP > 300 (ng/L)	27 (57.4)	17 (47.2)	10 (90.9)	**0.010**
CRP > 0.5 ml/dL	44 (93.6)	33 (91.7)	11 (100)	0.322
Cardiovascular risk factors				
Arterial hypertension	37 (78.7)	27 (75)	10 (90.9)	0.259
Dyslipidemia	24 (51.1)	20 (55.6)	4 (36.4)	0.229
Diabetes mellitus	12 (25.5)	9 (25)	3 (27.3)	0.880
Current smokers	1 (2.1)	0 (0)	1 (9.1)	0.571
Atrial fibrillation	10 (21.3)	6 (16.7)	4 (36.4)	0.178
Chronic kidney disease	7 (14.9)	5 (13.8)	2 (18.2)	0.726
Parameters of echocardiography				
Left ventricular ejection fraction, %	60 (60-60)	60 (60-60)	60 (60-60)	0.176
Right ventricular dilatation	15 (31.9)	11 (30.6)	4 (36.4)	0.229
Right ventricular function (TAPSE in mm)	20 (14.9-25.1)	20.5 (18-25.3)	19 (19-19)	0.524
Tricuspid regurgitation >1	6 (12.8)	4 (11.1)	2 (18.2)	0.494
Pericardial effusion	19 (40.4)	13 (36.1)	6 (54.5)	0.162
Pleural effusion	11 (23.4)	8 (22.2)	3 (27.3)	0.765
PAPsys (mmHg)	25 (20-30)	24 (20-30)	30 (24.8-47.3)	0.053
Concomitant cardiac medication at study entry				
Oral anticoagulation	2 (4.3)	2 (5.6)	0 (0)	0.869
ACE-I or ARB	30 (63.8)	24 (66.7)	6 (54.5)	0.464

Aldosterone inhibitors	6 (12.8)	4 (11.1)	2 (18.2)	0.300
Diuretics	19 (40.4)	16 (44.4)	3 (27.3)	0.720
Calcium channel blockers	13 (27.7)	10 (27.7)	3 (27.3)	0.586
Beta blockers	18 (38.3)	14 (38.9)	4 (36.4)	0.563
Statins	20 (42.6)	18 (50)	2 (18.2)	0.199
ASA	13 (27.7)	12 (33.3)	1 (9.1)	0.243
P2Y12 inhibitors	1 (2.1)	1 (2.8)	0 (0)	0.633
Parameters of electrocardiography				
Heart Rate (bpm)	77 (69.5-87.8)	77 (71-86.8)	74.5 (62.8-97.5)	0.595
Heart Rhythm				
- Sinus rhythm	29 (61.7)	22 (61.1)	7 (63.6)	
- Atrial fibrillation	6 (12.8)	4 (11.1)	2 (18.2)	0.861
- Pacemaker with ventricular pacing	3 (6.4)	1 (2.8)	2 (18.2)	
Laboratory parameters and biomarkers				
Leukocytes (1000/µL)	6080 (4190-7650)	5410 (4095-7637.5)	6840 (5980-8690)	0.315
Lymphocytes (1000/µL)	690 (590-970)	795 (632.5-1130)	580 (410-680)	**0.007**
Hb (g/dL)	13 (11.2-13.8)	13 (11.2-13.7)	13.3 (11.2-15.5)	0.407
Platelets (1000/µL)	169 (142-243)	171 (137.5-241.8)	164 (143-334)	0.821
INR (%)	1.1 (1-1.1)	1.1 (1-1.1)	1.1 (1-1.1)	0.820
PTT (s)	24 (22-28)	24 (22-27.8)	26 (23-31)	0.265
D-Dimer (µg/dL)	0.9 (0.7-1.7)	0.8 (0.5-1.1)	1.6 (0.9-2.6)	**0.034**
Creatinine (mg/dL)	0.9 (0.7-1.2)	0.9 (0.7-1.2)	1 (0.6-1.4)	0.791
GFR-MDRD (ml/m^2)	75.5 (58.3-98.9)	77.2 (58.6-96.9)	73.9 (48.3-100.6)	0.860
Sodium (mmol/L)	136 (134-140)	136 (135-139.8)	136 (132-140)	0.752
CRP (mg/dL)	4 (1.4-12.2)	2.6 (1.2-8)	12.2 (10.6-18.3)	**0.001**
PCT (ng/mL)	0.1 (0.1-0.2)	0.1 (0-0.2)	0.1 (0.1-0.2)	**0.045**
IL-6	13.5 (5.2-27.3)	13.4 (5.9-28.6)	11.7 (3-44.3)	0.690
TNF-α	143.6 (37.5-362.6)	61.7 (32.1-220.7)	272.5 (176.2-766.7)	**0.011**
hs TNI (ng/dL)	10 (3-25)	7.5 (2-18.5)	22 (13-101)	**0.010**

NT-pro-BNP (ng/L)	411 (132-3422)	316 (94.3-2511)	1588 (749-8845)	**0.018**
CK (U/L)	122 (66-250)	119 (65.3-249.5)	192 (116-266)	0.269
AST (U/L)	35 (20-43.5)	32.5 (20-40.3)	43 (25-70)	**0.025**
ALT (U/L)	27 (19-38)	27 (19.3-38.8)	26 (18-37)	0.669
LDH (U/L)	263.5 (210.3-332.5)	242 (197-309)	367 (279-445)	**0.002**
HbA1c (%)	6.2 (6-6.4)	6.1 (5.9-6.4)	6.3 (6.2-6.5)	0.331
Lactate (mmol/L)	1.4 (0.9-1.9)	1.5 (0.9-1.8)	1.3 (0.9-2.3)	0.836
pH	7.4 (7.4-7.5)	7.4 (7.4-7.5)	7.4 (7.4-7.5)	0.941
Intensive Care				
Bacterial co infection	4 (8.5)	0 (0)	4 (36.4)	**0.009**
Acute kidney injury	2 (4.3)	0 (0)	2 (18.2)	**0.038**
Acute hepatic injury	3 (6.4)	2 (5.6)	1 (9.1)	1.000
Vasopressors	6 (12.8)	1 (2.8)	5 (45.5)	**0.004**
Horovitz Index (mmHg)				
- > 300 mmHg	30 (63.8)	30 (83.3)	0 (0)	**<0.001**
- 201 - 300 mmHg	6 (12.8)	6 (16.7)	0 (0)	
- 101 - 200 mmHg	6 (12.8)	0 (0)	6 (54.5)	
- ≤ 100 mmHg	5 (10.6)	0 (0)	5 (45.5)	

Values are given as numbers (n) and percentage (%) or are given as median and interquartile range (IQR). Continuous, not normally distributed variables are expressed as median and IQR and were compared using Mann–Whitney U test for two group comparison and Kruskal-Wallis test for three group comparison, where applicable. Continuous parameters were dichotomized at established cut-off values if necessary. Categorical data are presented as total numbers and proportions and were analysed by chi-squared test. Comparisons were considered statistically significant if two-sided p-value was <0.05. ACE - Angiotensin Converting Enzyme, Afib - atrial fibrillation, ALT – alanine amino-tranferase, ARB - Angiotensin II Receptor Blockers**,** ASA – Acetylsalicylic acid , AST – aspartate-aminotransferase, BMI – body mass index, CAD – coronary artery disease, CK – creatinine kinase, CRP – C-reactive protein, GFR-MDRD – glomerular filtration rate, Hb – hemoglobin, Hs TNI - High sensitive Troponin I, INR – international normalized ratio, LDH – lactate dehydrogenase, NT-pro-BNP – N-Terminal pro-brain natriuretic peptide, Pap Sys – pulmonary arterial pressure systolic, PCT – procalcitonin, PTT – partial thromboplastin time, SARS-CoV-2 – severe acute respiratory syndrome coronavirus-2

Figure 1

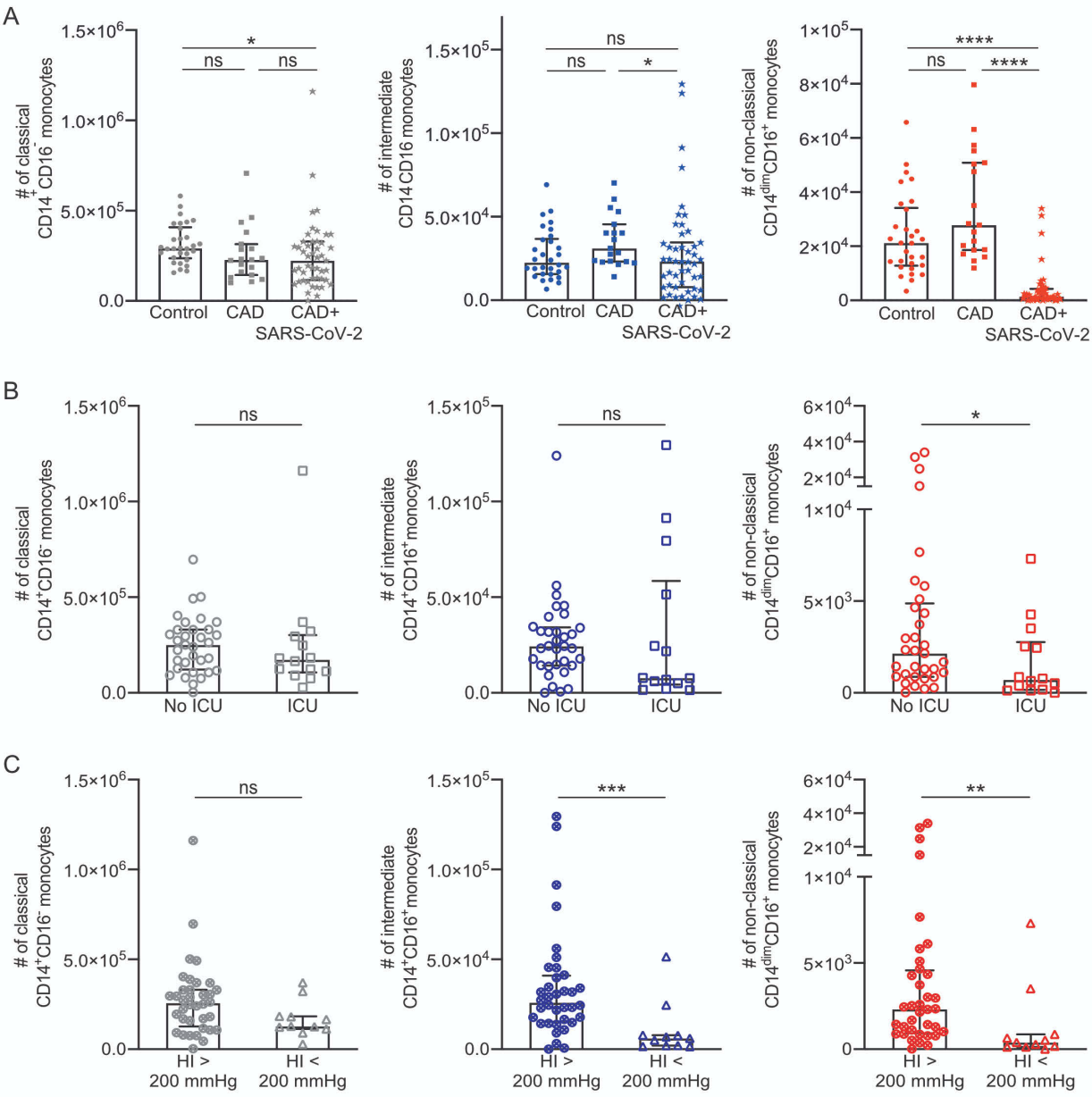
A
# of classical CD14+CD16- monocytes
1.5×10^6
1.0×10^6
5.0×10^5
0.0
*
ns
ns
Control
CAD
CAD+ SARS-CoV-2
# of intermediate CD14 CD16 monocytes
1.5×10^5
1.0×10^5
5.0×10^4
0.0
ns
ns
*
Control
CAD
CAD+ SARS-CoV-2
# of non-classical CD14dimCD16+ monocytes
1×10^5
8×10^4
6×10^4
4×10^4
2×10^4
0
****
ns
****
Control
CAD
CAD+ SARS-CoV-2
B
# of classical CD14+CD16- monocytes
1.5×10^6
1.0×10^6
5.0×10^5
0.0
ns
No ICU
ICU
# of intermediate CD14+CD16+ monocytes
1.5×10^5
1.0×10^5
5.0×10^4
0.0
ns
No ICU
ICU
# of non-classical CD14dimCD16+ monocytes
6×10^4
4×10^4
2×10^4
1×10^4
5×10^3
0
*
No ICU
ICU
C
# of classical CD14+CD16- monocytes
1.5×10^6
1.0×10^6
5.0×10^5
0.0
ns
HI > 200 mmHg
HI < 200 mmHg
# of intermediate CD14+CD16+ monocytes
1.5×10^5
1.0×10^5
5.0×10^4
0.0
***
HI > 200 mmHg
HI < 200 mmHg
# of non-classical CD14dimCD16+ monocytes
6×10^4
4×10^4
2×10^4
1×10^4
5×10^3
0
**
HI > 200 mmHg
HI < 200 mmHg

Figure 2

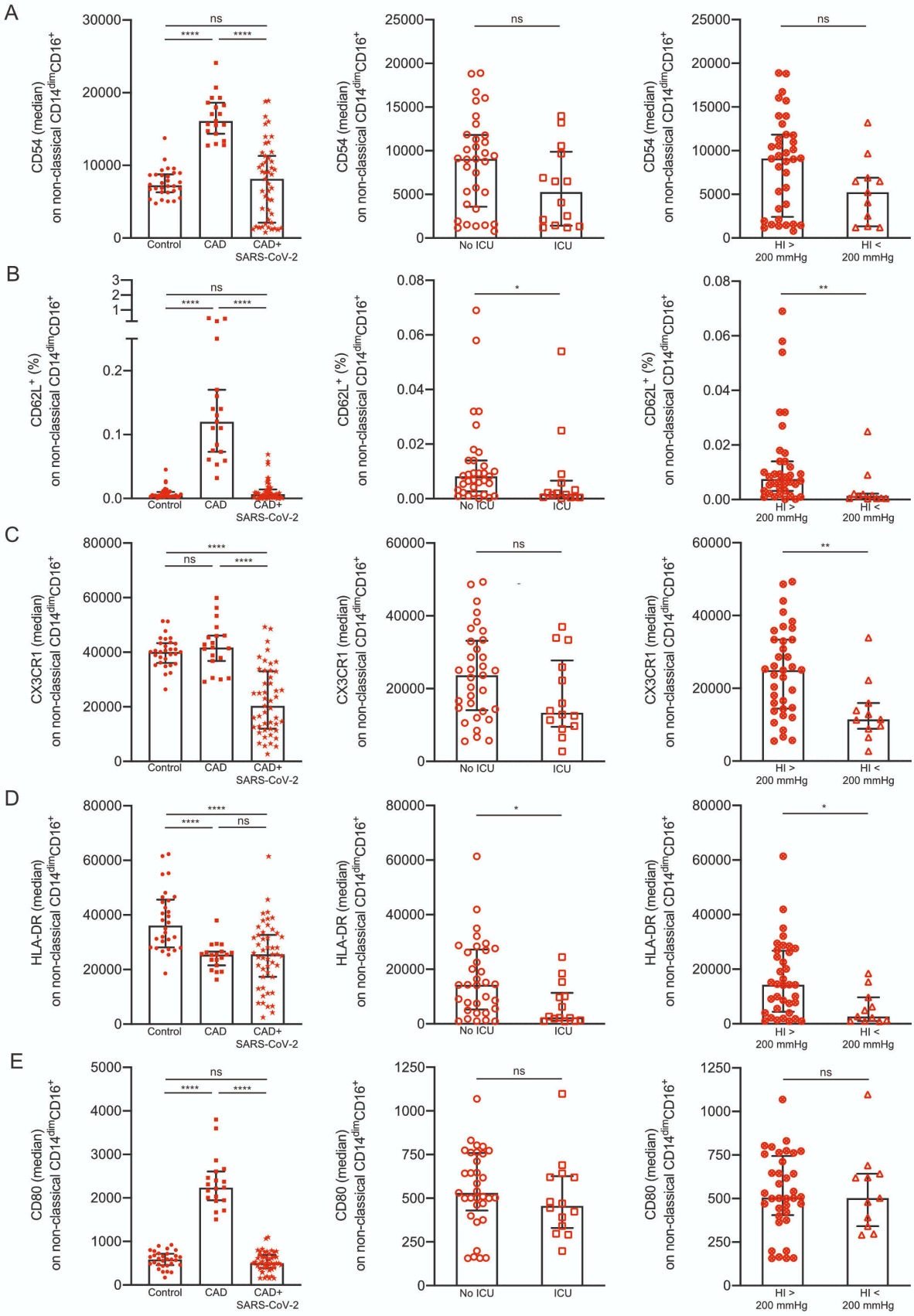
A
B
C
D
E
CD54 (median) on non-classical CD14dimCD16+
CD62L+ (%) on non-classical CD14dimCD16+
CX3CR1 (median) on non-classical CD14dimCD16+
HLA-DR (median) on non-classical CD14dimCD16+
CD80 (median) on non-classical CD14dimCD16+
Control
CAD
CAD+ SARS-CoV-2
No ICU
ICU
HI > 200 mmHg
HI < 200 mmHg
ns
****
*
**

Figure 3

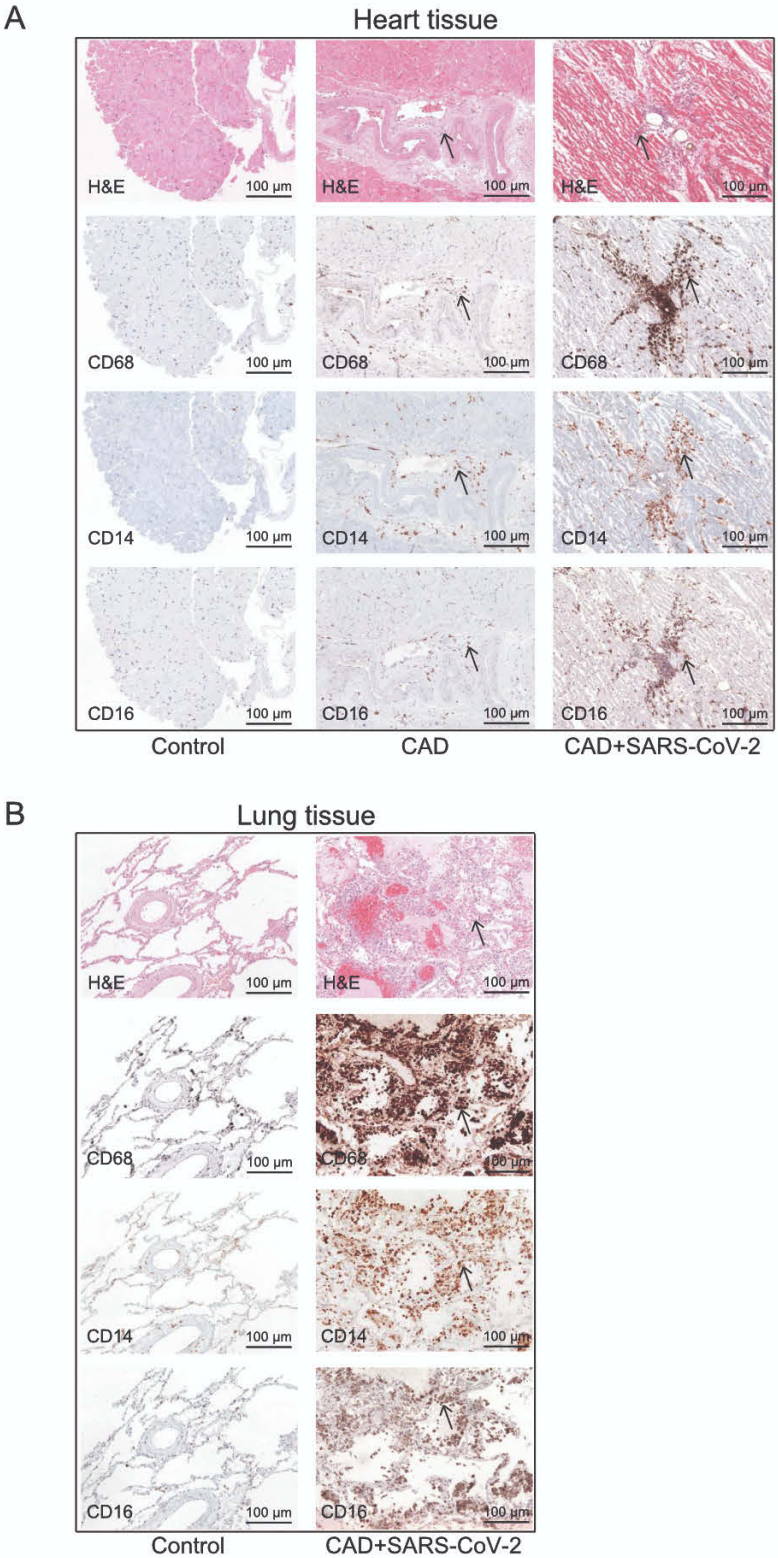
A
Heart tissue
H&E
CD68
CD14
CD16
100 μm
Control
CAD
CAD+SARS-CoV-2
B
Lung tissue
H&E
CD68
CD14
CD16
100 μm
Control
CAD+SARS-CoV-2

Figure 4

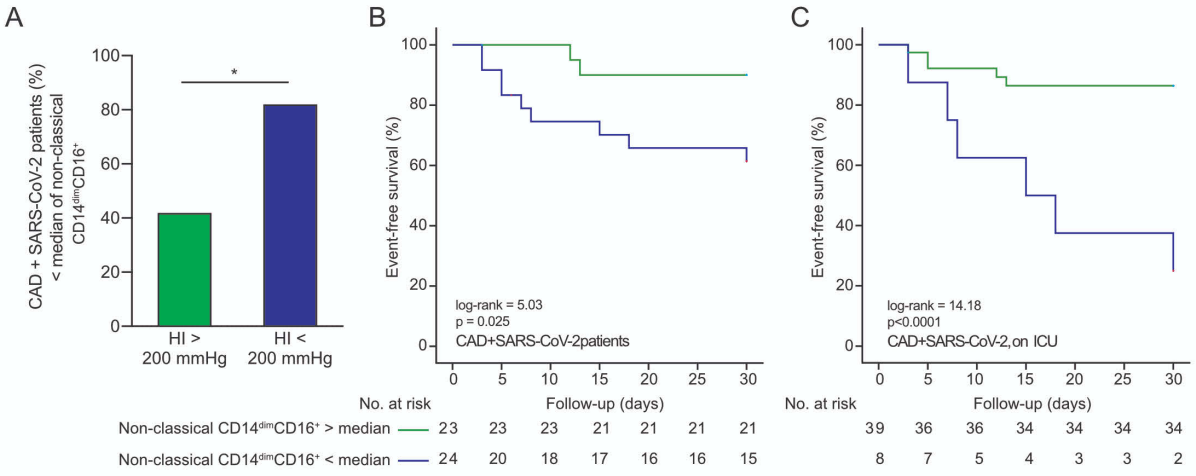
A
CAD + SARS-CoV-2 patients (%) < median of non-classical CD14dimCD16+
100
80
60
40
20
0
*
HI > 200 mmHg
HI < 200 mmHg
B
Event-free survival (%)
log-rank = 5.03
p = 0.025
CAD+SARS-CoV-2patients
0 5 10 15 20 25 30
Follow-up (days)
No. at risk
Non-classical CD14dimCD16+ > median 23 23 23 21 21 21 21
Non-classical CD14dimCD16+ < median 24 20 18 17 16 16 15
C
Event-free survival (%)
log-rank = 14.18
p<0.0001
CAD+SARS-CoV-2, on ICU
0 5 10 15 20 25 30
Follow-up (days)
No. at risk
39 36 36 34 34 34 34
8 7 5 4 3 3 2

Numbers and phenotype of non-classical CD14^{dim}CD16^{+} monocytes are predictors of adverse clinical outcome in patients with coronary artery disease and severe SARS-CoV-2 infection

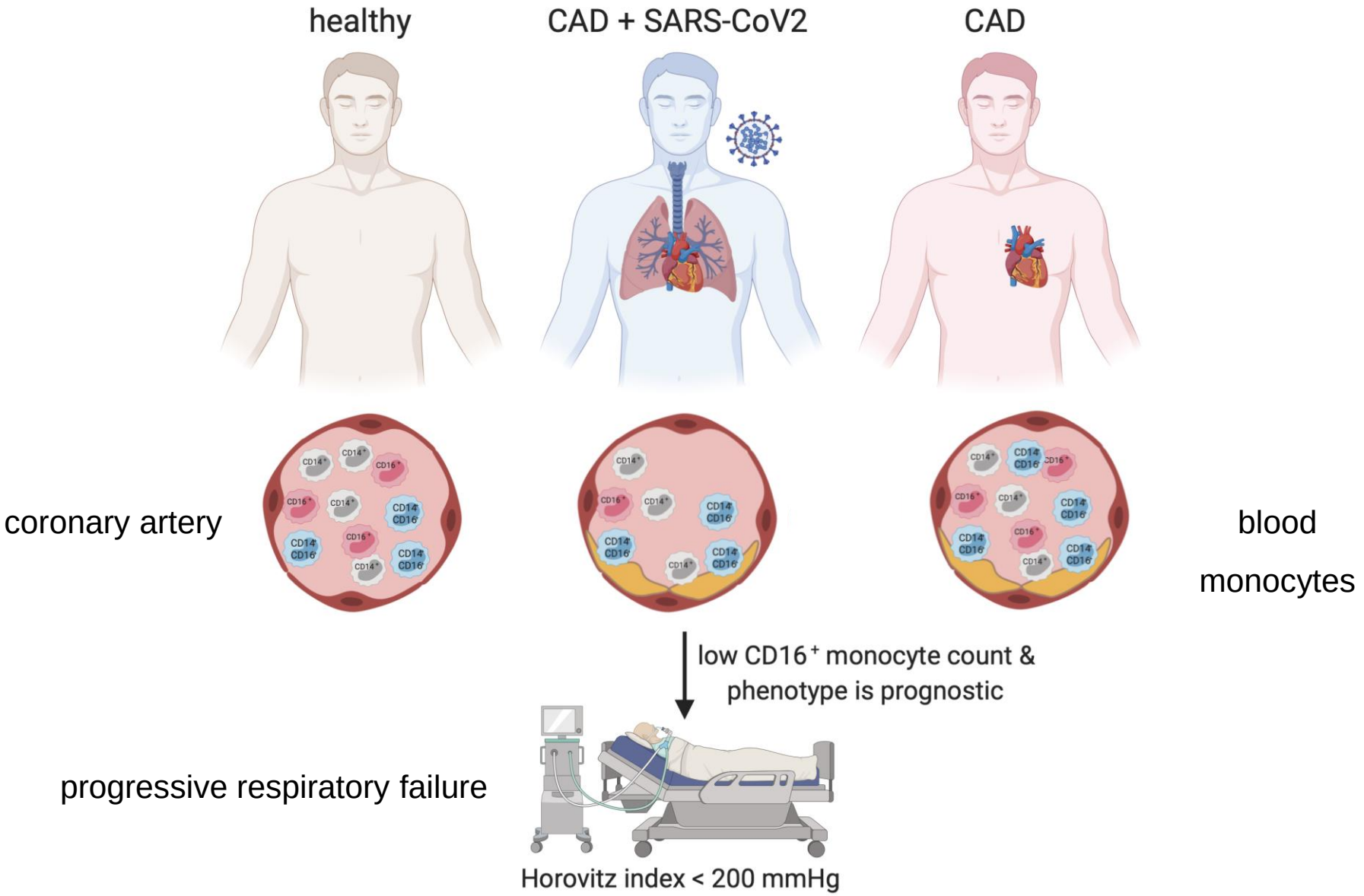

Recovery of systemic hyperinflammation in patients with severe SARS-CoV-2 infection

Carolin Langnau[1], Henrik Janing[1], Hüseyin Kocaman[1], Sarah Gekeler[1], Manina Günter[2,3], Álvaro Petersen-Uribe[1], Philippa Jaeger[1], Barbara Koch[1], Klaus-Peter Kreisselmeier[1], MD, Tatsiana Castor[1], PhD, Dominik Rath[1], MD, Meinrad Paul Gawaz[1], MD, Stella E. Autenrieth[2,3], PhD, Karin Anne Lydia Mueller[1*], MD

[1]University Hospital Tuebingen, Department of Cardiology and Angiology, Eberhard Karls University Tuebingen, Tuebingen, Germany

[2]University Hospital Tuebingen, Department of Hematology, Oncology, Clinical Immunology and Rheumatology, Eberhard Karls University Tuebingen, Tuebingen, Germany

[3]German Cancer Research Centre, Department of Dendritic Cells in Infection and Cancer, Heidelberg, Germany

Langnau, Carolin et al. “Recovery of systemic hyperinflammation in patients with severe SARS-CoV-2 infection.” Biomarkers : biochemical indicators of exposure, response, and susceptibility to chemicals, 1-14. 23 Nov. 2022, doi:10.1080/1354750X.2022.2148745

Biomarkers

ISSN: (Print) (Online) Journal homepage: https://www.tandfonline.com/loi/ibmk20

Recovery of systemic hyperinflammation in patients with severe SARS-CoV-2 infection

Carolin Langnau, Henrik Janing, Hüseyin Kocaman, Sarah Gekeler, Manina Günter, Álvaro Petersen-Uribe, Philippa Jaeger, Barbara Koch, Klaus-Peter Kreisselmeier, Tatsiana Castor, Dominik Rath, Meinrad Paul Gawaz, Stella E. Autenrieth & Karin Anne Lydia Mueller

To cite this article: Carolin Langnau, Henrik Janing, Hüseyin Kocaman, Sarah Gekeler, Manina Günter, Álvaro Petersen-Uribe, Philippa Jaeger, Barbara Koch, Klaus-Peter Kreisselmeier, Tatsiana Castor, Dominik Rath, Meinrad Paul Gawaz, Stella E. Autenrieth & Karin Anne Lydia Mueller (2022): Recovery of systemic hyperinflammation in patients with severe SARS-CoV-2 infection, Biomarkers, DOI: 10.1080/1354750X.2022.2148745

To link to this article: https://doi.org/10.1080/1354750X.2022.2148745

BIOMARKERS
https://doi.org/10.1080/1354750X.2022.2148745

Taylor & Francis
Taylor & Francis Group

ORIGINAL ARTICLE

Recovery of systemic hyperinflammation in patients with severe SARS-CoV-2 infection

Carolin Langnau[a], Henrik Janing[a], Hüseyin Kocaman[a], Sarah Gekeler[a], Manina Günter[b,c], Álvaro Petersen-Uribe[a], Philippa Jaeger[a], Barbara Koch[a], Klaus-Peter Kreisselmeier[a], Tatsiana Castor[a], Dominik Rath[a], Meinrad Paul Gawaz[a], Stella E. Autenrieth[b,c] and Karin Anne Lydia Mueller[a,#]

[a]Department of Cardiology and Angiology, Eberhard Karls University Tuebingen, University Hospital Tuebingen, Tuebingen, Germany; [b]Department of Hematology, Oncology, Clinical Immunology and Rheumatology, Eberhard Karls University Tuebingen, University Hospital Tuebingen, Tuebingen, Germany; [c]Department of Dendritic Cells in Infection and Cancer, German Cancer Research Centre, Heidelberg, Germany

ABSTRACT

Introduction: Patients with cardiovascular disease (CVD) and acute SARS-CoV-2 infection might show an altered immune response during COVID-19.

Material and methods: Twenty-three patients with CVD and SARS-CoV-2 infection were prospectively enrolled and received a cardiological assessment at study entry and during follow-up visit. Inclusion criteria of our study were age older than 18 years, presence of CVD, and acute SARS-CoV-2 infection. The median age of the patient cohort was 69 (IQR 55–79) years. 12 (52.2%) patients were men. Peripheral monocytes and chemokine/cytokine profiles were analysed.

Results: Numbers of classical and non-classical monocytes were significantly decreased during acute SARS-CoV-2 infection compared to 3-month recovery. While classical monocytes reached the expected level in peripheral blood after 3 months, the number of non-classical monocytes remained significantly reduced.

Discussion: All three monocyte subsets exhibited changes of established adhesion and activation markers. Interestingly, they also expressed higher levels of pro-inflammatory cytokines like macrophage migration inhibitory factor (MIF) at the time of recovery, although MIF was only slightly increased during the acute phase.

Conclusion: Changes of monocyte phenotypes and increased MIF expression after 3-month recovery from acute SARS-CoV-2 infection may indicate persistent, possibly long-lasting, pro-inflammatory monocyte function in CVD patients.

GRAPHICAL ABSTRACT

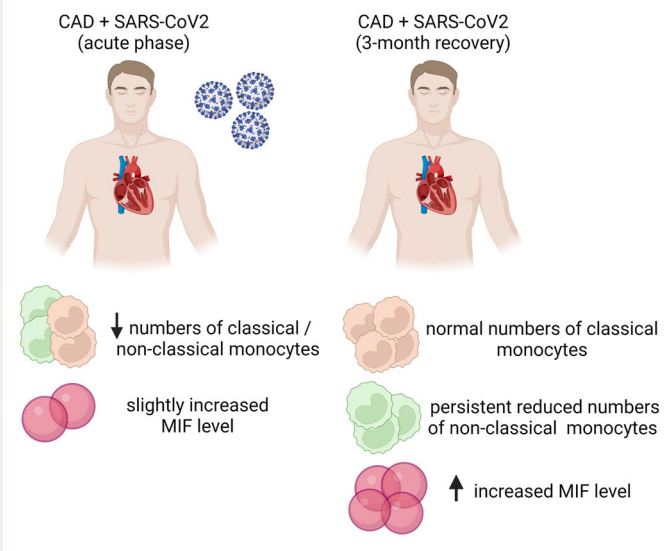

ARTICLE HISTORY

Received 23 June 2022
Accepted 12 November 2022

KEYWORDS

hyperinflammation; monocytes; platelets; recovery; SARS-CoV-2 infection

CONTACT Karin Anne Lydia Mueller k.mueller@med.uni-tuebingen.de Department of Cardiology and Angiology, University Hospital of the Eberhard Karls University Tuebingen, Otfried-Müller-Str. 10, 72076 Tuebingen, Germany
[#]Karin Anne Lydia Mueller is responsible for statistical design and analysis. Email: k.mueller@med.uni-tuebingen.de
Supplemental data for this article can be accessed online at https://doi.org/10.1080/1354750X.2022.2148745

Introduction

In the past two years, the COVID-19 pandemic has significantly threatened the health system worldwide. It has been rapidly recognised that patients with cardiovascular disease (CVD) or associated risk factors such as arterial hypertension, diabetes mellitus, renal failure, and obesity are at high risk for an unfavourable course of COVID-19 (Huang *et al.* 2020, Zhou *et al.* 2020). COVID-19 has been associated with severe systemic inflammatory response and cytokine storm leading to thrombotic complications, microcirculatory disturbances and organ failure (Huang *et al.* 2020, Zhou *et al.* 2020, Jose *et al.* 2020). Thus, SARS-CoV-2 infection may have a long-term impact not only on the cardiovascular system but also on the immune response (Xiong *et al.* 2020, Zheng *et al.* 2020, Task Force for the management of C-otESoC 2022). Recently, we found that patients with CVD are at increased risk of life-threatening heart and lung injury due to pro-inflammatory and prothrombotic responses during SARS-CoV-2 infection (Mueller *et al.* 2021). We identified phenotype changes of circulating monocyte subtypes together with reduced numbers of circulating non-classical $CD14^{dim}CD16^{+}$ monocytes and sequestration in affected organs precedes and predicts rapidly progressive respiratory and multiorgan failure (Mueller *et al.* 2021) Further, we and others found that platelet activation and hyperinflammation is associated with prognosis of patients with CVD and COVID-19 (Gu *et al.* 2021, Langnau *et al.* 2021). SARS-CoV-2 infection not only activates the antiviral immune response but, in addition, is responsible for uncontrolled immune responses in a number of cases, particularly increased release of pro-inflammatory cytokines. This in turn might induce lymphopenia, lymphocyte, granulocyte, and monocyte dysfunction and reduce immune cell numbers of clinical relevance (Yang *et al.* 2020). Another study showed that the numbers of intermediate monocytes producing interleukin (IL-) 6 were increased in patients that were admitted to intensive care unit (ICU) compared to patients with less severe courses of COVID-19 (Merad *et al.* 2020). Additionally, a significantly reduced amount of peripheral non-classical monocytes predicted an adverse clinical outcome in patients with CVD and severe SARS-CoV-2 infection (Mueller *et al.* 2021). To date, the long-term effects of SARS-CoV-2 infection have not been fully understood. Therefore, it is important to investigate the immune responses and immunophenotypes during acute phases and after recovery from SARS-CoV-2 infection. Along with clinically relevant complications and consequences such as fatigue, muscle weakness, dyspnoea, arrhythmias, anxiety, and depression, it is essential to investigate the long-term outcome of severe SARS-CoV-2 infection on immune cells and immune responses (Huang *et al.* 2021). The aim of the present study was to characterise the long-term changes of systemic inflammation in patients with severe acute SARS-CoV-2 infection on immune cells. We compared subgroups of circulating monocytes in the same group of COVID-19 patients in the acute phase of hyperinflammation and after 3-months recovery follow-up as well as a healthy control group using immunophenotyping by multicolour flow cytometry.

Materials and methods

Study design, study populations and inclusion criteria

In this study, we consecutively enrolled 23 patients at the Department of Cardiology and Angiology of the University Hospital Tübingen, Germany from February 2020 until September 2020. Twenty-three patients with pre-existing CAD and an acute, severe SARS-CoV-2 infection were included within 12 hours after hospital admission. As control, 40 healthy controls without SARS-CoV-2 infection were included in our study. The healthy control group showed a median age of 41 (IQR 28-53), 41% were men. Healthy controls did not suffer from any disease and did not take any relevant medication, especially no medication on daily basis. All 23 patients were analysed after a recovery period of 3 months in our department. None were lost to follow-up. All patients received a clinical and cardiac examination including echocardiography, electrocardiography, concomitant medication, comorbidities and blood sampling for routine laboratory parameters, marker expression on monocytes, and chemokine profiling. From nasopharyngeal secretions SARS-CoV-2 infection was confirmed by real-time reverse transcriptase polymerase chain reaction (PCR). Inclusion criteria of our study were age older than 18 years, confirmed CVD or CV risk factors, and acute SARS-CoV-2 infection. Exclusion criteria were other microbial infections. The study was approved by the local ethics committee (240/2018B02) and complies with the declaration of Helsinki and the good clinical practice guidelines on the approximation of the laws, regulations and administrative provisions of the member states relating to the implementation of good clinical practice in the conduct of clinical trials on medicinal products for human use. Written informed consent was obtained from every patient.

We determined N-terminal-pro-B-type natriuretic peptide (NT-pro-BNP, >300 ng/L), high sensitive troponin I (hs TNI, >37 ng/L), IL-6, and C-reactive protein (CRP, >0.5 mg/dL) as elevated laboratory markers of myocardial and inflammatory distress. As echocardiographic parameters the left and right ventricular function, right ventricular dilatation, presence of tricuspid valve regurgitation, and pericardial effusion were included according to current guidelines (Lang *et al.* 2015, Parasuraman *et al.* 2016).

Multicolour flow cytometry

46 blood samples of patients with CVD and SARS-CoV-2 infection and 40 healthy donors were collected in CPDA monovettes for phenotyping of platelets and monocytes for flow cytometry analysis. First, platelets were analysed in whole blood diluted 1:10 in HEPES-Tyrode's buffer (pH 7.4) in a 96 well plate (Falcon). For monocyte staining, whole blood was lysed in 10 x RBC Lysis buffer (BioLegend, San Diego, California, USA) diluted 1:10 in Millipore water and and incubated for 15 min at RT in the dark. After two washing steps with PBS containing 1% FCS, 2 mM EDTA and 1% sodium azide, cell count was adjusted to 3×10^6 cells per well. Human IgG (0.01 mg/ml; Sigma Aldrich Co. St. Luis, Missouri, USA)

was used to avoid unspecific binding by blocking the Fc part of receptors on cells during an incubation for 20 min at 4 °C. Extracellular monocyte staining was performed with fluorochrome-conjugated antibodies CX3CR1 PE/Dazzle (clone 2A9-1), CCR2 BV605 (clone K036C2) and CCR7 BV785 (clone G043H7) from BioLegend (San Diego, California, USA) for 1 h at 37 °C followed by staining with HLA-DR PerCP-Vio77 (clone REA805; Miltenyi Biotec, Bergisch Gladbach, Germany), CD3 BV510 (clone OKT3), CD15 BV510 (clone W603), CD19 BV510 (clone HLB19), CD20 BV510 (clone 2H7), CD56 BV510 (clone HCD56), CD14 FITC (clone M5E2), CD16 BV711 (clone 3G8), CD62L PE-Cy7 (clone DREG-56), CD11b BV605 (clone ICRF44), CD11a BV650 (clone HI1 11) from BioLegend (San Diego, California, USA) for 20 min at 4 °C. For Life/Dead staining Zombie NIR (BioLegend, San Diego, California, USA) was used and performed together with the extracellular antibody staining. Cells were fixed overnight with FoxP3 Staining Buffer Set (Thermo Fisher Scientific, Waltham, Massachusetts, USA) according to manufacturer's instructions. For permeabilization of monocytes, 1 x Perm buffer (eBioscience) was used followed by an intracellular staining for 1 h at RT with following fluorochrome-conjugated antibodies: anti-CXCL12 PE (clone 79019), anti-CXCL14 AF647 (clone MM0213-12B24) and anti-MIF AF594 (clone 932606) from R&D Systems (McKinley Place, Minneapolis, USA). Cells were washed after each staining with PBS containing 1% FCS, 2 mM EDTA and 1% sodium azide. Anti-CD3, -CD15, -CD19, -CD20, and CD56 were used as dump channels to remove T cells, NK cells, B cells, and granulocytes. Measurement was performed using the LSR Fortessa (BD Biosciences, Franklin Lakes, New Jersey, USA) and DIVA software (BD Biosciences, Franklin Lakes, New Jersey, USA) followed by data analysis with FlowJo software V.10.6.2 (BD Biosciences, Franklin Lakes, New Jersey, USA). Monocytes were gated as follows: time/singlets/leukocytes/living cells/lineage negative cells/CD14CD16. Classical monocytes were characterised as $CD14^{-}CD16^{+}$, intermediate as $CD14^{+}CD16^{+}$ and non-classical as $CD14^{dim}CD16^{+}$ (Supplemental Figure S1). Platelets and platelet/leukocyte co-aggregates were characterised according to their size and granularity and gated as follows: time/singlets/platelets/Life/Dead FSC-low or FSC-High. In particular, platelets were gated as follows: FSC-low/$CD41^{+}CD42b^{+}$ and platelet/leukocyte co-aggregates were gated as follows: FSC-high/$CD41^{+}CD42b^{+}$ (Supplemental Figure S1). Surface marker expression was quantified as median fluorescence intensity (MFI) and frequency of living cells. Fluorescence minus one (FMO) controls were used for gating on marker positive platelets.

Unsupervised data analysis as detailed below was done using OMIQ data analysis software (Omiq inc., Santa Clara, CA, USA). First, the data were manually gated to remove aggregates, dead cells, debris, and then the data were sub-sampled to include 1.0×10^{6} $CD14^{+}/CD16^{+}/CD14^{+}CD16^{+}$ cells/group. Next, flowAI (Monaco *et al.* 2016) was run to check for any aberrant regions of the files. FlowAI settings were as follows: all files used, all fluorescent channels and time selected, all methods used and default settings. Subsequently, dimension reduction analysis was performed using Uniform Manifold Approximation and Projection (UMAP) to visualise the different sub-populations of the cells (McInnes et al. 2018). For monocytes following UMAP settings were used: all files used, all fluorescent parameters were used, Neighbours = 15, Minimum Distance = 0.4, Components = 2, Metric = Euclidean, Learning Rate = 1, Epochs = 200, Random Seed = 8263, Embedding Initialisation = spectral. Following the UMAP analysis, PhenoGraph (Levine *et al.* 2015) was run to cluster the data. PhenoGraph settings for monocytes were as follows: all files used, clustering features CXCL14, ACKR3, CD11b, CXCR4, CD16, CCR7, CD14, CXCL12, CD62L, MIF, HLA-DR, (monocyte Panel 2: CD106, CD40, CCR2, CD11a, CD16, CD80, CD14, CD54, CD49a, CX3CR1, HLA-DR,) umap_1, umap_2, Distance Metric = euclidian, consensus metaclustering with k = 20, Louvain Seed = 9898. A heatmap was generated with the metaclusters obtained from PhenoGraph and clustered hierarchically on all surface markers with a euclidean distance metric to indicate the similarity of the populations.

Measurement of plasma levels of cytokines and chemokines (LEGENDPlex)

The concentrations of several cytokines and chemokines of 46 frozen plasma samples were determined by LEGENDPlex Inflammation Panel 1 (IL-1β, IFN-α2, IFN-γ, TNF-α, MCP-1 (CCL2), IL-6, IL-8 (CXCL8), IL-10, IL-12p70, IL-17A, IL-18, IL-23, and IL-33) and LEGENDPlex Proinflammatory Chemokine Panel (MCP-1 (CCL2), RANTES (CCL5), IP-10 (CXCL10), Eotaxin (CCL11), TARC (CCL17), MIP-1α (CCL3), MIP-1β (CCL4), MIG (CXCL9), MIP-3α (CCL20), ENA-78 (CXCL5), GROα (CXCL1), I-TAC (CXCL11) and IL-8 (CXCL8); Supplemental Table S3) (BioLegend, San Diego, California, USA). The assays were performed according to the manufacturer's manual. FACS Lyric (BD Biosciences, Franklin Lakes, New Jersey, USA) was used for the measurement and data analysis was performed with the LEGENDPlex Data Analysis Software (BioLegend, San Diego, California, USA).

Statistical analysis

Statistical analysis of participants' clinical and laboratory baseline characteristics in relation to measured monocyte and platelet phenotypes and marker expression was performed. Non-normally distributed continuous data are represented as median with interquartile range (IQR) and normally distributed continuous data are represented as mean with standard deviation (SD). Two group comparisons for non-normally distributed continuous variables were performed using a Mann-Whitney U test while normally distributed continuous variables were compared using Student's T-test. Paired non-normally distributed continuous variables were compared using Wilcoxon test. Three group comparisons for non-normally distributed continuous variables were performed using a Kruskal Wallis test while normally distributed continuous variables were compared using One Way ANOVA. Categorical variables are represented as total numbers and proportions of participants and comparison was performed

using chi-square test. Comparisons were considered statistically significant if two-sided p value was <0.05. All statistical analysis was performed with IBM SPSS Statistics software version 26 (SPSS, Inc.) and GraphPad Prism Version 8.4.0 (GraphPad Software). Unsupervised data analysis was done using OMIQ data analysis software (Omiq inc., Santa Clara, CA, USA). Heatmaps were generated with the metaclusters obtained from PhenoGraph and clustered hierarchically on all surface markers with a euclidean distance metric to indicate the similarity of the populations.

Results

Clinical characteristics of patients with severe SARS-CoV-2 infection

From February to September 2020, we prospectively studied a consecutive cohort of 23 patients at cardiovascular risk or with cardiovascular disease (CVD), who were treated for severe respiratory failure associated with acute SARS-CoV-2 infection in our hospital (Supplemental Table S1). 40 healthy participants served as controls. The healthy control group showed a median age of 41 (IQR 28-53), 41% were men. Healthy controls did not suffer from any disease and did not take any relevant medication, especially no medication on daily basis. Baseline characteristics and demographics of the overall cohort are given in Supplemental Table S1. The median age of the population was 69 (IQR 55–79) years. 12 (52.2%) patients were men. 11 (47.8%) patients presented with a Horovitz Index (HI) < 300 mmHg on admission (Supplemental Table S1). In the acute COVID-19 phase most prominent clinical signs were cough, dyspnoea, and fevers. All patients revealed radiological signs associated with their respiratory failure in the X-ray of the chest (Table 1). Pericardial and/or pleural effusion were present in 11 (48%) and 7 (30%) patients, respectively (Table 1). While there was no clinically relevant leukocytosis documented upon admission, we found lymphocytopenia of 660/µL (530-1150), elevated CRP and IL-6 levels of 2.5 mg/dL (1.3-12.5) and 27.3 (9.5-37.4), respectively (Table 1). Furthermore, NT-pro-BNP and D-Dimer were increased with 323 ng/L (132.5-825.5) and 0.9 µg/dL (0.6-1.9), respectively (Table 1). During their hospital stay, 9 (39.1%) patients were admitted to the intensive care unit (ICU) due to progressive respiratory failure requiring transient high-flow oxygen therapy ($n=4$) or mechanical ventilation ($n=5$) (Supplemental Table S1). At 3-months follow-up 43.5% of patients reported persistent dyspnoea as most prominent clinical symptom. Furthermore, one patient was re-hospitalized for acute Non-ST-elevation myocardial infarction during follow-up. 5 patients complained of chronic fatigue. No events of thrombosis, stroke, bleeding, or rhythm disturbances were evident (Supplemental Tables S1 and S2). In most patients pericardial and pleural effusion were absent in the recovery phase and radiological pulmonary pathologies recuperated (Table 1). Furthermore, initially impaired laboratory parameters including lymphocyte count, elevated CRP-, IL6-, NT-pro-BNP-, creatine kinase- (CK), lactate dehydrogenase- (LDH) levels during acute infection reached normal values at the follow up visit after three months (Table 1).

Characterisation of changes in immunophenotypes of circulating peripheral monocytes and platelets following SARS-CoV-2 infection

Recently, we found that in acute SARS-CoV-2 infection low numbers of $CD14^{dim}CD16^{+}$ non-classical monocytes were associated with rapidly progressive respiratory failure due to sequestration in affected inflamed lung and organ tissue (Mueller *et al.* 2021). In the present study, we compared subgroups of circulating monocytes in the same group of COVID-19 patients in the acute phase of hyperinflammation and after 3-months recovery follow-up as well as a healthy control group using immunophenotyping by multicolour flow cytometry. The white blood cell count was lower by trend in SARS-CoV-2-infected patients in the acute phase of hyperinflammation compared to the recovery phase after three months and to that of healthy controls (WBC count/ml; acute vs post vs healthy control; median + IQR; 4.3×10^6 (2.7×10^6-5.7×10^6) vs 5.4×10^6 (4.3×10^6-6.8×10^6) vs 5.25×10^6 (4.63×10^6-6.4×10^6); acute vs post $p=0.1126$; acute vs healthy $p=0.0702$; post vs healthy $p>0.9999$, Figure 1A). The platelet counts only showed differences by trend (platelet count/ml; acute vs post vs healthy control; median + IQR; 1.3×10^8 (9.6×10^7-1.8×10^8) vs 1.73×10^8 (1.43×10^8-2.29×10^8) vs 2.01×10^8 (1.71×10^8-2.37×10^8); acute vs post $p=0.4983$; acute vs healthy $p=0.0043$; post vs healthy $p=0.3112$, Figure 1B), however, platelet/leucocyte aggregates showed significantly different numbers in the recovery phase compared to the healthy controls (platelet/leucocyte aggregates count; acute vs post vs healthy control; median + IQR; 0.91×10^7 (6.9×10^6-1.3×10^7) vs 1.3×10^7 (8.9×10^6-2.1×10^7) vs 0.82×10^7 (5.74×10^6-1.5×10^7); acute vs post $p=0.0962$; acute vs healthy $p>0.9999$; post vs healthy $p=0.0202$, Figure 1C).

In line with our previous findings (Mueller *et al.* 2021), three months after SARS-CoV-2 infection the numbers of circulating $CD14^{dim}CD16^{+}$ non-classical monocytes was dramatically reduced in patients with acute SARS-CoV-2 infection and returned to near-normal levels three months later ($CD14^{dim}CD16^{+}$ non-classical monocytes; acute vs post vs healthy control; median + IQR; 1640 (526.3-6110) vs 12190 (2420-30020) vs 21905 (13883-36360); acute vs post $p=0.0013$; acute vs healthy $p<0.0001$; post vs healthy $p=0.0701$, Figure 1D). Similarly, the number of circulating $CD14^{+}CD16^{-}$ classical monocytes that were also slightly reduced during the acute phase of the infection and returned to normal levels after 3-months recovery ($CD14^{+}CD16^{-}$ classical monocytes; acute vs post vs healthy control; median + IQR; 193070 (122800-321180) vs 340280 (285140-491200) vs 292455 (240380-393835); acute vs post $p=0.0081$; acute vs healthy $p=0.0779$; post vs healthy $p=0.746$, Figure 1D) whereas the numbers of intermediate monocytes ($CD14^{+}CD16^{+}$) remained unchanged throughout the infection (Figure 1D). Previously, we found that the function of circulating monocytes was impaired in CVD patients with severe acute SARS-CoV-2 infection compared to CVD patients without SARS-CoV-2 infection, as indicated by low expression of CD62L, CX3CR1 and HLA-DR as established markers of adhesion, migration, and T-cell activation (Mueller *et al.* 2021). Here, we additionally assessed the expression of markers on subtypes of monocytes

Table 1. Clinical characteristics of patients during acute SARS-CoV-2 infection and after a three months recovery period.

Parameters	Acute Infection, n = 23	Post Infection, n = 23	*p*-value
Clinical characteristics			
Cough	12 (52.2)	1 (4.3)	**<0.001**
Dyspnoea	12 (52.2)	10 (43.5)	0.555
Fever	14 (60.9)	0 (0)	**<0.001**
NT-pro BNP > 300 (ng/L)	13 (56.5)	4 (17.4)	**0.037**
hs TNI > 15 (ng/L)	7 (30.4)	0 (0)	**0.007**
Parameters of echocardiography			
Left ventricular hypertrophy	11 (47.8)	11 (47.8)	0.763
Left ventricular ejection fraction (%)	60 (55-65)	60 (55-65)	0,989
Mitral regurgitation	16 (69.6)	18 (78.3)	0.164
Tricuspid regurgitation	11 (47.8)	15 (65.2)	0.132
Right ventricular function	1 (4.3)	0 (0)	0.334
Right ventricular dilatation	2 (8.7)	1 (4.3)	0.626
Pericardial effusion	11 (47.8)	3 (13)	**0.010**
Pleural effusion	7 (30.4)	2 (8.7)	**0.046**
PAPsys (mmHg)	25 (20-29.5)	20 (20-30.75)	0.696
Parameters of radiology			
Bilateral nodular opacities	13 (56.5)	0 (0)	**0.001**
Ground-glass opacities	4 (17.4)	1 (4.3)	0.155
Peribronchial thickening	1 (4.3)	1 (4.3)	1
Focal consolidations	4 (17.4)	1 (4.3)	0.155
Venous congestion	2 (8.7)	0 (0)	0.148
Atelectasis	0 (0)	1 (4.3)	0.312
Parameters of electrocardiography			
Heart Rate (bpm)	74 (68-86)	71 (63-79.5)	0.306
Systolic blood pressure (mmHg)	140 (120-150)	140 (130-150)	0.631
QRS (ms)	87.5 (80-100)	89 (81.5-93.5)	0.900
RBB	2 (8.7)	2 (8.7)	0.924
QTc (ms)	4 (17.4)	1 (4.3)	0.144
T-Neg	3 (12)	1 (4.3)	0.340
ST-Depression	2 (8.7)	0 (0)	0.167
Heart Rhythm			0.401
- Sinus rhythm	21 (91.3)	20 (86.9)	
- Atrial fibrillation	0 (0)	1 (4.3)	
- PM	1 (4.3)	0 (0)	
- SVT	1 (4.3)	0 (0)	
Laboratory parameters and biomarkers			
Leukocytes (1000/µL)	6550 (4090-8860)	7240 (6020-9110)	0.227
Lymphocytes (1000/µL)	660 (530-1150)	1540 (1280-2090)	**<0.001**
Hb (g/dL)	13.2 (11.7-14.3)	13 (12.5-14.9)	0.435
Platelets (1000/µL)	167 (143-228)	233 (191-297)	**0.024**
INR (%)	1.1 (1-1.1)	1 (1-1.1)	0.273
PTT (s)	24 (22-28)	23 (22-25)	0.991
D-Dimer (µg/dL)	0.9 (0.6-1.9)	–	–
Creatinine (mg/dL)	0.8 (0.7-1.2)	0.9 (0.6-1.2)	0.900
GFR-MDRD (ml/m^2)	82.3 (53.5-105.4)	84.1 (59.5-99.1)	0.820
Sodium (mmol/L)	136 (134-139)	141 (139-142)	**<0.001**
CRP (mg/dL)	2.5 (1.3-12.5)	0.1 (0.0-1.1)	**<0.001**
PCT (ng/mL)	0.1 (0.1-0.2)	–	–
IL-6	27.3 (9.5-37.4)	2.7 (2.7-4.2)	**<0.001**
hs TNI (ng/dL)	8.5 (3-18.5)	4 (3-8)	0.092
NT-pro-BNP (ng/L)	323 (132.5-825.5)	161 (44.5-326)	**0.048**
CK (U/L)	167.5 (71.5-260.8)	85 (62.5-123.5)	**0.045**
AST (U/L)	38 (20-46.5)	14 (12.8-21)	**<0.001**
ALT (U/L)	36 (19-44)	18 (12.8-26)	**0.006**
LDH (U/L)	263.5 (225-339.5)	191.5 (166.8-207)	**<0.001**
HbA1c (%)	6.3 (6-6.5)	5.8 (5.4-6.3)	**0.014**

Values are n (%) or are given as median and interquartile range (IQR). ACE - Angiotensin Converting Enzyme. Afib - atrial fibrillation. ALT – alanine amino-tranferase. ARB – Angiotensin II Receptor Blockers. ASA – Acetylsalicylic acid. AST – aspartate-aminotransferase. BMI – body mass index. CAD – coronary artery disease. CK – creatinine kinase. CRP – C-reactive protein. GFR-MDRD – glomerular filtration rate. Hb – haemoglobin. hs TNI – high sensitive Troponin I. INR – international normalised ratio. LDH – lactate dehydrogenase. NT-pro-BNP – N-terminal pro- brain natriuretic peptide. Pap Sys – pulmonary arterial pressure systolic. PCT – procalcitonin. PM – pace maker. PTT – partial thromboplastin time. SARS-CoV-2 – severe acute respiratory syndrome coronavirus-2.

important for adhesion, migration and T-cell activation such as CD11a, CD11b and CCR2. Most prominently, expression of the activation marker CD11b (MAC-1) was significantly higher on all subtypes of monocytes in the acute phase of the infection and normalised after 3-months (CD11b classical monocytes; acute vs post vs healthy control; median + IQR; 42753 (38630-48372) vs 26892 (21975-35937) vs 28654 (24018-34110); acute vs post $p < 0.0001$; acute vs healthy $p < 0.0001$; post vs healthy $p > 0.9999$; CD11b intermediate monocytes; acute vs post vs healthy control; median + IQR;

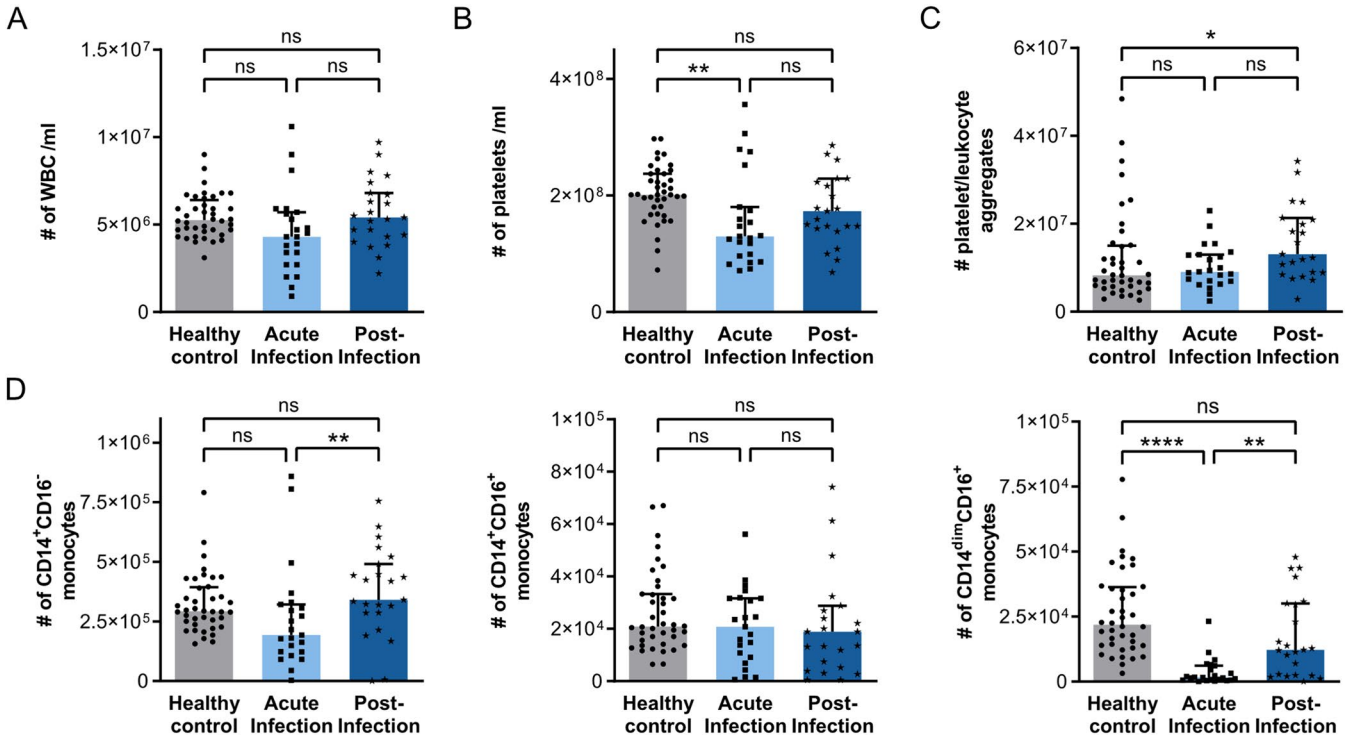

Figure 1. Classical and non-classical monocytes increasing to an original level after three months of SARS-CoV-2 infection. Flow cytometry analysis of 23 SARS-CoV-2 infected patients at acute stage and 3 months post-infection and 40 healthy controls was performed in whole blood for phenotyping of systemic monocytes, platelets and platelet/leukocyte aggregates. Following cell counts were measured: **(A)** WBC/ml **(B)** platelets/ml **(C)** platelet/leukocyte aggregates and **(D)** $CD14^{+}CD16^{-}$, $CD14^{+}CD16^{+}$ and $CD14^{dim}CD16^{+}$ monocytes. Plotted: Median with interquartile range (IQR); Statistics: Mann-Whitney U test. For this analysis a p-value ≤ 0.050 was considered significant, indicated by *, p-value ≤ 0.010 indicated by **, p-value ≤ 0.001 indicated by *** and p-value ≤ 0.0001 indicated by ****.

29097 (22716-36110) vs 19301 (14483-26384) vs 16497 (13806-19564); acute vs post $p = 0.0024$; acute vs healthy $p < 0.0001$; post vs healthy $p = 0.5101$; CD11b non-classical monocytes; acute vs post vs healthy control; median + IQR; 4623 (3214-5912) vs 1808 (1187-3113) vs 2705 (2293-3370); acute vs post $p < 0.0001$; acute vs healthy $p = 0.0003$; post vs healthy $p = 0.2849$, Figure 2A). The adhesion molecule CD11a (LFA-1) was higher expressed at least by trend in all monocyte subtypes at the time of acute SARS-CoV-2 infection compared to the same group of patients after recovery of 3 months (CD11a classical monocytes; acute vs post vs healthy control; median + IQR; 17045 (15171-20280) vs 11045 (7221-14316) vs 15437 (14054-16316); acute vs post $p < 0.0001$; acute vs healthy $p = 0.0502$; post vs healthy $p = 0.0231$; CD11a intermediate monocytes; acute vs post vs healthy control; median + IQR; 20715 (18676-25580) vs 15366 (11640-22730) vs 18787 (15655-20850); acute vs post $p = 0.0006$; acute vs healthy $p = 0.0396$; post vs healthy $p = 0.2514$; CD11a non-classical monocytes; acute vs post vs healthy control; median + IQR; 14857 (12611-17408) vs 11869 (8822-16445) vs 15582 (13189-18462); acute vs post $p = 0.2892$; acute vs healthy $p > 0.9999$; post vs healthy $p = 0.0253$, Figure 2B). This indicates, that the adhesive properties of all classical, intermediate and non-classical monocytes are altered during acute SARS-CoV-2 infection. Next, we analysed the levels of chemokine receptors that mediate migration (CCR2/CCL2 = MCP-2) and chemokine-induced survival (ACKR3/CXCL12). While CCR2 is by trend higher expressed on all monocyte subsets in patients with CVD and SARS-CoV-2 infection compared to healthy controls, CCR2 expression after 3-month recovery is comparable or even significantly lower to that of healthy controls on all subtypes of monocytes, indicating impaired migratory properties (CCR2 classical monocytes; acute vs post vs healthy control; 50531 (39765-54086) vs 35507 (23316-42239) vs 46367 (44521-51491); acute vs post $p < 0.0001$; acute vs healthy $p > 0.9999$; post vs healthy $p < 0.0001$; CCR2 intermediate monocytes; acute vs post vs healthy control; 13204 (7317-29730) vs 6025 (3469-15147) vs 7077 (4611-16606); acute vs post $p = 0.0543$; acute vs healthy $p = 0.1745$; post vs healthy $p > 0.9999$; CCR2 non-classical monocytes; acute vs post vs healthy control; 862 (613-1136) vs 168.5 (103.5-542.3) vs 690 (633-781.5); acute vs post $p < 0.0001$; acute vs healthy $p = 0.7055$; post vs healthy $p < 0.0001$, Figure 2C).

Similar to CCR2, ACKR3 is also increasingly expressed on monocytes in patients with acute SARS-CoV-2 infection, although here ACKR3 expression remains elevated in patients after 3-months of recovery compared to healthy controls (ACKR3/ACKR3 classical monocytes; acute vs post vs healthy control; median + IQR; 2804 (1991-5439) vs 3095 (1624-3967) vs 1535 (1226-2240); acute vs post $p > 0.9999$; acute vs healthy $p = 0.0006$; post vs healthy $p = 0.0213$; ACKR3/ACKR3 non-classical monocytes; acute vs post vs healthy control; median + IQR; 2452 (1612-5370) vs 3951 (2047-5122) vs 1204 (1038-1999); acute vs post $p > 0.9999$; acute vs healthy $p = 0.0012$; post vs healthy $p = 0.0002$; ACKR3/ACKR3 intermediate; acute vs post vs healthy control; median + IQR; 3034 (1784-5580) vs 4556 (2087-5291) vs 1340 (1114-2230); acute

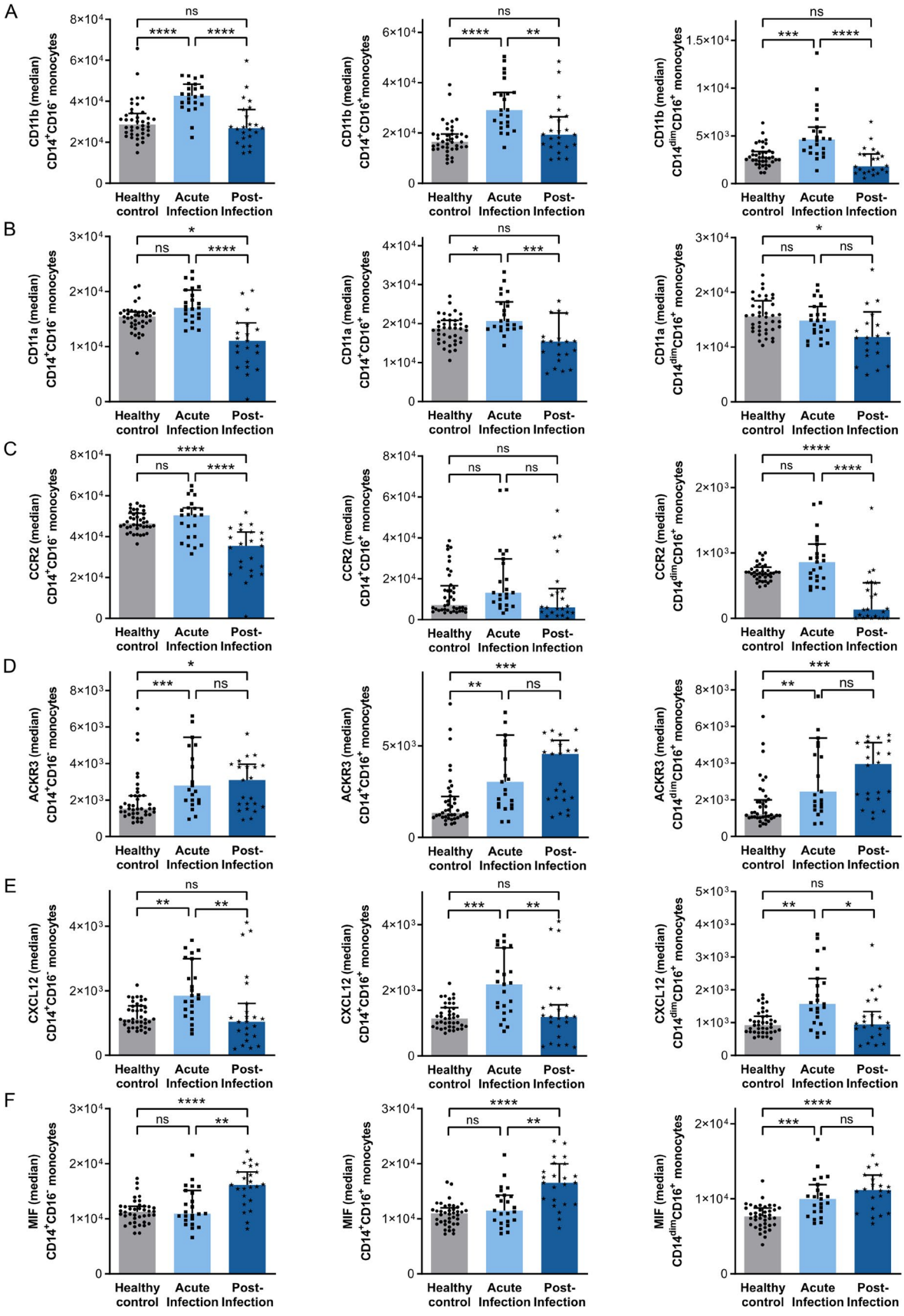

Figure 2. Activation and migration surface marker on monocyte subsets are significantly altered comparing acute and post SARS-CoV-2 infection. 23 SARS-CoV-2 infected patients at acute stage and 3 months post-infection as well as 40 healthy controls were analysed by flow cytometry staining in whole blood. Plots representing surface marker expression of $CD14^{+}CD16^{-}$, $CD14^{+}CD16^{+}$ and $CD14^{dim}CD16^{+}$ monocytes: **(A)** median of CD11b **(B)** median of CD11a **(C)** median of ACKR3 and **(D)** median of CCR2. Following marker were stained intracellularly: **(E)** median of CXCL12 **(F)** median of CXCL14 and **(G)** median of MIF. Plotted: Median with interquartile range (IQR); Statistics: Mann-Whitney U test. For this analysis a p-value ≤ 0.050 was considered significant, indicated by *, p-value ≤ 0.010 indicated by **, p-value ≤ 0.001 indicated by *** and p-value ≤ 0.0001 indicated by ****.

vs post $p > 0.9999$; acute vs healthy $p = 0.0013$; post vs healthy $p = 0.0004$ (Figure 2D).

For deeper characterisation of the immunophenotypes, we also analysed the intracellular expression of the chemokines CXCL12 and macrophage migration inhibitory factor (MIF) in all three subtypes of circulating monocyte. CXCL12 and MIF play important roles in inflammatory and atherosclerotic processes via chemotactic regulation of lymphocytes and monocytes (Calandra *et al.* 2003, van der Vorst *et al.* 2015, Gao *et al.* 2019). While CXCL12 expression was significantly increased in all monocyte subsets from patients in the acute phase of the infection and reached levels comparable to healthy controls after 3-months recovery (CXCL12 classical monocytes; acute vs post vs healthy control; median + IQR; 1849 (1335-2992) vs 1038 (591-1609) vs 1118 (915.3-1534); acute vs post $p = 0.0022$; acute vs healthy $p = 0.0037$; post vs healthy $p > 0.9999$; CXCL12 intermediate monocytes; acute vs post vs healthy control; median + IQR; 2185 (1368-3299) vs 1190 (579-1558) vs 1142 (893-1473); acute vs post $p = 0.0087$; acute vs healthy $p = 0.0003$; post vs healthy $p > 0.9999$; CXCL12 non-classical monocytes; acute vs post vs healthy control; median + IQR; 1573 (998-2346) vs 947 (612.3-1339) vs 928 (716.8-1199); acute vs post $p = 0.015$; acute vs healthy $p = 0.0023$; post vs healthy $p > 0.9999$, Figure 2E), the expression of MIF was significantly enhanced in monocytes from patients in the recovery phase (MIF classical monocytes; acute vs post vs healthy control; median + IQR; 10945 (9729-15135) vs 16154 (13327-18502) vs 11274 (9545-12268); acute vs post $p = 0.0018$; acute vs healthy $p > 0.9999$; post vs healthy $p < 0.0001$; MIF intermediate monocytes; acute vs post vs healthy control; median + IQR; 11507 (9513-14283) vs 16535 (12611-199995) vs 10958 (9142-11999); acute vs post $p = 0.0043$; acute vs healthy $p = 0.4345$; post vs healthy $p < 0.0001$; MIF non-classical monocytes; acute vs post vs healthy control; median + IQR; 9974 (8281-11881) vs 11159 (8515-13152) vs 7655 (6506-8770); acute vs post $p = 0.8634$; acute vs healthy $p = 0.0004$; post vs healthy $p < 0.0001$, Figure 2F).

These results indicate that monocyte chemotaxis, adhesion, migration, and B/T cell activation capabilities are influenced by acute SARS-CoV-2 infection and may recover three months after acute infection. However, several alterations of monocyte function do not recover during this three-month period back to expression levels of healthy controls (Figure 2). For a direct comparison of each patient during acute phase of infection and a recovery of 3 months, we prepared new figures for each cell count and investigated marker (Supplemental Figures S2 and S3).

Hierarchical clustering of monocyte subtypes identifies specific phenotypes in acute and recovery phase of SARS-CoV-2 infection

In addition to the manual gating strategy of multicolour-flow cytometry described above, we performed unsupervised data analysis by first applying uniform manifold approximation and projection (UMAP) (McInnes et al. 2018) dimension reduction of gated monocytes to group phenotypically similar events (Figures 3 and 4). This was followed by unsupervised clustering analysis using Phenograph (Levine *et al.* 2015), which uncovered distinct changes in monocyte marker profiles (Figures 3 and 4). Activation and migration surface markers such as CCR2 and CD11a are increased during acute phase of infection in cluster MT23, MT17 and MT14 comparable to our manual gating strategy (Figure 3). Unsupervised clustering with PhenoGraph resolved 28 clusters (MT01-MT28) for the monocyte chemokine receptor flow cytometry panel, of which 28 showed significant differences regarding the frequency of the clusters MT01-MT28 between patients with acute SARS-CoV-2 infection and patients after 3-month recovery. Only relevant significant clusters are shown in Figure 4. Here only seven relevant clusters are shown. Cluster MT03 and MT24 showing increased expression of intracellular CXCL12 and less CXCL14 in the acute phase compared to the recovery phase of SARS-CoV-2 infection, while MT27 showed an increase of both: CXCL12 and CXCL14 in patients during acute infection. Similar to our manual gating, the expression of CD11b is reduced in monocytes after 3-month of recovery in cluster MT27, MT14, MT03 and MT24 compared to the acute phase of infection. Moreover, we found that the median expression of monocytes shown by CD14 and CD16 surface expression was increased during the acute phase compared to the recovery phase in several clusters (Figure 4). Unsupervised OMIQ analysis confirmed our data obtained by our manual gating strategy.

Plasma levels of MIF and other pro-inflammatory cytokines in patients with acute SARS-CoV-2 infection were significantly increased in CAD patients

Next, we asked whether the assessment of systemic inflammation allows to characterise the acute phase of hyperinflammation compared to the recovery phase. We analysed plasma of CVD patient with acute SARS-CoV-2 infection and 3-months recovery with an inflammation panel of 26 chemokines/cytokines. The cytokines and chemokines were analysed as described in the method section. In particular, we found differences of the pro-inflammatory mediators CXCL10, IL-18, CCL2, IL-6, IL-8, IFN-γ, and CXCL11 which were significantly elevated in the plasma of CVD patient with acute SARS-CoV-2 infection compared to patients with 3-months recovery. Interestingly, also the cytokine MIF was significantly increased during the acute phase of infection (Figure 5A). MIF exhibit chemokine-like functions and is related to several acute and chronic inflammatory diseases as well as cardiovascular disease (Morand *et al.* 2006, Zernecke *et al.* 2008, Muller *et al.* 2014, Muller *et al.* 2015). Further, MIF is able to function as a pro-atherogenic factor and promote monocytes adhesion, migration and differentiation by interacting with CXCR2 and CXCR4 (Bernhagen *et al.* 2007, Cheng *et al.* 2010, Muller *et al.* 2015) Interestingly, IL-33, CXCL5, CCL11, CXCL1, IL-17A, CCL20, and CCL4 revealed significantly higher levels at 3-months of recovery compared to the acute phase (Figure 5B). Other tested mediators comprising IL-10, IFN-α, IL-23, IL-1ß, CXCL8, CCL5, CCL17, TNF-α, CXCL9, IL-12p70, and CCL3 showed similar plasma levels in both groups (Figure 5A and B).

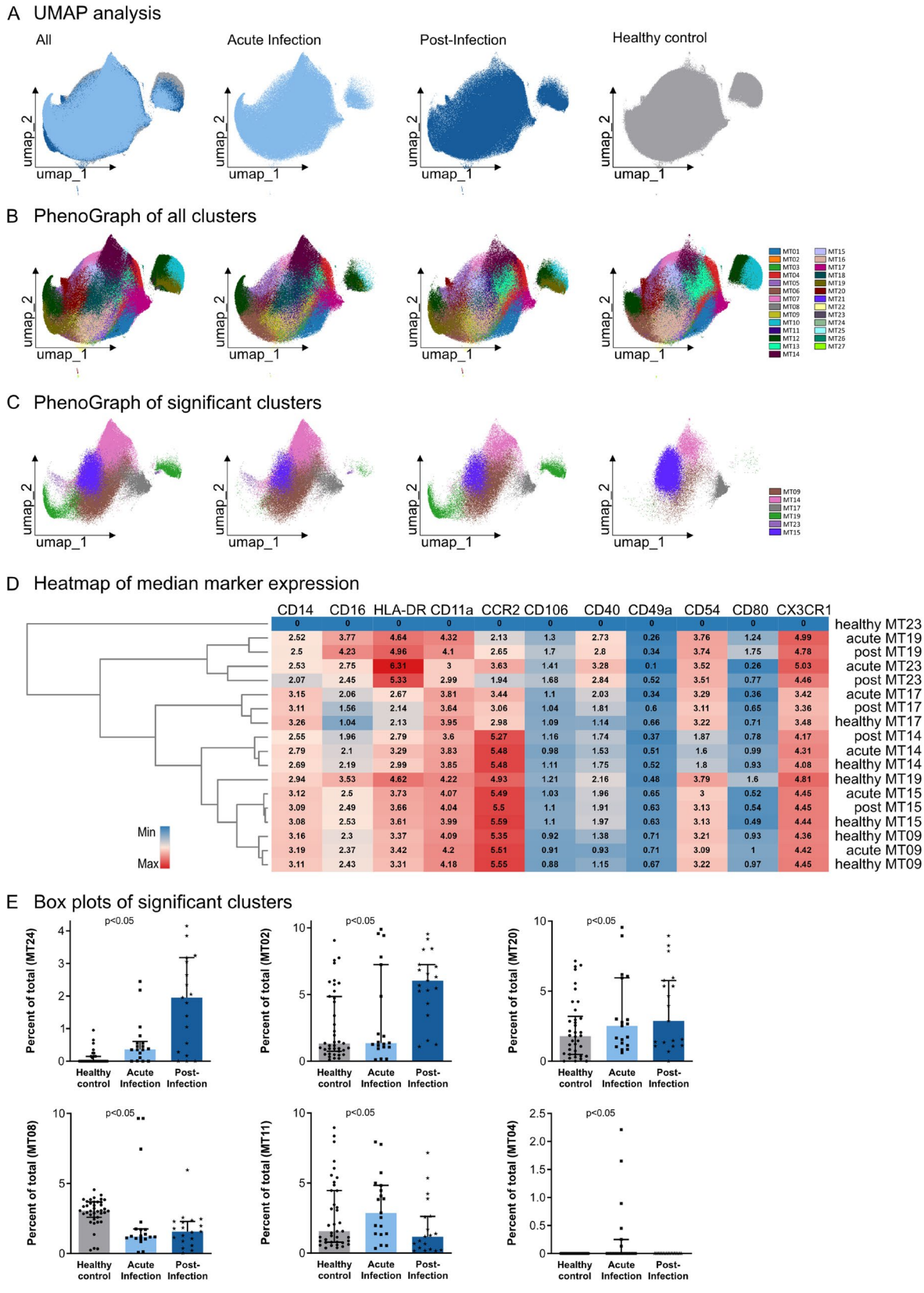

Figure 3. Immuno-phenotyping and high-dimensional analysis of monocytes. **(A)** UMAP analysis (neighbours n = 70) of monocyte flow cytometry activation panel of patients infected with SARS-CoV-2 at acute stage and 3 months post-infection. The left plot showing an overlay and the other two plots showing the individual patient groups as well as healthy controls. **(B)** Analysis of monocyte subpopulations. PhenoGraph algorithm was used (nearest neighbours k = 20) for unsupervised clustering of all patient samples (n = 86) measured by monocyte flow cytometry activation panel. Left plot representing an overlay of monocytes from acute and post infected patients and healthy controls followed by individual plots of monocytes of all clusters. **(C)** Same analysis of monocyte subpopulations is shown representing only significantly different monocyte clusters between acute stage and 3 months post-infection. **(D)** Clustered heatmap of significant different clusters MT23, MT19, MT17, MT14, MT15, and MT09 from (C) show median expression of indicated markers for comparison of acute and post-infected patients and healthy controls. **(E)** Box plots showing abundancy of cells for each cluster for each patient stratified into acute and post-infected patients as well as healthy controls. Only relevant plots are shown. Plotted: Median ± interquartile range (IQR); Statistics: Mann-Whitney U test. Plots were generated using OMIQ data analysis software.

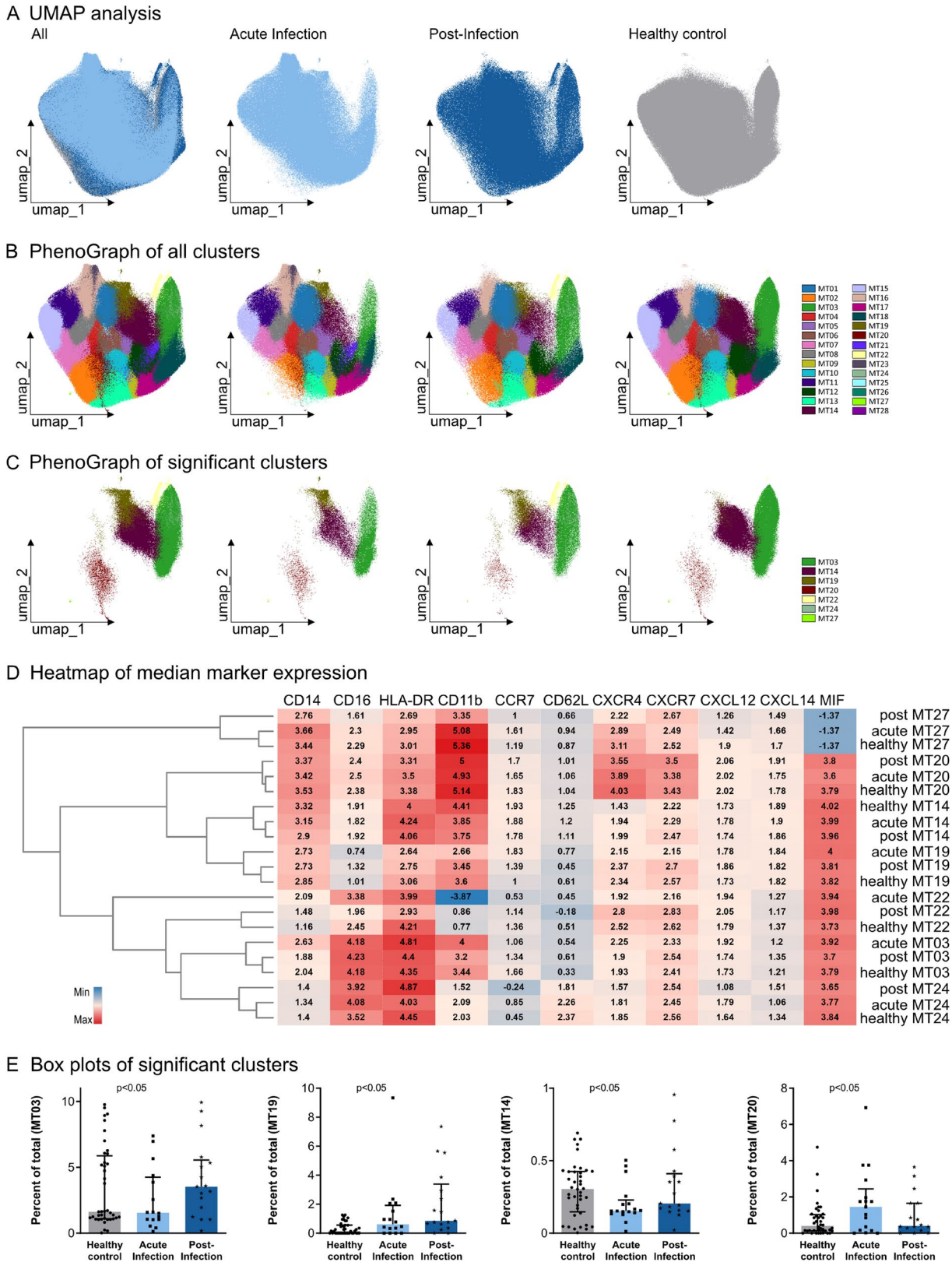

Figure 4. Immuno-phenotyping and high-dimensional analysis of monocytes. **(A)** UMAP analysis (neighbours n = 70) of monocyte flow cytometry chemokine receptor panel of patients infected with SARS-CoV-2 at acute stage and 3 months post-infection. The left plot showing an overlay and the other two plots showing the individual patient groups as well as healthy controls. **(B)** Analysis of monocyte subpopulations. PhenoGraph algorithm was used (nearest neighbours k = 20) for unsupervised clustering of all patient samples (n = 86) measured by monocyte flow cytometry chemokine receptor panel. Left plot representing an overlay of monocytes from acute and post infected patients as well as healthy controls followed by individual plots of monocytes of all clusters. **(C)** Same analysis of monocyte subpopulations is shown in lower plots representing only significantly different monocyte clusters between acute stage and 3 months post-infection. **(D)** Clustered heatmap of significant different clusters MT27, MT20, MT14, MT19, MT22, MT03 and MT24 from (C) show median expression of indicated markers for comparison of acute and post-infected patients. **(E)** Box plots showing abundancy of cells for each cluster for each patient stratified into acute and post-infected patients as well as healthy controls. Only relevant plots are shown. Plotted: Median ± interquartile range (IQR); Statistics: Mann-Whitney U test. Plots were generated using OMIQ data analysis software.

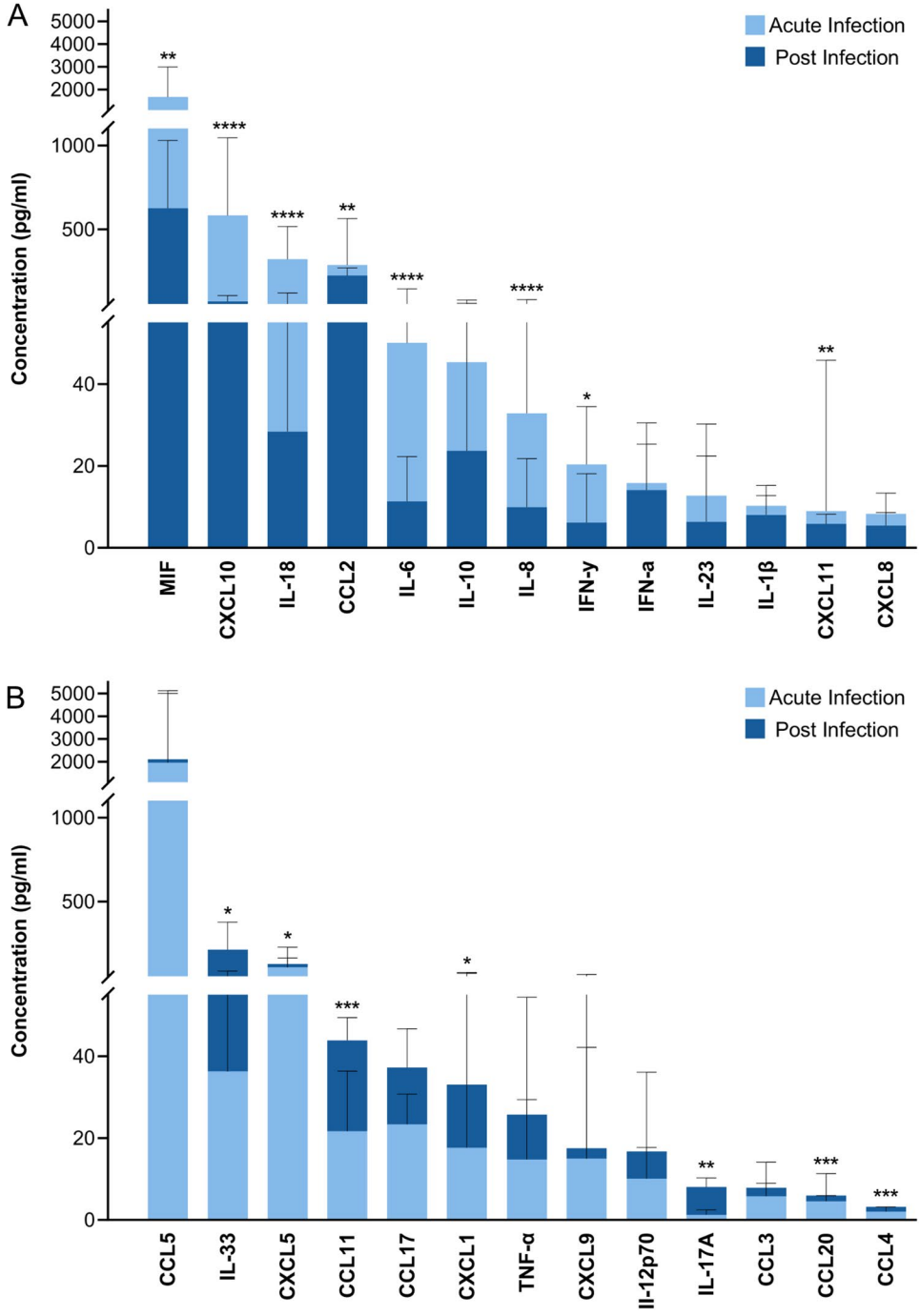

Figure 5. Plasma MIF concentration is significantly decreased in SARS-CoV-2 patients after 3 months post-infection compared to the acute stage.Several cytokine and chemokine concentration were analysed of 23 plasma samples of SARS-CoV-2 infected patients at acute stage and 3 months post-infection by LEGENDPlex as well as plasma MIF levels by ELISA. Plot represents concentration (pg/ml) of indicated cytokines/chemokines **(A)** MIF, CXCL10, IL-18, CCL2, IL-6, IL-10, IL-8, IFN-γ, IFN-α, IL-23, IL-1β, CXCL11, and CXCL8 (acute vs recovery phase; MIF: pg/mL; median + IQR; 1667 (1055-2994) vs 625.4 (424-1029), $p < 0.001$; CXCL10: pg/mL; median + IQR; 583 (116.7-1045) vs 80.44 (45.35-105.8), $p < 0.0001$; IL-18: pg/mL; median + IQR; 321.7 (189.1-516.8) vs 39.5 (13.69-116), $p < 0.0001$; CCL2: pg/mL; median + IQR; 287.4 (232.9-563.6) vs 226 (183.4-266.6), $p = 0.0027$; IL-6: pg/mL; median + IQR; 50.03 (29.14-145.8) vs 11.47 (8.2-21.04), $p < 0.0001$; IL-8: pg/mL; median + IQR; 32.81 (17.18-81.2) vs 7.92 (5.94-20.64), $p < 0.0001$; IFN-γ: pg/mL; median + IQR; 20.35 (13.56-34.5) vs 6.56 (3.2-19.4), $p < 0.023$; CXCL11: pg/mL; median + IQR; 8.97 (7.75-45.78) vs 6.32 (4.84-8.79), $p < 0.0023$) **(B)** CCL5, IL-33, CXCL5, CCL11, CCL17, CXCL1, TNF-α, CXCL9, IL-12p70, IL-17A, CCL3, CCL20, and CCL4 (acute vs recovery phase; IL-33: pg/mL; median + IQR; 36.23 (14.09-85.04) vs 177.3 (38.51-359.4), $p = 0.0108$; CXCL5: pg/mL; median + IQR; 107.9 (36.86-162.5) vs 150.9 (67.25-234.9), $p = 0.0441$; CCL11: pg/mL; median + IQR; 21.7 (15.84-36.35) vs 44.57 (35.99-49.4), $p = 0.0003$; CXCL1: pg/mL; median + IQR; 17.66 (17.66-71.47) vs 34.86 (20.74-77.64), $p = 0.0482$; IL-17A: pg/mL; median + IQR; 1.24 (0.55-2.45) vs 7.67 (2.78-12.65), $p = 0.0053$; CCL20: pg/mL; median + IQR; 4.56 (4.56-5.98) vs 5.98 (5.98-10.17), $p = 0.0009$; CCL4: pg/mL; median + IQR; 2.05 (2.05-3.18) vs 3.18 (3.18-3.2), $p = 0.0002$). Plotted: Median with interquartile range (IQR); Statistics: Mann-Whitney U test. For this analysis a p-value ≤ 0.050 was considered significant, indicated by *, p-value ≤ 0.010 indicated by **, p-value ≤ 0.001 indicated by *** and p-value ≤ 0.0001 indicated by ****.

We observed a significant increase of pro-inflammatory chemokines/cytokines like MIF, CCL2, IL-6 and IFN-y during the acute phase of infection compared to the timepoint of 3-months recovery.

Discussion

The major findings of the present study are: i) acute SARS-CoV-2 infection is associated with a significant decrease

of circulating nonclassical ($CD14^{dim}CD16^{+}$) monocytes that partially recover to normal levels after 3 months. ii) the adhesive ($CD11b^{+}$) and inflammatory ($ACKR3^{+}$, $CCR2^{+}$, $CXCL12^{+}$, $CXCL14^{+}$) phenotype of circulating monocytes is substantially altered in the acute phase of the infectious disease compared to control subjects. 3-months after infection, the phenotype of some monocyte subsets was recovered comparable to that of the control group. Most strikingly, MIF expression in all monocyte subtypes 3-months after infection was even higher than that in patients with acute SARS-CoV-2 infection as well as that in healthy controls. iii) Chemokine profiling revealed significant differences between the acute and the 3-months recovery phase. Whereas plasma levels of acute phase chemokines were significantly higher in patients with acute SARS-CoV2 infection compared to that of patients 3 months later, some chemokines (IL-33, CCL11, CXCL1, IL17A) were higher after 3-months of recovery.

Our data indicate that significant changes of circulating monocytes and chemokines occur in the acute and recovery phase of SARS-CoV-2 infection in CVD patients. The increased numbers of intracellular MIF expression in classical, intermediate, and non-classical monocytes and elevation of distinct chemokines in the recovery phase imply a sustained immune response following SARS-CoV-2 infection. Thus, it is tempting to speculate that monocytes are prominent inflammatory cells involved in the acute defense of the infectious disease and prominent changes of monocyte subgroups in the recovery phase may contribute to the prolonged immune response following SARS-CoV-2 infection.

COVID-19 has threatened our societies worldwide during the last 2 years. There is an unbelievable amount of scientific data available that disclosed the underlying pathophysiology in patients with SARS-CoV-2 infection. One major prominent aspect of severe SARS-CoV-2 infection is the systemic hyperinflammation associated with respiratory stress syndrome, microcirculatory dysfunction, and organ failure. Recently, we found that activation of monocytes occurs in severe COVID-19 with an enhanced pulmonary sequestration of especially non-classical ($CD14^{dim}CD16^{+}$) monocytes (Mueller *et al.* 2021, Chilunda *et al.* 2021, Degauque *et al.* 2021). These data suggested that monocyte contribute significantly to respiratory distress and organ failure in COVID-19.

The purpose of the present study was to characterise changes of monocyte subtypes and relevant plasma chemokines during the recovery phase of COVID-19 at 3-months follow-up in patients with cardiovascular disease. We focussed on CVD patients in our study because CVD, CAD patients or patients with cardiovascular comorbidities have an increased risk for life-threatening heart and lung injury and organ failure (Oren *et al.*, Task Force for the management of C-otESoC 2022). SARS-CoV-2 infection is characterised by pro-inflammatory and pro-thrombotic events causing in CVD patients acute coronary syndrome with subsequent impairment of left or right ventricular function (Xiong *et al.* 2020, Tang *et al.*). Further, acute right heart failure occurs in CVD or CAD patients due to pre-existing right heart and diastolic dysfunction (Oren *et al.*, Task Force for the management of C-otESoC 2022). Pneumatic infiltrates and lung involvement cause right heart dysfunction upon SARS-CoV-2 infection (Xiong *et al.* 2020). Furthermore, infiltration of inflammatory immune cells like monocytes or macrophages in CAD patients have been related to atherosclerotic lesions due to increased expression of cytokines (Woollard *et al.* 2010, Swirski *et al.* 2018, Wolf *et al.* 2019).

At 3-months follow-up almost half of the analysed patients (43.5%) reported persistent dyspnoea as most prominent clinical symptom and as a sign of possible long-COVID. Five patients complained of chronic fatigue. 56.5% of the enrolled patients revealed a complete clinical recovery from initially severe COVID-19 at the follow-up visit and were free from cardiovascular and neurological symptoms. Furthermore, we found that changes of monocyte subgroups were highly dynamic when comparing the acute to the recovery phase. One prominent finding was that the expression of MIF in monocytes was not altered in the acute phase of SARS-CoV-2 infection but increased 3-months later. MIF is an ubiquitously expressed chemokine-like protein which was found to be an important regulator of innate immunity (Calandra *et al.* 2003). Binding of MIF to cells promotes NF-κB activation and inflammation, migration or survival (Calandra *et al.* 2003, Kim *et al.* 2017). Our data further emphasise the role of MIF and circulating monocytes in the immuno-defense following viral infections such as SARS-CoV-2. A sustained expression of MIF in circulating monocytes may contribute to the cellular-based immuno-defense system in COVID-19. Monocytes are innate blood cells that are early cellular responders in acute infection (Jakubzick *et al.* 2017). Whereas classical monocytes ($CD14^{++}CD16^{-}$) are critical for the initial inflammatory response, nonclassical ($CD14^{dim}CD16^{+}$) "patrolling" monocytes are commonly viewed as anti-inflammatory guardians of the innate immune system (Buscher *et al.* 2017). Our results are in line with the current literature showing that circulating monocyte subsets return to normal proportions after a follow-up of six months upon infection (Utrero-Rico *et al.* 2021). Most of the literature are focussing on immune phenotyping of monocyte and macrophages during the acute phase of infection. Studies show that inflammatory monocytes are hyperactivated and secreting large amounts of pro-inflammatory cytokines (Merad *et al.* 2020, Knoll *et al.* 2021).

Thus, it is tempting to speculate, that especially MIF-positive monocytes are an imprint of severe SARS-CoV-2 infection that may contribute to immunity and re-infection. This conclusion is further substantiated by the fact that a variety of chemokines (e.g., IL-33, CCL17, CXCL1, IL-17A) were elevated months after SARS-CoV-2 infection. IL-33 is a cytokine that induces of T-helper 2 (Th2) cell priming (Komai-Koma *et al.* 2007). CCL17 is chemotactic for T-regulatory cells. CXCL1 serves as chemoattractant for neutrophils (Sawant *et al.* 2016, Metzemaekers *et al.* 2020). IL-17A has been implicated in immune response to infectious pathogens (Ge *et al.* 2020). Thereby, our observations indicate that these elevated cytokine/chemokine levels were also associated with altered and even partly enhanced immune response even after a 3-months recovery phase after COVID-19. However, at present we cannot provide evidence that here observed alterations of plasma chemokines and subsets of circulating monocytes play a role in a sustained protection for re-infection with SARS-CoV-2. We conclude that patients with CVD and acute

SARS-CoV-2 infection showed changes regarding their phenotype of monocytes and their chemokine profile after 3-months recovery. Altered monocyte function and increased MIF expression was characteristic for the recovery phase. One can speculate that MIF expression may serve as additional biomarker to identify patients at risk for an altered, possibly prolonged immune response after acute SARS-CoV-2 infection.

We are aware that our study is rather observational and hypothesis-generating, especially as the analysis is limited by the small patient number in the observed group. Furthermore, we can only provide data after 3-months of follow-up and cannot provide data after 6 or 12 months. Therefore, our data are also limited regarding their impact on long-COVID. Therefore, large scale randomised studies are essential for validation of our observations on the predictive value of MIF and other pro-inflammatory cytokines regarding the recovery of the immune response after acute COVID-19-infection as well as their impact to predict patients at risk for an unfavourable course of COVID-19 and long-COVID.

Conclusion

We found that the changes in immunophenotypes of circulating monocytes and plasma levels of most chemokines/cytokines that occurred or increased during the acute phase of severe SARS-CoV-2 infection normalised after a 3-month recovery. However, we also found that plasma levels of certain chemokines, in particular MIF, were still or newly elevated 3-months post COVID-19 compared to the acute infection phase, indicating a persistent alteration of the immune response after COVID-19 recovery.

Disclosure statement

No potential conflict of interest was reported by the authors.

Funding

This work was supported by the German Research Foundation (DFG) – Project number 374031971–TRR 240 and by the Ministry of Science, Research and the Arts of the State of Baden-Württemberg (COVID-19 Funding) grant to Meinrad Paul Gawaz. The funder had no role in study design, data collection, data analysis, data interpretation, or writing of the manuscript.

Data availability statement

The data that support the findings of this study are available from the corresponding author (KALM) upon reasonable request. The data are not publicly available due to the sensitive nature of the data collected for this study.

References

Bernhagen, J., *et al.*, 2007. MIF is a noncognate ligand of CXC chemokine receptors in inflammatory and atherogenic cell recruitment. *Nature medicine*, 13 (5), 587–596.

Buscher, K., *et al.*, 2017. Patrolling mechanics of non-classical monocytes in vascular inflammation. *Frontiers in cardiovascular medicine*, 4, 80.

Calandra, T., *et al.*, 2003. Macrophage migration inhibitory factor: a regulator of innate immunity. *Nature reviews. Immunology*, 3 (10), 791–800.

Cheng, Q., *et al.*, 2010. Macrophage migration inhibitory factor increases leukocyte-endothelial interactions in human endothelial cells via promotion of expression of adhesion molecules. *Journal of immunology (Baltimore, MD: 1950)*, 185 (2), 1238–1247.

Chilunda, V., *et al.*, 2021. Transcriptional changes in CD16+ monocytes may contribute to the pathogenesis of COVID-19. *Frontiers in immunology*, 12, 665773.

Degauque, N., *et al.*, 2021. Endothelial cell, myeloid, and adaptive immune responses in SARS-CoV-2 infection. *FASEB journal: official publication of the federation of American societies for experimental biology*, 35 (5), e21577.

Gao, J.H., *et al.*, 2019. CXC chemokine ligand 12 (CXCL12) in atherosclerosis: An underlying therapeutic target. *Clinica chimica acta; international journal of clinical chemistry*, 495, 538–544.

Ge, Y., *et al.*, 2020. Biology of interleukin-17 and its pathophysiological significance in sepsis. *Frontiers in immunology*, 11, 1558.

Gu, S.X., *et al.*, 2021. Thrombocytopathy and endotheliopathy: crucial contributors to COVID-19 thromboinflammation. *Nature reviews. Cardiology*, 18 (3), 194–209.

Huang, C., *et al.*, 2020. Clinical features of patients infected with 2019 novel coronavirus in Wuhan, China. *Lancet (London, England)*, 395 (10223), 497–506.

Huang, C., *et al.*, 2021. 6-month consequences of COVID-19 in patients discharged from hospital: a cohort study. *Lancet (london, England)*, 397 (10270), 220–232.

Jakubzick, C.V., *et al.*, 2017. Monocyte differentiation and antigen-presenting functions. *Nature reviews. Immunology*, 17 (6), 349–362.

Jose, R.J., *et al.*, 2020. COVID-19 cytokine storm: the interplay between inflammation and coagulation. *The lancet. respiratory medicine*, 8 (6), e46–e47.

Kim, M.J., *et al.*, 2017. Macrophage migration inhibitory factor interacts with thioredoxin-interacting protein and induces NF-kappaB activity. *Cellular signalling*, 34, 110–120.

Knoll, R., *et al.*, 2021. Monocytes and macrophages in COVID-19. *Frontiers in immunology*, 12, 720109.

Komai-Koma, M., *et al.*, 2007. IL-33 is a chemoattractant for human Th2 cells. *European journal of immunology*, 37 (10), 2779–2786.

Lang, R.M., *et al.*, 2015. Recommendations for cardiac chamber quantification by echocardiography in adults: an update from the American Society of Echocardiography and the European Association of Cardiovascular Imaging. *European heart journal. Cardiovascular imaging*, 16 (3), 233–270.

Langnau, C., *et al.*, 2021. Platelet activation and plasma levels of furin are associated with prognosis of patients with coronary artery disease and COVID-19. *Arteriosclerosis, thrombosis, and vascular biology*, 41 (6), 2080–2096.

Levine, J.H., *et al.*, 2015. Data-driven phenotypic dissection of AML reveals progenitor-like cells that correlate with prognosis. *Cell*, 162 (1), 184–197.

McInnes, L., Healy, J., and Melville, J., 2018. UMAP: Uniform manifold approximation and projection for dimension reduction. *Cornell university*. https://arxiv.org/abs/1802.03426

Merad, M., *et al.*, 2020. Pathological inflammation in patients with COVID-19: a key role for monocytes and macrophages. *Nature reviews. Immunology*, 20 (6), 355–362.

Metzemaekers, M., *et al.*, 2020. Neutrophil chemoattractant receptors in health and disease: double-edged swords. *Cellular & molecular immunology*, 17 (5), 433–450.

Monaco, G., *et al.*, 2016. flowAI: automatic and interactive anomaly discerning tools for flow cytometry data. *Bioinformatics (Oxford, England)*, 32 (16), 2473–2480.

Morand, E.F., *et al.*, 2006. MIF: a new cytokine link between rheumatoid arthritis and atherosclerosis. *Nature reviews. Drug discovery*, 5 (5), 399–410.

Mueller, K.A.L., *et al.*, 2021. Numbers and phenotype of non-classical CD14dimCD16+ monocytes are predictors of adverse clinical outcome in patients with coronary artery disease and severe SARS-CoV-2 infection. *Cardiovascular research*, 117 (1), 224–239.

Muller, I.I., *et al.*, 2014. Impact of counterbalance between macrophage migration inhibitory factor and its inhibitor Gremlin-1 in patients with coronary artery disease. *Atherosclerosis*, 237, 426–432.

Muller, K.A., *et al.*, 2015. Platelets, inflammation and anti-inflammatory effects of antiplatelet drugs in ACS and CAD. *Thromb haemost*, 114, 498–518.

Parasuraman, S., *et al.*, 2016. Assessment of pulmonary artery pressure by echocardiography-A comprehensive review. *International journal of cardiology. Heart & vasculature*, 12, 45–51.

Sawant, K.V., *et al.*, 2016. Chemokine CXCL1 mediated neutrophil recruitment: Role of glycosaminoglycan interactions. *Scientific reports*, 6, 33123.

Swirski, F.K., *et al.*, 2018. Cardioimmunology: the immune system in cardiac homeostasis and disease. *Nature reviews. Immunology*, 18 (12), 733–744.

Tang, N., *et al.*, 2020. Anticoagulant treatment is associated with decreased mortality in severe coronavirus disease 2019 patients with coagulopathy. *Journal of thrombosis and haemostasis: JTH*, 18 (5), 1094–1099.

Task Force for the management of C-otESoC. 2022. Corrigendum to: European Society of Cardiology guidance for the diagnosis and management of cardiovascular disease during the COVID-19 pandemic: part 1-epidemiology, pathophysiology, and diagnosis; and ESC guidance for the diagnosis and management of cardiovascular disease during the COVID-19 pandemic: part 2-care pathways, treatment, and follow-up. *European heart journal*, 43, 1776.

Utrero-Rico, A., *et al.*, 2021. Alterations in circulating monocytes predict COVID-19 severity and include chromatin modifications still detectable six months after recovery. *Biomedicines*, 9 (9), 1253.

van der Vorst, E.P., *et al.*, 2015. MIF and CXCL12 in cardiovascular diseases: Functional differences and similarities. *Frontiers in immunology*, 6, 373.

Wolf, D., *et al.*, 2019. Immunity and inflammation in atherosclerosis. *Circulation research*, 124 (2), 315–327.

Woollard, K.J., *et al.*, 2010. Monocytes in atherosclerosis: subsets and functions. *Nature reviews. Cardiology*, 7 (2), 77–86.

Xiong, T.Y., *et al.*, 2020. Coronaviruses and the cardiovascular system: acute and long-term implications. *European heart journal*, 41 (19), 1798–1800.

Yang, L., *et al.*, 2020. COVID-19: immunopathogenesis and Immunotherapeutics. *Signal transduction and targeted therapy*, 5 (1), 128.

Zernecke, A., *et al.*, 2008. Macrophage migration inhibitory factor in cardiovascular disease. *Circulation*, 117 (12), 1594–1602.

Zheng, Y.Y., *et al.*, 2020. COVID-19 and the cardiovascular system. *Nature reviews. Cardiology*, 17 (5), 259–260.

Zhou, F., *et al.*, 2020. Clinical course and risk factors for mortality of adult inpatients with COVID-19 in Wuhan, China: a retrospective cohort study. *Lancet (London, England)*, 395 (10229), 1054–1062.

Platelet Activation and Plasma Levels of Furin Are Associated With Prognosis of Patients With Coronary Artery Disease and COVID-19

Carolin Langnau,[1,*] Anne-Katrin Rohlfing,[1,*] Sarah Gekeler,[1] Manina Günter,[2,4] Simone Pöschel,[2] Álvaro Petersen-Uribe,[1] Philippa Jaeger,[1] Alban Avdiu,[1] Tobias Harm,[1] Klaus-Peter Kreisselmeier,[1] Tatsiana Castor,[1] Tamam Bakchoul,[3] Dominik Rath,[1] Meinrad Paul Gawaz,[1] Stella E. Autenrieth,[2,4] and Karin Anne Lydia Mueller[1]

[1]University Hospital Tuebingen, Department of Cardiology and Angiology, Eberhard Karls University Tuebingen, Tuebingen, Germany

[2]University Hospital Tuebingen, Department of Hematology, Oncology, Clinical Immunology and Rheumatology, Eberhard Karls University Tuebingen, Tuebingen, Germany

[3]University Hospital Tuebingen, Department of Clinical and Experimental Transfusion Medicine, Eberhard Karls University Tuebingen, Tuebingen, Germany

[4]German Cancer Research Centre, Department of Dendritic Cells in Infection and Cancer, Heidelberg, German

This is a non-final version of an article published in final form in Langnau, Carolin et al. “Platelet Activation and Plasma Levels of Furin Are Associated With Prognosis of Patients With Coronary Artery Disease and COVID-19.” Arteriosclerosis, thrombosis, and vascular biology vol. 41,6 (2021): 2080-2096. doi:10.1161/ATVBAHA.120.315698."

Langnau, Carolin et al. “Platelet Activation and Plasma Levels of Furin Are Associated With Prognosis of Patients With Coronary Artery Disease and COVID-19.” Arteriosclerosis, thrombosis, and vascular biology vol. 41,6 (2021): 2080-2096. doi:10.1161/ATVBAHA.120.315698

Objective:

Patients with coronary artery disease (CAD) are at increased risk for cardiac death and respiratory failure following severe acute respiratory syndrome coronavirus 2 (SARS-CoV-2) infection. Platelets are crucially involved in pathogenesis of CAD and might also contribute to pathophysiology of SARS-CoV-2 infection.

Approach and Results:

We enrolled a cohort of 122 participants from February 2020 to July 2020 including 55 patients with preexisting CAD and acute SARS-CoV-2 infection (CAD-SARS-CoV-2^{positive}), 28 patients with CAD and without SARS-CoV-2 (CAD-SARS-CoV-2^{negative}), and 39 healthy controls. Clinical and cardiac examination of the CAD-SARS-CoV-2positive group included blood sampling, echocardiography, and electrocardiography within 24 hours after hospital admission. Phenotyping of platelets was performed by flow cytometry; plasma levels of chemokines were analyzed by ELISA. Respiratory failure of patients was stratified by the Horovitz index as moderately/severely impaired when Horovitz index <200 mm Hg. The clinical end point was defined as Horovitz index <200 mm Hg with subsequent mechanical ventilation within a follow-up of 60 days. CAD-SARS-CoV-2^{positive} patients display a significant enhanced platelet activation and hyper-inflammation early at time of hospital admission. Circulating platelet/leukocyte co-aggregates correlate with plasma levels of cytokines/chemokines like IL (interleukin)-6, CCL2, and CXCL10 (chemokine [C-X-C motif] ligand) as well as activation of platelets is associated with CCL5 and elevation of pulmonary artery pressure. Furthermore, furin is stored and released from activated platelets. High furin plasma levels are associated with poor clinical prognosis in CAD-SARS-CoV-2^{positive} patients.

Conclusions:

Patients with CAD and SARS-CoV-2 infection exhibit elevated systemic platelet activation and enhanced plasma levels of the subtilisin-like proprotein convertase furin, which may contribute to an unfavorable clinical prognosis.

Keywords: coronary artery disease, cytokines, flow cytometry, furin, pulmonary artery

Graphical Abstract:

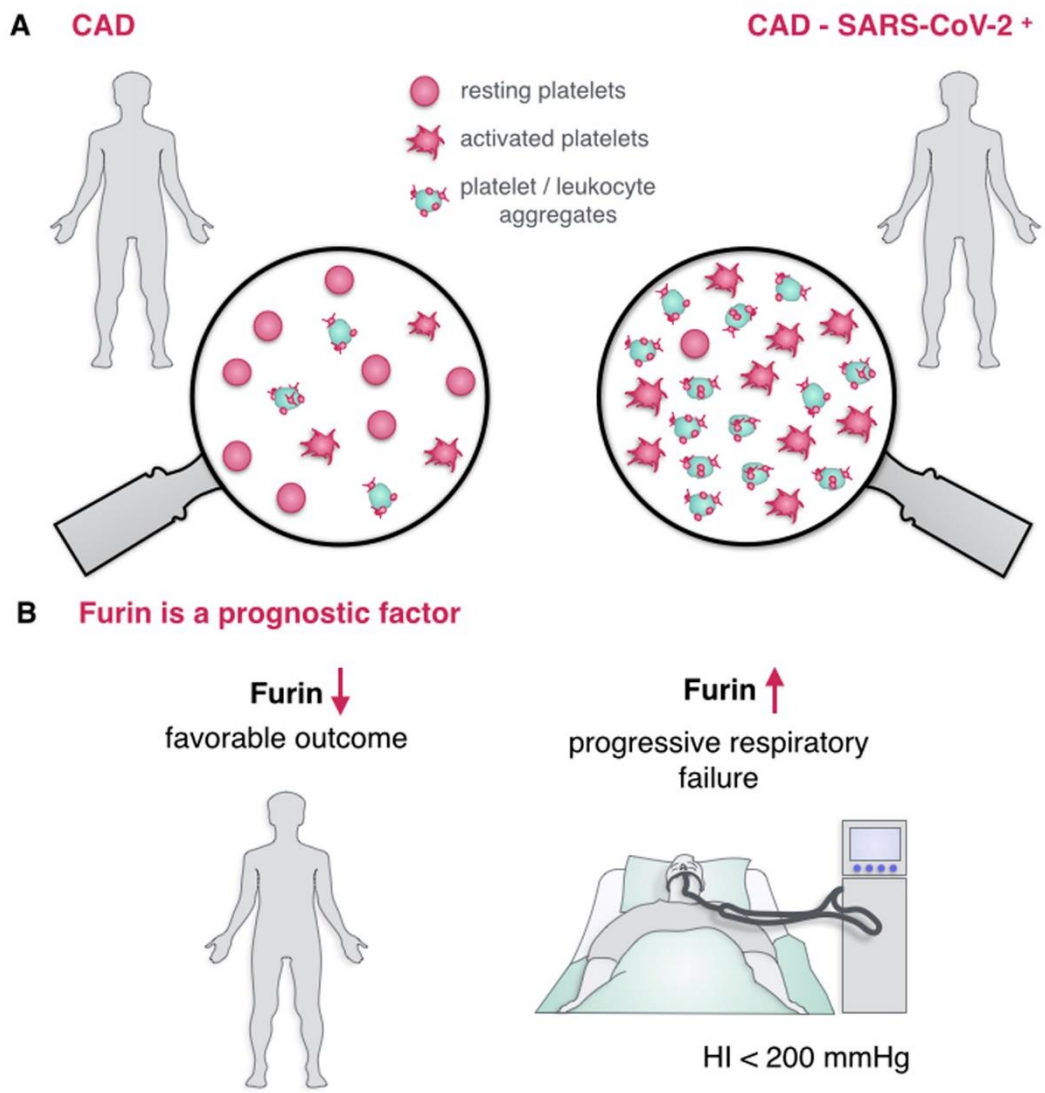

Highlights

- Significant changes in platelet activation, platelet/leukocyte co-aggregation, and plasma levels of cytokines and chemokines can already be detected in the very early phase of severe acute respiratory syndrome coronavirus 2 (SARS-CoV-2) associated infection of patients with coronary artery disease.
- Plasma levels of the subtilisin-like proprotein convertase furin released from activated platelets serve as independent prognostic factor for progression of respiratory failure in SARS-CoV-2 associated infection of patients with coronary artery disease.
- Platelets, platelet activation, and platelet-derived mediators play an important role in the immunodefense of SARS-CoV-2 infection in patients with coronary artery disease.
- Early phenotyping of platelets and platelet/leucocytes co-aggregates using simple flow cytometry along with simple analysis of furin plasma levels might predict worsening of respiratory failure at an early stage of SARS-CoV-2 infection in high-risk coronary artery disease patients.

- Targeting the release of platelet-derived furin may be a potential treatment strategy to interfere in the early course of disease progression of SARS-CoV-2 associated infection.

Introduction

Platelet activation and release of inflammatory mediators play a critical role in inflammation, atherosclerosis, and in infectious diseases.[1,2] Platelets interact with a variety of pathogens including bacteria and viruses.[2] Virus infection is often associated with systemic inflammation and changes in hemostasis (eg, platelet activation, thrombocytopenia) and coagulation (triggered by thrombin activation among others).[3] Virus-induced respiratory tract infection like an acute severe acute respiratory syndrome coronavirus 2 (SARS-CoV-2) infection is associated with platelet activation and characteristic coagulopathy resulting in thrombotic complications including deep vein thrombosis and pulmonary embolism.[4–6] In the case of RNA virus infections such as influenza, platelet activation and formation of platelet/leukocyte co-aggregates may occur early in the course of disease progression[7,8] followed by enhanced activation of coagulation and thrombin generation.[9] Enhanced platelet activation and formation of circulating platelet/leukocyte co-aggregates was additionally observed in SARS-CoV-2 infected patients[10] which is associated with a worse clinical outcome of patients with coronavirus disease 2019 (COVID-19).[11] The modulation of the renin-angiotensin-aldosterone system plays also an important role in this context.[12] Renin-angiotensin-aldosterone system is a cascade of peptides, which coordinate important processes in human physiology metabolizing angiotensin II (a potent vasoconstrictor) to generate angiotensin (1–7; a vasodilator). Renin-angiotensin-aldosterone system can interface with SARS-CoV-2 via ACE-2 (angiotensin-converting enzyme 2).[13,14] Therefore, ACE-2 has been described as key component during SARS-CoV-2 infections. ACE-2 is expressed on the surface of multiple immune cells like monocytes and macrophages as well as in respiratory and vascular endothelial cells and can enable viral entry into cells by binding to SARS-CoV-2 spike protein domains.[12,15,16] Recently, it was demonstrated, that ACE-2 is also expressed on the surface of platelets and thereby trigger thrombotic events in patients infected with SARS-CoV-2.[17] Enhanced ACE-2 expression may explain the predisposition to severe disease in certain patient groups, for example, patients with cardiovascular disease. Furthermore, viral attachment of SARS-CoV-2 is facilitated by various membrane and circulating proteases and convertases, such as the subtilisin-like proprotein convertase furin, minting severe clinical manifestations during infection.[18–21] Furin is expressed ubiquitously and regulates a variety of physiological functions and thus is involved in the blood-clotting and complement system as well as in the cleavage of membrane receptors, viral-envelope glycoproteins, and bacterial exotoxins.[22] Furin has been described to play a pivotal role in cardiovascular disease like

coronary artery disease (CAD) and cardiovascular risk factors like diabetes. A very recent publication also shows that furin plasma levels are associated with all-cause mortality and cardiovascular events in patients with acute myocardial infarction.[23] Additionally, furin was linked to atheroprogression. In advanced atherosclerotic plaques, furin is expressed primarily in macrophages. CAD-associated variants of furin were identified, and these variants altered furin expression are affecting monocyte/macrophage behavior.[24–29] But the role of platelet-derived furin has yet not been investigated thoroughly. A preexisting cardiovascular disease is linked to worse outcomes and increased risk of death in patients with COVID-19, whereas COVID-19 itself can also induce myocardial injury, arrhythmia, acute coronary syndrome, perimyocarditis, and venous thromboembolism. CAD, along with attributable other comorbidities like diabetes, has been identified as high-risk condition in patients with COVID-19 and is associated with all-cause mortality, a high risk for severe respiratory failure and organ failure following SARS-CoV-2 infection.[30–35] Concomitant CAD is present in ≈1 out of 10 patients hospitalized for COVID-19 but age and gender also are important risk factors.[36] Mechanisms underlying COVID-19-induced acute coronary syndrome might involve plaque rupture, coronary spasm or microthrombi owing to systemic inflammation or cytokine storm.[33,37] Potential drug–disease interactions affecting patients with COVID-19 and comorbid cardiovascular diseases are also becoming a serious concern and should be accounted for.[35] Finally, impaired cardiac function is associated with poor prognosis in COVID-19 positive patients. Consequently, treatment of these patients should include careful guideline-conform cardiovascular evaluation and treatment.[30] There is accumulating evidence that SARS-CoV-2 associated respiratory distress is associated with a hyper-thrombotic state and hyper-inflammation.[38,39] Further, platelets exhibit local and systemic thrombo-inflammatory activities and are able to alter immune cell functions inducing plaque formation in CAD. They function as connection between local inflammatory responses at vascular wall and development of an atherogenetic milieu.[40,41] Further, it could be shown that platelet survival is shortened in patients with CAD.[42]

We hypothesized that changes in platelet activity and systemic thrombo-inflammation at an early stage of SARS-CoV-2 infection is of prognostic relevance for the course of the disease. We found that significant changes in platelet activation, platelet/leukocyte co-aggregation, and plasma levels of cytokines and chemokines occur initial in the early phase of SARS-CoV-2 associated infection. We identified the plasma levels of furin released from activated platelets as critical prognostic factor for progression of respiratory failure. Targeting release of platelet-derived furin may be a potential target to interfere in the course of the disease progression.

Material and Methods

Because of the sensitive nature of the data collected for this study, requests to access the data set from qualified researchers trained in human subject confidentiality protocols may be sent to Carolin Langnau at University Hospital Tuebingen, Department of Cardiology and Angiology, Eberhard Karls University Tuebingen, Germany.

Study Design, Study Populations, and Inclusion Criteria

In this study, 122 participants were consecutively enrolled at the Department of Cardiology and Angiology of the University Hospital Tübingen, Germany from February 2020 until July 2020. Fifty-five patients with preexisting CAD and an acute SARS-CoV-2 infection were included within 24 hours after hospital admission (CAD-SARS-CoV-2positive). Twenty-eight patients with CAD but with-out SARS-CoV-2 infection (CAD-SARS-CoV-2negative) were included in the study as well as 39 healthy controls. All patients received a clinical and cardiac examination including echocardiography, electrocardiography, concomitant medication, comorbidities and blood sampling for routine laboratory parameters, marker expression on platelets, and chemokine profiling. SARS-CoV-2 infection was confirmed by real-time reverse transcriptase-polymerase chain reaction from nasopharyngeal secretions. CAD was determined by coronary angiography and was characterized as >25% to 50% stenosis of one or more coronary vessels.

Inclusion criteria of our study were age older than 18 years, confirmed CAD and subsequent SARS-CoV-2 infection. Exclusion criteria were other microbial infections. The study was approved by the local ethics committee (240/2018B02) and complies with the declaration of Helsinki and the good clinical practice guidelines on the approximation of the laws, regulations, and administrative provisions of the member states relating to the implementation of good clinical practice in the conduct of clinical trials on medicinal products for human use. Written informed consent was obtained from every patient.

We determined NT-proBNP (N-terminal pro-B-type natriuretic peptide, >300 ng/L), hs TNI (high sensitive troponin I, >37 ng/L), and CRP (C-reactive protein, >0.5 mg/dL) as elevated laboratory markers of myocardial and inflammatory distress. As echocardiographic parameters, the left and right ventricular function, right ventricular dilatation, presence of tricuspid valve regurgitation, and pericardial effusion were included according to current guidelines.[43,44]

Clinical Follow-Up

The clinical study end point was characterized as rapidly progressive respiratory failure with indication to mechanical ventilation. Respiratory failure was defined by a moderately to severely impaired Horovitz index (moderately impaired HI defined as 101–200 mm Hg, severely impaired HI defined as ≤100 mm Hg). The occurrence of the clinical study end point HI <200 mm Hg was obtained during a follow-up period of 60 days.

Flow Cytometry Staining

One hundred twenty-two blood samples of patients with CAD (with or without SARS-CoV-2 infection) and healthy controls were collected in citrat-phosphat-dextrose-adenin monovette for flow cytometry to characterize platelets and platelet/leukocyte co-aggregates. Platelets were analyzed in 5 µL whole blood, diluted 1:10 in HEPES Tyrode buffer (pH 7.4) in a 96 well plate. To avoid unspecific binding, the Fc part of cellular receptors was blocked using human IgG (0.01 mg/mL; Sigma Aldrich Co St Luis, MO) and incubated for 20 minutes at 4 °C. Extracellular staining of platelets was performed for 20 minutes at 4 °C using following fluorochrome-conjugated antibodies: CD41 PaBl (clone HIP8), CD42b PerCP-Cy5.5 (clone HIP1), CD62P PE-Cy7 (clone AK4), CD61 FITC (clone VIPL2), and CD31 BV711 (clone WM59; BioLegend, San Diego, California). For life/dead staining Zombie NIR (BioLegend, San Diego, California) was used and performed together with the extracellular anti-body staining in one master mix tube. Zombie NIR from BioLegend is an amine-reactive fluorescent dye which is permeant to the cells with compromised membranes in contrast to non permeant live cells. Low-temperature incubations did not influence platelet activation, tested by measurement of CD62P surface expression (data not shown). Cells were fixed overnight with FoxP3/transcription factor staining buffer set containing formaldehyde (Thermo Fisher Scientific, Waltham, MA) according to manufacturer's instructions. After each staining, cells were washed with PBS containing 1% FCS, 2 mmol/L EDTA, and 1% sodium azide. At least 100 000 cells were acquired using a LSR Fortessa flow cytometer with the DIVA software and were further analyzed using FlowJo 10.6.2 software (all from BD Biosciences, Franklin Lakes, New Jersey). Platelets and platelet/leukocyte co-aggregates were characterized according their size and granularity. All samples were gated as follows: time/singlets/platelets/LiveDead FSC-low or FSC-high. Platelets (blue plots) were gated as follows: FSC-low/$CD41^+CD42b^+$. Platelet/leukocyte co-aggregates (green plots) were gated as follows: FSC-high/$CD42b^+CD61^+$ and for highly activated $CD42b^+$ platelet/leukocyte co-aggregates expression of $CD41^+CD61^+CD62P^+$ was measured (Figure IA in the Data Supplement). Compensation was measured and calculated by FACS DIVA software. Surface marker expression was quantified as median fluorescence intensity and frequency of living cells. Fluorescence minus one controls were used for gating on marker positive platelets.

Activation of Platelets and Flow Cytometry Staining

Blood samples of healthy controls were collected in citrat-phosphat-dextrose-adenin monovette to quantify furin surface expression upon activation. Platelet-rich plasma was prepared by centrifugation for 20 minutes at 210g without a break. For each sample, 1×10^4 platelets were incubated with either 5 µmol/L ADP, 10 µmol/L TRAP (thrombin receptor activating peptide; TRAP6, F. HOFFMANN LA-ROCHE AG, BASEL, SWITZERLAND), 1

µg/mL CRP (CRP-XL, CambCol, Cambridge, United King-dom), or 1 U/mL Thrombin (F. Hoffmann La-Roche AG, Basel, Switzerland). Platelet surface staining was performed with the following fluorochrome-conjugated antibodies: CD62P PE (clone CLBThromb/6, Beckman-Coulter, Brea, CA) and furin AF488 (clone 222722, R&D Systems, Minneapolis, MN) for 30 minutes at room temperature in combination with the agonists. Platelets were fixed with 0.5% formaldehyde for 30 minutes in the dark. To measure the effects of the PAR-1 (pro-tease-activated receptor-1) inhibitor ML161, samples were preincubated for 5 minutes with 50 µmol/L ML161 at RT before activation and staining for 30 minutes as described above. Measurements were performed using a Calibur (BD Biosciences, Franklin Lakes, NJ) and DIVA software (BD Biosciences, Franklin Lakes, NJ) followed by data analysis with FlowJo software V.10.6.2 (BD Biosciences, Franklin Lakes, NJ).

Imaging Flow Cytometry

Imaging flow cytometry was performed of CAD-SARS-CoV-2negative patients in the same way as de-scribed above for the flow cytometry staining of platelets. Following fluorochrome-conjugated antibodies were used: CD42b PerCP-Cy5.5 (clone HIP1) and CD14 FITC (clone M5E2) from BioLegend, San Diego, CA. For live/dead staining, Zombie Aqua (BioLegend, San Diego, California) was included. For gating of platelet/leukocyte co-aggregates CD14 and CD42b surface expression was performed. Platelet/leukocyte co-aggregates were gated as follows: fo-cus/cells/lymphocytes/live/$CD14^+$/$CD42b^+$/platelet-monocyte-complex (Figure IB in the Data Supplement). Measurements were performed with an Amnis Image Stream MK II (Luminex, Austin, TX), and data analysis was done with the software IDAS Version 6.2.

Determination of Plasma Levels of Cytokines/Chemokines (LEGENDPlex)

To quantify the concentrations of several chemokines and cytokines in human plasma, a LEGEND-Plex inflammation panel 1 (BioLegend, San Diego, CA) and LEGENDPlex proinflammatory chemokine panel (BioLegend, San Diego, CA) were performed. Only 79 frozen plasma samples were avail-able and could be analyzed, consisting of 19 CAD-SARS-CoV-$2^{negative}$, 31 CAD-SARS-CoV-$2^{positive}$ patients, and 29 healthy controls. The assays were performed according to the manufacturers' manual. FACS Lyric (BD Biosciences, Franklin Lakes, NJ) was used for the measurement and data analysis was performed with the LEGENDPlex Data Analysis Software (BioLegend, San Diego, CA).

Isolation of Human Platelets

Human washed platelets were isolated as previously described.[45] Washed platelets were resus-pended in HEPES Tyrode buffer (pH 7.4, supplemented with 1 mmol/L CaCl2) or lysed in RIPA lysis buffer for further experiments. For activation, isolated platelets were stimulated with CRP (CRP-XL, CambCol, Cambridge, United Kingdom), TRAP (TRAP6, F. Hoffmann La-

Roche AG, Basel, Switzer-land), or thrombin (F. Hoffmann La-Roche AG, Basel, Switzerland). Individual concentrations and exposure times are indicated within figures and legends.

Generation of Supernatant From Activated Platelets

To gain activated platelet supernatant, washed platelets were activated by addition of 1 U/mL thrombin (F. Hoffmann La-Roche AG, Basel, Switzerland) and incubated at room temperature for 30 minutes each. Afterwards, samples were centrifuged at 340g for 5 minutes, and the supernatants were used for further experiments. The protein concentration of the activated platelet supernatant was determined by a standard Bradford Assay.46

Determination of Plasma Levels of Furin

To quantify furin concentration in human plasma, a furin human ELISA Kit (R&D Systems, Minneapolis, MN) was performed. Frozen plasma samples of CAD-SARS-CoV-2negative (n=20), CAD-SARS-CoV-$2^{positive}$ patients (n=35), and healthy controls (n=28) were measured.

To quantify platelet furin levels, we used lysates from resting human platelets and activated plate-let supernatant from platelets activated with 1 U/mL thrombin (F. Hoffmann La-Roche AG, Basel, Switzerland). Each sample was prepared from a suspension containing 2×10^9 washed platelets/mL. The assays were performed according to the manufacturer manuals.

Immunofluorescence Microscopy

Isolated human platelets in PBS (4×10^8 platelets/mL) were supplemented with 1 mmol/L $CaCl_2$, activated with 1 µg/mL CRP (CRP-XL CambCol, Cambridge, United Kingdom), and incubated on poly-L-Lysin coated coverslips for 30 minutes at room temperature. The platelets were fixated with 2% formaldehyde and blocked with BSA. The samples were stained with anti-mouse furin AF488 con-jugated antibody (Mouse monoclonal IgG_{2B}, clone 222722 R&D Systems, Minneapolis, MN). An IgG_{2B} antibody (Mouse monoclonal IgG2B Isotype control, clone 20116, R&D Systems, Minneapolis, MN) with an AF568 secondary antibody (A1161, invitrogen) was used as isotype control. The coverslips were mounted onto slides and several images from randomly selected areas were taken (Nikon Eclipse Ti2-A, 100×DIC [differential interference contrast] objective). The images were analyzed with the NIS-Elements AR software (Nikon, Japan).

Furin Activation Assay

To analyze the furin enzyme activity of platelets, the fluorogenic peptide substrate pERTKR-AMC Substrate (100 µmol/L; R&D Systems, Minneapolis, MN) was combined with 200 ng furin or isolated platelets (5×107/mL) stimulated with CRP (CRP-XL CambCol, Cambridge, United Kingdom), TRAP (TRAP6, F. HOFFMANN LA-ROCHE AG, BASEL, SWITZERLAND) or

thrombin (F. Hoffmann La-Roche AG, Basel, Switzerland).47,48 Additionally, experiments were performed in the same manner with isolated platelets (1×109/mL) diluted in Tyrode buffer (pH 7.4) or platelet-poor plasma derived from the donor of the sample by 10 minutes centrifugation of PRP at 2500g. The resulting fluorescent signal of the digested peptide was immediately detected over 60 minutes using a plate reader (380/460 nm; Glomax, Promega, Madison, WI).

Statistical Analysis

Statistical analysis of participants' clinical and laboratory baseline characteristics in relation to measured platelet phenotypes, and marker expression was performed. Non-normally distributed continuous data are represented as median with interquartile range (IQR) and normally distributed continuous data are represented as mean with SD. Two group comparisons for non-normally distributed continuous variables were performed using a Mann-Whitney U test while normally distributed continuous variables were compared using Student t test. One-Way ANOVA was performed for >2 group comparison and for post hoc analysis and multiple comparison Dunnett test was used. Categorical variables are represented as total numbers, and proportions of participants and comparison was performed using $\chi 2$ test. Survival curves of patients were calculated by Kaplan-Meier analyses and compared using the log-rank test. Correlation analysis was calculated by Spearman rank correlation coefficient. Cox proportional-hazards regression analysis was performed for multi-variable analysis to assess furin plasma level association with progressive respiratory failure (HI <200 mm Hg). Volcano plots were performed with JMP Version 15.0. Each data point was tested using Mann-Whitney U test. Comparisons were considered statistically significant if 2-sided P value was ≤0.050. All statistical analysis was performed with IBM SPSS Statistics software version 26 (SPSS, Inc) and GraphPad Prism Version 8.4.0 (GraphPad Software).

Results

Demographic and Clinical Characteristics of Patients With CAD and SARS-CoV-2-Associated Respiratory Failure

We prospectively studied a consecutive cohort of 55 patients in spring 2020 during the first wave of symptomatic patients with CAD that were admitted to our hospital for suspected respiratory infection and found to be positive for SARS-CoV-2 (CAD-SARS-CoV-2^{positive}; Table 1). Twenty-eight patients with symptomatic CAD without any signs of respiratory infection and with a negative reverse transcriptase-polymerase chain reaction test for SARS-CoV-2 (CAD-SARS-CoV-2^{negative}) were matched by age, gender, and presence of stable CAD on admission to the CAD-SARS-CoV-2^{positive} group (Table 1). The median age of the population was 63.5 (IQR, 47–78) years; 57 (46.7%) patients were men (Table 1). About one-fourth (21.8%) of

CAD-SARS-CoV-2^{positive} patients showed a BMI ≥30 compared with 10.7% of CAD-SARS-CoV-2^{negative} patients and to 10.3% of healthy control group (P=0.045). Pericardial effusion was significantly more often present in the CAD-SARS-CoV-2^{positive} group, possible mirroring concomitant perimyocarditis (P<0.001; Table 1). Interestingly, there were no significant differences of D-dimer levels between groups upon admission (P=0.882). Progressive respiratory failure as indicated by an HI of ≥200 mm Hg was found in 35 (63.6%) of CAD-SARS-CoV-2^{positive} patients. Out of 55 patients, 22 (36.4%) required mechanical ventilation in the time course during their hospital stay (Table 2).

Table 1. Baseline characteristics of patient population

Parameters	**All Patients. N=122**	**CAD-SARS-CoV-2^{positive}. N=55**	**CAD-SARS-CoV-2^{negative}. N=28**	**Control. N=39**	***P* value**
Clinical characteristics					
Age. y	63.5 (47-78)	76 (62-82)	70.5 (63-78)	41 (28-53)	<0.001 *
Male	57 (46.7)	27 (49.1)	14 (50)	16 (41)	0.686
BMI (kg/m²)	25 (22.3-28.1)	27.7 (25.1-31.1)	24.9 (23-26.5)	22 (21-25)	0.005 *
BMI (kg/m^2) ≥ 30	19 (15.6)	12 (21.8)	3 (10.7)	4 (10.3)	0.045 *
Fever	30 (24.6)	30 (54.5)	0 (0)	0 (0)	<0.001 *
Cardiovascular risk factors					
Arterial hypertension	71 (58.2)	47 (85.5)	23 (82.1)	1 (2.6)	<0.001 *
Dyslipidemia	52 (42.6)	32 (58.2)	19 (67.9)	1 (2.6)	<0.001 *
Diabetes mellitus	22 (18)	18 (32.7)	3 (10.7)	1 (2.6)	0.004 *
Current smokers	11 (9)	3 (5.5)	4 (14.3)	4 (10.3)	0.392
Atrial fibrillation	25 (20.5)	14 (25.5)	11 (39.3)	0 (0)	<0.001 *
Chronic kidney disease	13 (10.7)	11 (20)	2 (7.1)	0 (0)	0.007 *
Parameters of echocardiography					
Left ventricular ejection fraction. %	60 (60-60)	60 (60-60)	60 (51.3-60)	60 (60-60)	0.001 *
Right ventricular dilatation	18 (14.8)	17 (30.9)	1 (3.6)	0 (0)	<0.001 *
Tricuspid regurgitation >1	4 (3.3)	3 (5.5)	1 (3.6)	0 (0)	0.584
Pericardial effusion	27 (22.1)	25 (45.5)	2 (7.1)	0 (0)	<0.001 *
Pleural effusion	14 (11.5)	13 (23.6)	1 (3.6)	0 (0)	0.003 *
PAPsys (mmHg)	25 (21-34.5)	25 (21-33)	24 (20-36)	-	-
Concomitant cardiac medication at study entry					
Oral anticoagulation	18 (14.8)	8 (14.5)	10 (35.7)	0 (0)	0.007 *
ACE-I or ARB	52 (42.6)	36 (65.5)	16 (57.1)	0 (0)	0.017 *
Aldosterone inhibitors	13 (10.7)	8 (14.5)	5 (17.9)	0 (0)	0.025 *
Diuretics	29 (23.8)	25 (45.5)	4 (14.3)	0 (0)	<0.001 *
Calcium channel blockers	19 (15.6)	14 (25.5)	5 (17.9)	0 (0)	0.002 *

Beta blockers	39 (32)	27 (49.1)	12 (42.9)	0 (0)	<0.001 *
Statins	39 (32)	26 (47.3)	13 (46.4)	0 (0)	<0.001 *
ASA	26 (21.3)	17 (30.9)	9 (32.1)	0 (0)	<0.001 *
P2Y12 inhibitors	2 (1.6)	1 (1.8)	1 (3.6)	0 (0)	0.643
Parameters of electrocardiography					
Heart Rate (bpm)	75 (65-81.8)	76 (67.3-84)	69 (62.5-81.5)	61 (58-74)	0.058
Heart Rhythm					
Sinus rhythm	58 (47.5)	36 (65.5)	22 (78.6)	0 (0)	
Atrial fibrillation	9 (7.4)	7 (12.7)	2 (7.1)	0 (0)	<0.001 *
Pacemaker with ventricular pacing	4 (3.3)	2 (3.6)	2 (7.1)	0 (0)	
Laboratory parameters and biomarkers					
Leukocytes (1000/µL)	6760 (5112.5-8672.5)	6180 (4590-8860)	7150 (6010-8475)	6890 (5700-7670)	0.452
Lymphocytes (1000/µL)	910 (662.5-1622.5)	780 (610-1150)	1790 (1380-2135)	2110 (1550-2410)	<0.001 *
Hb (g/dL)	13.1 (11.7-14)	12.5 (11.1-13.8)	13.7 (12.6-14.3)	13.8 (12.6-14.2)	0.544
Platelets (1000/µL)	139.4 (97.5-177.2)	120.4 (74.9-148.4)	160.1 (111.1-187.3)	178.6 (145.7-213.8)	<0.001 *
INR (%)	1.1 (1-1.1)	1.1 (1-1.2)	1 (1-1.1)	1 (1-1)	0.347
PTT (s)	24.5 (22.3-29)	24 (22-29)	25 (23-31)	24 (23-24.5)	0.304
D-Dimer (µg/dL)	1 (0.7-1.8)	1 (0.7-1.9)	0.31 (0.31-0.31)	0.23 (0.23-0.23)	0.882
Creatinine (mg/dL)	0.8 (0.7-1)	0.9 (0.7-1.3)	0.8 (0.7-0.9)	0.7 (0.6-0.8)	0.062
GFR-MDRD (ml/m^2)	77.9 (60.5-97.5)	74.1 (50.5-95.5)	83 (71.8-101.7)	107.1 (86.7-119.7)	0.001 *
Sodium (mmol/L)	138 (136-140)	137 (135-139)	140 (139-141)	140 (138.8-142)	<0.001 *
CRP (mg/dL)	1.6 (0.3-8.7)	4 (1.2-12.2)	0.1 (0-0.6)	0.12 (0.1-0.5)	<0.001 *
PCT (ng/mL)	0.1 (0.1-0.3)	0.1 (0.1-0.3)	-	-	-
IL-6	28.6 (10-49.4)	28.6 (10-49.4)	-	-	-
hs TNI (ng/dL)	9.5 (4-27.3)	13.5 (5-47.8)	4.5 (3-7.3)	1.5 (0.0-3)	0.129
NT-pro-BNP (ng/L)	595 (133-3592)	749 (136-4731)	261 (106.8-899)	55 (34.8-120)	0.746
CK (U/L)	103.5 (63-194.3)	117 (63-250)	80 (57-120.5)	95 (68-162)	0.031 *
AST (U/L)	28 (17.5-45)	38 (20-53)	17.5 (14-21)	18 (15.5-25)	0.001 *
ALT (U/L)	24.5 (17.3-37.8)	27 (19-38)	20 (14.5-36.5)	24 (18-32)	0.543
LDH (U/L)	218 (190-318)	270 (204-362.5)	195 (172.5-207.5)	155 (141.3-208.8)	<0.001 *
HbA1c (%)	6.1 (5.8-6.4)	6.2 (6-6.6)	5.8 (5.6-6)	5.4 (5-5.8)	0.006 *
Lactate (mmol/L)	1.5 (0.9-1.8)	1.5 (0.9-1.8)	-	-	-
pH	7.4 (7.4-7.5)	7.4 (7.4-7.5)	-	-	-
Horovitz Index (mmHg)					
≥ 200 mmHg	102 (83.6)	35 (63.6)	28 (100)	39 (100)	<0.001 *

< 200 mmHg	20 (16.4)	20 (36.4)	0 (0)	0 (0)

Table 2. Baseline characteristics of patient population stratified by the occurrence of the clinical endpoint (progressive respiratory failure defined by Horovitz Index HI < 200 mmHg and mechanical ventilation)

Parameters	**CAD-SARS-CoV-2^{positive} (n=55)**	**HI > 200mmHg (n=35)**	**HI ≤ 200mmHg (n=20)**	**p-value**
Clinical characteristics				
Age. y	76 (62-82)	68 (57-81)	79 (73-85.5)	0.003 *
Male	27 (49.1)	17 (48.6)	10 (50)	0.919
BMI (kg/m²)	27.7 (25.1-31.1)	27.7 (25.2-32)	27.5 (25-29.6)	0.783
Fever	30 (54.5)	19 (54.3)	11 (55)	0.799
Cardiovascular risk factors				
Arterial hypertension	47 (85.5)	28 (80)	19 (95)	0.129
Dyslipidemia	32 (58.2)	24 (68.6)	8 (40)	0.039 *
Diabetes mellitus	18 (32.7)	11 (31.4)	7 (35)	0.410
Current smokers	3 (5.5)	3 (8.6)	0 (0)	0.178
Atrial fibrillation	14 (25.5)	7 (20)	7 (35)	0.219
Chronic kidney disease	11 (20)	5 (14.3)	6 (30)	0.161
Parameters of echocardiography				
Left ventricular ejection fraction. %	60 (60-60)	60 (60-60)	60 (55-60)	0.597
Right ventricular dilatation	17 (30.9)	12 (34.3)	5 (25)	0.134
Tricuspid regurgitation >1	3 (5.5)	2 (5.7)	1 (5)	0.693
Pericardial effusion	25 (45.5)	15 (42.9)	10 (50)	0.701
Pleural effusion	13 (23.6)	8 (22.9)	5 (25)	0.821
PAPsys (mmHg)	25 (21-33)	25 (20-30.8)	30 (25.5-41)	0.039 *
Concomitant cardiac medication at study entry				
Oral anticoagulation	8 (14.5)	5 (14.3)	3 (15)	0.348
ACE-I or ARB	36 (65.5)	24 (68.6)	12 (60)	0.768
Aldosterone inhibitors	8 (14.5)	6 (17.1)	2 (10)	0.614
Diuretics	25 (45.5)	16 (45.7)	9 (45)	0.692
Calcium channel blockers	14 (25.5)	10 (28.6)	4 (20)	0.657
Beta blockers	27 (49.1)	18 (51.4)	9 (45)	0.918
Statins	26 (47.3)	18 (51.4)	8 (40)	0.768
ASA	17 (30.9)	14 (40)	3 (15)	0.107
P2Y12 inhibitors	1 (1.8)	1 (2.9)	0 (0)	0.475
Parameters of electrocardiography				
Heart Rate (bpm)	76 (67.3-84)	76 (68.5-81)	74.5 (65.5-94)	0.787
Heart Rhythm				
Sinus rhythm	36 (65.5)	24 (68.6)	12 (60)	0.390
Atrial fibrillation	7 (12.7)	6 (17.1)	1 (5)	
Pacemaker with ventricular pacing	2 (3.6)	2 (5.7)	0 (0)	
Laboratory parameters and biomarkers				
Leukocytes (1000/µL)	6180 (4590-8860)	6070 (4250-8860)	6295 (5275-9057.5)	0.449

Lymphocytes (1000/µL)	780 (610-1150)	890 (690-1320)	655 (530-817.5)	0.019 *
Hb (g/dL)	12.5 (11.1-13.8)	13 (11.7-13.8)	12.1 (10-13.9)	0.643
Platelets (1000/µL)	184 (143-243)	184 (147-243)	174 (130.8-240.8)	0.615
INR (%)	1.1 (1-1.2)	1 (1-1.1)	1.1 (1-1.2)	0.612
PTT (s)	24 (22-29)	24 (22-27)	26.5 (23.3-31)	0.680
D-Dimer (µg/dL)	1 (0.7-1.9)	0.8 (0.5-1.4)	1.8 (1-2.6)	0.728
Creatinine (mg/dL)	0.9 (0.7-1.3)	0.9 (0.7-1.2)	1 (0.6-1.6)	0.894
GFR-MDRD (ml/m^2)	74.1 (50.5-95.5)	75.5 (58.3-86)	73 (39.9-97.6)	0.951
Sodium (mmol/L)	137 (135-139)	137 (135-139)	136 (132.5-139.8)	0.366
CRP (mg/dL)	4 (1.2-12.2)	1.9 (0.9-4.5)	12.3 (7.4-20.3)	<0.001 *
PCT (ng/mL)	0.1 (0.1-0.3)	0.1 (0-0.2)	0.1 (0.1-0.6)	0.238
IL-6	28.6 (10-49.4)	13.6 (8-28)	42.1 (31.6-60.5)	0.328
hs TNI (ng/dL)	13.5 (5-47.8)	8.5 (2.3-21.5)	23.5 (16-105.8)	0.294
NT-pro-BNP (ng/L)	749 (136-4731)	316 (92.5-1107.8)	3068 (793.5-17373.5)	0.823
CK (U/L)	117 (63-250)	114 (63-252)	119.5 (55.8-229.5)	0.801
AST (U/L)	38 (20-53)	34 (19.8-44.5)	48 (38-77)	0.154
ALT (U/L)	27 (19-38)	27 (20-38)	26 (18-53.5)	0.738
LDH (U/L)	270 (204-362.5)	242 (190-320)	337 (252-445)	0.006 *
HbA1c (%)	6.2 (6-6.6)	6.1 (6-6.6)	6.3 (5.9-6.5)	0.479
Lactate (mmol/L)	1.5 (0.9-1.8)	1.5 (0.9-1.8)	1.4 (1-2.2)	0.915
pH	7.4 (7.4-7.5)	7.4 (7.4-7.5)	7.4 (7.4-7.5)	0.650
Horovitz Index (mmHg)				
≥ 200 mmHg	35 (63.6)	35 (100)	0 (0)	<0.001 *
< 200 mmHg	20 (36.4)	0 (0)	20 (100)	

Values are n (%) or are given as median and interquartile range (IQR). ACE - Angiotensin Converting Enzyme. Afib - atrial fibrillation. ALT – alanine amino-tranferase. ARB - Angiotensin II Receptor Blockers. ASA – Acetylsalicylic acid. AST – aspartate-aminotransferase. BMI – body mass index. CAD – coronary artery disease. CK – creatinine kinase. CRP – C-reactive protein. GFR-MDRD – glomerular filtration rate. Hb – hemoglobin. hs TNI - high sensitive Troponin I. INR – interna-tional normalized ratio. LDH – lactate dehydrogenase. NT-pro-BNP – N-terminal pro- brain natriuretic peptide. Pap Sys – pulmonary arterial pressure systolic. PCT – procalcitonin. PTT – partial thromboplastin time. SARS-CoV-2 – severe acute respiratory syndrome coronavirus-2. P values <0.05 we considered significant and indicated with *.

CAD-SARS-CoV-2^{positive} Patients Show Significantly Higher Systemic Platelet Activation and Hyper-Inflammation

At time of hospital admission all patients received a prespecified complete clinical assessment and evaluation of ECG, echocardiography, and extensive routine laboratory parameters including troponin I, NT-proBNP, and D-dimers. Blood samples were characterized by flow cytometric platelet activation parameters and cytokine/chemokine plasma profiling.

CAD-SARS-CoV-2^{positive} patients showed a significantly reduced peripheral platelet count compared with CAD-SARS-CoV-2^{negative} patients and healthy controls (healthy control versus CAD-SARS-CoV-2^{positive} versus $^{-negative}$; median, IQR; 1.79×10^8/mL (1.46×10^8×/mL–2.14×10^8/mL) versus 1.20×10^8/mL (0.75×10^8/mL–1.48×10^8/mL) versus 1.60×10^8/mL (1.11×10^8/mL–1.87×10^8/mL); healthy control versus CAD-SARS-CoV-2^{positive} P<0.0001, healthy control versus CAD-SARS-CoV-2^{negative} P=0.4610, CAD-SARS-CoV-2^{positive} versus $^{-negative}$ P=0.0365; Figure 1A). Further, activation of circulating platelets of CAD-SARS-CoV-2^{positive} patients, determined by surface expression of CD62P, was significantly enhanced in the infected group compared with uninfected CAD patients and the healthy control group (%CD62P$^+$ platelets; healthy control versus CAD-SARS-CoV-2^{positive} versus $^{-negative}$; median (IQR); 13.5% (9.7%–19.3%) versus 18.7% (14.6%–25.2%) versus 10.8% (7.4%–15.5%); healthy control versus CAD-SARS-CoV-2^{positive} P=0.0139, healthy control versus CAD-SARS-CoV-2^{negative} P=0.4994, CAD-SARS-CoV-2^{positive} versus $^{-negative}$ P=0.0002; Figure 1B). Further significantly enhanced CD42b$^+$CD61$^+$ platelet/leukocyte co-aggregates were observed in the infection group compared with CAD-SARS-CoV-2^{negative} patients and the healthy control group (healthy control versus CAD-SARS-CoV-2^{positive} versus $^{-negative}$; median (IQR); 4.6% (3.4%–7.1%), 8.4% (5.6%–11.2%) versus 4.4% (3.3%–5.0%); healthy control versus CAD-SARS-CoV-2^{positive} P=0.0002, healthy control versus CAD-SARS-CoV-2^{negative} P=0.7580, CAD-SARS-CoV-2^{positive} versus $^{-negative}$ P<0.0001; Figure 1C). Moreover, enhanced platelet activation in CAD-SARS-CoV-2^{positive} patients was reflected by an increase of CD41$^+$CD61$^+$CD62P$^+$ surface expression of CD42b$^+$ platelet/leukocyte co-aggregates in comparison to healthy and CAD-SARS-CoV-2^{negative} patients (Figure 1D). Platelet/leukocyte co-aggregates were gated first for double-positive CD41$^+$CD61$^+$ and further for CD62P$^+$ representing highly activated platelet/leukocyte co-aggregates. For visualization of the platelet/leukocyte co-aggregates, we performed imaging flow cytometry analysis and showed that CD42b$^+$ platelets adhere to CD14$^+$ monocytes, represented by red and green fluorescence, respectively (Figure 1E).

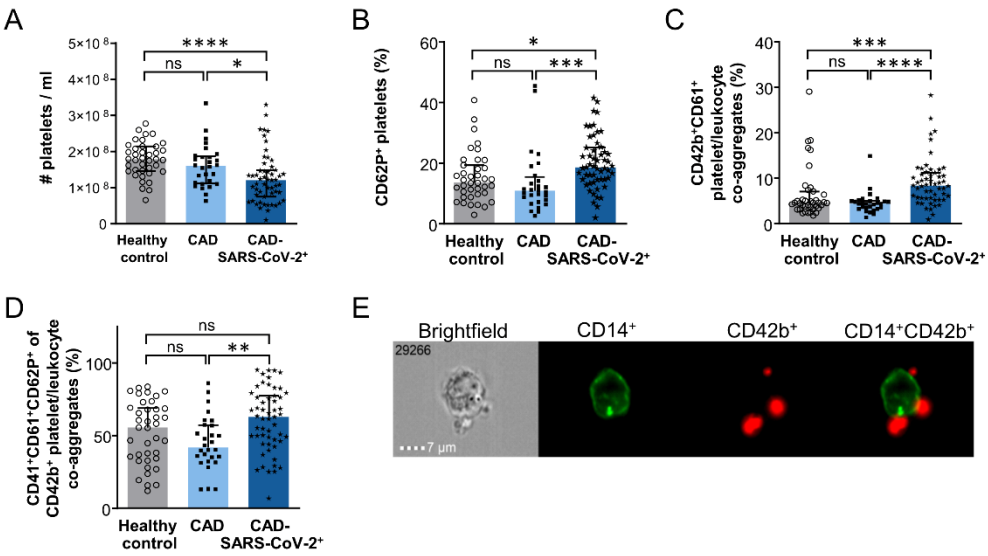

Figure 1. Coronary artery disease severe acute respiratory syndrome coronavirus 2 (CAD-SARS-CoV-2)^{positive} patients present with reduced platelet count but show increased platelet activation and platelet/leukocyte co-aggregates in peripheral blood. Human platelets were analyzed by flow cytometry in whole blood of healthy controls (n=39), CAD-SARS-CoV-2^{negative} patients (CAD; n=28), and patients with CAD with subsequent SARS-CoV-2 infection (CAD-SARS-CoV-2^{positive}; n=55). Graphs show (**A**) cell count of platelets/mL, (**B**) frequency of CD62P^{+} platelets (%), (**C**) frequency of CD42b^{+}CD61^{+} platelet/leukocyte co-aggregates (%), and (**D**) frequency of CD41^{+}CD61^{+}CD62P^{+} of CD42b^{+} plate-let/leukocyte co-aggregates (%). **E**, Imaging flow cytometry was performed to analyze platelet/leukocyte co-aggregates by staining with CD42b-PerCP-Cy5.5 and CD14-FITC antibodies. Representative brightfield and fluorescence images are shown. **A–D**, Plotted: Median with interquartile range (IQR); Statistics: Mann-Whitney U test. ns indicates not significant; *P≤0.050, **P≤0.010, ***P≤0.001, and ****P≤0.0001.

Thus, in contrast to patients with CAD with a negative test for SARS-CoV-2, the virus infection was associated with enhanced platelet activation.

We next measured plasma levels of hyper-inflammation markers in our patient cohort. Among the 17 tested inflammation markers 10 cytokines/chemokines were significantly different expressed at time of hospital admission in CAD-SARS-CoV-2^{positive} in contrast to CAD-SARS-CoV-2^{negative} patients and healthy controls. IFN (interferon)-γ, IL (interleukin) 18, IL-1β, IL-33, CCL2, CXCL8 (chemokine [C-X-C motif] ligand), CXCL9, CXCL10, CXCL11, and furin were significantly increased. IL-6, IL-10, IFN-α, TNF (tumor necrosis factor)-α IL-12p70, CCL5, and CXCL5 were not differently expressed (Figure 2A through 2Q).

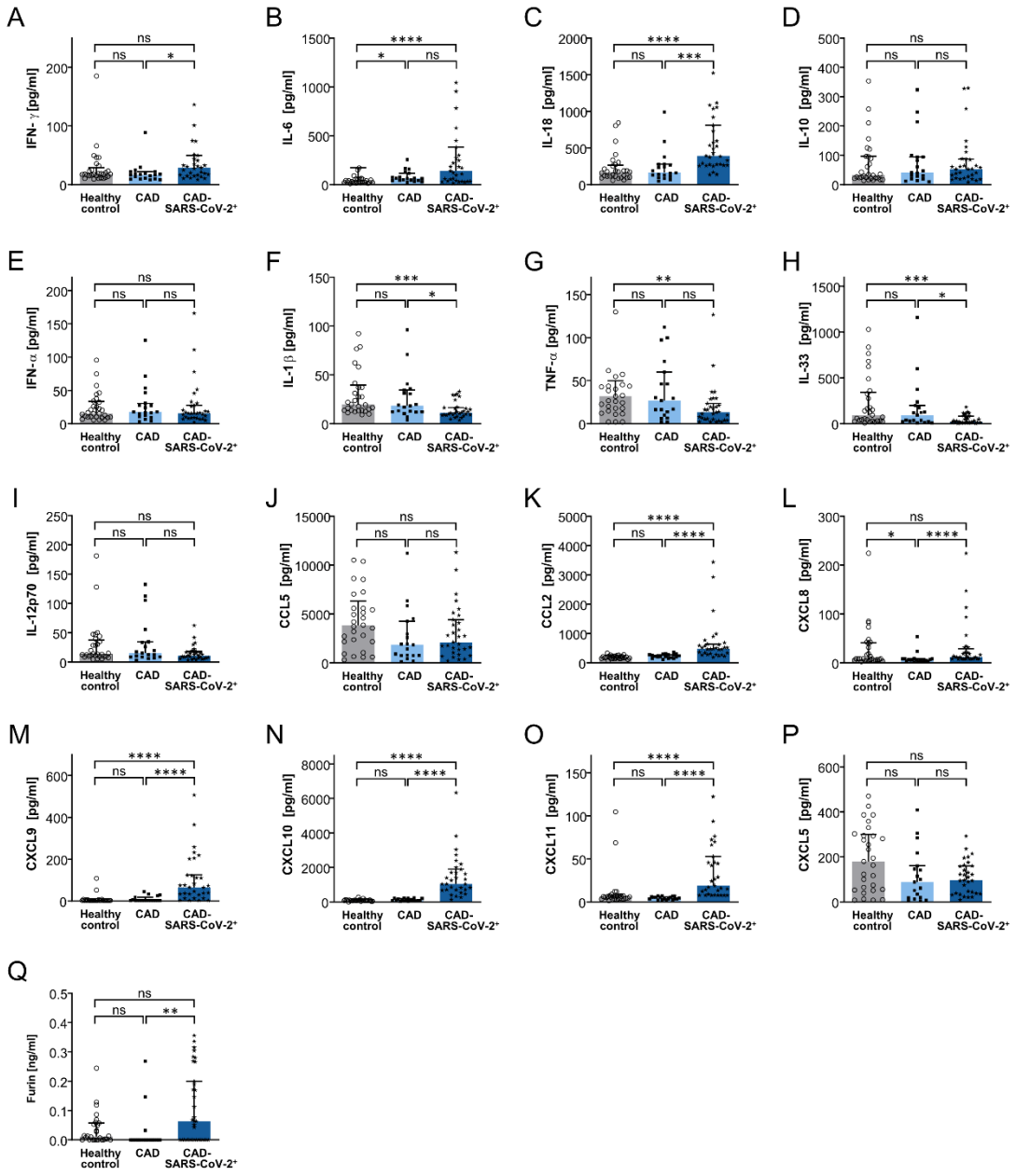

Figure 2. Coronary artery disease severe acute respiratory syndrome coronavirus 2 (CAD-SARS-CoV-2)^{positive} patients showed highly increased plasma concentration of furin and several inflammatory cytokines. LEGENDPlex assays were performed for measuring plasma concentrations of healthy controls (n=29), CAD-SARS-CoV-2^{negative} (n=19), and CAD-SARS-CoV-2^{positive} patients (n=31). Graphs display concentration (pg/mL) of (**A**) IFN (interferon)-γ, (**B**) IL (interleukin)-6, (**C**) IL-18, (**D**) IL-10, (**E**) IFN-α, (**F**) IL-1ß, (**G**) TNF (tumor necrosis factor)-α, (**H**) IL-33, (**I**) IL-12p70, (**J**) CCL5, (**K**) CCL2, (**L**) CXCL8 (chemokine [C-X-C motif] ligand), (**M**) CXCL9, (**N**) CXCL10, (**O**) CXCL11, and (**P**) CXCL5. **Q**, Plasma concentration (ng/mL) of Furin in healthy controls (n=28), CAD-SARS-CoV-2^{negative} (n=20) and CAD-SARS-CoV-2^{positive} patients (n=35) was analyzed by ELISA. **A–Q**, Plotted: Median with interquartile range (IQR); Statistics: Mann-Whitney U test, ns indicates not significant; *P≤0.050, **P≤0.010, ***P≤0.001, and ****P≤0.0001.

Further we found that platelet activation, as indicated by surface expression of the degranulation marker CD62 (P-selectin), correlates with plasma levels of CCL5 (RANTES; r=0.454, P=0.010), which is a prominent platelet chemokine released upon activation (Figure IIIA in the Data Supplement). Further, circulating CD42b+CD61+ platelet/leukocyte co-

aggregates correlated with IL-6 (r=0.398, P=0.027) as well as chemokines CCL2 (r=0.481, P=0.006) and CXCL10 (r=0.537, P=0.002) indicating that platelet activation and interaction with leukocytes is a trigger of hyper-inflammation (Figure 3B through 3D in the Data Supplement). Further, in CAD-SARS-CoV-2^{positive} patients, platelet activation and platelet/leukocyte co-aggregation are associated with elevation of pulmonary artery pressure (r=0.428, P=0.007) and plasma levels of TNI (troponin I; r=0.302, P=0.033; Figure 3E and 3F in the Data Supplement).

Plasma Levels of Furin Are Associated With Poor Clinical Prognosis in SARS-CoV-2-Positive CAD Patients, and Furin Is Released From Activated Platelets

We found that plasma levels of furin that has been postulated to activate the spike protein of the SARS-CoV-2 virus and facilitates cell fusion is enhanced in plasma of CAD-SARS-CoV-2^{positive} versus $^{-negative}$ patients (Figure 2Q).

Further, we observed increased furin plasma levels in CAD-SARS-CoV-2^{positive} patients requiring in-tensive care unit (ICU) treatment. Thus, furin levels on hospital admission are an early marker for progressive respiratory failure and requirement of ICU treatment (Figure 3A). Moreover, plasma levels of furin significantly correlate with numbers of circulating CD42b^{+}CD61^{+} platelet/leukocyte co-aggregates (r=0.460, P=0.009; Figure 3B). Thus, in CAD-SARS-CoV-2^{positive} patients, platelet activation is associated with enhanced plasma levels of furin. Next, we performed Kaplan-Meier analyses to identify whether plasma furin levels can be used as prognostic marker for patients with CAD infect-ed with SARS-CoV-2. We divided CAD-SARS-CoV-2^{positive} patients according to the calculated median concentration of furin (0.064 ng/mL) into 2 groups. We found that increased plasma levels of the serine protease furin is associated with adverse clinical outcome (ventilation therapy and overall mortality) in CAD-SARS-CoV-2^{positive} patients (log-rank=3.68, P=0.05; Figure 3C; Table 3). In our cohort, 11/55 CAD-SARS-CoV-2^{positive} patients reached the primary end point after 60 days defined as the occurrence of a HI <200 mm Hg and mechanical ventilation. Results showed that significantly more often CAD-SARS-CoV-2^{positive} patients with a furin concentration above the median reached the clinical end point (Figure 3C). Cox regression analysis adjusted for age, gender, pulmonary artery pressure, platelet count, and platelet activation showed that early determination of plasma levels of furin is predictive for progression of respiratory failure in CAD-SARS-CoV-2^{positive} patients (Table 3). Interestingly, 6 events of venous thromboembolism occurred during the 60 days of follow-up within the CAD-SARS-CoV-2^{positive} group of 55 patients. Four patients experienced a deep vein thrombosis and 2 patients a combination of deep vein thrombosis and pulmonary embolism. All events occurred in the CAD-SARS-CoV-2^{positive} patients admitted to ICU.

Table 3. Results of unadjusted and adjusted Cox regression analysis of progressive respiratory failure (Horovitz index HI < 200 mmHg)

Prediction of progressive respiratory failure (Horovitz index HI < 200 mmHg)	**Model 1: unadjusted HR (95% CI)**	***P* value**	**Model 2: adjusted HR (95% CI)***	***P* value**
Furin plasma levels, ng/mL	300.5 (5.01-18019)	0.006t	1802.97 (2.65-1226451)	0.024

Cox Regression analysis: model 1, *P* value=0.006; model 2: *P* value=0.024. Groups in each model were matched by age, gender, and smoking status. HI indicates Horovitz index; HR hazard ratio, and PAPsys, pulmonary artery pressure.

*Model 2 adjusted for PAPsys, platelet count, and platelet activation ($CD62P^+$ platelets, $CD61^+CD31^+CD41^+CD62P^+$ platelets/leucocytes co-aggregates).

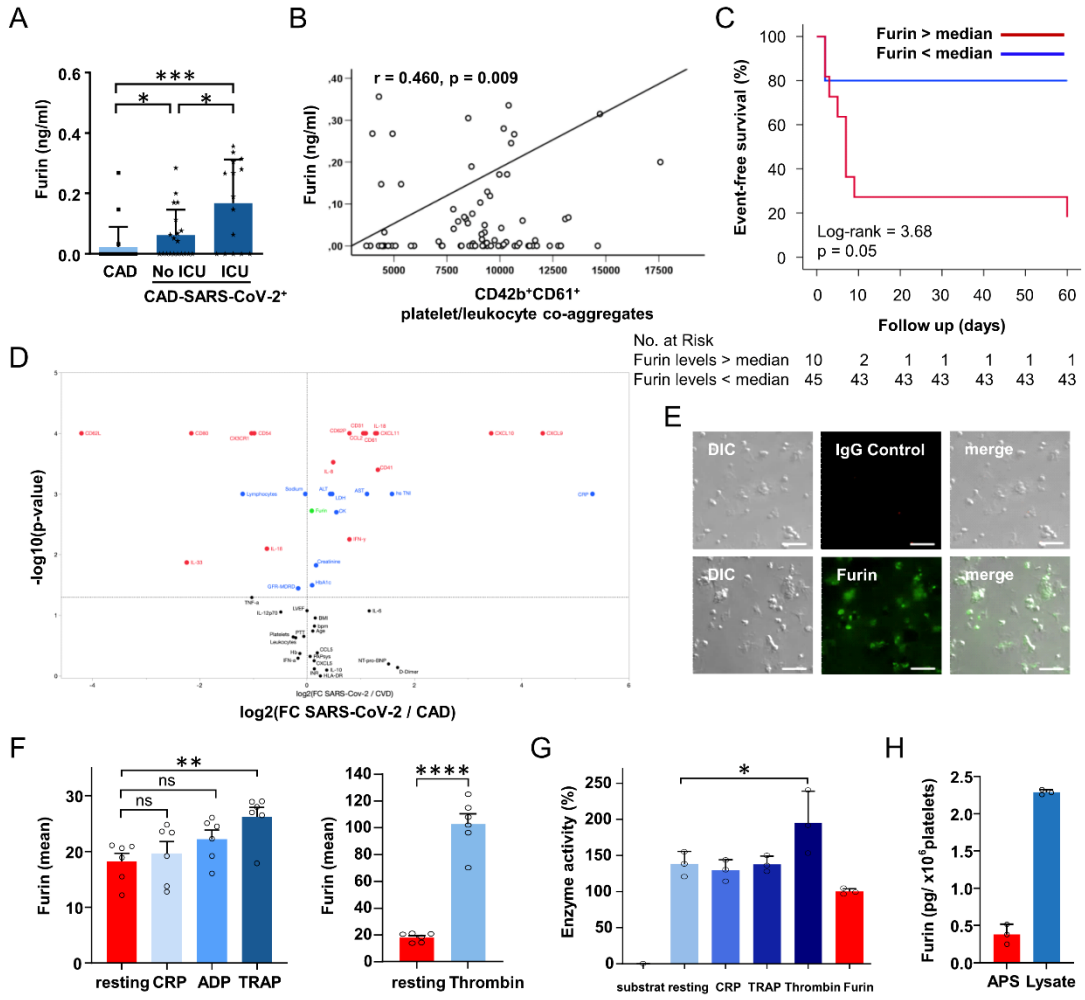

Figure 3. Furin is stored in platelets and furin plasma levels are associated with clinical outcome of coronary artery disease severe acute respiratory syndrome coronavirus 2 (CAD-SARS-CoV-2)^{positive} patients, platelet activation, and presence of platelet/leucocyte co-aggregates. A, Furin plasma levels (ng/mL) were measured by ELISA and stratified by CAD (CAD-SARS-CoV-2^{negative}; n=20) and CAD-SARS-CoV-2^{positive} status (subgroup of CAD-SARS-CoV-2^{positive} admitted to the intensive care unit [ICU; n=15] compared with no ICU [n=20] admission). Plotted: Mean±SD; statistics: 1-way ANOVA (Dunnett), *P≤0.050 and ***P≤0.001. **B**, Pearson correlation analysis was performed to evaluate associations be-tween $CD42b^+CD61^+$ platelet/leukocyte co-aggregates (median) and furin (ng/mL; r=0.460, P=0.009). Statistics: Pearson correlation coefficient r, **P≤0.010. **C**, Plasma concentration of furin of CAD-SARS-CoV-2^{positive} infected patients was divided into 2 groups based on the calculated median of furin concentration (median 0.064 ng/mL). Kaplan-Meier curve represents the occurrence of

the clinical study end point stratified according to furin plasma concentration of all CAD-SARS-CoV-2^{positive} patients within a follow-up time of 60 days. During these 60 days, 11/55 (20%) reached the end point. The clinical study end point was defined as rapidly progressive respiratory failure with a Horovitz index <200 mm Hg and required mechanical ventilation. Nine out of 11 (81.8%) patients had a furin plasma concentration above the calculated median (log-rank 3.68, P=0.05). **D**, Volcano plot displays analysis of clinical data and flow cytometry and LEGENDPlex measurements. y axis displays P (log10) with cut-off 1.3=−log10(0.05) and x axis fold change between the median of CAD (CAD-SARS-CoV-2^{negative}) and CAD-SARS-CoV-2^{positive}. Test was performed by JMP Version 15.0 Statistics: Mann-Whitney U test. **E**, Immunofluorescence microscopy was performed to analyze whether platelets store furin. Graph shows images of representative immunofluorescence microscopy pictures of spreaded human platelets stained with furin antibody (AF488) or an IgG_{2B} control antibody (AF568). Responding differential interference contrast (DIC) and merge images are supplied (scale=10 µm). **F**, For comparison of furin surface expression between differently activated platelets (n=6), graphs display mean fluorescence intensity of furin. Plotted: mean±SD; statistics: Student t test, ns=not significant; **P≤0.010 and **** P≤0.0001. **G**, For analysis of enzyme activity assay, a pERTKR-AMC fluorogenic peptide substrate was used. Graph shows the statistical end point analysis of the enzyme activity after 60 min incubation with of the fluorogenic peptide substrate with 5×107 platelets and activators (n=3). Plotted: mean±SD; Statistics: 1-way ANOVA (Dunnett), *P≤0.050. **H**, To quantify platelet furin levels we used lysates from resting human platelets and APS from platelets activated with 1 U/mL thrombin. Each sample was prepared from a platelet suspension of 2×10^9 cells/mL. For comparison of furin amount in platelets, supernatant of activated platelets (APS) and resting platelet lysate was performed and furin concentration (pg/1×10^6 platelets) was measured by ELISA (n=3). CRP indicates C-reactive protein; and TRAP, thrombin receptor activating peptide.

Volcano plot analysis confirms that furin plasma levels (green spot) are significantly elevated in CAD-SARS-CoV-2^{positive} patients compared with CAD-SARS-CoV-2^{negative} patients (Figure 3D).

Previously, others and we described platelets as a major source of inflammatory mediators, which play a critical role in atheroprogression and thrombo-inflammation.[1,49] Since platelet activation is associated with enhanced plasma levels of furin in CAD-SARS-CoV-2^{positive} patients, we asked whether furin is present in platelets and released upon activation. As shown by immunofluorescence studies, furin is stored in significant amounts in platelets (Figure 3E). Upon activation with TRAP6 or most prominently thrombin, furin is significantly expressed on the platelet surface (flow cytometry; Figure 3F). Furthermore, the enhanced furin expression by TRAP6 can be significantly suppressed with the PAR-1 inhibitor ML161 (10 µmol/L). This result was expected; as TRAP6 mediated activation is solely depended on the PAR-1 receptor (Figure IV in the Data Supplement). In contrast, the thrombin-induced furin expression is only partially inhibited in samples treated with 0.1 U/mL thrombin and 40 µmol/L ML161. When we used 1 U/mL of thrombin activation failed to be inhibited by 40 µmol/L ML161 (Figure IV in the Data Supplement). In both cases, ML161 was used to the maximum applicable concentration, due to the solubility limit of ML161. These findings indicate, that thrombin-induced furin expression is dependent on the PAR-1 as well as the PAR-4 signaling pathway and that pathway involvement may be dependent on the thrombin concentration. CRP activation was used as control for the ML161 specificity. No inhibitory effect of ML161 on CRP activation could be observed (Figure IV in the Data Supplement). The sample activation was confirmed by CD62P expression, which was significantly increased in all samples measured (Figures II and

IV in the Data Supplement). Further, comparison of washed platelets and platelet poor plasma regarding enzyme activity upon platelet activation display increased furin activity in the presence of plasma (Figure V in the Data Supplement). Additionally, platelets have the potential ability to degrade the SARS-CoV-2 spike protein indicated by the furin activity assay performed (Figure 3G). To quantify platelet furin levels, we used lysates from resting human platelets and activated platelet supernatant from platelets activated with 1 U/mL thrombin. Each sample was prepared from a platelet sus-pension of 2×10^9 cells/mL. Quantification by ELISA revealed that resting platelets contain 2.291±0.0348 (pg/1×10^6 platelets) furin and release approximately 20% furin upon activation (0.382±0.1225 pg/1×10^6 platelets; Figure 3H). In summary, platelets are a major source of furin that is released upon activation and may be critical for progression of respiratory failure in SARS-CoV-2^{positive} patients with CAD.

Discussion

The major findings of our present study are (1) patients with CAD and SARS-CoV-2 infection already exhibit a significantly enhanced platelet activation (Figure 1B) and hyper-inflammation at time of hospital admission (Figure 2) and (2) plasma levels of furin are associated with poor clinical outcome in CAD-SARS-CoV-2^{positive} patients (Figure 3C), in addition, furin is stored and released from activated platelets (Figure 3E and 3F). Our data imply that a prothrombotic state of circulating platelets is critically involved in development of systemic thrombo-inflammation (hyper-inflammation) early in the development of SARS-CoV-2 infection. Moreover, release of the SARS-CoV-2 activated serin protease furin from platelets may promote infection of the RNA virus.

Targeting platelet activation and attenuating release of inflammation markers at an early state of the infection may help to control progression of COVID-19. Former studies showed that acute SARS-CoV-2 infection is associated with platelet activation, increased amount of platelet/leucocyte co-aggregates and characteristic coagulopathy resulting in thrombotic complications including deep vein thrombosis and pulmonary embolism.[4–6,10] Platelet activation and platelet/leucocyte co-aggregates can predict an unfavorable clinical outcome of patients with COVID-19.[11] This might be in particular be relevant for patients with CAD due to their increased risk of mortality, respiratory, and organ failure. Mechanisms underlying COVID-19-induced acute coronary syndrome might involve plaque rupture, coronary spasm, or microthrombi owing to systemic inflammation or cytokine storm. Potential drug–disease interactions affecting patients with COVID-19 and comorbid cardio-vascular diseases are also becoming a serious concern and should be accounted for. Therefore, addressing platelet activation and release of mediators like furin as therapeutic target might be of clinical relevance to improve outcome of these patients.[32–35,50] Furthermore, it has been described that platelet activation and the amount of circulating platelet/leucocyte co-aggregates are associated with

the stability of CAD and can serve as reliable biomarkers during atheroprogression in cardiovascular disease.[51–54] In our cohort, we could not observe statistically significant differences in platelet activation and the amount of platelet/leukocyte co-aggregates between healthy controls and CAD-SARS-CoV-2^{negative} patients, while CAD-SARS-CoV-2^{positive} patients were characterized by significantly increased platelet activation and elevated numbers of platelet/leukocyte co-aggregates. As we analyzed a relatively small patient cohort this might explain why we did not detect statistically significant differences in platelet activation and amount of platelet/leukocyte co-aggregates between healthy controls and CAD-SARS-CoV-2^{negative} patients as described before.[51–54] On the contrary, we included patients with stable CAD that were on long-term antiplatelet therapy during their course of the disease. This aspect might also explain why there was no statistically significant difference between healthy controls and CAD-SARS-CoV-2^{negative} patients reflecting efficient antiplatelet treatment in this subgroup. Patients with acute coronary syndrome and myocardial infarction were explicitly excluded, while this subgroup has been investigated thoroughly in former studies and was also characterized by enhanced platelet activation and increased amount of platelet/leukocyte co-aggregates.[51–56]

An underlying cardiac disease is a major risk factor for unfavorable clinical outcome in COVID-19.[30,57,58] Platelet hyper-reactivity promotes development of acute coronary syndromes,[59] and COVID-19 has been described to be associated with myocardial injury and mortality.[60,61]

In line with previous findings, we found that 21.8% in CAD-SARS-CoV-2^{positive} patients showed a BMI ≥30 compared with 10.7% in the CAD-SARS-CoV-2negative group and 10.3 % in the healthy control group (Table 1; P=0.045). With this significant difference between the groups, BMI might be another confounding factor regarding outcome, in particular of the end point defined as respiratory failure. Recent studies have shown that obesity is a risk factor of unfavorable outcome and progressive respiratory failure. Obesity increases risk for hospitalization, ICU admission, requirement of invasive mechanical ventilation, and death among patients with COVID-19.[62–64]

A prothrombotic disease state has been recognized as critical factor in COVID-19.[5] Patients with SARS-CoV-2 infection are at increased risk for thrombosis (deep vein thrombosis and pulmonary embolism) and for multiple organ failure most likely due to microcirculatory arrest.[65,66] Recently, it has been shown that development of thrombocytopenia, elevated D-dimers and markers of systemic inflammation are of prognostic relevance in SARS-CoV-2-positive patients.[67,68] In our cohort, there were no significant differences between groups in their D-dimer levels upon admission (Table 1). This might be explained by the low patient number and by the time point when samples for D-dimer measurements were obtained. All blood samples were taken within 24 hours of hospital admission and, therefore, also correlated

our findings and presented baseline characteristics including laboratory parameters upon admission. There were no associations of D-dimer levels on admission and outcome. However, we did not correlate repeated D-dimer levels during the course of the disease and correlated these with the occurrence of the clinical outcome, which might ex-plain the observed difference. The impact of D-dimer has been discussed controversially and studies showed miscellaneous aspects and impacts of D-dimer. D-dimer was independently associated with incidence of critical illness, thrombosis, acute kidney injury, and all-cause mortality.[69] Another study showed that D-dimer levels could not predict thrombotic events.[70] Thus, levels of D-dimer may help to estimate the individual risk for an unfavorable course of the disease and to identify patients at risk. In regards to our findings, we have to take into account comorbidities and other clinical features in addition to D-dimer levels to estimate patients' prognosis. Therefore, the additive analysis of furin levels and platelet-derived furin can improve an intensified risk assessment of patients with COVID-19 regarding an unfavorable course of the disease depending on their furin levels as additional biomarker. Our findings implicate, that several biomarkers and clinical parameters should be taken into account, to identify patients at risk of an unfavorable course of the dis-ease, for example, furin.[69,70]

Patients with uncontrolled hyper-inflammation are at high risk to develop progressive respiratory failure, multiple organ failure, or of death.[4,71] In the present study, we evaluated whether changes of platelet activation occur in an early state of SARS-CoV-2 infection defined as time of hospital ad-mission. Beyond thrombosis, platelets are key mediators of inflammation and thrombo-immunity.[2] During pathogen infections, platelets release a variety of potent cytokines or chemokines[72,73] and interact with leukocytes as well as endothelial cells and propagate vascular and tissue inflamma-tion.[8,74] It is well known that virus infections are associated with thrombocytopenia, platelet hyper-reactivity, and formation of platelet/leukocyte co-aggregates leading to enhanced sequestration within the microcirculation.[75] In critically affected patients, nonsurvivors showed a trend towards a drop in platelet count and leukocytosis.[76] Recently, in critical COVID-19 ICU patients an enhanced platelet apoptosis has been described[77] and excessive platelet and neutrophil activation.[38,39] Our data confirm and extent the published findings and show that platelet activation not only is evident in progressive SARS-CoV-2 associated infection but substantially is present at an early disease stage as soon as SARS-CoV-2 infection was verified by reverse transcriptase polymerase chain reaction. Most strikingly, our study shows that platelet activation and $CD42b^{+}CD61^{+}$ platelet/leukocyte co-aggregates correlate with enhanced plasma levels of cytokine IL-6 and chemokines CCL2, CCL5, and CXCL10 which represent prominent markers of hyper-inflammation (Figure III in the Data Supplement). Platelet activation was also associated with enhanced pulmonary artery pressure and elevation of the cardiac injury marker troponin I indicating its linkage to myocardial stretch and subsequent myocardial necrosis in our patient

cohort. Further, $CD42b^{+}CD61^{+}$ platelet/leukocyte co-aggregates correlate with furin plasma levels, which in turn is associated with progression of respiratory failure and poor clinical prognosis (Figure 3B). Furin has been suggested to cleave the SARS-CoV-2 spike protein, a putative critical mechanism for syncytium formation and virus replica-tion.[18,19,78] Platelets contain significant amounts of furin.[50] We further showed that furin is re-leased from activated platelets implying that platelets are a major source of furin in the microenvironment of platelet activation (Figure 3F). Although we do not provide direct evidence that plate-let-derived furin is involved in SARS-CoV-2 activation, it is tempting to speculate that activated platelets promote vascular and tissue inflammation and might contribute to virus-induced cell fusion and replication. Limiting platelet release of furin by antithrombotic therapy early in the disease state may be a feasible and effective prevention for worse clinical outcome and thromboembolic events. This might be most relevant in patients with underlying cardiovascular diseases to prevent progression of CAD and threatening organ failure.

Furthermore, the thrombin-specific phenotype observed must be transmitted via the thrombin receptors PAR1 or PAR4 (Figure IV in the Data Supplement). The TRAP-6 did also induce a significant increase in furin, even though the effect is not as prominent as the Thrombin activation. This effect is, as expected, fully inhibited by the PAR-1 receptor inhibitor ML161, therefore, PAR1 is probably involved in furin activation. But this does not exclude PAR4 as additional pathway and the involvement of both receptors may explain the strong activation. By activation with thrombin or TRAP, more furin will be available especially free furin, which is responsible for the measured increase in enzyme activity. Some studies suggest that the dual receptor system PAR1 and PAR4 offers an intriguing possibility of pharmacologically fine-tuning thrombin signaling in platelets by taking ad-vantage of the individual contributions of PAR1 and PAR4, but with distinct kinetics. PAR1 is de-scribed to respond to much lower concentrations of thrombin than PAR4 suggesting that PAR4 might only be a backup thrombin receptor. Indeed, our results do match with this hypothesis. We did observe, that low concentration of thrombin (0.1 U/mL) stimulation could be partially inhibited by the PAR-1 inhibitor ML161 but not high concentration like 1 U/mL thrombin, which were unaffected by the inhibitor even at maximum concentrations. These results imply the involvement of the PAR4 signaling pathway upon strong thrombin activation. Blocking the sustained signaling from PAR4 may limit thrombosis, while leaving the transient PAR1 signaling mechanism available to initiate hemostasis and limit bleeding. The first in-class antiplatelet therapy targeting PAR1, vorapaxar, was approved by the Food and Drug Administration in 2014 for secondary prevention of thrombotic events in stable patients. Importantly, vorapaxar was approved for use in addition to the standard antiplatelet therapy, but not as a stand-alone therapy or as a substitute for aspirin or clopidogrel. Recent data support the hypothesis that blocking PAR4-mediated sustained signaling for stable thrombus formation, while preserving PAR1 signaling

for initial thrombus formation, may be a safe and effective antithrombotic strategy. Vorapaxar has not gained widespread clinically use. One issue is a difficult clinical management due to its pharmacokinetics and pharmacodynamics. The reversibility and elimination characteristics of the PAR4 inhibitor BMS-986120 may prove to be advantageous in this regard. PAR1 and PAR4 inhibition might regulate furin signaling and, therefore, serve as therapeutic targets among others. But larger studies focusing on underlying mechanisms and clinical relevance are needed to clarify these questions.[79–87]

Therefore, we investigated the prognostic impact of platelet activation, platelet-derived furin and furin plasma levels along with other established risk factors for unfavorable outcome of COVID-19. Blocking the activity of furin might reduce severity of viral infections and cardiovascular damage and could be beneficial for the treatment of both, SARS-CoV-2 infection and cardiovascular diseases.

Sources of Funding

This work was supported by the German Research Foundation (DFG)—Project number 374031971–TRR 240 and by the Ministry of Science, Research and the Arts of the State of Baden-Württemberg (COVID-19 funding). The funder had no role in study design, data collection, data analysis, data in-terpretation, or writing of the article.

Disclosures

None.

References

1. Gawaz M, Langer H, May AE. Platelets in inflammation and atherogenesis. J Clin Invest. 2005;115:3378–3384. doi: 10.1172/JCI27196 [PMC free article] [PubMed] [Google Scholar]

2. Koupenova M, Clancy L, Corkrey HA, Freedman JE. Circulating platelets as mediators of immunity, inflamma-tion, and thrombosis. Circ Res. 2018;122:337–351. doi: 10.1161/CIRCRESAHA.117.310795 [PMC free article] [PubMed] [Google Scholar]

3. Koupenova M, Corkrey HA, Vitseva O, Manni G, Pang CJ, Clancy L, Yao C, Rade J, Levy D, Wang JP, et al. . The role of platelets in mediating a response to human influenza infection. Nat Commun. 2019;10:1780. doi: 10.1038/s41467-019-09607-x [PMC free article] [PubMed] [Google Scholar]

4. Guzik TJ, Mohiddin SA, Dimarco A, Patel V, Savvatis K, Marelli-Berg FM, Madhur MS, Tomaszewski M, Maffia P, D'Acquisto F, et al. . COVID-19 and the cardiovascular system: implications for risk assessment, diagnosis, and treatment options. Cardiovasc Res. 2020;116:1666–1687. doi: 10.1093/cvr/cvaa106 [PMC free article] [Pub-Med] [Google Scholar]

5. Connors JM, Levy JH. COVID-19 and its implications for thrombosis and anticoagulation. Blood. 2020;135:2033–2040. doi: 10.1182/blood.2020006000 [PMC free article] [PubMed] [Google Scholar]

6. Zaid Y, Puhm F, Allaeys I, Naya A, Oudghiri M, Khalki L, Limami Y, Zaid N, Sadki K, El Haj RB, et al. . Platelets can associate with SARS-Cov-2 RNA and are hyperactivated in covid-19. Circ Res. 2020;127:1404–1418. doi: 10.1161/CIRCRESAHA.120.317703 [PMC free article] [PubMed] [Google Scholar]

7. Lê VB, Schneider JG, Boergeling Y, Berri F, Ducatez M, Guerin JL, Adrian I, Errazuriz-Cerda E, Frasquilho S, An-tunes L, et al. . Platelet activation and aggregation promote lung inflammation and influenza virus pathogenesis. Am J Respir Crit Care Med. 2015;191:804–819. doi: 10.1164/rccm.201406-1031OC [PubMed] [Google Scholar]

8. Dib PRB, Quirino-Teixeira AC, Merij LB, Pinheiro MBM, Rozini SV, Andrade FB, Hottz ED. Innate immune recep-tors in platelets and platelet-leukocyte interactions. J Leukoc Biol. 2020;108:1157–1182. doi: 10.1002/JLB.4MR0620-701R [PubMed] [Google Scholar]

9. Boilard E, Paré G, Rousseau M, Cloutier N, Dubuc I, Lévesque T, Borgeat P, Flamand L. Influenza virus H1N1 activates platelets through FcγRIIA signaling and thrombin generation. Blood. 2014;123:2854–2863. doi: 10.1182/blood-2013-07-515536 [PubMed] [Google Scholar]

10. Manne BK, Denorme F, Middleton EA, Portier I, Rowley JW, Stubben C, Petrey AC, Tolley ND, Guo L, Cody M, et al. . Platelet gene expression and function in patients with COVID-19. Blood. 2020;136:1317–1329. doi: 10.1182/blood.2020007214 [PMC free article] [PubMed] [Google Scholar]

11. Hottz ED, Azevedo-Quintanilha IG, Palhinha L, Teixeira L, Barreto EA, Pão CRR, Righy C, Franco S, Souza TML, Kurtz P, et al. . Platelet activation and platelet-monocyte aggregate formation trigger tissue factor expression in patients with severe COVID-19. Blood. 2020;136:1330–1341. doi: 10.1182/blood.2020007252 [PMC free arti-cle] [PubMed] [Google Scholar]

12. Clarke NE, Turner AJ. Angiotensin-converting enzyme 2: the first decade. Int J Hypertens. 2012;2012:307315. doi: 10.1155/2012/307315 [PMC free article] [PubMed] [Google Scholar]

13. Jarcho JA, Ingelfinger JR, Hamel MB, D'Agostino RB, Sr, Harrington DP. Inhibitors of the renin-angiotensin-aldosterone system and covid-19. N Engl J Med. 2020;382:2462–2464. doi: 10.1056/NEJMe2012924 [PMC free article] [PubMed] [Google Scholar]

14. Vaduganathan M, Vardeny O, Michel T, McMurray JJV, Pfeffer MA, Solomon SD. Renin-angiotensin-aldosterone system inhibitors in patients with covid-19. N Engl J Med. 2020;382:1653–1659. doi: 10.1056/NEJMsr2005760 [PMC free article] [PubMed] [Google Scholar]

15. Datta PK, Liu F, Fischer T, Rappaport J, Qin X. SARS-CoV-2 pandemic and research gaps: Understanding SARS-CoV-2 interaction with the ACE2 receptor and implications for therapy. Theranostics. 2020;10:7448–7464. doi: 10.7150/thno.48076 [PMC free article] [PubMed] [Google Scholar]

16. Abassi Z, Knaney Y, Karram T, Heyman SN. The lung macrophage in SARS-CoV-2 infection: a friend or a foe? Front Immunol. 2020;11:1312. doi: 10.3389/fimmu.2020.01312 [PMC free article] [PubMed] [Google Scholar]

17. Zhang S, Liu Y, Wang X, Yang L, Li H, Wang Y, Liu M, Zhao X, Xie Y, Yang Y, et al. . SARS-CoV-2 binds platelet ACE2 to enhance thrombosis in COVID-19. J Hematol Oncol. 2020;13:120. doi: 10.1186/s13045-020-00954-7 [PMC free article] [PubMed] [Google Scholar]

18. Coutard B, Valle C, de Lamballerie X, Canard B, Seidah NG, Decroly E. The spike glycoprotein of the new coronavirus 2019-nCoV contains a furin-like cleavage site absent in CoV of the same clade. Antiviral Res. 2020;176:104742. doi: 10.1016/j.antiviral.2020.104742 [PMC free article] [PubMed] [Google Scholar]

19. Hoffmann M, Kleine-Weber H, Schroeder S, Krüger N, Herrler T, Erichsen S, Schiergens TS, Herrler G, Wu NH, Nitsche A, et al. . SARS-CoV-2 cell entry depends on ACE2 and TMPRSS2 and is blocked by a clinically proven protease inhibitor. Cell. 2020;181:271–280.e8. doi: 10.1016/j.cell.2020.02.052 [PMC free article] [PubMed] [Google Scholar]

20. Walls AC, Park YJ, Tortorici MA, Wall A, McGuire AT, Veesler D. Structure, function, and antigenicity of the SARS-CoV-2 spike glycoprotein. Cell. 2020;181:281–292.e6. doi: 10.1016/j.cell.2020.02.058 [PMC free article] [PubMed] [Google Scholar]

21. Shang J, Wan Y, Luo C, Ye G, Geng Q, Auerbach A, Li F. Cell entry mechanisms of SARS-CoV-2. Proc Natl Acad Sci USA. 2020;117:11727–11734. doi: 10.1073/pnas.2003138117 [PMC free article] [PubMed] [Google Schol-ar]

22. Nakayama K. Furin: a mammalian subtilisin/Kex2p-like endoprotease involved in processing of a wide variety of precursor proteins. Biochem J. 1997;327(pt 3):625–635. doi: 10.1042/bj3270625 [PMC free article] [Pub-Med] [Google Scholar]

23. Wang YK, Tang JN, Han L, Liu XD, Shen YL, Zhang CY, Liu XB. Elevated FURIN levels in predicting mortality and cardiovascular events in patients with acute myocardial infarction. Metabolism. 2020;111:154323. doi: 10.1016/j.metabol.2020.154323 [PubMed] [Google Scholar]

24. Adu-Agyeiwaah Y, Grant MB, Obukhov AG. The potential role of osteopontin and furin in worsening disease outcomes in COVID-19 patients with pre-existing diabetes. Cells. 2020;9:E2528. doi: 10.3390/cells9112528 [PMC free article] [PubMed] [Google Scholar]

25. Yakala GK, Cabrera-Fuentes HA, Crespo-Avilan GE, Rattanasopa C, Burlacu A, George BL, Anand K, Mayan DC, Corlianò M, Hernández-Reséndiz S, et al. . FURIN inhibition reduces vascular remodeling and atherosclerotic lesion progression in mice. Arterioscler Thromb Vasc Biol. 2019;39:387–401. doi: 10.1161/ATVBAHA.118.311903 [PMC free article] [PubMed] [Google Scholar]

26. Zhao G, Yang W, Wu J, Chen B, Yang X, Chen J, McVey DG, Andreadi C, Gong P, Webb TR, et al. . Influence of a coronary artery disease-associated genetic variant on FURIN expression and effect of furin on macrophage be-havior. Arterioscler Thromb Vasc Biol. 2018;38:1837–1844. doi: 10.1161/ATVBAHA.118.311030 [PMC free article] [PubMed] [Google Scholar]

27. Yang X, Yang W, McVey DG, Zhao G, Hu J, Poston RN, Ren M, Willeit K, Coassin S, Willeit J, et al. . FURIN ex-pression in vascular endothelial cells is modulated by a coronary artery disease-associated genetic variant and influences monocyte transendothelial migration. J Am Heart Assoc. 2020;9:e014333. doi: 10.1161/JAHA.119.014333 [PMC free article] [PubMed] [Google Scholar]

28. Stawowy P, Kallisch H, Borges Pereira Stawowy N, Stibenz D, Veinot JP, Gräfe M, Seidah NG, Chrétien M, Fleck E, Graf K. Immunohistochemical localization of subtilisin/kexin-like proprotein convertases in human atheroscle-rosis. Virchows Arch. 2005;446:351–359. doi: 10.1007/s00428-004-1198-7 [PubMed] [Google Scholar]

29. Fernandez C, Rysä J, Almgren P, Nilsson J, Engström G, Orho-Melander M, Ruskoaho H, Melander O. Plasma levels of the proprotein convertase furin and incidence of diabetes and mortality. J Intern Med. 2018;284:377–387. doi: 10.1111/joim.12783 [PMC free article] [PubMed] [Google Scholar]

30. Rath D, Petersen-Uribe A, Avdiu A, Witzel K, Jaeger P, Zdanyte M, Heinzmann D, Tavlaki E, Muller K, Gawaz MP. Impaired cardiac function is associated with mortality in patients with acute covid-19 infection. Clin Res Cardiol. 2020;109:1491–1499. doi: 10.1007/s00392-020-01683-0 [PMC free article] [PubMed] [Google Schol-ar]

31. Zheng YY, Ma YT, Zhang JY, Xie X. COVID-19 and the cardiovascular system. Nat Rev Cardiol. 2020;17:259–260. doi: 10.1038/s41569-020-0360-5 [PMC free article] [PubMed] [Google Scholar]

32. Xie J, Tong Z, Guan X, Du B, Qiu H. Clinical characteristics of patients who died of coronavirus disease 2019 in China. JAMA Netw Open. 2020;3:e205619. doi: 10.1001/jamanetworkopen.2020.5619 [PMC free article] [PubMed] [Google Scholar]

33. Xiong TY, Redwood S, Prendergast B, Chen M. Coronaviruses and the cardiovascular system: acute and long-term implications. Eur Heart J. 2020;41:1798–1800. doi: 10.1093/eurheartj/ehaa231 [PMC free article] [Pub-Med] [Google Scholar]

34. Nishiga M, Wang DW, Han Y, Lewis DB, Wu JC. COVID-19 and cardiovascular disease: from basic mechanisms to clinical perspectives. Nat Rev Cardiol. 2020;17:543–558. doi: 10.1038/s41569-020-0413-9 [PMC free article] [PubMed] [Google Scholar]

35. European Society of Cardiology. Esc guidance for the Diagnosis and Management of CV Disease during the Covid-19 Pandemic. 2020. https://www.escardio.org/Education/COVID-19-and-Cardiology/ESCCOVID-19-Guidance. Accessed February 13, 2021

36. Li B, Yang J, Zhao F, Zhi L, Wang X, Liu L, Bi Z, Zhao Y. Prevalence and impact of cardiovascular metabolic dis-eases on COVID-19 in China. Clin Res Cardiol. 2020;109:531–538. doi: 10.1007/s00392-020-01626-9 [PMC free article] [PubMed] [Google Scholar]

37. Tang N, Bai H, Chen X, Gong J, Li D, Sun Z. Anticoagulant treatment is associated with decreased mortality in severe coronavirus disease 2019 patients with coagulopathy. J Thromb Haemost. 2020;18:1094–1099. doi: 10.1111/jth.14817 [PubMed] [Google Scholar]

38. Nicolai L, Leunig A, Brambs S, Kaiser R, Weinberger T, Weigand M, Muenchhoff M, Hellmuth JC, Ledderose S, Schulz H, et al. . Immunothrombotic dysregulation in COVID-19 pneumonia is associated with respiratory failure and coagulopathy. Circulation. 2020;142:1176–1189. doi: 10.1161/CIRCULATIONAHA.120.048488 [PMC free article] [PubMed] [Google Scholar]

39. Mueller KAL, Langnau C, Günter M, Pöschel S, Gekeler S, Petersen-Uribe Á, Kreisselmeier KP, Klingel K, Bösmüller H, Li B, et al. . Numbers and phenotype of non-classical CD14dimCD16+ monocytes are predictors of adverse clinical outcome in patients with coronary artery disease and severe SARS-CoV-2 infection. Cardiovasc Res. 2021;117:224–239. doi: 10.1093/cvr/cvaa328 [PMC free article] [PubMed] [Google Scholar]

40. Wirtz TH, Tillmann S, Strüßmann T, Kraemer S, Heemskerk JW, Grottke O, Gawaz M, von Hundelshausen P, Bernhagen J. Platelet-derived MIF: a novel platelet chemokine with distinct recruitment properties. Atheroscle-rosis. 2015;239:1–10. doi: 10.1016/j.atherosclerosis.2014.12.039 [PubMed] [Google Scholar]

41. Reinthaler M, Braune S, Lendlein A, Landmesser U, Jung F. Platelets and coronary artery disease: Interac-tions with the blood vessel wall and cardiovascular devices. Biointerphases. 2016;11:029702. doi: 10.1116/1.4953246 [PubMed] [Google Scholar]

42. Steele P, Battock D, Genton E. Effects of clofibrate and sulfinpyrazone on platelet survival time in coronary artery disease. Circulation. 1975;52:473–476. doi: 10.1161/01.cir.52.3.473 [PubMed] [Google Scholar]

43. Parasuraman S, Walker S, Loudon BL, Gollop ND, Wilson AM, Lowery C, Frenneaux MP. Assessment of pul-monary artery pressure by echocardiography-A comprehensive review. Int J Cardiol Heart Vasc. 2016;12:45–51. doi: 10.1016/j.ijcha.2016.05.011 [PMC free article] [PubMed] [Google Scholar]

44. Lang RM, Badano LP, Mor-Avi V, Afilalo J, Armstrong A, Ernande L, Flachskampf FA, Foster E, Goldstein SA, Kuznetsova T, et al. . Recommendations for cardiac chamber quantification by echocardiography in adults: an update from the American Society of Echocardiography and the European Association of Cardiovascular Imaging. Eur Heart J Cardiovasc Imaging. 2015;16:233–270. doi: 10.1093/ehjci/jev014 [PubMed] [Google Scholar]

45. Borst O, Schmidt EM, Münzer P, Schönberger T, Towhid ST, Elvers M, Leibrock C, Schmid E, Eylenstein A, Kuhl D, et al. . The serum- and glucocorticoid-inducible kinase 1 (SGK1) influences platelet calcium signaling and func-tion by regulation of Orai1 expression in megakaryocytes. Blood. 2012;119:251–261. doi: 10.1182/blood-2011-06-359976 [PubMed] [Google Scholar]

46. Bradford MM. A rapid and sensitive method for the quantitation of microgram quantities of protein utilizing the principle of protein-dye binding. Anal Biochem. 1976;72:248–254. doi: 10.1006/abio.1976.9999 [PubMed] [Google Scholar]

47. Ferguson TE, Reihill JA, Walker B, Hamilton RA, Martin SL. A selective irreversible inhibitor of furin does not prevent pseudomonas aeruginosa exotoxin A-induced airway epithelial cytotoxicity. PLoS One. 2016;11:e0159868. doi: 10.1371/journal.pone.0159868 [PMC free article] [PubMed] [Google Scholar]

48. Huygens C, Liénart S, Dedobbeleer O, Stockis J, Gauthy E, Coulie PG, Lucas S. Lysosomal-associated trans-membrane protein 4B (LAPTM4B) decreases transforming growth factor β1 (TGF-β1) production in human regu-latory T cells. J Biol Chem. 2015;290:20105–20116. doi: 10.1074/jbc.M115.655340 [PMC free article] [Pub-Med] [Google Scholar]

49. Massberg S, Brand K, Grüner S, Page S, Müller E, Müller I, Bergmeier W, Richter T, Lorenz M, Konrad I, et al. . A critical role of platelet adhesion in the initiation of atherosclerotic lesion formation. J Exp Med. 2002;196:887–896. doi: 10.1084/jem.20012044 [PMC free article] [PubMed] [Google Scholar]

50. Leblond J, Laprise MH, Gaudreau S, Grondin F, Kisiel W, Dubois CM. The serpin proteinase inhibitor 8: an endogenous furin inhibitor released from human platelets. Thromb Haemost. 2006;95:243–252. doi: 10.1160/TH05-08-0561 [PubMed] [Google Scholar]

51. Linden MD, Furman MI, Frelinger AL, 3rd, Fox ML, Barnard MR, Li Y, Przyklenk K, Michelson AD. Indices of platelet activation and the stability of coronary artery disease. J Thromb Haemost. 2007;5:761–765. doi: 10.1111/j.1538-7836.2007.02462.x [PubMed] [Google Scholar]

52. Allen N, Barrett TJ, Guo Y, Nardi M, Ramkhelawon B, Rockman CB, Hochman JS, Berger JS. Circulating mono-cyte-platelet aggregates are a robust marker of platelet activity in cardiovascular disease. Atherosclerosis. 2019;282:11–18. doi: 10.1016/j.atherosclerosis.2018.12.029 [PubMed] [Google Scholar]

53. Furman MI, Benoit SE, Barnard MR, Valeri CR, Borbone ML, Becker RC, Hechtman HB, Michelson AD. In-creased platelet reactivity and circulating monocyte-platelet aggregates in patients with stable coronary artery disease. J Am Coll Cardiol. 1998;31:352–358. doi: 10.1016/s0735-1097(97)00510-x [PubMed] [Google Scholar]

54. Brambilla M, Camera M, Colnago D, Marenzi G, De Metrio M, Giesen PL, Balduini A, Veglia F, Gertow K, Biglioli P, et al. . Tissue factor in patients with acute coronary syndromes: expression in platelets, leukocytes, and plate-let-leukocyte aggregates. Arterioscler Thromb Vasc Biol. 2008;28:947–953. doi: 10.1161/ATVBAHA.107.161471 [PubMed] [Google Scholar]

55. Ibrahim H, Kleiman NS. Platelet pathophysiology, pharmacology, and function in coronary artery disease. Coron Artery Dis. 2017;28:614–623. doi: 10.1097/MCA.0000000000000519 [PubMed] [Google Scholar]

56. Malakar AK, Choudhury D, Halder B, Paul P, Uddin A, Chakraborty S. A review on coronary artery disease, its risk factors, and therapeutics. J Cell Physiol. 2019;234:16812–16823. doi: 10.1002/jcp.28350 [PubMed] [Google Scholar]

57. Clerkin KJ, Fried JA, Raikhelkar J, Sayer G, Griffin JM, Masoumi A, Jain SS, Burkhoff D, Kumaraiah D, Rabbani L, et al. . COVID-19 and cardiovascular disease. Circulation. 2020;141:1648–1655. doi: 10.1161/CIRCULATIONAHA.120.046941 [PubMed] [Google Scholar]

58. Inciardi RM, Adamo M, Lupi L, Metra M. Atrial fibrillation in the COVID-19 era: simple bystander or marker of increased risk? Eur Heart J. 2020;41:3094. doi: 10.1093/eurheartj/ehaa576 [PMC free article] [PubMed] [Google Scholar]

59. Martin JF, Kristensen SD, Mathur A, Grove EL, Choudry FA. The causal role of megakaryocyte–platelet hyper-activity in acute coronary syndromes. Nat Rev Cardiol. 2012;9:658–670. doi: 10.1038/nrcardio.2012.131 [Pub-Med] [Google Scholar]

60. Bonow RO, O'Gara PT, Yancy CW. Cardiology and COVID-19. JAMA. 2020;324:1131–1132. doi: 10.1001/jama.2020.15088 [PubMed] [Google Scholar]

61. Guo T, Fan Y, Chen M, Wu X, Zhang L, He T, Wang H, Wan J, Wang X, Lu Z. Cardiovascular implications of fatal outcomes of patients with coronavirus disease 2019 (COVID-19). JAMA Cardiol. 2020;5:811–818. doi: 10.1001/jamacardio.2020.1017 [PMC free article] [PubMed] [Google Scholar]

62. Huang Y, Lu Y, Huang YM, Wang M, Ling W, Sui Y, Zhao HL. Obesity in patients with COVID-19: a systematic review and meta-analysis. Metabolism. 2020;113:154378. doi: 10.1016/j.metabol.2020.154378 [PMC free arti-cle] [PubMed] [Google Scholar]

63. Soeroto AY, Soetedjo NN, Purwiga A, Santoso P, Kulsum ID, Suryadinata H, Ferdian F. Effect of increased BMI and obesity on the outcome of COVID-19 adult patients: a systematic review and meta-analysis. Diabetes Metab Syndr. 2020;14:1897–1904. doi: 10.1016/j.dsx.2020.09.029 [PMC free article] [PubMed] [Google Scholar]

64. Tamara A, Tahapary DL. Obesity as a predictor for a poor prognosis of COVID-19: a systematic review. Diabe-tes Metab Syndr. 2020;14:655–659. doi: 10.1016/j.dsx.2020.05.020 [PMC free article] [PubMed] [Google Scholar]

65. Lax SF, Skok K, Zechner P, Kessler HH, Kaufmann N, Koelblinger C, Vander K, Bargfrieder U, Trauner M. Pul-monary arterial thrombosis in COVID-19 with fatal outcome: results from a prospective, single-center, clinico-pathologic case series. Ann Intern Med. 2020;173:350–361. doi: 10.7326/M20-2566 [PMC free article] [Pub-Med] [Google Scholar]

66. Poissy J, Goutay J, Caplan M, Parmentier E, Duburcq T, Lassalle F, Jeanpierre E, Rauch A, Labreuche J, Susen SLille ICU Haemostasis COVID-19 Group. Pulmonary embolism in patients with COVID-19: awareness of an in-creased prevalence. Circulation. 2020;142:184–186. doi: 10.1161/CIRCULATIONAHA.120.047430 [PubMed] [Google Scholar]

67. Gu SX, Tyagi T, Jain K, Gu VW, Lee SH, Hwa JM, Kwan JM, Krause DS, Lee AI, Halene S, et al. . Thrombocytopa-thy and endotheliopathy: crucial contributors to COVID-19 thromboinflammation. Nat Rev Cardiol. 2021;18:194–209. doi: 10.1038/s41569-020-00469-1 [PMC free article] [PubMed] [Google Scholar]

68. Levi M, Thachil J, Iba T, Levy JH. Coagulation abnormalities and thrombosis in patients with COVID-19. Lancet Haematol. 2020;7:e438–e440. doi: 10.1016/S2352-3026(20)30145-9 [PMC free article] [PubMed] [Google Scholar]

69. Berger JS, Kunichoff D, Adhikari S, Ahuja T, Amoroso N, Aphinyanaphongs Y, Cao M, Goldenberg R, Hinden-burg A, Horowitz J, et al. . Prevalence and outcomes of D-dimer elevation in hospitalized patients with COVID-19. Arterioscler Thromb Vasc Biol. 2020;40:2539–2547. doi: 10.1161/ATVBAHA.120.314872 [PMC free article] [PubMed] [Google Scholar]

70. Elbadawi A, Elgendy IY, Sahai A, Bhandari R, McCarthy M, Gomes M, Bishop GJ, Bartholomew JR, Kapadia S, Cameron SJ. Incidence and outcomes of thrombotic events in symptomatic patients with COVID-19. Arterioscler Thromb Vasc Biol. 2021;41:545–547. doi: 10.1161/ATVBAHA.120.315304 [PMC free article] [PubMed] [Google Scholar]

71. Jose RJ, Manuel A. COVID-19 cytokine storm: the interplay between inflammation and coagulation. Lancet Respir Med. 2020;8:e46–e47. doi: 10.1016/S2213-2600(20)30216-2 [PMC free article] [PubMed] [Google Scholar]

72. Yeaman MR. Platelets in defense against bacterial pathogens. Cell Mol Life Sci. 2010;67:525–544. doi: 10.1007/s00018-009-0210-4 [PMC free article] [PubMed] [Google Scholar]

73. Maouia A, Rebetz J, Kapur R, Semple JW. The immune nature of platelets revisited. Transfus Med Rev. 2020;34:209–220. doi: 10.1016/j.tmrv.2020.09.005 [PMC free article] [PubMed] [Google Scholar]

74. Li C, Li J, Ni H. Crosstalk between platelets and microbial pathogens. Front Immunol. 2020;11:1962. doi: 10.3389/fimmu.2020.01962 [PMC free article] [PubMed] [Google Scholar]

75. Rapkiewicz AV, Mai X, Carsons SE, Pittaluga S, Kleiner DE, Berger JS, Thomas S, Adler NM, Charytan DM, Gasmi B, et al. . Megakaryocytes and platelet-fibrin thrombi characterize multi-organ thrombosis at autopsy in COVID-19: a case series. EClinicalMedicine. 2020;24:100434. doi: 10.1016/j.eclinm.2020.100434 [PMC free article] [PubMed] [Google Scholar]

76. Rondina MT, Tatsumi K, Bastarache JA, Mackman N. Microvesicle tissue factor activity and interleukin-8 levels are associated with mortality in patients with influenza A/H1N1 infection. Crit Care Med. 2016;44:e574–e578. doi: 10.1097/CCM.0000000000001584 [PMC free article] [PubMed] [Google Scholar]

77. Althaus K, Marini I, Zlamal J, Pelzl L, Haeberle H, Mehrlaender M, Hammer S, Schulze H, Bitzer M, Malek N, et al. . Severe covid-19 infection is associated with increased antibody-1 mediated platelet apoptosis. Blood. 2021. doi: 10.1101/2020.09.03.20187286 [Google Scholar]

78. Cheng YW, Chao TL, Li CL, Chiu MF, Kao HC, Wang SH, Pang YH, Lin CH, Tsai YM, Lee WH, et al. . Furin inhibi-tors block SARS-CoV-2 spike protein cleavage to suppress virus production and cytopathic effects. Cell Rep. 2020;33:108254. doi: 10.1016/j.celrep.2020.108254 [PMC free article] [PubMed] [Google Scholar]

79. Hasan A, Paray BA, Hussain A, Qadir FA, Attar F, Aziz FM, Sharifi M, Derakhshankhah H, Rasti B, Mehrabi M, et al. . A review on the cleavage priming of the spike protein on coronavirus by angiotensin-

converting enzyme-2 and furin. J Biomol Struct Dyn. 2021;39:3025–3033. doi: 10.1080/07391102.2020.1754293 [PMC free article] [PubMed] [Google Scholar]

80. Thomas G. Furin at the cutting edge: from protein traffic to embryogenesis and disease. Nat Rev Mol Cell Biol. 2002;3:753–766. doi: 10.1038/nrm934 [PMC free article] [PubMed] [Google Scholar]

81. Schoergenhofer C, Schwameis M, Gelbenegger G, Buchtele N, Thaler B, Mussbacher M, Schabbauer G, Wojta J, Jilma-Stohlawetz P, Jilma B. Inhibition of protease-activated receptor (PAR1) reduces activation of the endo-thelium, coagulation, fibrinolysis and inflammation during human endotoxemia. Thromb Haemost. 2018;118:1176–1184. doi: 10.1055/s-0038-1655767 [PubMed] [Google Scholar]

82. Cheng JW. Impact of selective platelet inhibition in reducing cardiovascular risk - role of vorapaxar. Vasc Health Risk Manag. 2016;12:263–268. doi: 10.2147/VHRM.S81342 [PMC free article] [PubMed] [Google Schol-ar]

83. Han X, Nieman MT. PAR4 (Protease-Activated Receptor 4): PARticularly important 4 antiplatelet therapy. Arterioscler Thromb Vasc Biol. 2018;38:287–289. doi: 10.1161/ATVBAHA.117.310550 [PMC free article] [Pub-Med] [Google Scholar]

84. Li S, Tarlac V, Hamilton JR. Using PAR4 inhibition as an anti-thrombotic approach: why, how, and when? Int J Mol Sci. 2019;20:E5629. doi: 10.3390/ijms20225629 [PMC free article] [PubMed] [Google Scholar]

85. Rovai ES, Alves T, Holzhausen M. Protease-activated receptor 1 as a potential therapeutic target for covid-19. Exp Biol Med (Maywood). 2021;246:688–694. doi: 10.1177/1535370220978372 [PMC free article] [PubMed] [Google Scholar]

86. Hosokawa K, Ohnishi T, Miura N, Sameshima H, Koide T, Tanaka KA, Maruyama I. Antithrombotic effects of PAR1 and PAR4 antagonists evaluated under flow and static conditions. Thromb Res. 2014;133:66–72. doi: 10.1016/j.thromres.2013.10.037 [PubMed] [Google Scholar]

87. Wu CC, Huang SW, Hwang TL, Kuo SC, Lee FY, Teng CM. YD-3, a novel inhibitor of protease-induced platelet activation. Br J Pharmacol. 2000;130:1289–1296. doi: 10.1038/sj.bjp.0703437 [PMC free article] [PubMed] [Google Scholar]

Supplementary Material

Major Resources Table

In order to allow validation and replication of experiments, all essential research materials listed in the Methods should be included in the Major Resources Table below. Authors are encouraged to use public repositories for protocols, data, code, and other materials and provide persistent identifiers and/or links to repositories when available. Authors may add or delete rows as needed.

Animals (in vivo studies)

Species	Vendor or Source	Background Strain	Sex	Persistent ID / URL
N/A				

Genetically Modified Animals

	Species	Vendor or Source	Background Strain	Other Information	Persistent ID / URL
Parent - Male	N/A				
Parent - Female	N/A				

Antibodies

Target antigen	Vendor or Source	Catalog #	Working concentration	Lot # (preferred but not required)	Persistent ID / URL
CD41 Pacific Blue (clone HIP8)	BioLegend	303714	Dilution of 1:50		https://www.biolegend.com/en-us/products/pacific-blue-anti-human-cd41-antibody-6994
CD42b PerCP-Cy5.5 (clone HIP1)	BioLegend	303918	Dilution of 1:20		https://www.biolegend.com/en-us/products/percp-cyanine5-5-anti-human-cd42b-antibody-13187
CD62P PE-Cy7 (clone AK4)	BioLegend	304922	Dilution of 1:100		https://www.biolegend.com/en-us/products/pe-cyanine7-anti-human-cd62p-p-selectin-antibody-13066
CD61 FITC (clone VI-PL2)	BioLegend	336404	Dilution of 1:50		https://www.biolegend.com/en-us/products/fitc-anti-human-cd61-antibody-5338
CD31 BV711 (clone WM59)	BioLegend	303136	Dilution of 1:80		https://www.biolegend.com/en-us/products/brilliant-violet-711-anti-human-cd31-antibody-14948
Zombie NIR	BioLegend	423106	Dilution of 1:500		https://www.biolegend.com/en-us/products/zombie-nir-fixable-viability-kit-8657
CD14 FITC (clone M5E2)	BioLegend	301804	Dilution of 1:80		https://www.biolegend.com/en-us/products/fitc-anti-human-cd14-antibody-794
Furin AF488 (clone 222722)	R&D Systems	IC1503G-100UG	Dilution of 1:20		https://www.rndsystems.com/products/human-furin-alexa-fluor-488-conjugated-antibody-222722_ic1503g
AF568 secondary antibody	invitrogen	A-11061	5 µg/ml		https://www.thermofisher.com/antibody/product/Rabbit-anti-Mouse-IgG-H-L-Cross-Adsorbed-Secondary-Antibody-Polyclonal/A-11061
IgG_{2B} antibody (clone 20116)	R&D Systems	MAB004	1 µg/ml		https://www.rndsystems.com/products/mouse-igg2b-isotype-control_mab004
CD62P PE (clone CLBThromb/6)	Beckman-Coulter	IM1759U	Dilution of 1:10		https://www.beckman.de/reagents/coulter-flow-cytometry/antibodies-and-kits/single-color-antibodies/cd62p/im1759u

DNA/cDNA Clones

Clone Name	Sequence	Source / Repository	Persistent ID / URL
N/A			

Cultured Cells

Name	Vendor or Source	Sex (F, M, or unknown)	Persistent ID / URL
N/A			

Data & Code Availability

Description	Source / Repository	Persistent ID / URL
N/A		

Other

Description	Source / Repository	Persistent ID / URL
N/A		

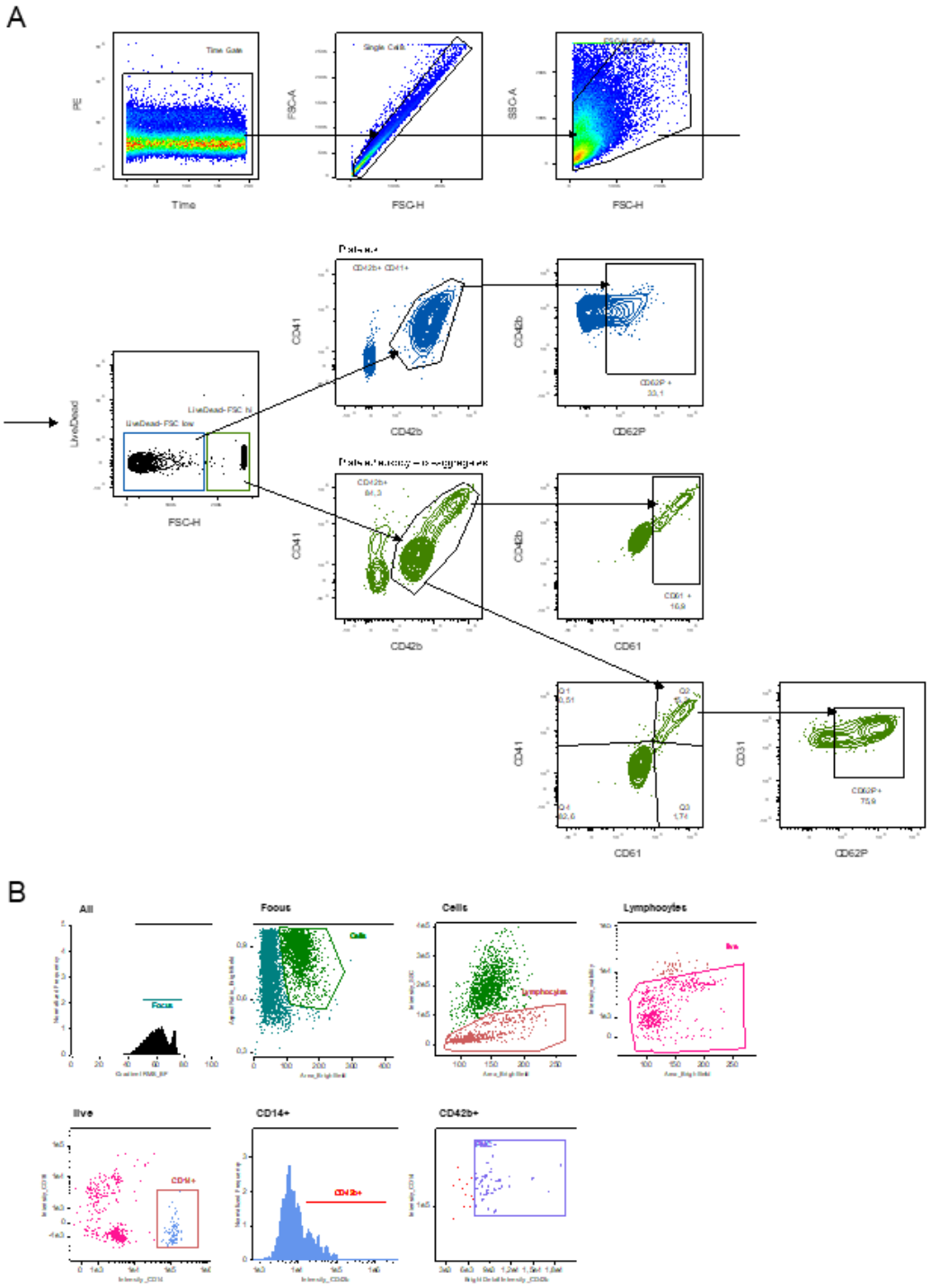

Supplementary Figure I: Gating strategy of human platelets and platelet/leukocyte co-aggregates. (**A**) One representative gating strategy of human platelets and platelet/leukocyte co-aggregates is shown. Platelets were stained and measured by flow cytometry analysis in whole blood of CAD-SARS-CoV-2^{negative} patients (n=28), CAD-SARS-CoV-2^{positive} patients (n=55) and healthy controls (n=39). All samples were gated as follows: time/ singlets/ platelets/ live FSC-low or FSC-High. Platelets (blue plots) were gated as follows: FSC-low/CD41^{+}CD42b^{+}. Platelet/leukocyte co-aggregates (green plots) were gated as follows: FSC-high/ CD42b^{+}/CD61^{+} and for highly activated CD42b^{+} platelet/leukocyte co-aggregates expression of CD41^{+}CD61^{+}CD62P^{+} was measured. For gating of positive cell populations for each marker, fluorescence minus one (FMOs) were used. FlowJo software 10.6.2 (Treestar) was used for compensation and analysis of measured data. (**B**) Platelets/leukocyte co-aggregates were stained and measured by Imaging flow cytometry in whole blood of a CAD-SARS-

CoV-2^{negative} patient. Platelet/leukocyte co-aggregates were gated as follows: focus/ cells/ lymphocytes/ live/ CD14^{+}/ CD42b^{+}/ platelet-monocyte-complex (PMC). The last gating step for platelet-monocyte complexes (PMC) describes gating on cells only with high CD14^{+} and CD42b^{+} intensity to exclude unspecific background signal. Data were analyzed using IDAS software 6.2.

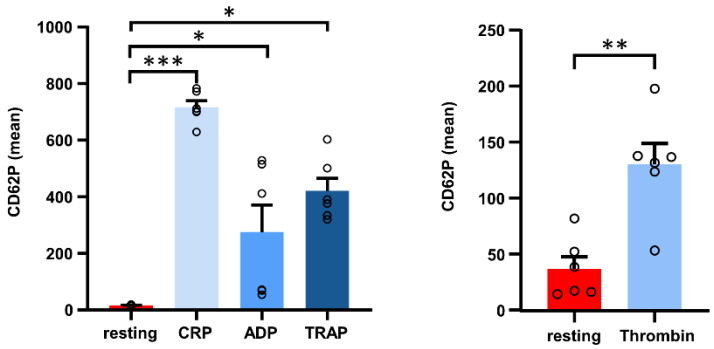

Supplementary Figure II: Surface CD62P expression on platelets upon activation. Graphical presentation of CD62P sur-face expression on platelets measured by flow cytometry upon activation with CRP, ADP, TRAP (n=6); Plotted: Mean ± SEM; * p ≤ 0.05, ** p ≤ 0.01, *** p ≤ 0.001.

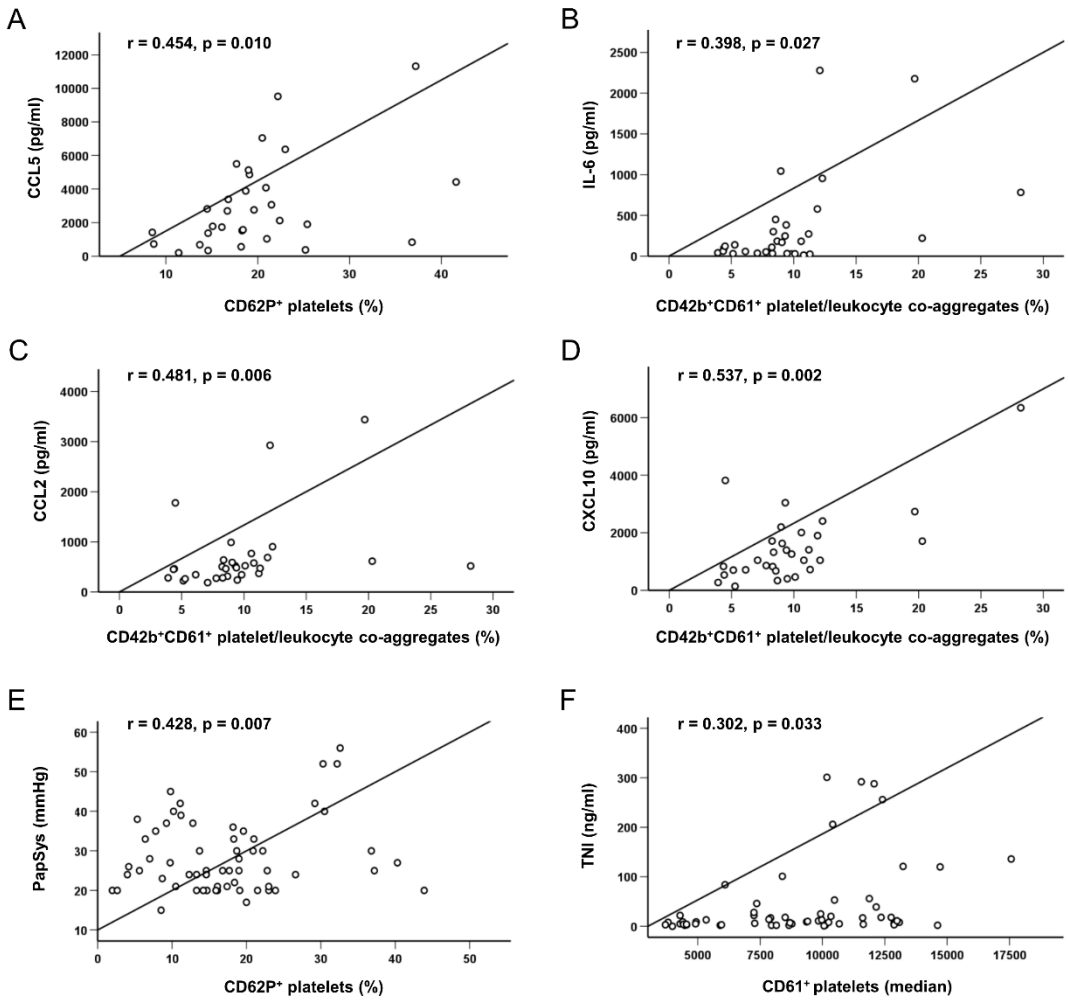

Supplementary Figure III: Platelet activation and the amount of platelet/leukocyte co-aggregates correlate with inflammatory plasma markers and clinical parameters. Pearson's correlation was performed to evaluate correlations between activation of platelets and platelet/leukocyte co-aggregates

and measured furin and inflammatory cytokine markers. Following correlations were performed: (A) Positive correlation between activation (CD62P+) of platelets and CCL5 (pg/ml) (r=0.454, p-value=0.010), (B) Positive correlation between CD42b+CD61+ platelet/leukocyte co- aggregates (%) and IL-6 (pg/ml) (r=0.398, p-value=0.027), (C) Positive correlation between CD42b+CD61+ platelet/leukocyte co-aggregates (%) and CCL2 (pg/ml) (r=0.481, p-value=0.006), (D) Positive correlation between CD42b+CD61+ plate-let/leukocyte co-aggregates (%) and CXCL10 (ng/ml) (r=0.537, p-value=0.002), (E) Positive correlation between activation (CD62P+) of platelets and pulmonary artery pressure PapSys (mmHg) (r=0.428, p- value=0.007) and (F) CD61 (medi-an) on platelets and Troponin I TNI (ng/ml) (r=0.302, p-value=0.033). (A-F) Statistics: Pearson's correlation coefficient r, ns = not significant, * p-value ≤ 0.050, ** p-value ≤ 0.010.

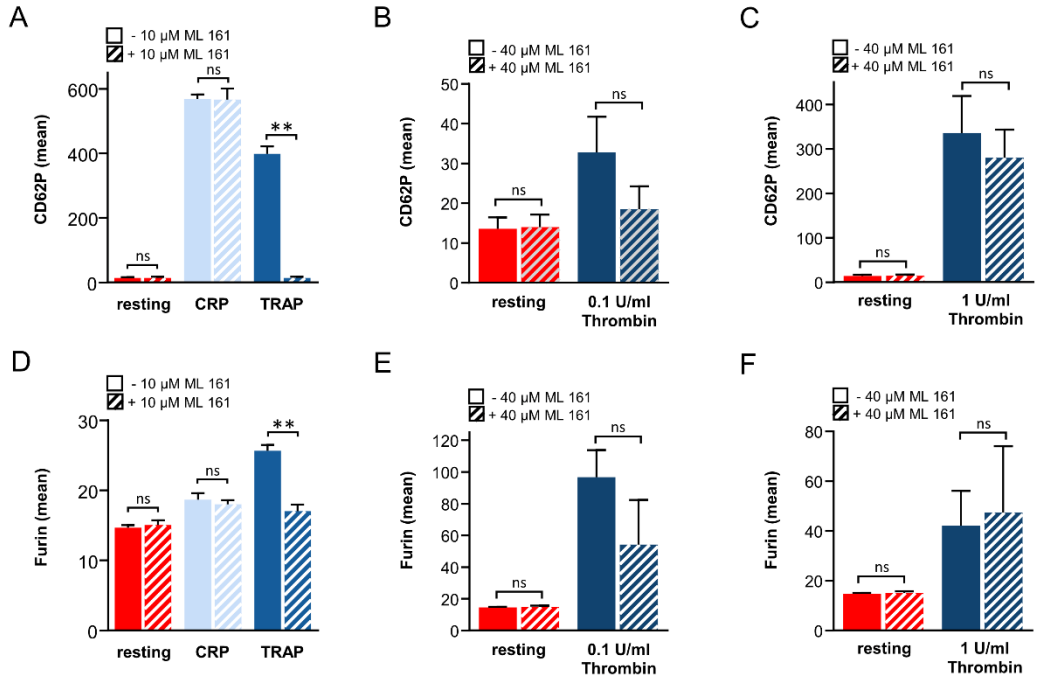

Supplementary Figure IV: TRAP induced furin expression can be inhibited by the PAR-1 inhibitor ML 161, whereas Thrombin activation cannot be suppressed by ML161. (A-C) For comparison of CD62P surface expression between differently activated platelets with or w/o PAR-1 inhibitor ML161 at indicated concentrations (n=3), graphs display mean fluorescence intensity of CD62P. Plotted: Mean ± SD; Statistics: one-way ANOVA (Dunnett), ns = not significant, ** p-value ≤ 0.010. (D-F) For comparison of furin surface expression between differently activated platelets with or w/o PAR-1 inhibitor ML161 at indicated concentrations (n=3), graphs display mean fluorescence intensity of furin. Plotted: Mean ± SD; Statistics: one-way ANOVA (Dunnett), ns = not significant, ** p-value≤ 0.010.

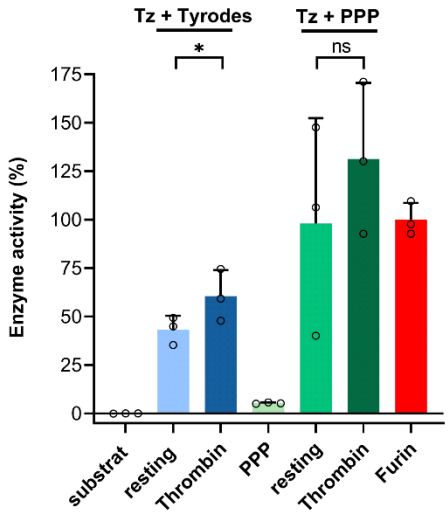

Supplementary Figure V: Furin enzyme activity assay performed with 1 x 109 washed platelets diluted in HEPES-Tyrodes (pH 7.4) compared to platelet poor plasma (PPP). Thrombin was used at 1 U/ml, (n=3). Plotted: Mean ± SD. Statistic one-way ANOVA; n.s. = not significant; * p-value ≤ 0.050

Macrophage migration inhibitory factor (MIF) promotes local and systemic thrombo-inflammation in fast progressive aortic stenosis and predicts unfavorable outcome (*in revision*)

Running title: Thromboinflammation in progressive aortic stenosis

Karin Anne Lydia Mueller[1*], MD, Carolin Langnau[1], Tobias Harm[1], Manuel Sigle[1], Michal Droppa[1], MD, Madeleine Ilg[1], Anne-Katrin Rohlfing[1], PhD, Sarah Gekeler[1], Bo Li[1], MD, Manina Günter[2,3], Nora Goebel[4], MD, Ulrich F.W. Franke[4], MD, Medhat Radwan[5], MD, Christian Schlensak[5], MD, Nura Susann Rashed[1], Henrik Janning[1], Zeanub Khan[1], Dominik Rath[1], MD, Klaus-Peter Kreisselmeier[1], MD, Tatsiana Castor[1], PhD, Iris Irmgard Mueller[1], MD, Stella E. Autenrieth[2,3#], PhD, Meinrad Paul Gawaz[1#], MD

[1]University Hospital Tuebingen, Department of Cardiology and Angiology, Eberhard Karls University Tuebingen, Tuebingen, Germany

[2]University Hospital Tuebingen, Department of Hematology, Oncology, Clinical Immunology and Rheumatology, Eberhard Karls University Tuebingen, Tuebingen, Germany

[3]Dendritic Cells in Infection and Cancer, German Cancer Research Center (DKFZ), Heidelberg, Germany

[4]Robert-Bosch Hospital, Department of Cardiovascular Surgery, Stuttgart, Germany

[5]University Hospital Tuebingen, Department of Thoracic and Cardiovascular Surgery, Eberhard Karls University Tuebingen, Tuebingen, Germany

[#]contributed equally

*Corresponding author:

Karin Anne Lydia Mueller, MD

Department of Cardiology and Angiology

University Hospital of the Eberhard Karls University Tuebingen

Otfried-Mueller-Str.10, 72076 Tuebingen, Germany

Tel: +49-7071-29-83688

Fax: +49-7071-29-5749

E-mail: k.mueller@med.uni-tuebingen.de

Abstract

Background: Aortic stenosis (AS) is driven by progressive inflammatory and fibro-calcific processes regulated by circulating inflammatory and valve resident endothelial (VEC) and interstitial cells (VIC). The impact of platelets, platelet-derived mediators, and platelet monocyte interactions on the acceleration of local valvular inflammation and mineralization is presently unknown.

Methods: We prospectively enrolled 475 consecutive patients with severe symptomatic AS undergoing aortic valve (AV) replacement. Patients were stratified into slow (SP-) and fast progressive (FP-) AS by repetitive echocardiography. Cardiac workup included echocardiography, blood sampling for laboratory parameters, chemokine profiling, and phenotyping of platelets and monocytes as well as collection of explanted valve tissue for further analysis of protein and gene expression.

Results: Macroscopic and immuno-histological analysis of AVs revealed substantially enhanced infiltrating inflammatory cells and platelet accumulation predominantly in the lamina fibrosa on the aortic side ($p<0.001$) with less calcification in FP-AS compared to SP-AS ($p<0.0001$). Furthermore, pro-inflammatory macrophage inhibitory factor (MIF)-associated gene expression was significantly enhanced in FP-AS. Tissue expression of MIF correlated with tissue infiltration of macrophages, monocytes, and platelets ($p<0.05$). This was accompanied by significantly elevated MIF plasma levels ($p<0.05$) and increased platelet activation in FP-AS ($p<0.05$) with decreased intracellular MIF expression indicating an enhanced MIF release upon platelet activation ($p<0.0001$). Moreover, intracellular MIF expression was increased in intermediate and non-classical monocytes in patients with FPcompared to SP-AS ($p<0.05$) and correlated with the degree of platelet activation ($p<0.0001$) and inversely with MIF expression in platelets ($p<0.001$). In-depth phenotyping uncovered disease-specific changes in platelet and monocyte marker profiles in FP- and SP-AS ($p<0.05$). Finally, linear regression analysis confirmed that plasma and cell-based MIF markers are strongly associated with FP-AS. Thus, patients with FP-AS are characterized by significant alterations of systemic MIF expression comprising plasma, circulating platelets and monocytes which can be linked to accelerated inflammation of AV tissue in FP-AS.

Conclusions: Our findings suggest a key role for the platelet-derived mediator MIF and its interplay with circulating and valve resident monocytes/macrophages in local and systemic thrombo-inflammation associated with fast progression of AS. “MIF-biomarkers” in peripheral blood may help to identify patients at risk for fast progressive disease.

Abbreviations

AS – aortic stenosis; AVA – aortic valve area; BMI – body mass index; BMP-2 – bone morphogenic protein 2; DAVD - degenerative aortic valve disease; CAD - coronary artery disease; CI – confidence interval; CRP – C-reactive protein; EP – clinical endpoint; FP – fast progressive; GP – glycoprotein; HR – hazard ratio; hsTNI – high sensitive troponin I; IL - interleukin; IQR – interquartile range; LV – left ventricle, MIF – macrophage migration inhibitory factor; PAPsys – pulmonary artery pressure; RNA – ribonucleic acid; Runx2 – run-related transcription factor 2; TGF-ß1 – transforming growth factor ß1; SD – standard deviation; SP – slow progressive; UMAP – uniform manifold approximation and projection; VECs – valve resident endothelial cells; VICs – valve interstitial cells; Wnt – wingless and Int-1; w/o – without

Introduction

Aortic stenosis (AS) is the most prevalent heart valve pathology worldwide, especially in the aging population, and is associated with a poor prognosis once symptoms occur.[1] AS is defined as a progressive disease with increasing hemodynamic severity over time. Accelerating inflammation, fibrotic and calcific remodeling, thickening, and finally osteogenic formation of the aortic valve (AV) cusps leads to valve obstruction[2, 3] followed by surgical or transcatheter AV replacement.[4, 5] No pharmacotherapy has been established to prevent the development and progression of degenerative aortic valve disease (DAVD) resulting in AS, however, clinical trials targeting inflammatory and calcium metabolic pathways are ongoing.[6-8] Thus, none of the suggested therapeutic strategies addresses early stages of DAVD and AS to inhibit acceleration of inflammatory, fibrotic, and, finally, osteogenic formation and thereby improve prognosis and shift AV replacement to the latest time point possible. Therefore, the development of pharmacological treatment strategies targeting early regulatory mechanisms of inflammation and fibrosis within the valve tissue still is an unmet clinical need to delay DAVD and AS progression.

Presumed underlying cellular and molecular pathophysiology is complex and comprises mechanical stress, endothelial damage, dysfunction of valvular endothelial cells (VEC) followed by lipid accumulation, and differentiation of myofibroblasts and valvular interstitial cell (VIC) to calcifying phenotypes.[1, 2, 6] Furthermore, circulating immune cells are activated and subsequently infiltrate valve tissue and accelerate myofibroblastic and osteoblastic differentiation of valve resident cells thereby advancing tissue calcification.[6, 9, 10] The differentiation of VICs into myofibroblastic and osteoblastic phenotypes is a pivotal step during the propagation phase of AS and seems to be regulated by cytokines/chemokines and extracellular vesicles that are secreted by platelets and immune cells like monocytes/macrophages.[11] However, it is unclear whether, similar as described in atherosclerosis, the underlying pathophysiology of AS may also be triggered by interactions of platelets and immune cells like monocytes / macrophages[10, 12, 13] and which inflammatory mediators are responsible for disease acceleration in AS. The clinical course of AS is highly variable regarding its progression 110 over time, its hemodynamic relevance and the presentation of symptoms.[14, 15] Several recent studies have defined the clinical progress of AS by its echocardiographic parameters and their change during disease progression. To distinguish between fast and slow progressive AS, the change of the peak velocity over the AV (ΔVmax) or the decrease of the aortic valve area (AVA) within one year has been proposed.[14-19] However, the underlying mechanisms triggering fast disease progression remain unclear and patients at risk for fast progression are not well defined.[4, 5, 20] Thus, we hypothesized that changes in platelet activity, platelet-derived mediators and platelet monocyte

interactions during systemic thrombo-inflammation in AS are of prognostic relevance for an accelerated course of the disease leading to fast progression as defined by repetitive echocardiography. In the present study we found in a large cohort of patients that significant changes in platelet activation, platelet/leukocyte co-aggregation and plasma levels of cytokines and chemokines occur in association with local disease progression. We identified the plasma level of MIF released from activated platelets as critical prognostic factor for patients at risk for fast progressive AS. Targeting release of platelet-derived MIF may be a potential strategy to interfere in the course of the disease progression and to decelerate inflammatory, fibro-calcific and osteogenic processes.

Methods

Detailed descriptions of study design, patient cohort (supplemental Figure S1-S2), blood sampling, valvular tissue procurement, multicolor flow cytometry (supplemental Figure S3-S8), chemokine profiling, RNA gene expression analysis by Nanostring technology, morphological analysis by computed tomography scans (supplemental Figure S9), and statistical analysis (supplemental Figure S10) are provided as Supplemental Data. In brief, we prospectively enrolled 475 consecutive patients with severe symptomatic (NYHA class ≥ 2) AS with indication for AV repair. The design of the patient cohort is shown in supplemental Figure S1. All patients underwent clinical and cardiac examination including repetitive echocardiography, electrocardiography, assessment of medical history at baseline, concomitant medication, comorbidities, and blood sampling for routine laboratory parameters, marker expression on platelets and monocytes, as well as chemokine profiling. Tissue samples of explanted AVs were obtained from patients who underwent surgical valve replacement and were analyzed by histology, immunohistochemistry, and gene expression analysis using Nanostring technology. Echocardiographic assessment of AS and standard measurements were performed in all patients according to the European Association of Echocardiography/American Society of Echocardiography (EAE/ASE) guidelines.[4, 5] Furthermore, we defined two subgroups of patients with symptomatic AS regarding fast and slow disease progression by repetitive transthoracic echocardiographic assessment in a retrospective analysis of our digital echocardiographic database. Here, we determined the rate of disease progression by the change of the maximum transvalvular flow velocity (ΔVmax) over time and established an annualized progression rate ΔVmax as described before.[4, 5, 16-18] The median annualized ΔVmax was used as cut-off and thereby two subgroups of patients were evident with either FP-AS (ΔVmax ≥ 0.45 m/s/year) or SP-AS (ΔVmax < 0.45 m/s/year) until onset of severe symptoms occurred that warranted surgical valve replacement (supplemental Figure S2).18

Results

Clinical characteristics and valve pathology of patients with slow and fast progressive aortic stenosis reveal significant differences between both groups

Progression of AS is highly variable in affected patients. However, the underlying mechanisms remain unclear and patients at risk for fast progression are not well defined.[18, 27] To get a deeper insight into the pathophysiological mechanisms of fast (FP-) and slow progressive (SP-) AS, we prospectively studied a large consecutive cohort of 475 patients which were admitted to our hospital for symptomatic severe AS with indication for surgical valve replacement (Table 1). We identified the two subgroups of patients by repetitive transthoracic echocardiographic assessment and symptom duration as described in the supplemental method sectiondata (Supplemental Figure S2). Hereby, 237 (49.9 %) patients were classified as FP-AS, while 238 (50.1 %) were categorized as SP-AS by the median ΔVmax < 0.45 m/s/year. Patients with FP-AS were younger (SP-AS versus (vs) FP-AS; median, interquartile range (IQR); 79 (71 - 83) vs 76 (69 – 81), p<0.001), had a slightly lower risk score defined by the Society of Thoracic Surgeons (STS)[4, 5] (p=0.021), and showed a lower incidence of atrial fibrillation (p=0.012). Transvalvular flow velocity indicated by the mean and peak pressure gradient (Pmean, Pmax), the aortic valve area (AVA), and the stroke volume was similar in both groups (Table 1). There were no statistical differences between both groups regarding gender, body mass index (BMI), NYHA classification, cardiovascular comorbidities or comedication at time of valve replacement (Table 1). In a subgroup of n=134 patients computed tomography (CT) scan of the aortic valve and the aorta was performed before valve replacement. However, CT scans did neither reveal significant morphological differences regarding the degree of valve calcification nor regarding distribution patterns of calcified areas within the AV between FP-AS and SP-AS (supplemental Figure S9).

Assessment of gross pathology of the explanted valves revealed a significant higher calcification grade of AV cusps in SP-AS compared to FP-AS (SP-AS vs FP-AS; %; median, IQR; 0.62 (0.56-0.71) vs 182 0.48 (0.36-0.54), p<0.0001) (Figure 1A). The degree of macroscopic calcification did not correlate with the echocardiographic parameters Pmean or AVA, while age was significantly associated with calcification area in gross pathology of AV tissue (p=0.0045) (Figure 1B). Interestingly, histological analysis showed that collagen content (visualized by pentachrome staining) of AV tissue from FP-AS was significantly increased (SP-AS vs FP-AS; mm2; median, IQR; 16.91 (7.36-27.54) vs 33.66 (21.24-55.2), p<0.0001) (Figure 1C lower panel). In contrast, mineralization (depicted by van Kossa staining in histology) of the AV was significantly enhanced in SP-AS vs FP-AS (SP-AS vs FP-AS; mm2; median, IQR; 33.74 (27.82-41.86) vs 20.54 (13.52-33.41), p<0.0001) (Figure 1C upper panel). We performed additional analysis of lipid accumulation in a subgroup of n=64 patients (n=32 with FP-AS and n=32 with SP-AS) by using the RedOil staining technique (Figure 1D). Lipid accumulation

assessed by RedOil staining was not different between both groups (Figure 1D). Further immunohistochemical assessment of AV tissue showed that cellularity was significantly increased in FP-AS (SP-AS vs FP-AS; n; median, IQR; 247 (142.3-504) vs 717.5 (360.5-1234), p<0.0001) (Figure 1E) suggesting an extravasation and infiltration of immune cells into AV tissue. Immunostaining also revealed a remarkably higher tissue content of $CD16^+$ monocytes (SP-AS vs FP-AS; cells/mm2; median, IQR; 1 (0-6) vs 10 (2-12), p<0.0001) and $CD68^+$ macrophages (SP-AS vs FP-AS; cells/mm2, median, IQR; 51 (32-76.25) vs 128.5 (75-147.8), p<0.0001) in explanted valves derived from patients with FP-AS (Figure 1E). Most strikingly, platelet accumulation ($CD42b^+$ area) was significantly enhanced in FP-AS (SP-AS vs FP-AS; mm2; median, IQR; 0.78 (0-1.54) vs 1.7 (0.77-2.66), p<0.0001) (Figure 1E). Topical analysis revealed that platelet and cellular infiltration occurs predominantly on the aortic (lamina fibrosa) and substantially less on the ventricular side (lamina ventricularis) of the AV of FP-AS (cellularity aortal: SP-AS vs FP-AS; n; median, IQR; 111 (77-133) vs 183 (135.8-258.5), p=0.0005; cellularity ventricular: SP-AS vs FP-AS; n; median, IQR; 23 (18-27) vs 76 (52.25-93.5), p<0.0001; $CD42b^+$ area aortal: SP208 AS vs FP-AS; mm2; median, IQR; 0.07 (0.02-0.12) vs 1.33 (0.92-1.7), p<0.0001; $CD42b^+$ area ventricular: SP-AS vs FP-AS; mm2; median, IQR; 0.02 (0-0.03) vs 0.09 (0-0.24), p=0.1105) (Figure 1F). Histological and immunohistochemical 210 results indicate that FP-AS valve tissue is characterized by substantially enhanced infiltration of inflammatory cells and platelets as well as less calcification compared to SP-AS.

Characterization of local tissue inflammation in explanted aortic valves of patients with fast and slow progressive aortic stenosis shows significant differences between both patient groups

To further assess inflammation of explanted valves of patients with FP-AS and SP-AS, we performed gene expression analysis of 594 predefined genes using the nCounter Human Immunology v2 Panel by NanoString technology (supplemental Table I). Ribonucleic acid (RNA) profiling was evaluated after total RNA extraction from formalin-fixed paraffin embedded valve tissues (Supplemental Methods). Hierarchical cluster analysis of the top 50 differentially expressed genes showed significantly different RNA expression levels in valve tissue derived from FP- and SP-AS patients (Figure 2A). Among 594 tested genes, 23 genes, mainly inflammatory genes, were significantly upregulated (p<0.05), whereas two genes were downregulated in the AVs of FP-AS compared to SP-AS patients (p<0.05) as shown by scatter as well as volcano plot (Figure 2B-C). The most prominently downregulated gene expression signals involved key regulators of the toll-like receptor/inflammasome pathway (transforming growth factor-ß1 (TGF-ß1) and MAP kinase activated protein kinase 2 (MAPKAPK2)), while pro-inflammatory and/or apoptotic signaling, e.g. mediated by NF-κB or MIF is upregulated in

FP-AS (Figure 2B-C). Furthermore, heatmap analysis with row-wise comparisons of Nanostring® data28 disclosed remarkable differences in the TGF-ß1- and MIF-dependent pathways between the two patient groups (Figure 2). Compared to AV tissue derived from SP-AS patients MIF-associated gene expression was significantly enhanced in FP-AS (Figure 2D). In contrast, TGF-ß1- associated gene regulation was a prominent feature in SP-AS (Figure 2D). Pathway enrichment analysis (KEGG pathways) of the up-regulated genes in FP-AS valve tissue identified the protein translation-related categories “complement and coagulation cascade”, “toll-like receptor signaling”, “Th17 cell 237 differentiation”, and “B cell receptor signaling pathway” (Figure 2E).

A term-gene-graph highlights subnetworks and significantly differently regulated genes and the referring KEGG pathway in FP-AS (Figure 2F). To further highlight the importance of MIF regulated signaling in patients with FP-AS, MIF was added to the network analysis displaying its interactions with significantly enriched GeneOntology pathways ($p<0.01$) (Figure 2F). This observation is further substantiated by immunohistochemistry of AV tissue on protein expression level. MIF immunostaining is significantly enhanced in AV of FP-AS (Figure 2G). Interestingly, not only the overall MIF expression of valve resident cells of FP-AS patients was enhanced (SP-AS vs FP-AS; cells/mm2; median, IQR; 30 (24.75-36.25) vs 37 (29-50.75), $p<0.0001$), but most prominent MIF expression was detected in cells of the lamina fibrosa on the aortal side of the AV cusps (MIF expression, aortal: SP-AS vs FP-AS; cells/mm2; median, IQR; 13 (7-21) vs 23.5 (20.25-32), $p=0.0058$; MIF expression, ventricular: SP-AS vs FP-AS; cells/mm2; median, IQR; 1 (0-7) vs 1.5 (0-7), $p=0.7483$) (Figure 2G+H). However, TGF-ß1 expression signals were remarkably lower in FP-AS (SP-AS vs FP-AS; mm2; median, IQR; 3 (2-3) vs 2 (1-3), $p<0.0001$) (Figure 2G). Furthermore, tissue expression of MIF correlated with tissue cell infiltration of macrophages ($CD68^+$; $r=0.1445$, $p=0.0330$), monocytes ($CD16^+$, $r=0.1751$, $p=0.0096$), and platelets ($CD42b^+$, $r=0.2684$, $p<0.0001$) (Figure 2I). Thus, our results imply that MIF and its related pathways are a predominant regulator of local valve tissue inflammation in patients with FP-AS.

Characterization of systemic thrombo-inflammation in patients with slow and fast progressive aortic stenosis identifies disease-related phenotypes

Next, we asked whether the assessment of systemic inflammation allows to discriminate AS progression and whether it is associated with the degree of local valve inflammation. We did not find any associations between established markers of inflammation like leukocyte count or levels of C-reactive protein and progression of AS (Table 1). To further characterize systemic inflammation in AS, we performed chemokine profiling and analyzed an inflammation panel of 26 chemokines/cytokines. 264 MIF plasma levels were significantly elevated in FP-AS (SP-AS vs FP-AS; MIF: pg/mL; mean ± standard error of the mean (SEM); 6877±379.1 vs 9959±749.1,

p=0.0003; SP-AS vs FP-AS) (Figure 3A). Further, levels of interleukin (IL)-12p70 were reduced by trend in FP-AS (SP-AS vs FP-AS; pg/mL; mean ± SEM; 2.675±0.7134 vs 1.008±0.4442, p=0.0572) (Figure 3A), whereas the other tested mediators, e.g. IL-6, IL-1ß or TNF, showed similar plasma levels in both groups.

Platelets and platelet-derived mediators play a critical role in inflammation.29 Multi-color flow cytometry analysis performing classical manual gating revealed that although the numbers of circulating platelets (defined as FSClowCD42b+ cells, gating see supplemental Figure S4A) were similar in FP-AS and SP-AS patients (Figure 3B), their activation status was significantly increased in FP-AS demonstrated by platelet CD62P+ expression (SP-AS vs FP-AS; CD62P; %; median, IQR; 16.8 (11.58-23.8) vs 20.55 (12.48-32.28), p=0.0045), CD41 expression (SP-AS vs FP-AS; CD41; median, IQR; 3159 (1432-5816) vs 3949 (2567-5843), p=0.0304), and CD31 expression (SP-AS vs FP-AS; CD31; median, IQR; 4087 (2918-5515 vs 5147 (3349-6733), p=0.0006) (Figure 3B). In contrast, MIF expression in platelets was significantly decreased in FP-AS indicating an enhanced release reaction of MIF due to increased platelet activation in patients with FP-AS (SP-AS vs FP-AS; MIF; %; median, IQR; 4.85 (1.48-9.75) vs 2.3 (0.78-5.9), p<0.0001) (Figure 3B).

In addition to this manual gating strategy, we performed unsupervised data analysis by first applying uniform manifold approximation and projection (UMAP) dimension reduction to group phenotypically similar events (supplemental Figure S4)25 followed by unsupervised clustering analysis using PhenoGraph26 which uncovered distinct changes in platelet marker profiles in FP- and SP-AS (Figure 3C). PhenoGraph analysis resolved 42 clusters (P01- P42), of which seven showed significant differences between SP-AS and FP-AS patients (Figure 3C-D, supplemental Figure S8). We confirmed the finding obtained by manual gating strategy by clustered heatmap analysis of the clusters acquired by PhenopGraph clustering. Clusters P35, P03, P06, and P38 of platelets expressing either high or even increased amounts of intracellular MIF 291 in SP-AS patients were more abundant in SP-AS compared to FP-AS patients (p<0.05) (Figure 3D). In contrast, cluster 24 showing increased expression of CD62P and CD31 and less intracellular CXCL12 was more abundant in FP-AS than in SP-AS patients.

As high infiltration of monocytes and macrophages was observed in immunohistochemistry staining of AVs from FP-AS compared to SP-AS patients, we addressed the differences in abundancy and immunophenotype of circulating monocyte subsets in this patient cohort to link local and systemic inflammation regulated by monocytes and macrophages. Similar numbers of white blood cells (SP-AS vs FP-AS; WBCs; median, IQR; $5.2x10^6$ ($4.2x10^6$- $6.43x10^6$) vs $5.5x10^6$ ($4.5x10^6$-$6.5x10^6$), p=0.1667) as well as circulating classical ($CD14^+CD16^-$; SP-AS vs FP-AS; median, IQR; $3.1x10^5$ ($2.2x10^5$-$4.1x10^5$) vs $3.2x10^5$ ($2.3x10^5$-$4.2x10^5$), p=0.9089), intermediate ($CD14^+CD16^+$,SP-AS vs FP-AS; median, IQR; $4.6x10^4$ ($2.9x10^4$-$6.6.x10^4$) vs

$5.2x10^4$ ($3.1x10^4$-$7.7x10^4$), p=0.0717) and non-classical monocytes ($CD14^{dim}CD16^+$,SP-AS vs FP-AS; median, IQR; $2.5x10^4$ ($1.5x10^4$-$4.1x10^4$) vs $2.6x10^4$ ($1.4x10^4$-$4.1x10^4$), p=0.9751) were observed in both patient groups (Figure 4A, gating see supplemental Figure S3). Intracellular MIF expression was highest in classical and intermediate monocytes (Figure 4B), while not all monocytes regardless their subtype showed a high MIF content (supplemental Figure S5). In particular, intracellular MIF expression was increased most prominently in intermediate (SP-AS vs FP-AS; MIF; median, IQR; 12396 (10076-16051) vs 13419 (10718-19324), p=0.0186) and non-classical monocytes (SP-AS vs FP-AS; MIF; median, IQR; 7488 (5593-10185) vs 8601 (6180-12053), p=0.0073) in patients with FP- compared to SP-AS ($p<0.05$) (Figure 4B). MIF expression in monocyte subtypes correlated with the degree of platelet activation indicated by CD62P expression ($CD62P^+$ platelets and $MIF^+CD14^+CD16^+$: r=0.2533, $p<0.0001$; $CD62P^+$ platelets and $MIF^+CD14^{dim}CD16^+$: r=0.2660, $p<0.0001$) and inversely with MIF expression in platelets (MIF^+ platelets and $MIF^+CD14^+CD16^+$: r=-0.2098, p=0.0003; MIF^+ platelets and $MIF^+CD14^{dim}CD16^+$: r=-0.2831, $p<0.0001$) (Figure 4C). Thus, changes of plasma and intracellular MIF levels (monocytes, platelets) are associated with FP-AS.

To gain insight into 319 monocyte activation patterns in both, FP- and SP-AS, we also used a comprehensive high-dimensional flow cytometric activation marker panel and performed unsupervised data analysis on pre-gated total monocytes using UMAP and PhenoGraph algorithms as described above (Figure 4D-E, supplemental Figures S5-S7). We obtained 35 clusters (MT1-35), of which five showed significant differences between SP-AS and FP-AS (Figure 4D). Clustered heatmap analysis of these five clusters revealed distinct activation states (CD11b, CD62L, HLA-DR) and expression of MIF, CXCL12, CXCL14, and their receptors CXCR4 and CXCR7 ($p<0.05$) (Figure 4E). The MT30 cluster is significantly reduced in FP-AS patients showing a clear difference in MIF but also CXCR4 expression (Figure 4E). In summary, we found substantial differences in systemic inflammation markers in monocytes between the two groups of AS with prominent changes in MIF-associated markers.

Plasma and cell-associated levels of MIF are significantly related to findings of local aortic valve tissue inflammation and predict progression of aortic stenosis

MIF plays a critical role in monocyte function and regulation, and platelets are an important source of MIF, which is therefore central for platelet-monocyte interactions.[30-32] AV tissue derived from patients with FP-AS is characterized by enhanced infiltration of $CD16^+$ monocytes and $CD68^+$ macrophages as well as platelet accumulation. We hypothesized that changes of plasma and/or cell-associated MIF (MIF in platelets and monocytes) levels might reflect the degree of local valvular inflammation and the amount of infiltrating immune cells. We performed extensive correlation analysis of important clinical factors and thrombo-inflammation-related parameters in patients with FP- and SP-AS. Correlation coefficient Spearman´s ρ is given in

the correlation matrix, color, color intensity and size are plotted proportional to correlation coefficients (Figure 5A). We found that plasma levels of MIF correlate significantly with AV tissue cell infiltration and collagen content ($p<0.001$) (Figure 5B). Furthermore, platelet-MIF correlates inversely with monocyte and platelet tissue accumulation, while it also correlates positively with calcification area ($p<0.05$) (Figure 5B). Thus, patients with FP-AS are characterized by significant 346 alterations of “systemic” MIF expression comprising plasma and circulating platelets and monocytes, implying that this cytokine plays a critical role in accelerated valvular inflammation and thereby disease progression of AS. A chord diagram (Figure 5C) shows the synopsis of significant MIF- associated gene expression, markers of local valve inflammation and systemic immunophenotypes of circulating platelets and monocytes in patients with FP-AS and SP-AS. Significant ($p<0.05$) changes of clinical parameters and ex vivo data, as well as differentially expressed gene pathways between patients with FP-AS (blue) and SP-AS (orange) were presented and colored according to their assay. Strikingly, patients with FP-AS share elevated MIF levels and MIF-regulated pathways, whereas TGF-ß1 is a prominent regulating factor in patients with SP-AS (Figure 5C). In conclusion, the chord diagram links local protein and gene expression within the AV to systemic MIF- and TGF-ß1-related mediators and clinical features pointing out that MIF-regulated pathways are of great importance in FP-AS. Next, we asked, whether MIF plasma levels and platelet MIF are of prognostic value for the prediction of FP-AS independent from potential demographic, clinical, or functional cofounders. In a step-wise linear regression analysis, we found that plasma and cell-based MIF markers summarized as “liquid biopsy” is strongly associated with FP-AS, independent of cardiovascular comorbidities and valvular function parameters as depicted in Table 2. “Liquid biopsy” remained significantly associated with FP-AS in all models shown ($p<0.05$). Furthermore, multivariate Cox regression analysis identifies plasma levels of MIF and MIF expression in platelets summarized as markers of “liquid biopsy” and age as independent predictors of FP-AS among all risk factors tested (liquid biopsy: hazard ratio (HR) 0.366; 95% confidence interval (CI) 0.157–0.855, $p=0.020$; age: HR 0.88; 95% CI 0.82–0.95, $p<0.001$) (Table 3). Additionally, we also tested for possible confounding effects of cardiovascular risk factors (diabetes mellitus type 2, smoking status, arterial hypertension, hyperlipidemia), comedication (P2Y12 inhibitors), and comorbidities (heart failure defined by NYHA class, symptomatic coronary artery disease, chronic kidney disease, atrial fibrillation) on the progression rate of AS. Here, we confirmed that none of the tested clinical parameters showed a significant influence on the progression rate of AS (supplemental Figure S10).

Discussion

The underlying pathophysiological mechanisms of AS are only incompletely understood as described in various studies before.5, 16 Therefore, we hypothesized that changes in platelet activity, platelet-derived mediators and platelet-monocyte interactions during systemic thrombo-inflammation are of prognostic relevance for an accelerated course of the disease leading to FP-AS. Here, we present data showing that: i) patients with FP-AS reveal an inflammatory phenotype of the affected AV which significantly differ from a calcifying, pro-osteogenic valve pathology in patients with SP-AS. ii) MIF-related pathways are predominantly regulated in valvular tissue of FP-AS patients. iii) platelet activity along with plasma and cell-based markers of systemic inflammation are associated with local valvular inflammation and allow to discriminate an “accelerated inflammatory” and a “calcifying” pathological valvular phenotype. iv) peripheral MIF-based biomarkers (“liquid biopsy” comprising high MIF plasma levels and lower MIF expression in platelets) may be useful to predict FP-AS and are independent from demographic, clinical, and functional confounders. Our findings imply that targeting MIF secretion and/or MIF regulated processes pharmacologically may be a future treatment option to delay/prevent progression of DAVD and AS.

To date a “watch-and-wait” strategy is generally performed in all patients with AS irrespective of disease progression rate.[2, 4, 5] The development of an effective prevention strategy of AS is an unmet need in modern patient care.[6]

We found that platelets substantially accumulate within AVs derived from individuals with FP-AS. Presence of local platelet accumulation is associated with enhanced tissue inflammation and activation of circulating platelets. The infiltration of immune cells and the differentiation of VICs into myofibroblastic and osteoblastic phenotypes is a pivotal step during the development of DAVD and is regulated by cytokines and extracellular vesicles that are secreted by platelets and immune cells.[11] These intercellular communications are potential key players to regulate cellular functions during DAVD and might influence phenotypic switching of VICs and VECs resulting in accelerated disease progression.[1, 6]

Our findings extent the current knowledge as we demonstrate that local platelet accumulation is associated with an inflammatory valvular phenotype that shows enhanced numbers of infiltrating macrophages and monocytes. This suggests that platelet and immune cells, both might influence the differentiation of VICs and VECs leading finally to fibrosis and calcification. Platelet-triggered local inflammation might be another key component in the complex mechanisms of DAVD. We suggest an important impact of platelet activation and secretion not only locally but also in systemic thrombo-inflammation during the course of DAVD. Platelets have been well recognized to play a critical role in inflammation and atherogenesis[10, 12, 33] but also seem to regulate important processes in AS. Our findings are in line with other studies that describe a platelet mediated osteogenic differentiation of AS10 and add a deeper insight

in platelet-regulated processes along with its associations with disease progression.Besides hemostasis and thrombosis platelets are critical in vascular inflammation (thrombo-inflammation)33 Various mediators are involved in platelet-endothelial cell interaction. In mice, early inhibition of platelet adhesion results in attenuation of inflammation of the aortic root and reduces atheroprogression.[12, 33] Inhibition of platelet adhesion attenuates vascular inflammation and plaque formation[33] in humans and in animal models. For example, inhibition of platelet aggregation via glycoprotein (GP) Ibα profoundly reduced leukocyte accumulation and attenuated atherosclerotic lesion formation of aortic sinus/cusps in ApoE$^{-/-}$ mice[33] suggesting an important role in local inflammation/calcification. These findings establish platelets as major players in the initiation of pro-inflammatory and atherogenic processes in line with our findings. Furthermore, platelet activation occurs in AS as a result of shear stress.[10] Upon adhesion platelets are activated and secrete a variety of inflammatory mediators including chemokines/cytokines that boost vascular inflammation.[34-36] In this context, we also found that significant changes in platelet activation and plasma levels of cytokines/chemokines occur in association with AS progression. Our study highlights that the presence of platelets within the AV tissue is associated with enhanced local inflammation and activation of circulating platelets. As platelet-triggered inflammation might be one of the most important underlying mechanisms in the genesis and progression of AS, further studies are needed to get a deeper insight in platelet-mediated pathways.

In addition to platelets, inflammatory cells like monocytes/macrophages secrete cytokines and chemokines, which may cause further invasion of inflammatory cells leading to lipid accumulation, local inflammation and formation of fibrotic and calcifying nodules.[35-39] Because of the monocyte and macrophage “continuum” of subtypes shown by our findings of significantly altered clusters in unsupervised PhenoGraph analysis, so far established hypothesis of three monocyte subsets and just two classical pro-inflammatory and anti-inflammatory (M1 and M2) types of macrophages seems to be obsolete. This group of immune cells seems to comprise far more subsets which might be disease-related and might be of importance to better understand inflammatory regulations and mineral uptake capacity of osteoclast-like cells derived from specific subsets in cardiovascular disease, especially AS.[1, 6, 12, 13] Specific platelet and monocyte phenotypes can not only help to identify patients with DAVD that are at risk for fast progression but may also be addressed by novel anti-inflammatory therapeutic strategies in the future. Therefore, anti-inflammatory strategies should be further investigated in larger clinical studies.

Most interestingly, in the present study we found that MIF expression by circulating platelets is reduced in FP-AS and is associated with enhanced MIF expression in circulating intermediate and non-classical monocytes. MIF is a cytokine that has broad effects on the inflammatory

response and the immune system signals via CXCR2/4 and CD74 thereby initiating, among others, inflammatory cell recruitment and pro-inflammatory gene expression.**32** Moreover, MIF plays a pivotal role in atherogenesis and atheroprogression as deficiency of MIF reduces atherogenesis in LDLR-/- mice.[40] Our study is the first to show that MIF might be of great importance in the regulatory processes of local and systemic thrombo inflammation during AS. Platelets are a major source of MIF and other pro-inflammatory cytokines/chemokines that are released upon activation.[32, 36] Our present findings imply that circulating platelets in fast progressive AS degranulate (CD62P expression), release MIF, and interact with circulating monocytes. In the murine system MIF promotes migration of classical Ly6C^{high} monocytes, which are the corresponding classical CD14^{+} monocyte subtypes in the human system.[41] Further studies are needed to dissect the direct interaction of platelets with the various monocyte subsets e.g. by using a more advanced flow cytometry panel addressing platelet/monocyte interactions.

We also identified the plasma levels of MIF released from activated platelets as critical prognostic factor for patients at risk for fast progressive AS. Thus, inhibition of platelet degranulation or direct inhibition of MIF through antagonists may be a possible pharmacological strategy to modulate accelerated local valve inflammation and thereby, progression of AS. Additionally, MIF is involved in cardiovascular disease and linked to atheroprogression[38, 42] and a very recent publication shows that MIF plasma levels are associated with all-cause mortality and cardiovascular events in patients with acute myocardial infarction.[43] MIF antagonists have been developed preclinically and attenuate atherosclerosis.[44] Another interesting mediator is the bone morphogenetic protein antagonist Gremlin-1 which has been shown to inhibit MIF-related monocyte function and attenuates atherosclerotic plaque growth in ApoE$^{-/-}$ mice.[38, 45] Thus, early recognition of inflammatory phenotypes of DAVD by MIF-related biomarkers may offer a treatment option to decelerate disease progression before irreversible calcification of the aortic valve occurs. Given the prominent role of immune cells and possibly platelets in all stages of DAVD and AS, an elegant way to inhibit local inflammation and fibro-calcific remodeling would be to specifically target platelet-monocyte interactions or macrophages responsible for the differentiation of immune cells and valve resident cells to pro-inflammatory and osteogenic phenotypes.

Current anti-inflammatory strategies in cardiovascular diseases have been shown to be effective at least in CAD. Our data suggest that modulating inflammatory processes that are regulated by a critical inflammatory mediator, MIF, may be promising in prevention of accelerating AS. According to our results MIF levels are associated with valve inflammation and the inhibition of this cytokine-like mediator may have a significant impact on valve inflammation.[45]

At present, several preclinical and clinical compounds are available to modulate the function of MIF in vitro and in vivo.[46-49] One promising compound might be the phosphodiesterase-(PDE)4-inhibitor ibudilast which has a high allosteric anti-MIF activity. Ibudilast has potent anti-inflammatory activity 48 and inhibits platelet aggregation48. Thus, addressing a trigger event of inflammation in the early course of accelerated AS might be a novel and promising strategy.

Furthermore, several previous studies have investigated possible clinical confounders which might be associated with an accelerated progression of AS like diabetes mellitus type 2, CAD, hyperlipidemia or, chronic kidney disease.[4, 5, 15, 16, 18, 19, 50] In our analysis, there were no patients included that underwent hemodialysis for renal failure before aortic valve replacement. We have tested possible clinical confounders in association with disease progression extensively and found no association with progression of AS. However, MIF plasma levels and MIF expression in platelets remained associated with fast progression of AS indicating that these parameters might serve as additional novel biomarkers to identify patients at risk. However, further clinical studies are needed to evaluate the diagnostic impact of this “MIF-based liquid biopsy” in early and in progressive stages of AS. Here, the underlying signaling pathways mediated by MIF should also be further characterized in mild and moderate AS regarding its role in triggering an “accelerated inflammatory” valvular phenotype compared to a “calcifying” phenotype.

In conclusion, our study is the first to show that patients with FP-AS show an enhanced platelet- and monocyte mediated systemic inflammatory response, enhanced plasma levels of MIF, and an accelerated local inflammation within the aortic valve tissue.

Acknowledgments

None

Sources of Funding

This work was supported by the German Research Foundation (DFG) – Project number 374031971–TRR 240 and by the Ministry of Science, Research and the Arts of the State of Baden-Württemberg (COVID-19 Funding). The funder had no role in study design, data collection, data analysis, data interpretation, or writing of the manuscript.

Disclosures

None

References

1. Pawade TA, Newby DE and Dweck MR. Calcification in Aortic Stenosis: The Skeleton Key. J Am Coll Cardiol. 2015;66:561-77.

2. Dweck MR, Khaw HJ, Sng GK, Luo EL, Baird A, Williams MC, Makiello P, Mirsadraee S, Joshi NV, van Beek EJ, Boon NA, Rudd JH and Newby DE. Aortic stenosis, atherosclerosis, and skeletal bone: is there a common link with calcification and inflammation? Eur Heart J. 2013;34:1567-74.

3. Aikawa E and Libby P. A Rock and a Hard Place: Chiseling Away at the Multiple Mechanisms of Aortic Stenosis. Circulation. 2017;135:1951-1955.

4. Vahanian A, Beyersdorf F, Praz F, Milojevic M, Baldus S, Bauersachs J, Capodanno D, Conradi L, De Bonis M, De Paulis R, Delgado V, Freemantle N, Gilard M, Haugaa KH, Jeppsson A, Juni P, Pierard L, Prendergast BD, Sadaba JR, Tribouilloy C, Wojakowski W and Group EESD. 2021 ESC/EACTS Guidelines for the management of valvular heart disease. Eur J Cardiothorac Surg. 2021.

5. Otto CM, Nishimura RA, Bonow RO, Carabello BA, Erwin JP, 3rd, Gentile F, Jneid H, Krieger EV, Mack M, McLeod C, O'Gara PT, Rigolin VH, Sundt TM, 3rd, Thompson A and Toly C. 2020 ACC/AHA Guideline for the Management of Patients With Valvular Heart Disease: A Report of the American College of Cardiology/American Heart Association Joint Committee on Clinical Practice Guidelines. Circulation. 2021;143:e72-e227.

6. Goody PR, Hosen MR, Christmann D, Niepmann ST, Zietzer A, Adam M, Bonner F, Zimmer S, Nickenig G and Jansen F. Aortic Valve Stenosis: From Basic Mechanisms to Novel Therapeutic Targets. Arterioscler Thromb Vasc Biol. 2020;40:885-900.

7. Myasoedova VA, Ravani AL, Frigerio B, Valerio V, Moschetta D, Songia P and Poggio P. Novel pharmacological targets for calcific aortic valve disease: Prevention and treatments. Pharmacol Res. 2018;136:74-82.

8. Zheng KH, Tsimikas S, Pawade T, Kroon J, Jenkins WSA, Doris MK, White AC, Timmers N, Hjortnaes J, Rogers MA, Aikawa E, Arsenault BJ, Witztum JL, Newby DE, Koschinsky ML, Fayad ZA, Stroes ESG, Boekholdt SM and Dweck MR. Lipoprotein(a) and Oxidized Phospholipids Promote Valve Calcification in Patients With Aortic Stenosis. J Am Coll Cardiol. 2019;73:2150-2162.

9. Raddatz MA, Madhur MS and Merryman WD. Adaptive immune cells in calcific aortic valve disease. Am J Physiol Heart Circ Physiol. 2019;317:H141-H155.

10. Bouchareb R, Boulanger MC, Tastet L, Mkannez G, Nsaibia MJ, Hadji F, Dahou A, Messadeq Y, Arsenault BJ, Pibarot P, Bosse Y, Marette A and Mathieu P. Activated platelets promote an osteogenic programme and the progression of calcific aortic valve stenosis. Eur Heart J. 2019;40:1362-1373. 11. Jansen F, Xiang X and Werner N. Role and function of extracellular vesicles in calcific aortic valve disease. Eur Heart J. 2017;38:2714-2716.

12. Huo Y, Schober A, Forlow SB, Smith DF, Hyman MC, Jung S, Littman DR, Weber C and Ley K. Circulating activated platelets exacerbate atherosclerosis in mice deficient in apolipoprotein E. Nat Med. 2003;9:61-7.

13. Otto CM, Kuusisto J, Reichenbach DD, Gown AM and O'Brien KD. Characterization of the early lesion of 'degenerative' valvular aortic stenosis. Histological and immunohistochemical studies. Circulation. 1994;90:844-53.

14. Rosenhek R, Binder T, Porenta G, Lang I, Christ G, Schemper M, Maurer G and Baumgartner H. Predictors of outcome in severe, asymptomatic aortic stenosis. New Engl J Med. 2000;343:611-617.

15. Chan KL, Teo K, Dumesnil JG, Ni A, Tam J and Investigators A. Effect of Lipid lowering with rosuvastatin on progression of aortic stenosis: results of the aortic stenosis progression observation: measuring effects of rosuvastatin (ASTRONOMER) trial. Circulation. 2010;121:306-14.

16. Surendran A, Edel A, Chandran M, Bogaert P, Hassan-Tash P, Kumar Asokan A, Hiebert B, Solati Z, Sandhawalia S, Raabe M, Kass M, Shah A, Jassal DS, Jaleel A and Ravandi A. Metabolomic Signature of Human Aortic Valve Stenosis. JACC Basic Transl Sci. 2020;5:1163-1177.

17. Yilmaz MB, Guray U, Guray Y, Cihan G, Caldir V, Cay 596 S, Kisacik HL and Korkmaz S. Lipid profile of patients with aortic stenosis might be predictive of rate of progression. Am Heart J. 2004;147:915-8.

18. Mateos N, Gomez M, Homar A, Garcia-Elias A, Yanez L, Tajes M, Molina L, Ble M, Cladellas M, Roqueta C and Benito B. Plasmatic PCSK9 Levels Are Associated with Very Fast Progression of Asymptomatic Degenerative Aortic Stenosis. J Cardiovasc Transl Res. 2021.

19. Salinger T, Hu K, Liu D, Taleh S, Herrmann S, Oder D, Gensler D, Muntze J, Ertl G, Lorenz K, Frantz S, Weidemann F and Nordbeck P. Association between Comorbidities and Progression of Transvalvular Pressure Gradients in Patients with Moderate and Severe Aortic Valve Stenosis. Cardiol Res Pract. 2018;2018:3713897.

20. Baumgartner H, Hung J, Bermejo J, Chambers JB, Evangelista A, Griffin BP, Iung B, Otto CM, Pellikka PA, Quinones M, American Society of E and European Association of E. Echocardiographic assessment of valve stenosis: EAE/ASE recommendations for clinical practice. J Am Soc Echocardiogr. 2009;22:1-23; quiz 101-2.

21. Glodny B, Helmel B, Trieb T, Schenk C, Taferner B, Unterholzner V, Strasak A and Petersen J. A method for calcium quantification by means of CT coronary angiography using 64-multidetector CT: very high correlation with Agatston and volume scores. Eur Radiol. 2009;19:1661-8.

22. Fujita B, Kutting M, Seiffert M, Scholtz S, Egron S, Prashovikj E, Borgermann J, Schafer T, Scholtz W, Preuss R, Gummert J, Steinseifer U and Ensminger SM. Calcium distribution patterns of the aortic valve as a risk factor for the need of permanent pacemaker implantation after transcatheter aortic valve implantation. Eur Heart J Cardiovasc Imaging. 2016;17:1385-1393.

23. Mosch J, Gleissner CA, Body S and Aikawa E. Histopathological assessment of calcification and inflammation of calcific aortic valves from patients with and without diabetes mellitus. Histol Histopathol. 2017;32:293-306.

24. Monaco G, Chen H, Poidinger M, Chen J, de Magalhaes JP and Larbi A. flowAI: automatic and interactive anomaly discerning tools for flow cytometry data. Bioinformatics. 2016;32:2473-80.

25. McInnes L HJ, Melville J. . UMAP: Uniform Manifold Approximation and Projection for Dimension Reduction. Cornell University. 2018.

26. Levine JH, Simonds EF, Bendall SC, Davis KL, Amir el AD, Tadmor MD, Litvin O, Fienberg HG, Jager A, Zunder ER, Finck R, Gedman AL, Radtke I, Downing JR, Pe'er D and Nolan GP. Data-Driven Phenotypic Dissection of AML Reveals Progenitor-like Cells that Correlate with Prognosis. Cell. 2015;162:184-97.

27. Otto CM and Prendergast B. Aortic-valve stenosis--from patients at risk to severe valve obstruction. N Engl J Med. 2014;371:744-56.

28. GeneCardsSuite. 2021;2021.

29. Gawaz M, Langer H and May AE. Platelets in inflammation and atherogenesis. J Clin Invest. 2005;115:3378-84.

30. Zernecke A, Bernhagen J and Weber C. Macrophage migration inhibitory factor in cardiovascular disease. Circulation. 2008;117:1594-602.

31. Schober A, Bernhagen J, Thiele M, Zeiffer U, Knarren S, Roller M, Bucala R and Weber C. Stabilization of atherosclerotic plaques by blockade of macrophage migration inhibitory factor after vascular injury in apolipoprotein E-deficient mice. Circulation. 2004;109:380-5.

32. Bernhagen J, Krohn R, Lue H, Gregory JL, Zernecke A, Koenen RR, Dewor M, Georgiev I, Schober A, Leng L, Kooistra T, Fingerle-Rowson G, Ghezzi P, Kleemann R, McColl SR, Bucala R, Hickey MJ and Weber C. MIF is a noncognate ligand of CXC chemokine receptors in inflammatory and atherogenic cell recruitment. Nat Med. 2007;13:587-96.

33. Massberg S, Brand K, Gruner S, Page S, Muller E, Muller I, Bergmeier W, Richter T, Lorenz M, Konrad I, Nieswandt B and Gawaz M. A critical role of platelet adhesion in the initiation of atherosclerotic lesion formation. J Exp Med. 2002;196:887-96.

34. Bakogiannis C, Sachse 651 M, Stamatelopoulos K and Stellos K. Platelet-derived chemokines in inflammation and atherosclerosis. Cytokine. 2019;122:154157.

35. Strussmann T, Tillmann S, Wirtz T, Bucala R, von Hundelshausen P and Bernhagen J. Platelets are a previously unrecognised source of MIF. Thromb Haemost. 2013;110:1004- 13.

36. Wirtz TH, Tillmann S, Strussmann T, Kraemer S, Heemskerk JW, Grottke O, Gawaz M, von Hundelshausen P and Bernhagen J. Platelet-derived MIF: a novel platelet chemokine with distinct recruitment properties. Atherosclerosis. 2015;239:1-10.

37. Zernecke A and Weber C. Inflammatory mediators in atherosclerotic vascular disease. Basic Res Cardiol. 2005;100:93-101.

38. Muller, II, Chatterjee M, Schneider M, Borst O, Seizer P, Schonberger T, Vogel S, Muller KA, Geisler T, Lang F, Langer H and Gawaz M. Gremlin-1 inhibits macrophage migration inhibitory factor-dependent monocyte function and survival. Int J Cardiol. 2014;176:923-9.

39. Erdogan M, Ozturk S, Kardesler B, Yigitbasi M, Kasapkara HA, Bastug S, Erdol MA, Akar Bayram N, Akcay M and Durmaz T. The relationship between calcific severe aortic stenosis and systemic immune-inflammation index. Echocardiography. 2021;38:737-744.

40. Pan JH, Sukhova GK, Yang JT, Wang B, Xie T, Fu H, Zhang Y, Satoskar AR, David JR, Metz CN, Bucala R, Fang K, Simon DI, Chapman HA, Libby P and Shi GP. Macrophage migration inhibitory factor deficiency impairs atherosclerosis in low-density lipoprotein receptor-deficient mice. Circulation. 2004;109:3149-53.

41. Ruiz-Rosado Jde D, Olguin JE, Juarez-Avelar I, Saavedra R, Terrazas LI, Robledo- Avila FH, Vazquez-Mendoza A, Fernandez J, Satoskar AR, Partida-Sanchez S and Rodriguez-Sosa M. MIF Promotes Classical Activation and Conversion of Inflammatory Ly6C(high) Monocytes into TipDCs during Murine Toxoplasmosis. Mediators Inflamm. 2016;2016:9101762.

42. Muller, II, Muller KA, Karathanos A, Schonleber H, Rath D, Vogel S, Chatterjee M, Schmid M, Haas M, Seizer P, Langer H, Schaeffeler E, Schwab M, Gawaz M and Geisler T. Impact of counterbalance between macrophage migration inhibitory factor and its inhibitor Gremlin-1 in patients with coronary artery disease. Atherosclerosis. 2014;237:426-32.

43. Zhao Q, Men L, Li XM, Liu F, Shan CF, Zhou XR, Song N, Zhu JJ, Gao XL, Ma YT, Du XJ, Gao XM and Yang YN. Circulating MIF Levels Predict Clinical Outcomes in Patients With ST-Elevation Myocardial Infarction After Percutaneous Coronary Intervention. Can J Cardiol. 2019;35:1366-1376.

44. Kontos C, El Bounkari O, Krammer C, Sinitski D, Hille K, Zan C, Yan G, Wang S, Gao Y, Brandhofer M, Megens RTA, Hoffmann A, Pauli J, Asare Y, Gerra S, Bourilhon P, Leng L, Eckstein HH, Kempf WE, Pelisek J, Gokce O, Maegdefessel L, Bucala R, Dichgans M, Weber C, Kapurniotu A and Bernhagen J.

Designed CXCR4 mimic acts as a soluble chemokine receptor that blocks atherogenic inflammation by agonist-specific targeting. Nat Commun. 2020;11:5981.

45. Muller I, Schonberger T, Schneider M, Borst O, Ziegler M, Seizer P, Leder C, Muller K, Lang M, Appenzeller F, Lunov O, Buchele B, Fahrleitner M, Olbrich M, Langer H, Geisler T, Lang F, Chatterjee M, de Boer JF, Tietge UJ, Bernhagen J, Simmet T and Gawaz M. Gremlin-1 is an inhibitor of macrophage migration inhibitory factor and attenuates atherosclerotic plaque growth in ApoE-/- Mice. J Biol Chem. 2013;288:31635-45.

46. Tilstam PV, Pantouris G, Corman M, Andreoli M, Mahboubi K, Davis G, Du X, Leng L, Lolis E and Bucala R. A selective small-molecule inhibitor of macrophage migration inhibitory factor-2 (MIF-2), a MIF cytokine superfamily member, inhibits MIF-2 biological activity. J Biol Chem. 2019;294:18522-18531.

47. Jin K, Zheng L, Ye L, Xie Z, Gao J, Lou C, Pan W, Pan B, Liu S, Chen Z and He D. Chicago sky blue 6B (CSB6B), an allosteric inhibitor of macrophage migration inhibitory factor (MIF), suppresses osteoclastogenesis and promotes osteogenesis through the inhibition of the NF-kappaB signaling pathway. Biochem Pharmacol. 2021;192:114734.

48. Oliveros G, Wallace CH, Chaudry O, Liu Q, Qiu Y, Xie L, Rockwell P, Figueiredo- Pereira ME and Serrano PA. Repurposing ibudilast to mitigate Alzheimer's disease by targeting inflammation. Brain. 2022.

49. Lee JY, Cho E, Ko YE, Kim I, 707 Lee KJ, Kwon SU, Kang DW and Kim JS. Ibudilast, a phosphodiesterase inhibitor with anti-inflammatory activity, protects against ischemic brain injury in rats. Brain Res. 2012;1431:97-106.

50. Capoulade R, Yeang C, Chan KL, Pibarot P and Tsimikas S. Association of Mild to Moderate Aortic Valve Stenosis Progression With Higher Lipoprotein(a) and Oxidized Phospholipid Levels: Secondary Analysis of a Randomized Clinical Trial. JAMA Cardiol. 2018;3:1212-1217.

Figures and Tables

Tables

Table 1. Baseline characteristics of patient population

Parameters	All Patients, N=475	Slow AS, N=238	Fast AS, N=237	p-value
Clinical characteristics				
Age, y	77 (69-82)	79 (71-83)	76 (69-81)	**<0.001**
Male	287 (60.4)	139 (58.4)	148 (62.4)	0.368
BMI (kg/m²)	27.1 (24.3-31.1)	27.2 (24.1-31.2)	27.0 (24.4-31.0)	0.725
Systolic blood pressure	135 (120-150)	140 (120-150)	133 (120-150)	0.728
NYHA class > 2	258 (54.3)	129 (54.2)	129 (54.4)	0.788
Cardiovascular risk factors and co-morbidities				
Coronary artery disease				
- 1-vessel	80 (16.8)	36 (15.1)	44 (18.6)	
- 2-vessel	69 (14.5)	36 (15.1)	33 (13.9)	0.850
- 3-vessel	95 (20)	48 (20.2)	47 (19.8)	
- CABG	23 (4.8)	13 (5.5)	10 (4.2)	
Myocardial infarction	32(15.8)	19 (14.7)	13 (16.9)	0.230

Smoking	75 (15.8)	35 (14.7)	40 (16.9)	0.615
Hyperlipidemia	224 (47.2)	118 (49.6)	106 (44.7)	0.244
Diabetes mellitus	116 (24.4)	59 (24.8)	57 (24.1)	0.960
Hypertension	387 (81.5)	195 (81.9)	192 (81.0)	0.871
Atrial fibrillation	161 (33.9)	94 (39.5)	67 (28.3)	**0.012**
Pulmonary	208 (43.8)	111 (46.6)	97 (40.9)	0.231
Bicuspid aortic valve	33 (6.9)	14 (5.9)	19 (8.0)	0.353
STS-Score	2.8 (1.6-6.7)	2.8 (1.6-10.1)	2.7 (1.5-5.2)	**0.021**
Parameters of echocardiography and electrocardiography				
Left ventricular ejection	60 (46-60)	60 (49-60)	60 (45-60)	0.892
Stroke volume (mL)	76.8 (60-96.5)	73.1 (60.5-91.9)	81.9 (58.9-100)	0.060
Stroke volume index (	40.6 (31.7-52.5)	39.4 (32.2-49.5)	44 (30.8-57.2)	0.083
Mean pressure gradient	42 (32-50)	43 (33-50.3)	41 (31-50)	0.458
Peak pressure gradient	70 (56-84)	71 (59-84)	68.5 (54-85)	0.220
AVA (cm^2)	0.7 (0.6-0.9)	0.7 (0.6-0.9)	0.7 (0.6-0.9)	0.616
Heart Rate (bpm)	72.5 (64-85)	72.5 (65-84)	72.5 (64-87)	0.875
Medication at study entry				
ASA	229 (48.2)	114 (47.9)	115 (48.5)	0.721
Antiplatelet therapy	82 (17.3)	41 (17.2)	41 (17.3)	0.877
Oral anticoagulation	105 (22.1)	60 (25.2)	45 (19)	0.103
Antihypertensive	304 (64.0)	153 (64.3)	151 (63.7)	0.950
Aldosterone inhibitors	76 (16.0)	38 (15.9)	38 (16.0)	0.964
Diuretics	234 (49.3)	118 (49.6)	116 (48.9)	0.974
Beta blockers	229 (48.2)	117 (49.2)	112 (47.2)	0.702
Statins	256 (53.9)	132 (55.5)	124 (52.3)	0.499
Laboratory parameters and biomarkers				
Leukocytes (1000/µL)	7100 (6090-8485)	7000 (5920-8300)	7200 (6245-8660)	0.200
Hb (g/dL)	12.8 (11.5-13.9)	12.7 (11.3-13.9)	12.9 (11.7-13.9)	0.397
Platelets (1000/µL)	212 (181-259)	212 (181-247.5)	212 (180-265)	0.460
GFR-MDRD (ml/m^2)	70 (53-85.4)	68.8 (52.5-85.3)	73.2 (54-85.7)	0.190
CRP (mg/dL)	1 (0.8-1.2)	0.23 (0.1-0.85)	0.32 (0.1-0.95)	0.233
hs TNI (mg/L)	0.06 (0.03-5)	0.06 (0.03-2.5)	0.06 (0.03-10)	0.524
NT-pro-BNP (ng/L)	429 (203-1190)	429 (221-1059)	400.5 (156.3-1350)	0.486
Serum Creatinine	1 (0.8-1.2)	1.0 (0.8-1.2)	0.95 (0.8-1.2)	0.516
Total Cholesterol	171 (141.8-203)	165 (140-200)	175 (142.8-211)	0.161
LDL (mg/dL)	96 (69.3-129)	90 (68-126)	102 (72-129)	0.250

Values are given as numbers (n) and percentage (%) or are given as median and interquartile range (IQR). AS – aortic stenosis, ASA – Acetylsalicylic acid , AV – aortic valve, AVA – aortic valve area, BMI – body mass index, CAD – coronary artery disease, CABG - coronary artery bypass grafting, CK – creatinine kinase, CRP – C-reactive protein, GFR-MDRD – glomerular filtration rate, Hb – hemoglobin, HDL – high density lipoprotein, hs TNI - High sensitive Troponin I, LDL – low density lipoprotein, NT-pro-BNP – N-terminal pro-B-type natriuretic peptide, STS - Society of Thoracic Surgeons.

Table 2. Linear regression analysis identifies liquid biopsy as independent predictors of fast progressive aortic valve stenosis

Model	Parameter	Unstandardized Coefficients		Standardized Coefficients		
		Beta	Std error	Beta	t-value	p-value
1	Liquid biopsy	0.164	0.051	0.397	3.21	**0.002**
2	Liquid biopsy	0.142	0.043	0.370	3.33	**0.003**
3	Liquid biopsy	0.147	0.050	0.388	2.967	**0.008**
4	Liquid biopsy	0.151	0.053	0.394	2.839	**0.013**

Adjusted Beta Coefficients are given. Dependent Variable: Fast progressive aortic valve stenosis.

Model 1: Unadjusted. **Model 2**: Adjusted for age, STS score, mean pressure gradient (mmHg), peak pressure gradient (mmHg). **Model 3**: Adjusted for age, STS score, mean pressure gradient (mmHg), peak pressure gradient (mmHg), HTN, HLP, DM, CRP, CAD, NYHA class, and smoking status. **Model 4**: Adjusted for age, STS score, mean pressure gradient (mmHg), peak pressure gradient (mmHg), HTN, HLP, DM, CRP, CAD, NYHA class, smoking status, ASA, LDL, and LVEF. Liquid biopsy remained significantly associated with fast progressive aortic valve stenosis in all models shown. P-values < 0.05 were defined as statistically significant. Significant p-values are bolded. Abbreviations: ASA – Acetylsalicylic acid, CAD – coronary artery disease, CRP – C-reactive protein, DM – diabetes mellitus, HLP – hyperlipidemia, HTN – arterial hypertension, LDL – low density lipoprotein, NYHA - New York Heart Association, Std. Error - Standard Error, STS - Society of Thoracic Surgeons.

Table 3. Cox regression analysis identifies liquid biopsy, age, and gender as independent predictors of fast progressive aortic valve stenosis

Variable	Cox regression analysis	
	HR (95% CI)	p-value
Bicuspid AV	1.772 (0.116 – 27.006)	0.681
Peak pressure gradient (mmHg) AV	1.245 (0.938 – 1.654)	0.130
STS Score	1.047 (0.619 – 1.769)	0.864
Left ventricular ejection fraction	0.997 (0.863 – 1.152)	0.973
Age	0.756 (0.611 – 0.935)	**0.010**
Mean pressure gradient (mmHg) AV	0.668 (0.434 – 1.028)	0.067
Liquid biopsy	0.087 (0.008 – 0.977)	**0.048**
Gender	0.008 (0.00 – 0.611)	**0.029**
Hyperlipidemia	0.005 (0.00 – 2.266)	0.089

Figure 1

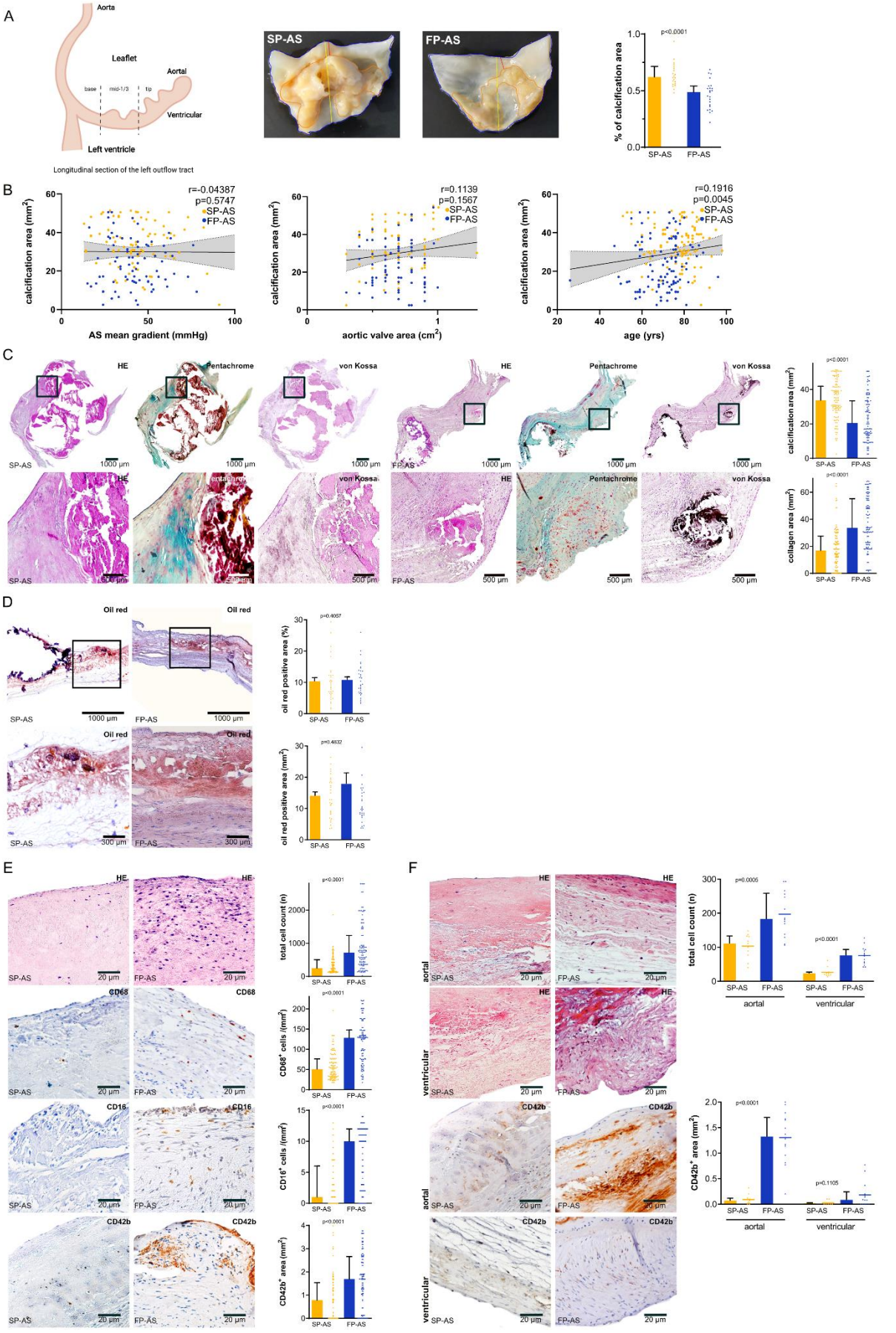
A
Aorta
Leaflet
Aortal
Ventricular
base
mid-1/3
tip
Left ventricle
Longitudinal section of the left outflow tract
SP-AS
FP-AS
% of calcification area
p<0.0001
B
r=-0.04387
p=0.5747
r=0.1139
p=0.1567
r=0.1916
p=0.0045
calcification area (mm²)
AS mean gradient (mmHg)
aortic valve area (cm²)
age (yrs)
C
HE
Pentachrome
von Kossa
calcification area (mm²)
collagen area (mm²)
D
Oil red
oil red positive area (%)
oil red positive area (mm²)
E
CD68
CD16
CD42b
total cell count (n)
CD68⁺ cells /(mm²)
CD16⁺ cells /(mm²)
CD42b⁺ area (mm²)
F
aortal
ventricular

Figure 1: Patients with fast progressive AS are characterized by enhanced collagen content, higher cellularity, and an increased number of CD68+ macrophages, CD16+ monocytes and CD42+ platelets within the aortic valve. (A) Morphological analysis of patients with either slow (n=22) or fast (n=23) progressive AS. **(A)** Morphological analysis of patients with either slow (n=22) or fast (n=23) progressive AS. Left graphic shows overview chart of a longitudinal section of the left outflow tract. The middle panel shows the representative gross pathology of explanted AV cusps and the analysis of SP-AS and FP-AS patients regarding the degree of mineralization and calcification. Right plot shows quotient of calcification area in proportion to total area (%). Plotted: Median ± interquartile range (IQR); Statistics: Mann-Whitney U test. **(B)** Spearman´s correlation analysis of slow (n=238) and fast (n=237) progressive AS patients to evaluate associations between: calcification area (mm^2) and AS mean gradient (mmHg) (r=-0.04387, p=0.5747), calcification area (mm^2) and aortic valve area (cm^2) (r=0.1139, p=0.1567), and calcification area (mm^2) and age (yrs) (r=0.1916, p=0.0045). Statistics: Spearman´s correlation coefficient r. **(C)** Representative histological stainings of aortic valves of patients with slow and fast progression AS. Upper panel shows 4x magnification and lower panel a 40x magnification of the aortic valves. Hematoxylin eosin (HE), Movat pentrachrome and von Kossa staining were performed. Calcification area (mm^2) and collagen area (mm^2) of slow (n=110) and fast (n=108) AS patients was calculated. Plotted: Median ± interquartile range (IQR); Statistics: Mann-Whitney U test. **(D)** Representative histological stainings of aortic valves of patients with slow (n=32) and fast (n=32) progression AS. Upper panel shows 10x magnification and lower panel a 40x magnification of the aortic valves. Oil red staining was performed. Oil red positive area (%, mm2) was calculated. Plotted: Median ± interquartile range (IQR); Statistics: Mann-Whitney U test. **(E)** Representative immunohistological stainings of aortic valves of patients with slow (n=110) and fast (n=108) progression AS. Upper panel shows HE staining to calculate total aortic valve cell count (n) between slow and fast progressive AS. Second panel shows staining of $CD68^+$ macrophages and calculation of $CD68^+$ cells /mm^2. Third panel represents staining of $CD16^+$ monocytes and calculation of $CD16^+$ cells /mm^2. Last panel represents staining of $CD42b^+$ platelets and calculation of $CD42b^+$ area (mm^2). Plotted: Median ± interquartile range (IQR); Statistics: Mann-Whitney U test. **(F)** Representative immunohistological stainings of aortic valves comparing aortal and ventricular aortic valve side of patients with slow (n=11) and fast (n=14) progression AS. Upper panels show HE staining to analyze the cell count (n) in the aortal and the ventricular side of the AV in slow and fast progressive AS. Lower panel represents staining of $CD42b^+$ positive areas indicating platelets. The distribution of $CD42b^+$ positive area (mm^2) in the aortal and the ventricular side of the AV is shown in the right graph and illustrate the different expression in SP-AS compared to FP-AS. Plotted: Median ± interquartile range (IQR); Statistics: Mann-Whitney U test.

Figure 2

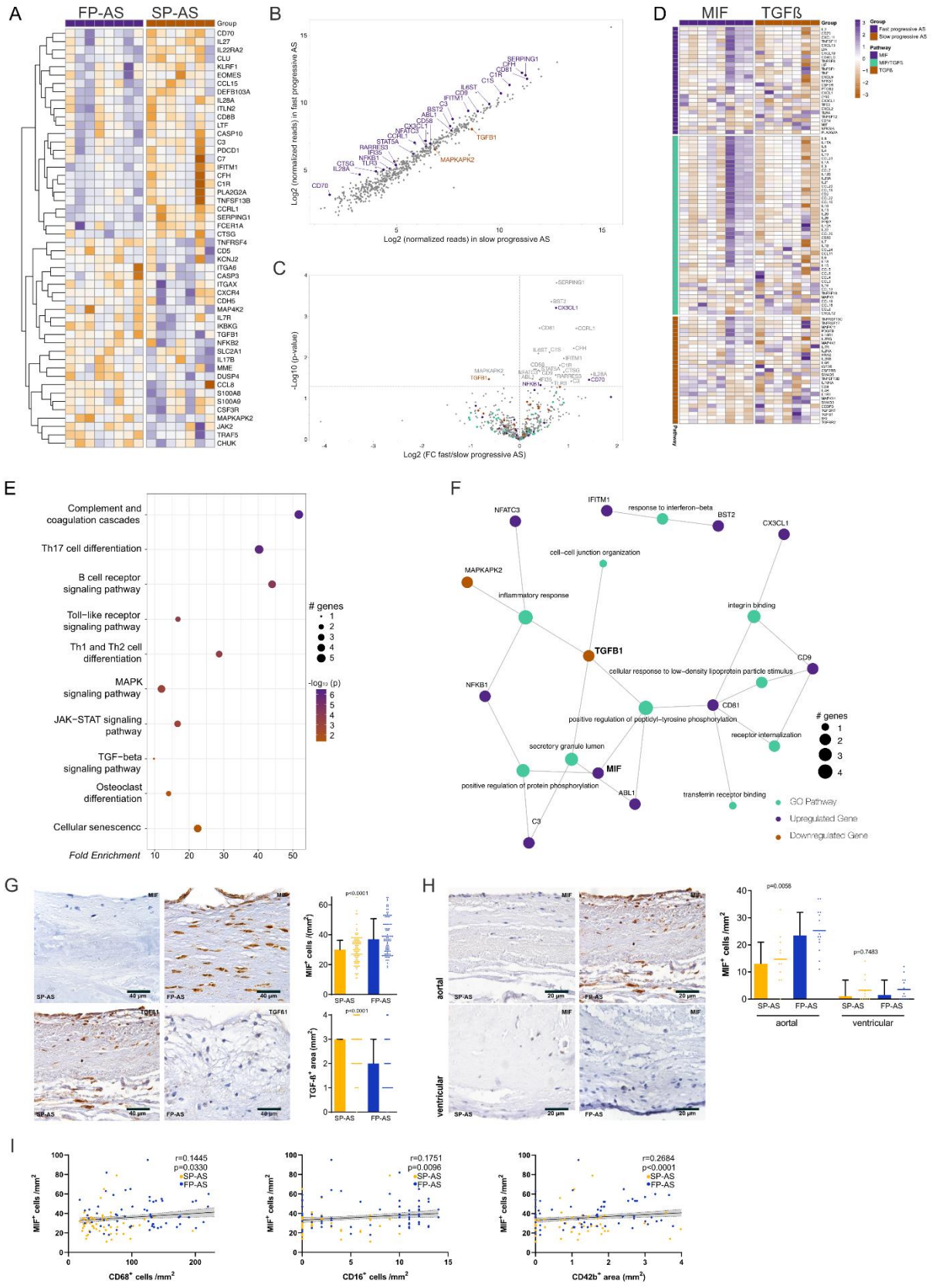

Figure 2: MIF associated gene expression is upregulated in fast progressive AS patients along with an increased MIF expression within the aortic valve tissue. (A) Hierarchical clustering analysis of the top 50 differentially expressed genes of Nano- String mRNA profiling. Z-scores of means were colored according to upregulation in fast (FP-AS, blue) or slow progressive aortic stenosis (SP-AS,

orange). **(B)** Results of Nanostring® data were Log2-transformed and fold change of means was plotted in scatter plot displaying significant ($p<0.05$) alterations between patients with fast and slow progressive aortic stenosis. To evaluate whether the gene expression is dependent on the progression of the disease, mean normalized reads of distinct genes between patients with fast and slow progressive aortic stenosis were compared. **(C)** Results of Nanostring® data were Log2- transformed, and fold change of means was plotted in volcano plot displaying significant ($p<0.05$) alterations between patients with fast and slow progressive aortic stenosis. To evaluate whether the gene expression is dependent on the progression of the disease, mean normalized reads of distinct genes between patients with fast and slow progressive aortic stenosis were compared. (B+C) Test was performed by JMP Version 15.0. Plotted: fold change of means; Statistics: Student's test. **(D)** Heatmap with row-wise comparisons of Nanostring® data. Observed z-scores of genes belonging to the MIF pathway (blue) and TGF-ß1 pathway (orange) were plotted according to PathCards online database. **(E)** KEGG (Kyoto Encyclopedia of Genes and Genomes) pathway analysis was performed. The top ten significantly enriched KEGG pathways subsuming the 25 significantly regulated genes in fast progressive AS were plotted. Log10-transformed p-values of enriched terms were colored and the size of each term adapted to the number of genes. Plotted: Log10-transformed p-values; Statistics: Bonferroni $p<0.01$, greedy algorithm active subnetwork search method. **(F)** A term-gene-graph highlights subnetworks and regulations of significantly regulated genes and the referring KEGG pathway in fast progressive AS. To further highlight the importance of MIF in patients with fast progressive AS, MIF was added to the network analysis displaying its interactions with significantly ($p<0.01$) enriched GeneOntology pathways. **(G)** Representative immunohistological stainings of aortic valves of patients with slow (n=110) and fast (n=108) progression AS. Upper panel shows staining of MIF^+ cells and calculation of MIF^+ cells /mm^2. Lower panel represents staining of TGFß-1^+ area and calculation of TGFß- 1^+ area (mm^2). Plotted: Median ± interquartile range (IQR); Statistics: Mann-Whitney U test. **(H)** Representative immunohistological stainings of aortic valves comparing aortal and ventricular aortic valve side of patients with slow (n=11) and fast (n=14) progression AS. Upper panel represents staining of MIF^+ cells and calculation of MIF^+ cells /mm^2. Plotted: Median ± interquartile range (IQR); Statistics: Mann-Whitney U test. **(I)** Spearman´s correlation analysis of slow and fast progressive AS patients was performed to evaluate associations between: MIF^+ cells /mm^2 and $CD68^+$ cells /mm^2 ($r=0.1445$, $p=0.0330$), MIF^+ cells /mm^2 and $CD16^+$ cells /mm2 ($r=0.1751$, $p=0.0096$), MIF^+ cells /mm^2 and $CD42b^+$ area (mm^2) ($r=0.2684$, $p<0.0001$), Statistics: Spearman´s correlation coefficient r.

Figure 3

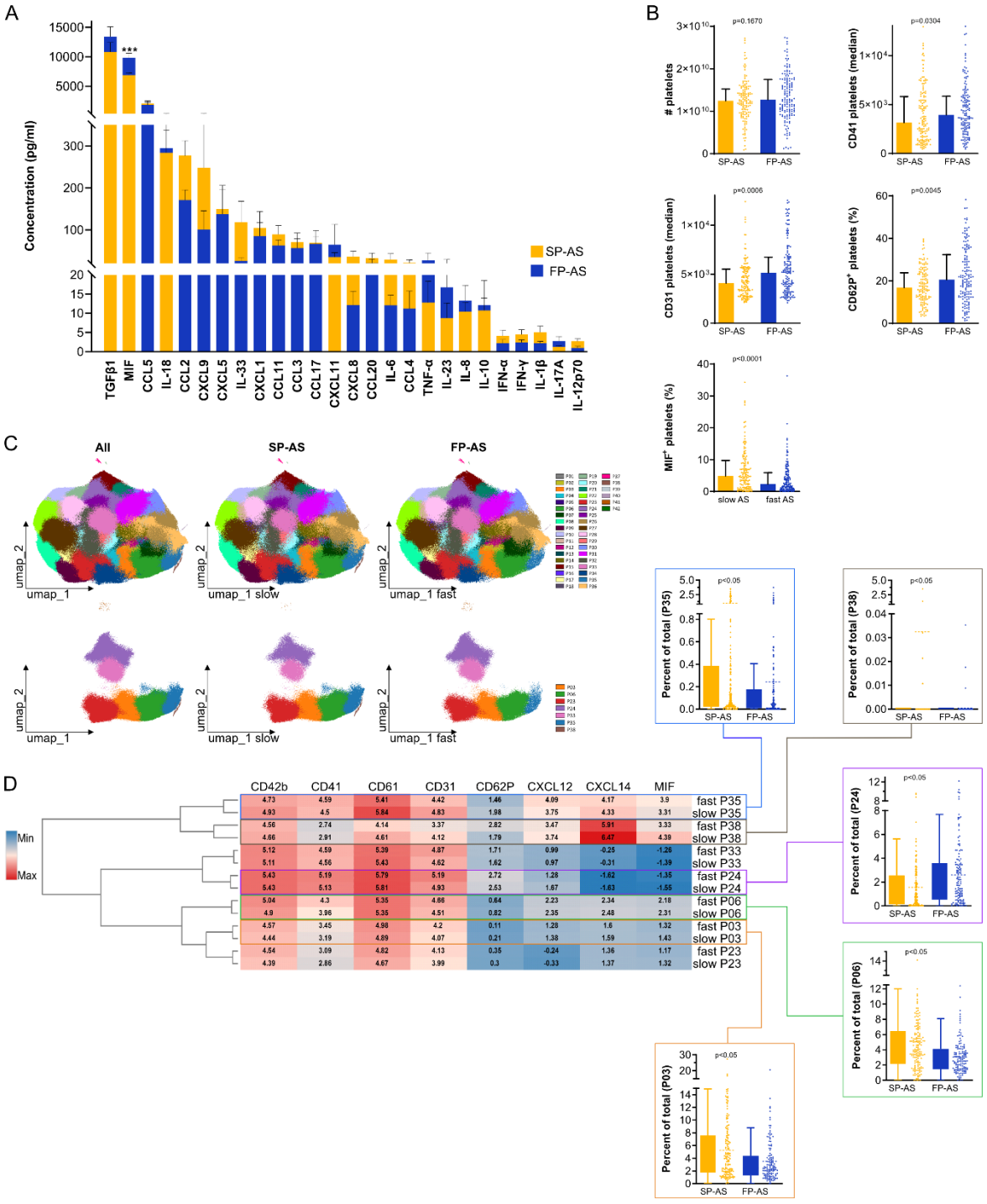

Figure 3: Immunophenotyping and high-dimensional analysis of platelets show differences in platelet activation and in the expression of MIF between fast and slow progressive aortic stenosis. **(A)** Plasma concentration of several inflammatory cytokines and chemokines including MIF (LegendPlex and ELISA). Plot represents concentration (pg/ml) of indicated cytokines / chemokines for slow (n=98) and fast progressive AS patients (n=95). Plotted: Mean ± standard error of the mean (SEM); Statistics: unpaired T-test. **(B)** Platelets were analyzed by flow cytometry of slow (n=142) and fast (n=150) progressive AS patients. Graphs show following marker expression: cell count of platelets, median of CD41 on platelets, median of CD31 on platelets, frequency of $CD62P^+$ platelets (%), and frequency of MIF^+ platelets (%). Plotted: Median ± interquartile range (IQR); Statistics: Mann-Whitney U test. **(C)** Analysis of platelet subpopulations. PhenoGraph algorithm was used (nearest neighbors k=20) for unsupervised clustering of patient samples (n=270) measured by platelet flow cytometry panel. Left plot

represents an overlay of platelets from slow and fast progressive patients followed by individual plots of platelets from slow and fast progressive patients of all clusters. Same analysis of platelet subpopulations is shown in lower plots representing only significantly different clusters. **(D)** Clustered heatmap of significant different clusters P35, P38, P24, P03, and P06 from (C) show median expression of indicated markers for comparison of slow and fast progressive AS patients. Abundancy of cells in each cluster for each patient are shown as box plots stratified into slow and fast progressive AS. Plotted: Median ± interquartile range (IQR); Statistics: Mann-Whitney U test. Plots were generated using OMIQ data analysis software.

Figure 4

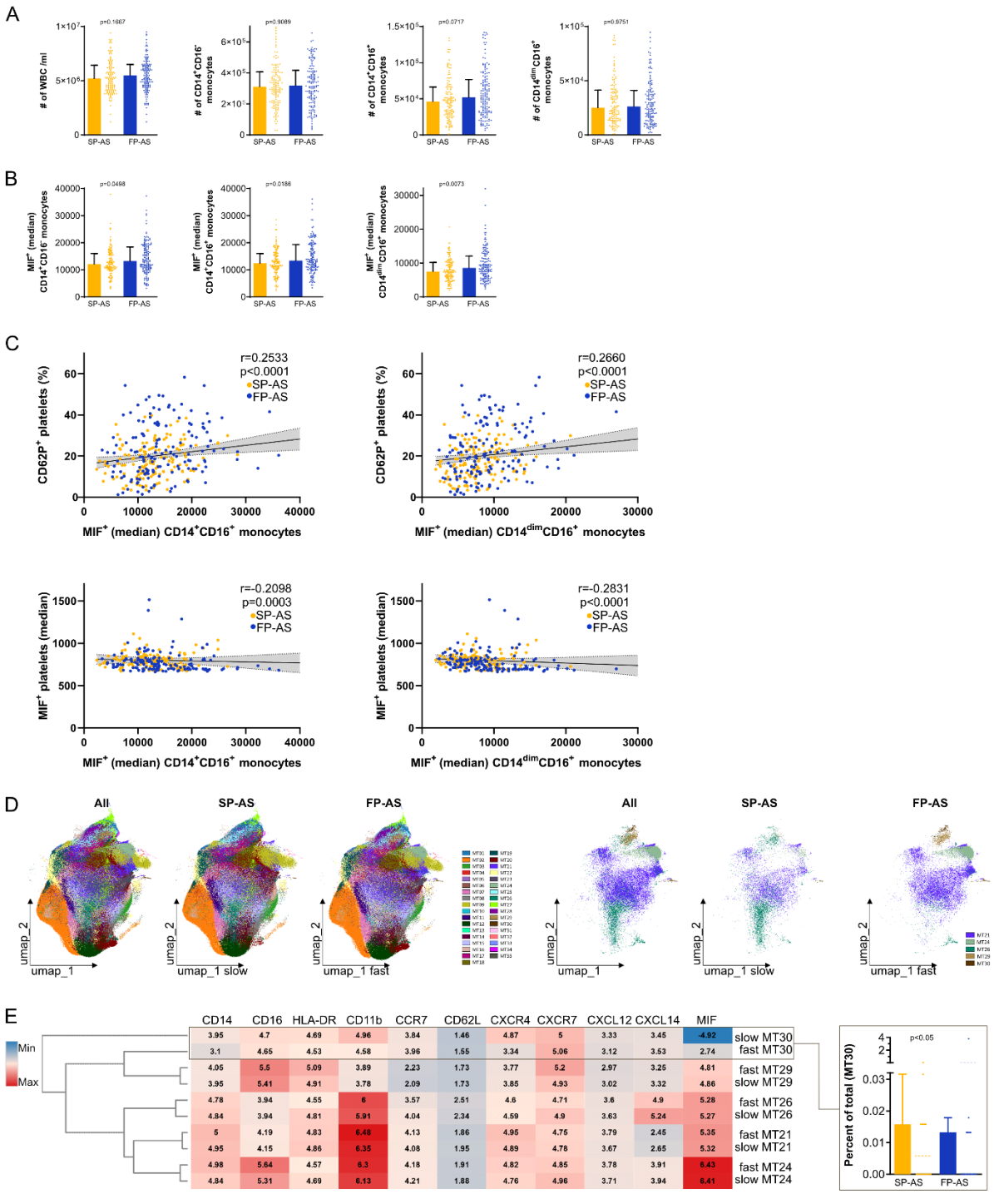

Figure 4: Surface expression of MIF in monocyte subsets is significantly elevated in fast progressive AS patients and correlates with MIF expression in platelets. (A) Monocytes were

analyzed by flow cytometry of slow (n=142) and fast (n=150) progressive AS patients. Graphs show: cell count of WBC/ml and of monocyte subsets. **(B)** Flow cytometry analysis of intracellular MIF expression (median) by monocyte subsets. (A+B) Plotted: Median ± interquartile range (IQR); Statistics: Mann-Whitney U test. **(C)** Spearman´s correlation analysis of slow and fast progressive AS patients to evaluate associations between: $CD62P^+$ platelets (%) and MIF^+ $CD14^+CD16^+$ monocytes (median) (r=0.2533, p<0.0001), $CD62P^+$ platelets (%) and MIF^+ $CD14^{dim}CD16^+$ monocytes (median) (r=0.2660, p<0.0001), MIF^+ platelets (median) and MIF^+ $CD14^+CD16^+$ monocytes (median) (r=-0.2098, p=0.0003), MIF^+ platelets (median) and MIF^+ $CD14^{dim}CD16^+$ monocytes (median) (r=-0.2831, p<0.0001). Statistics: Spearman´s correlation coefficient r. **(D)** Analysis of monocyte subpopulations. PhenoGraph algorithm was used (nearest neighbors k=20) for unsupervised clustering of patient samples (n=260) of monocyte flow cytometry. Left plot representing an overlay of monocytes from slow and fast progressive patients followed by individual plots of monocytes from slow and fast progressive patients of all clusters. Same analysis of monocyte subpopulations is shown in lower plots representing only significant different clusters. **(E)** Clustered heatmap of significant different clusters from (D) show median expression of indicated markers for comparison of slow and fast progressive AS patients. Abundancy of cells in each cluster for each patient are shown as box plots stratified into slow and fast progressive AS. Plotted: Median ± interquartile range (IQR); Statistics: Mann-Whitney U test. Plots were generated using OMIQ data analysis software.

Figure 5

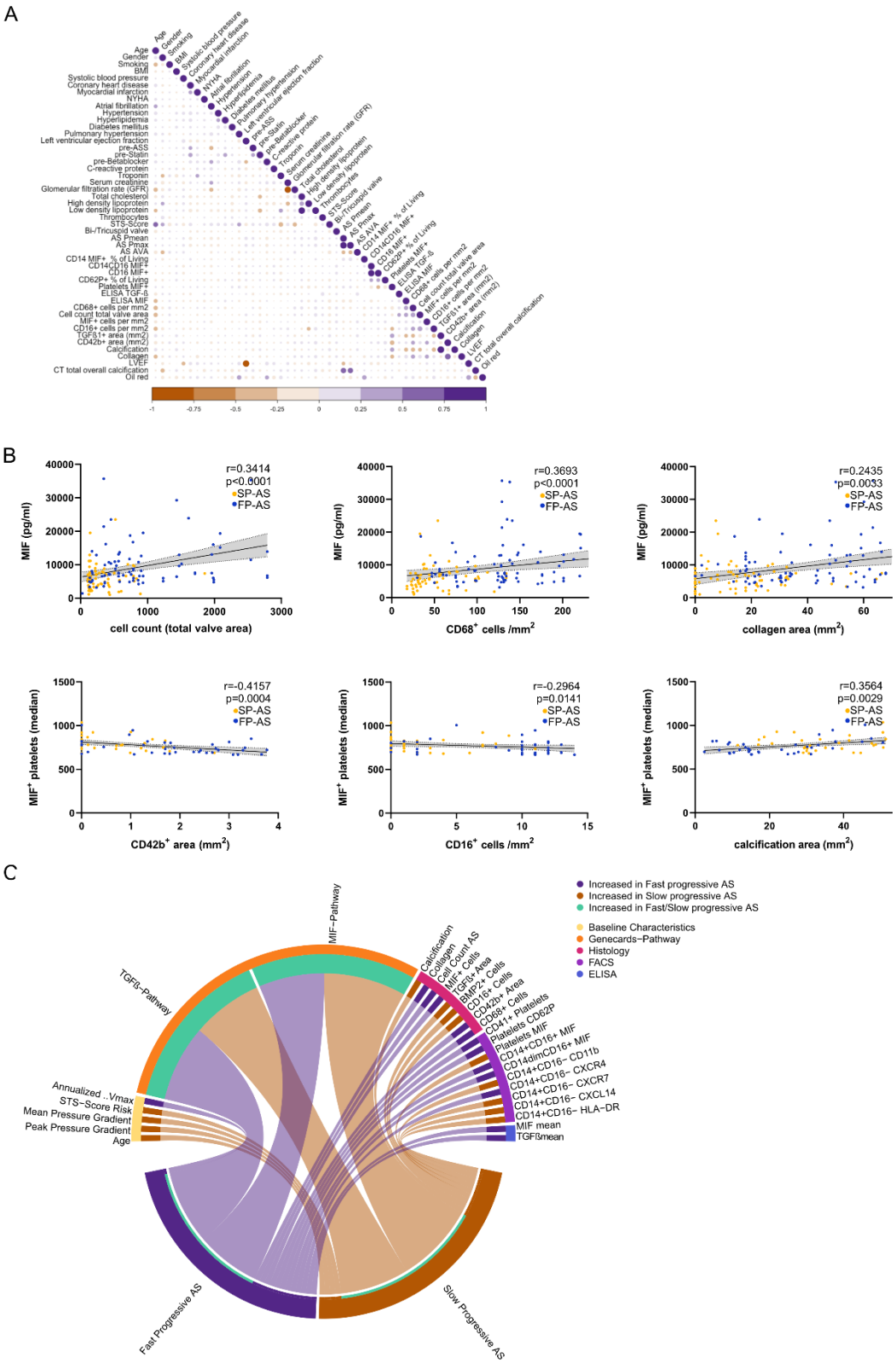

Figure 5: Plasma levels of MIF and MIF in platelets correlate with migrated immune cells within the aortic valve. (A) Correlation matrix was performed with Rstudio package “corrplot” displaying correlations of clinical parameters alongside ex vivo assays. Spearman´s ρ is colored and color intensity and size are plotted proportional to correlation coefficients. **(B)** Spearman´s correlation analysis of slow (n=110) and fast (n=83) progressive AS patients to evaluate associations between following parameter: MIF (pg/ml) and cell count (total valve area) (r=0.2576, p-value=0.0003), MIF (pg/ml) and CD68⁺ cells

/mm^2 (r=0.2662, p-value=0.0002), MIF (pg/ml) and collagen area (mm^2) (r=0.2102, p-value=0.0034), MIF$^+$ platelets (median) and CD42b$^+$ area (mm^2) (r=-0.2433, p-value=0.0296), MIF$^+$ platelets (median) and CD16$^+$ cells /mm^2 (r=-0.2855, p-value=0.0103), calcification area (mm^2) (r=0.2601, p-value=0.0198). Statistics: Spearman´s correlation coefficient r. **(C)** A synopsis of important findings in this study is displayed by chord diagram using Rstudio package “Circlize”. Significant ($p<0.05$) changes of clinical parameters and ex vivo data, as well as differently expressed gene pathways between patients with fast (blue) and slow (orange) progressive aortic stenosis are illustrated and colored according to the performed assays as indicated in the figure caption.